THERMAL MODELLING OF HIGHLY GLAZED SPACES

Peter Pfrommer

Ph. D.

1995

Thermal Modelling of Highly Glazed Spaces

Peter Pfrommer

A thesis submitted in partial fulfilment
of the requirements of De Montfort University
for the degree of Doctor of Philosophy

April 1995

ECADAP Centre
Institute of Energy and Sustainable Development
De Montfort University Leicester

and

Department of Building-Physics
Fachhochschule für Technik Stuttgart

ABSTRACT

Within the UK, and elsewhere, there is a growing interest in the Passive Solar Design for dwellings and commercial buildings. The aim is to make greater use of the *renewable* energy source, the sun, to provide space heating energy and (in commercial buildings) lighting energy. Such buildings often have large equator-facing glazed areas, attached conservatories, or large atria. The trend towards greater areas of glass is, for energy and aesthetic reasons, likely to continue.

Thermal simulation models such as ESP, HTB2, and SERI-RES have been used extensively to study the design of highly glazed buildings. However, recent work at De Montfort University Leicester has indicated that approximate methods used to model the glazing, solar distribution, and solar shading can severely compromise the accuracy of the predictions. This was confirmed for both direct-gain spaces and conservatories in early work in this project.

To improve the simulation of highly glazed spaces, new algorithms and calculation models for the transmission of solar radiation through windows, and the distribution of the transmitted solar radiation to internal surfaces, have been developed. A new calculation model allows the incidence angle dependent direct transmittance and absorptance, the diffuse transmittance and absorptance, and the effective total solar energy transmittance of glazing systems to be calculated. The main feature of the model is its applicability to any combination of coated or tinted glass, with no limitation on the number or sequence of the layers. The influence of internal or external slat-type blinds can also be simulated.

An internal solar distribution model has also been developed which can calculate the time-varying internal solar distribution in a room. It considers radiation transmission through any glazing system, radiation re-transmission through the other windows, backloss of the reflected radiation, and interzonal radiation transfer.

The new calculation models were formulated as independent pre-processing programs which produce the necessary input values for thermal simulation programs. The program HTB2 was used to illustrate the different links. The new programs were validated by comparing their predictions with measured values, known analytical solutions, or the results of other reputable programs.

Simulation studies examined the thermal consequences of using the new calculation models rather than applying conventional approximations. It was concluded that the application of all the new simulation aspects leads to a more authentic prediction of the environmental conditions in highly glazed spaces.

Finally, the new modelling possibilities were used to produce widely applicable information about the design, energy saving potential, and internal comfort conditions, of domestic conservatories.

ACKNOWLEDGEMENTS

This research was carried out at De Montfort University Leicester (UK), in the Environmental Computer Aided Design and Performance (ECADAP) group, working in collaboration with the Fachhochschule für Technik Stuttgart (Germany), department of Building-Physics. This work could not have been completed without the support and help of many people in both institutions.

I am especially grateful to Dr. Kevin J. Lomas for his encouragement and enthusiastic support and for his carefully and critical review of this thesis. I am also deeply indebted to Professor Christian Kupke who encouraged me to do the work and who has given me guidance and support in so many ways.

I would like to thank Prof. Neil Bowman and Prof. Dr. Martin Stohrer who - as leaders of the School of the Built Environment (De Montfort University) and the Fachhochschule für Technik, respectively - took care that the collaboration between both schools was possible and successful.

This work could not have succeeded without the funding of different institutions, to which I would like to express my gratitude:

- the British Council for early travel grants;
- the Deutsche Akademische Austauschdienst (DAAD) for British-German Academic Research Collaboration (ARC) - project funding;
- the Joseph-von-Egle Institut of the Fachhochschule für Technik Stuttgart; and
- the Knödler Stiftung (Club of the Friends of the Fachhochschule für Technik Stuttgart).

While realizing that a complete listing of all people which supported this work is impossible I would gratefully acknowledge the following.

- Herbert Eppel whose experience with thermal simulation programs and UNIX workstations helped me in many ways and for his organisation talent and much more.
- Colin Seale for proofreading the theory of thin films, and all the other members of the ECADAP research group for creating an atmosphere in which it was a pleasure to be a guest.
- the students Thomas Sehorsch and Oliver Küster who considerably contributed to this research during their diploma works, mainly by participating the developement of the computer programs GLSIM and SUNSIM.
- all members of the department of Building-Physics for their help and assistance.

Finally, I want to thank my parents who gave me the opportunity to study and which always stand by me helpfully.

I declare that the content of the submission represents solely my own work. The contents of the work have not been submitted for any other academic or professional award. I acknowledge that the thesis is submitted on the conditions in the Regulations. I declare that the work was carried out as part of the course of study for which I was registered and not previously or subsequently; and I draw attention to any relevant considerations of rights of third parties or of security which might merit a restriction on loan or access.

Peter Pfrommer, April 1995

CONTENTS

LIST OF SYMBOLS

English Letter Symbols

A: surface area, m^2

az: azimuth angle, *deg* or *rad*

c: velocity of light in vacuum, *m/s*

c_η: glazing tilt correction for the equivalent incidence angle of the diffuse radiation, *deg*

cc: cloud cover fraction, -

d: thickness of layer, *m*

di: distance, *m*

dP_V: reduction factor of the ventilation heat losses at any time, -

$\mathcal{E}$: electric field strength, *V/m*

E: radiation energy, *kWh*

E: net electric field strength (only chapter 5), *V/m*

f: view factor, -

fr: fraction of secondary heat flow directed inwards, -

h: height angle above horizon, *deg* or *rad*

h': projected sun height angle, *deg*

H: height above sea level, *km*

isw: illuminated slat width, same unit as used for slat distance (*sd*)

k: absorption index, -

I: radiation intensity, W/m^2

L: radiance, $W/sr\ m^2$

M: layer matrix, -

n: refractive index, -

n': complex refractive index, -

N: interface matrix, -

nr: number of reflections (in a sequence of inter-reflections), -

o: opening angle, *deg*

p: glazing property (transmittance, absorptance, reflectance etc.), -

p: portion of ventilation air from a conservatory to the total ventilation air quantity (only chapter 9), -

Po: specular transmitted radiation portion, -

Q: radiation power, W

r: interface amplitude reflection coefficient, -

R: surface resistance, m^2K/W

R: multi-layer total amplitude reflection coefficient (only chapter 5), -

red: reduction of the temperature difference between inside and outside, -

sd: slat distance, any unit

sh: shaded area, same unit as used for slat distance (*sd*)

si: slat inclination angle (positive upwards; negative downwards), *deg*

sp: absorptance-split, -

sw: slat width, same unit as used for slat distance (*sd*)

t: time variable, *s*

t: interface amplitude transmission coefficient (only chapter 5), -

T: multi-layer total amplitude transmission coefficient, -

T_L: Linke turbidity index (DIN 5034, 1983), -
U: U-value, W/m^2K
v: wind speed, m/s
x,y,z: coordinates, m

Greek Letter Symbols

α: absorptance, -
β: surface heat transfer coefficient, W/m^2K
Δ: attenuation factor, -
ε: angle between zenith and a sky point, *rad*
ζ: height integration angle, *rad* or *deg*
η: inclination angle between surface normal and a vertical plane (e.g. 0° or 0 rad for horizontal surfaces), *deg* or *rad*
θ: angle between direct radiation incidence and surface normal, *deg*
λ: wavelength, m
Λ: thermal resistance, m^2K/W
μ: angle between the sun position and a sky point, *rad*
ξ: integration angle of the sky/ground slices, *rad* or *deg*
ρ: reflectance, -
σ: shining factor, -
τ: transmittance, -
τ_{tot}: total solar energy transmittance, -
φ: emittance or incidence angle of a diffuse radiation portion (in relation to the surface normal vector), *deg* or *rad*
χ: angle between surface azimuth and wind direction, *rad* or *deg*
ψ: angle between direct radiation incidence onto an internal surface and surface normal, *deg*
ω: spatial integration angle, *rad*
ω: angular frequency (only chapter 5), *rad/s*
Ω: profile angle (projected height angle of diffuse radiation portions), *deg*
$\Omega 1$: cutoff angle1, *deg*
$\Omega 2$: cutoff angle2, *deg*

Subscripts

ab: absorbed radiation
at,d: direct transmittance of the Raleigh-atmosphere
at,a: total transmittance of the Raleigh-atmosphere inclusive absorption
c: relating to convection
con: relating to conservatory
d: relating to direct radiation
df: relating to direct-to-diffuse reflected radiation
ds: relating to specular-reflected direct radiation
e: emitted radiation
f: relating to diffuse radiation
f: relating to thin layer (film) (only chapter 5)
ff: relating to diffuse-reflected diffuse radiation
gr: relating to ground

i: inside (medium)
in: into the room
o: outside (medium)
on: onto the outer glazing surface
p: relating to sky or ground point
ref: reflected radiation
s: relating to sun
s: relating to thick layer (substrate) (only chapter 5)
sky: relating to sky
tr: transmitted radiation
w: relating to window surface
z: relating to zenith

Superscripts

a: annual effective (energy averaged)
b: relating to blind
e: effective (energy averaged)
E: electric field
g: relating to glazing
i: inside
I: intensity
o: outside
P: P-polarization
r: relative to normal radiation incidence ($\theta = 0°$)
n: for normal radiation incidence ($\theta = 0°$)
m: monthly effective (energy averaged)
S: S-polarization
T: total (transmittance, absorptance or reflectance of a multi-layered glazing or glazing/blind system)

CHAPTER 1

INTRODUCTION

1.1 BACKGROUND

Within the UK, and elsewhere, there is a growing interest in the Passive Solar Design for dwellings and commercial buildings. The aim is to make greater use of the *renewable* energy source, the sun, to provide space heating energy and (in commercial buildings) lighting energy. Passive solar dwellings often have large equator-facing glazed areas (i.e. south-facing glazing in high northern latitudes[1]) and they may include attached conservatories. Commercial buildings may incorporate large atria. The ratio of the glazed area to the area of the opaque building elements is growing.

Atria and conservatories are increasingly popular in new buildings and as retrofitted additions to older properties. They can provide attractive spaces which may be habitable for a large part of the year, even without heating. They may reduce the cost of heating the building to which they are attached. Aria and conservatories are, however, poorly understood spaces when considered from the perspective of their environmental performance. Their thermal environment is produced by a complex interaction between solar gains, heat losses through the glazing, air flow and thermal storage. Since atria and conservatories are often neither mechanically heated nor mechanically cooled, their time of habitability, the thermal comfort conditions and the time of overheating are very important issues. Issues, which, however, are very difficult to resolve.

One route to an improved understanding of glazed spaces, and to their effective design, is to use Detailed thermal Simulation Models (DSMs). In these programs, the energy transport through the individual building components is calculated on the basis of hourly values for the external climatic conditions and the assumed behaviour of the building occupants. The resulting predictions of the indoor temperature, and the necessary heating or cooling energies arise from the balance of the different energy fluxes. DSMs play a key role in the Passive Solar Design Program (PSP) of the UK Department of Energy (now in the Department of Trade and Industry (DTI)) as, potentially, they provide the most cost-effective way of resolving many of the key issues encountered in the thermal design of buildings.

[1]This thesis is written from the perspective of energy-efficient design at high, northern latitudes, considering the UK and Germany in particular. Therefore, the term south-facing, rather than equator-facing, is used throughout.

In the UK, thermal models such as ESP (Clark and McLean 1988), HTB2 (Lewis and Alexander 1985) and SERI-RES (Palmiter and Wheeling 1983) have been used extensively to study the design of passive solar buildings, conservatories and commercial atria. For example, the program SERI-RES was used in the PSP to study the effect of glazing types, glazing areas, glazing orientations, and conservatories, on the energy demands of passive solar dwellings (Yannis 1994). Also in the PSP the program ESP was used to predict the energy demand of commercial atria (BDP 1991). The program FRED (Penz 1983) was used by Baker (1985) to study the energy demands of dwellings with conservatories, as well as the internal air temperatures, the habitabilities, and the incidences of overheating in the conservatories themselves. In Germany, well-known studies of conservatories have also been based on DSM simulations (Hauser 1984, 1986).

1.2 MODELLING ASPECTS OF HIGHLY GLAZED SPACES

In highly glazed spaces the internal environmental conditions depend mainly on the energy transport through the window, while all the other energy fluxes (fabric heat losses through opaque walls and ground, internal small power heat gains etc.) loose importance. The energy transport through windows can be divided into two main mechanisms:

(i) the heat transport through the window; and
(ii) the transmittance of solar radiation energy through the glazing.

Taken together, these two mechanisms will be termed the "glazing model" in this thesis, however, DSMs may use quite different models for each of the components.

1.2.1 Heat transport through glazing

The heat transport through the window includes the following aspects: the longwave (infrared) radiation exchange either externally (to the sky and to the surroundings) or internally to the room surfaces; the convective energy transport from the room air to the internal window surface and from the external window surface to the outside air; and the conductance through the window itself (Fig. 1.1).

The heat-transport through the window consists of one portion, which is transport through the frame, and another portion which is transport through the glazing. Since, especially for large glazing areas, the heat transport through the glazing dominates, in this work, the problem of modelling windows was reduced to that of modelling glazing. (Since frames can be produced with thermal resistances, which are similar to those of the glazings, frames are usually not explicitly modelled by thermal simulation programs).

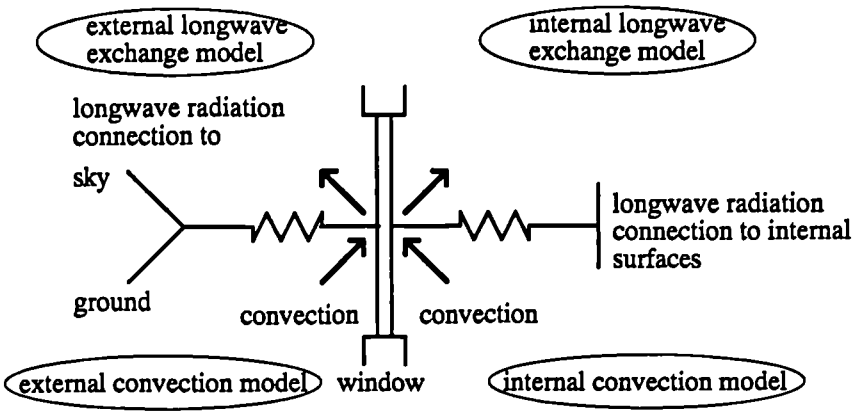

Figure 1.1: Heat transport through glazing.

The heat conduction through glazings depends mainly on the thermal resistance of the air cavity between the glass panes (for multi-layered glazings); the thermal resistance of the glass panes is unimportant. Conduction is modelled in a similar way by most DSMs but they may adopt quite different algorithms, and sub-models, for the internal and external radiant and convective exchanges. In this thesis, the sum of all the different heat transport algorithms will be termed the "thermal model of glazing".

1.2.2 Solar radiation energy transport through glazing

The solar radiation gains to a room through a glazing, depend on: the external solar radiation; the transfer of the incident radiation through the glazing; and the distribution of the transmitted shortwave radiation to internal surfaces (Fig 1.2).

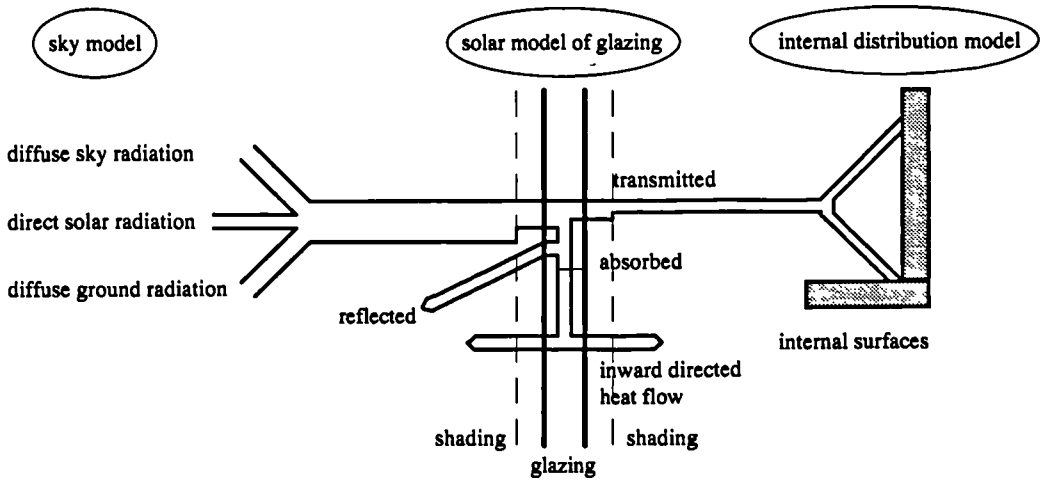

Figure 1.2: Solar radiation transfer through glazing.

Solar radiation has direct (beam) and diffuse components. The direct radiation intensity onto the glazing is determined: by the position of the sun in the sky (sun height and azimuth); by the position of the glazing (orientation and tilt); and by conditions of the atmosphere (turbidity; clouds etc.). The diffuse radiation onto a tilted surface consists of portions from the sky, ground and surroundings. Each radiation portion has different incidence an-

gles and intensities. These are influenced by any shading due to either external objects or the building itself, e.g. side-fines, overhangs, window reveals, external blinds. In this thesis, the combination of all the algorithms which influence the solar radiation incident on the glazing will be termed the "sky model".

The transfer of radiation through the glass involves the transmittance, absorptance and reflectance of the radiation. The magnitude of these components is determined by the thicknesses and optical properties of the glass panes. Traditionally, clear (float) glass is used in buildings, however, the use of coated and tinted glass is growing - in this thesis, these are termed "special glazings". The portion of transmitted radiation entering the internal space is also affected by curtains, blinds or other internal shading devices. The absorbed radiation energy in the glass panes is transformed into heat and transported to the room and to the outside by longwave radiation and convection; this is often termed "secondary heat flow". The solar transfer and the heat transfer issues therefore interact. In this thesis, these algorithms, which together describe the solar energy transmission, will be termed "solar model of glazing".

Finally, the thermal reaction of a room to solar energy gains depends on the absolute amount of radiation energy entering the room and on the interactions of the solar radiation with the internal wall surfaces and furnishing. These interactions influence the way the solar energy is distributed around internal surfaces (sun patching), absorbed at surfaces, transmitted straight back to the outside (re-transmission), reflected onto other internal surfaces or back to the outside (backloss) or transmitted through internal glazings into adjacent spaces (interzonal radiation transfer) (Fig. 1.3). In this thesis these processes together are termed the "internal solar distribution model". In a modestly glazed room radiation backloss is small, interzonal radiation transfer happens rarely, solar distribution can be easily determined, and finally the overall solar energy gains are limited. In highly glazed spaces these processes may be important.

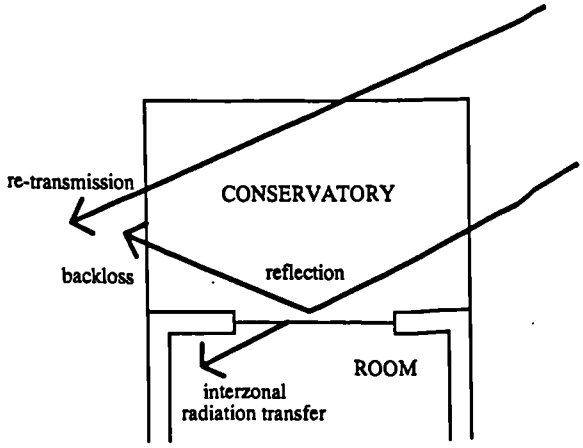

Figure 1.3:

Plan view of a conservatory with attached room to illustrate radiation re-transmission, backloss and interzonal radiation transfer.

1.2.3 Other important aspects

In highly glazed spaces other thermal aspects gain importance.

- The high solar gains in conservatories and atria often precipitates the need for an intensive ventilation (with outside air) to reduce overheating. Therefore, aspects of air flow (natural and mechanical ventilation) become important.
- The solar pre-heated air in conservatories (or atria) can be used to ventilate the parent building, which is called "Solar Pre-heating of Ventilation air" (SPV). This topic includes aspects of air flow through ducts, openings and cracks, distribution of ventilation air in the building, forced and free convection etc.
- The high solar gains, and low insulation levels, often lead to big temperature variations in free-floating (unheated) highly glazed spaces. Furthermore marked temperature stratification is frequently encountered in tall (atrium) spaces.

With regard to thermal simulations, all these aspects can be attributed to the modelling problem of air flow and ventilation within one space or between spaces (interzonal airflow).

1.3 REVIEW OF PREVIOUS WORK

To appreciate why the research presented in this thesis was felt to be necessary, it is important to briefly review previous relevant work.

It has been shown (Bland 1992 and Martin et al. 1994) that DSMs usually calculate conduction through solid building elements very accurately. However there is an awareness that the theoretical basis of even the most sophisticated codes may not be adequate for spaces with large glazing areas. To illustrate this problem, consider the study in which expert users of ESP, HTB2 and SERI-RES were requested to predict the annual energy demands of a direct gain passive solar house, the Linford house (Everett et al. 1985). Wildly differing predictions were obtained for the absolute annual auxiliary energy demand and, even more significantly, the trends in energy demand as the window area and type were varied (Fig. 1.4). The poor results for the Linford house were attributed to a poor building specification and errors in interpretation of the specification. They may also be due to the inherent differences in the algorithms used by the programs (see Lomas 1992).

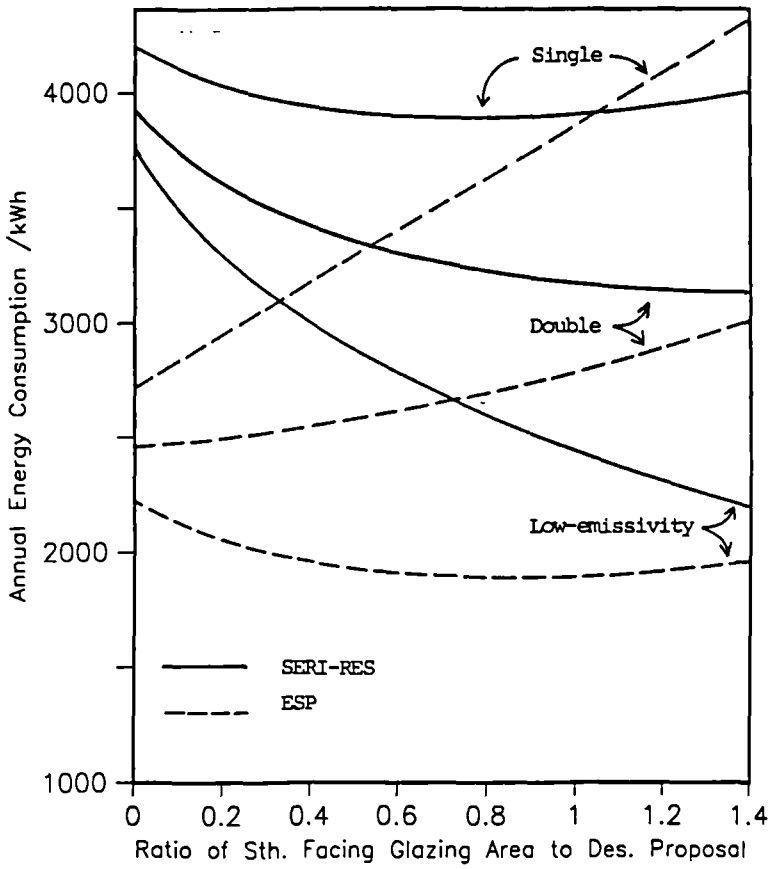

Fig. 1.4:

Comparison of annual auxiliary heating energy demand predictions made by ESP and SERI-RES for the Linford passive solar house (after Lomas et al. 1991).

Because of these results the UK DTI initiated Applicability Study 1, a seven man year initiative aimed at enhancing the usability and credibility of DSMs for the design of passive solar dwellings. The work concentrated on inter-model comparisons with the programs ESP, HTB2 and SERI-RES. This work was led by De Montfort University in Leicester and confirmed that the approximate methods used to model some aspects of windows and glazings can severely compromise the accuracy of the program predictions (Lomas et al. 1989, 1991). For example, the three programs produced large variations in daily energy demand predictions for typical domestic scale buildings as the glazing area (Fig. 1.5) and glazing type of the building was varied. In some cases (as demonstrated in Fig. 1.5) the optimal design solution depended on the DSM used for the analysis. Results such as this seriously undermine the credibility of DSMs for the analysis of highly glazed spaces. Since the investigated DSMs (SERI-RES; ESP and HTB2) differed highly in their approach to modelling the thermal conductance through glazing (thermal model of glazing), the inter-program variations were first attributed to this issue (Lomas et al. 1991).

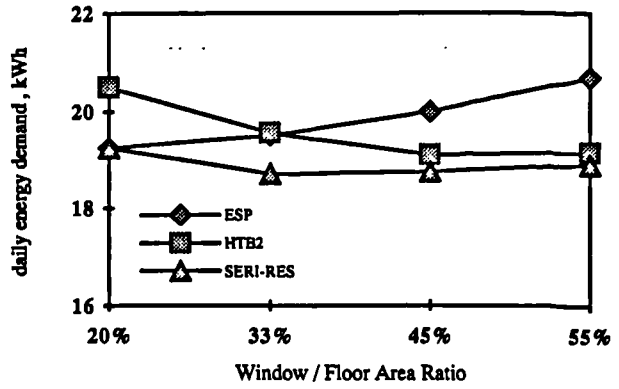

Figure 1.5:

Predicted influence of window area on the energy demand of a domestic living-room (with one, single-glazed, south-facing window) on a sunny winter's day.

A similar conclusion was drawn as a result of inter-program comparisons done as part of the IEA Annex XII work (Frank and Püntener 1987). The work was aimed to identify the problem areas responsible for large differences in heating and cooling loads predicted by DSMs and compare the calculation procedures connected with windows. The chosen strategy was to perform a detailed code-to-code comparison (inter-model comparison) based on a given standard test room subjected to Geneva climate conditions. The room was very sensitive to the energy transport through the window. The calculations included simplified checks using steady-state boundary conditions, 10-days simulations, and predictions of the seasonal heating demand. The deviations in the predictions of seasonal heating demand and the hourly peak loads and zone temperatures were mainly attributed to differences in the approach to treating heat transfer between window surfaces and room air (thermal model of glazing). Other factors were also indicated to have a significant influence on the results (such as the internal distribution of solar gains, see Frank and Püntener 1987).

Within International Energy Agency (IEA) Task VIII, passive and hybrid solar low energy buildings, a validation study was undertaken which included the most prominent simulation programs of the day. The study comprised of three empirical validation test cases: Direct Gain, Trombe Wall and Attached Sunspace, followed by code-to-code comparisons on yearly data sets. These results are documented in a work report edited by Mørck 1986. In addition, inter-program comparisons studied the annual heating and cooling energy demand predictions for a test room with attached sunspace subjected to Copenhagen and Denver climate conditions (see also Judkoff 1988).

As a result of these studies, the major source of error and disagreement among the programs used to model passive and hybrid low energy buildings was attributed to differences in the algorithms related to the handling, distribution and storage of solar energy (see Mørck 1986 and Judkoff 1988). This would include algorithms of incident and transmitted solar radiation, modelling of radiative and convective surface coefficients, natural convection heat transfer and stratification (see section 1.2). Judkoff (1988) concluded, that the presence of strong solar forcing functions in the building exacerbated the inaccuracies caused by the above algorithms and subroutines.

Unfortunately, since the DSM predictions were influenced by many different algorithms, none of the above studies could determine the particular sensitivity of the results to specific algorithms.

1.4 THE PROJECT "THERMAL MODELLING OF HIGHLY GLAZED SPACES"

The foregoing studies indicated, that design guidelines on aspects of glazing area and glazing type derived from DSM predictions, as given in many passive solar design studies, must be treated with caution. The studies suggest that, at least for some circumstances, programs give divergent results because of their glazing models. Since domestic conservatories and commercial atria (as well as glazed halls, greenhouses etc.) are particularly sensitive to the energy transport through glazing, the credibility of the design statements is even more questionable. This was the starting point of the project "Thermal Modelling of Highly Glazed Spaces" described in this thesis.

The project was an international research programme between the De Montfort University (DMU) Leicester (UK) and the Fachhochschule für Technik Stuttgart (Germany). The Environmental Computer Aided Design and Performance (ECADAP) research group in Leicester has extensive experiences in the area of detailed simulation programs and program validation. The department of Building-Physics in Stuttgart concentrates on the theoretical investigation of physical phenomenon in buildings and its practical consequences in modern building design. Hence the collaborative research work offered the advantage of combining: theoretical aspects; their realisation in thermal simulation programs; validation of new assumptions; and their application to building design.

The aims of this project were:

- to illustrate the weakness of existing models for calculating the heating energy demand of houses with attached, or incorporated, highly glazed spaces;
- to improve the credibility of simulations of highly glazed spaces;
- to explore the internal temperatures in-, and energy demands of-, highly glazed spaces.

In this thesis, different DSMs are reviewed and/or used for thermal simulations. It was agreed to concentrate on the programs ESP, HTB2 and SERI-RES to maintain continuity with previous studies at De Montfort University Leicester (see section 1.3). In some cases, the performance of the programs TRNSYS (Klein et al. 1988) and ZB-SIMULAP (Zimmermann and Becker 1992) were also considered. These programs were available at the Fachhochschule für Technik in Stuttgart and had been used in many previous research projects (see for example Spitzner 1991).

To achieve the aims of the project a programme of work with six phases was devised. The purpose of each phase was as follows:

(i) to review the theoretical basis of the glazing, shading and solar distribution algorithms used within DSMs. This included parametric studies with the currently available DSMs to investigate the variability in their predictions of the environment in highly glazed spaces. Inter-model comparisons would be used to understand the differences and the impact of the different physical approaches in the algorithms.

(ii) to identify the specific areas of weakness in the DSMs, e.g. solar gains, solar shading, internal solar radiation distribution, stratification, convection etc. The consequences of the algorithmic approximations for energy demand and temperature predictions were to be determined.

(iii) to investigate alternative theoretical approaches to improving the programs. This task was to include the development of new appropriate algorithms and programming work. Ideally, it would lead to standalone program modules, which could be used in connection with more than one DSM. Alternatively it may require the improvement of a DSM in order to incorporate the new algorithms.

(iv) to investigate the impact of the newly developed algorithms using sensitivity studies and realistic buildings. This was intended to lead to guidance about when a more accurate treatment of a phenomenon is necessary, or how big the error potential will be when a simplified approach is used. The effect of the new algorithms could also be judged by rerunning some of the simulations undertaken in activity (i).

(v) to validate the improved programs by comparing their predictions with measured values, and/or analytical tests.

(vi) to use the improved program to predict the energy saving potential of domestic conservatories and atria.

The investigations into the modelling capabilities of DSMs (phase i) are presented in Chapter 2 of this thesis. As a result of these investigations, the specific areas of weakness of DSMs (phase ii) are indicated. Chapter 3 discusses the key aspects for further investigations and model implementations. It also deals with general aspects for the development and testing of new algorithms (phase iii). The various aspects of developing improved calculation models were divided into five main problem areas, these are discussed in Chapters 4 to 8. Each of these Chapters summarises: the theory of the newly developed algorithms and computer models; their testing; and their validation (phases iv and v). Finally, Chapter 9 deals with the application of the improved modelling methods to the study of conservatory designs (phase vi). Rather than listing the conclusions of each piece of work at the end of

the relevant Chapter, all the conclusions are presented together in Chapter 10. This Chapter also outlines suggestions for further work.

Each phase, and the intermediate results, have been described in 14 "Interim Reports". These reports are not fully polished public domain documents, but they may be interesting for some readers, since they contain additional, more detailed, information which could not be fully presented within this thesis. A list of these reports is given in the Bibliography; they are refered to in the main text as follows, IR1, IR2 etc. The reports can be requested from ECADAP research group at DMU or from the department of Building-Physics in the Fachhochschule für Technik Stuttgart. (For contact names and addresses see the Bibliography).

CHAPTER 2

WEAKNESSES IN THERMAL MODELLING OF HIGHLY GLAZED SPACES

2.1 INTRODUCTION

Previous studies (see section 1.3) suggest that, at least for some circumstances, DSMs give divergent results because of the models used to simulate aspects of glazing and solar radiation. However, the particular sensitivity of the DSM predictions to specific algorithms; and the accuracy of these algorithms was not determined. This Chapter seeks to identify the main areas of weakness; two methods were used:

- inter-model comparisons using the currently available DSMs to investigate the variability in their predictions of the environment in highly glazed spaces; and
- a theoretical review of algorithms used within DSMs.

Inter-model comparisons were used to understand the differences in the algorithms currently employed in DSMs and to illustrate the consequences of using simplified methods rather than more detailed approaches. The comparison of the program predictions quantified the sensitivity of algorithms to the special environment in highly glazed spaces. Clearly, these investigations were restricted to the algorithms currently employed in DSMs.

The aim of the theoretical review was to establish the mathematical differences in the algorithms used by different DSMs and the significance of these differences. This also highlighted the limitations of some algorithms and the implications for their use in particular applications. Although the theoretical review was useful to establish modelling weaknesses, the thermal consequences of the assumptions could not be quantified. This was done later, when more rigorous algorithms were available (Chapters 4 to 8).

The review concentrated on the programs ESP (Clark and McLean 1988), HTB2 (Lewis and Alexander 1985) and SERI-RES (Palmiter and Wheeling. 1983), however approaches used by the programs TRNSYS (Klein et al. 1988) and ZB-SIMULAP (Zimmermann and Becker 1992) were also considered.

The programs can be characterised as follows:

(i) ESP (Environmental Systems Performance) was developed at the University of Strathclyde in Glasgow (UK). It is a transient energy simulation system which is capable of modelling the energy and fluid flows within combined building and plant systems. The program is comprised of several interrelating program modules ad-

dressing input management, simulation, results output, database management and several simulation support functions.

The program requires the input of the exact building geometry. Because of this, it is able to consider geometrical factors when calculating the view factors, the internal long-wave radiation exchange, the external shading etc. ESP adopts a mixed, equally-weighted, implicit and explicit Finite Difference approach (i.e. the Crank-Nicholson method) to solving the partial differential equations which are required to predict the energy flow through walls, floors and roofs. Unfortunately, because of its complexity, the internal operation of the program is difficult to trace.

(ii) HTB2 is a computer program designed for simulating the thermal performance of energy efficient occupied buildings. It was developed at the Welsh School of Architecture, UWIST, in Cardiff (UK) and has been intended primarily as an investigative research tool rather than a simple design tool. In order to achieve this, HTB2 has been written in a modular format in which each sub-system has been isolated and localised in specific subroutines.

Compared to ESP, HTB2 is less rigorous in the calculation detail (e.g. it is non-geometric and has an explicit calculation method based on small time-steps). However, since the programming has been made as explicit as possible, its internal operation can be easily understood (see also Chapter 3, section 3.2).

(iii) SERI-RES is a non-geometric dynamic simulation program, which simulates a building's thermal and energy performance, based on a backward finite difference approach. It was developed at the Solar Energy Research Institute (SERI) in Golden, Colorado (USA) and incorporates several additional features for calculating passive solar systems (e.g. Trombe Wall simulations, external shading etc.).

Compared to ESP and HTB2, the input requirements of SERI-RES are less extensive and the program operates much faster, however, the internal algorithms are also less detailed (e.g SERI-RES does not model internal long-wave radiation exchange, uses constant internal and external surface coefficients, and treates glazings with a simple U-value model).

(iv) TRNSYS (Transient System Simulation Program) is a library of program modules to calculate transient technical systems, mainly active and passive solar systems and buildings. TRNSYS was developed at the Solar Energy Laboratory in Madison, Wisconsin (USA) sponsored by the American government. Although the program was originally not aimed for building simulations (the building module TYPE 56 was added later), the program is increasingly used to this end. The level of detail of the building module can be best compared with that of SERI-RES.

(v) ZB-SIMULAP is a transient program to simulate heating and cooling plant systems in multi-zone commercial buildings. It is the advancement of one of the first dynamic simulation programs (developed in the early 1970s) and is based on a calculation model, which represents the thermal behaviour of walls using electric circuit theory (see Rouvel 1972). Since it is not intended for modelling passive solar systems in detail, it uses simplified calculation methods for solar gains.

All these DSMs represent different calculation methods and algorithms which should illustrate the diversity of approaches used by the current generation of DSMs. The complexity of the programs decreases from (i) to (v). While programs (i) - (iii) normally require the computer power of an UNIX Workstation, the latter two programs easily run on a PC. (All the programs are written in Fortran77.)

For each program, the algorithmic approaches could be determined by investigating the source code, by comparing the input possibilities, and by a detailed review of previous investigations into the modelling techniques (Allen and Whittle 1988; Bland et al. 1988; Parand and Lomas 1988 and 1989; Pinney 1990).

The inter-program comparisons and the theoretical review concentrated on:

(i) thermal models of glazing (section 2.2 and 2.3);
(ii) internal solar radiation distribution (section 2.3);
(iii) solar models of glazing (section 2.4); and
(iv) air-flow and temperature stratification (section 2.5).

These are the most important modelling aspects for (passive, low-energy) buildings with strong solar exposure (see section 1.2). The results of the review are summarised in section 2.6.

2.2 COMPARISON OF THERMAL MODELS OF GLAZING FOR DIRECT-GAIN SPACES

2.2.1 Introduction

Although the thermal modelling of glazings is one of the most important aspects of detailed thermal simulations programs there are still great differences in the level of detail and accuracy of these models. In general, there are two different approaches.

(i) The glazing is represented by a single thermal resistance between the zone air and the external environment (U-value model). The detailed effects of thermal storage in the glass, absorption in the glass (the inwards directed secondary heat flow is calculated using total solar energy transmittance values), and longwave (infrared) radiation ex-

change either to the sky or to the room surfaces, are neglected. For example, this approach is used by SERI-RES, TRNSYS and ZB-SIMULAP.

(ii) The glazing is treated as a transparent multi-layered construction (TMC) in which each layer of glass has thermal properties just like any other opaque material (TMC model). Thus, in the TMC approach, the effects of thermal storage, absorption and longwave radiation exchange are considered in detail. For example, this approach is used by ESP and HTB2. It should be noted, that the TMC models used by ESP and HTB2 differ in their treatment of internal and external convection coefficients, as well as in their calculation of the longwave radiation exchange.

Both ESP and HTB2 consider the thermal resistance of the air-gap as a constant fixed value. The resistance actually depends on the longwave (infrared) radiation exchange, convection, and conduction in the air cavity; these are highly dependent on the boundary conditions (surface temperatures) (Erhorn 1983). A similar problem occurs for glazing systems with internal blinds, where the heat transport through the system depends highly on the convective and radiative conditions in the cavity between the glass pane and the blind.

The studies outlined in Chapter 1 (section 1.3) compared numerous DSM predictions. Whilst the researchers felt that the key algorithms influencing the performance of DSMs were those describing the thermal conductance through glazings, the detailed effects of different thermal models of glazing were not studied. Therefore, as a first step, an investigation was conducted to determine the sensitivity of the predicted heating energy demands of domestic-scale buildings to the algorithmic differences in the thermal models of glazing. Inter-model comparisons were used to study the impact of the different approaches in the algorithms more closely.

The investigation concentrated on the program ESP, since it provides the possibility of modelling windows in different levels of detail. By using one program, which offers different thermal models of the glazing, there is the big advantage that all the other algorithms remain unchanged. Therefore, variations in the results can be entirely attributed to the thermal glazing algorithms.

2.2.2 Alternative algorithms

Three methods of modelling the heat transport through windows were studied.

(i) A simple, fixed, user-specified, U-value (U_f). The fixed values chosen imply the standard Chartered Institution of Building Services Engineers (CIBSE) values for the inside and outside combined surface coefficients, which are for vertical glazing 8.3 W/m²K and 16.7 W/m²K respectively (see also DIN 67507, 1980). (This represents the approach in SERI-RES, TRNSYS and ZB-SIMULAP.)

(ii) A time varying U-value (U_V), in which the standard (CIBSE) external convection coefficient is subtracted from the user specified U-value and replaced by an internally calculated coefficient based on wind speed and direction. The external convection coefficient β_c is calculated by ESP as follows:

(2.1) leeward surface: $\beta_c = 2.8 + 0.75 * v * \sin|\chi|$

(2.2) windward surface, $\beta < 10°$ $\beta_c = 2.8 + 0.75 * v$

(2.3) windward surface, $\beta > 10°$ $\beta_c = 2.8 + 3.0 * v * \sin|\chi|$

where, v is the wind speed and χ the angle between surface azimuth and wind direction. Thus, for wind speeds between 0 and 10 m/s, β_c varies between 2.8 W/m²K and 32.8 W/m²K. (This approach is unique to ESP.)

(iii) A rigorous transparent multi-layer construction (TMC) approach, in which each layer of glass has thermal properties just like any other opaque material. The external and internal surface coefficients are determined by ESP at each time-step. (This approach is also used in HTB2.)

2.2.3 The building description

The different thermal models of glazing were compared for the simple hypothetical direct gain test room (Appendix A.1) used in previous work at DMU (Lomas et al. 1989) (Fig. 2.1). The room represents a typical UK domestic scale living-space, however, it may also represent an office room in a commercial building. It was south orientated, with two walls (south and west) treated as external. The room was continuously heated to 18°C. (The low temperature set-point was chosen as being appropriate for passive solar buildings, where lower set-points lead to lower energy demands.) The room was assumed to be well sealed with a low air-change rate of 0.35. To exaggerate any effect that the glazing algorithms may have on the inside climate of the room, occupancy, lighting and small power heat gains were neglected.

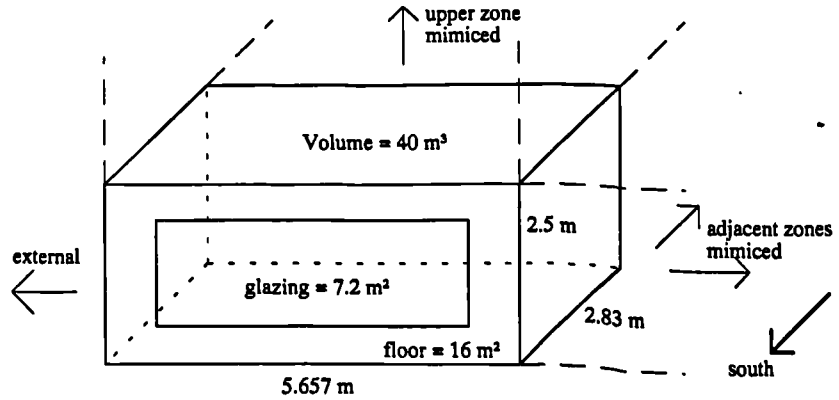

Figure 2.1:

One-zone module of a typical UK domestic scale living-room.

The room was located at Kew near London (UK): latitude = 51.5° North; longitude = 0°. It was unobstructed with respect to the wind and sun (no shading from other buildings was considered).

In this study two constructions, representing the extremes in terms of insulation levels, were studied. One was a traditional heavyweight construction with an average U-value of 1.4 W/m²K and the other was an advanced well-insulated (heavyweight) construction with an average U-value of 0.3 W/m²K. For both constructions, the energy demand was studied for four different window areas (20%; 33%; 45%; and 55% of the floor area). In connection with each of these, three different window types (single glazing; double glazing; low-emittance glazing) were used.

Both annual and daily simulations were undertaken. For the daily simulations, two UK design days generated by Loxsom (1985) were used: a cloudy winter's day; and a sunny winter's day (Appendix B). All combinations of construction, window type and window area were examined. The annual energy demand was studied for different window types only (the window area was 45% of the floor area or 7.2 m²). Weather data of Kew in London was used.

2.2.4 Predicted differences between the two U-value models

A comparison of the results predicted by the two U-value models (U_f and U_v) indicated that the energy loss of a room can be very sensitive to the external surface convection coefficient. The predicted differences were greatest for a single glazed, highly insulated room (with a high portion of window area), but the differences decreased as the insulation properties of the glass increased. For example, the fixed U-value model (U_f) predicted higher annual energy demands than the variable U_v model. The differences were 35% for a single glazed room (45% window to floor area ratio), but decreased to less than 8%, for low-emittance glazing (Fig. 2.2). In contrast, for the daily simulations, the fixed U-value model (U_f) produced lower values for energy demand irrespective of the glazing area, glazing type, construction mode and design day (e.g. see Fig. 2.3).

The apparent contradiction between the daily and annual results occurred because the external convection coefficient (used by U_v) depends on the wind speed and on the angular difference between surface azimuth and wind direction (equations 2.1 to 2.3).

Early in the study it became clear that the external convection coefficient algorithm in ESP had curious properties. In particular, there was a step-wise change in the coefficient. In a small side study, the change in daily energy demand of a single glazed, well-insulated room on a sunny winter's day was calculated as the wind direction was changed from 270° to 271°. For that building, a swing in the wind direction from exactly parallel to the glazing to just 1° off parallel halved the energy demand! Physically this scenario seems doubtful and,

unfortunately, because the wind direction had been arbitrarily set to 270° in the daily weather files the U_v model was using a windward coefficient which produced very large heat losses (for the daily simulations).

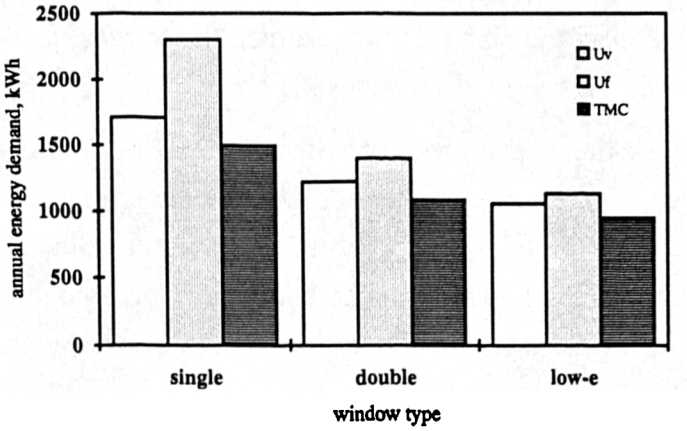

Figure 2.2

Influence of the thermal models of glazing on annual energy demand as the window type is varied (advanced well-insulated building; 45% window area to floor area ratio).

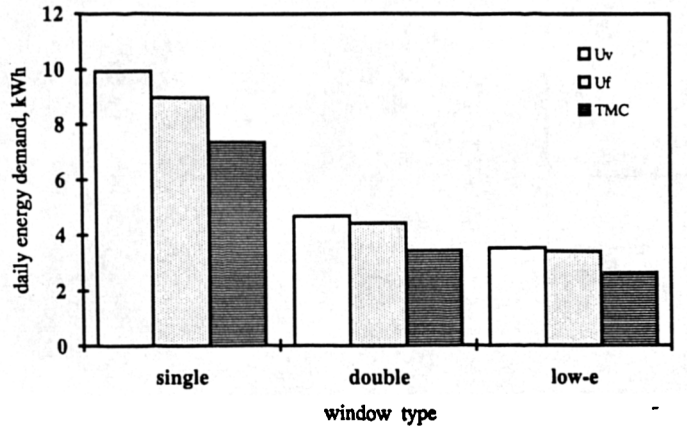

Figure 2.3

Influence of the thermal models of glazing on the daily energy demand on a sunny winter's day as the window type is varied (advanced well-insulated building; 45% window area to floor area ratio).

2.2.5 Predicted differences between the U-value and TMC models

The forgoing considerations indicate, that for daily comparisons between U-value and TMC models, the variable (U_v) model is more suitable (since both models consider the same variable external surface coefficient). For annual simulations, where the wind direction changes numerous times, results for all three algorithms can be compared.

For all buildings, irrespective of the glazing area, glazing type, construction mode and design day, the U_v specifications always predicted a higher daily energy demand than the TMC specification (e.g. see Fig. 2.3). For a sunny winter's day and a traditional construction, the difference was up to 23% for a single-glazed room with a large area of glass but it decreased with the window area and the insulation properties of the glass to as little as 2% for a modestly glazed room (20% of the floor area) with low-emittance glazing.

The TMC specification generated significantly lower values than either U-value model for the absolute annual energy demand (Fig. 2.2). Again, the difference was greatest for poorly

insulated single glazing (800 kWh; 41%) less for double glazing (300 kWh; 25%) and least for low-emittance glazing (200 kWh; 15%). These differences were obtained for the well-insulated room. The traditional construction led to similar absolute differences but to lower relative differences (since the absolute energy demand predictions were higher). Clearly, irrespective of whether daily or annual energy demand is being studied the thermal model of glazing can have a significant impact on the energy demand results obtained.

In general, the trends in daily energy demand, as the window area changed, were not influenced by the thermal models of glazing. One notable exception was for the traditional, single glazed building at a sunny winter's day. Here, the U_V (and U_f) specification indicated an increase in the daily energy demand whereas the TMC specification indicated a continuous decrease (Fig. 2.4). Thus, in this case, the selection of an optimum design is affected by the chosen thermal model of glazing.

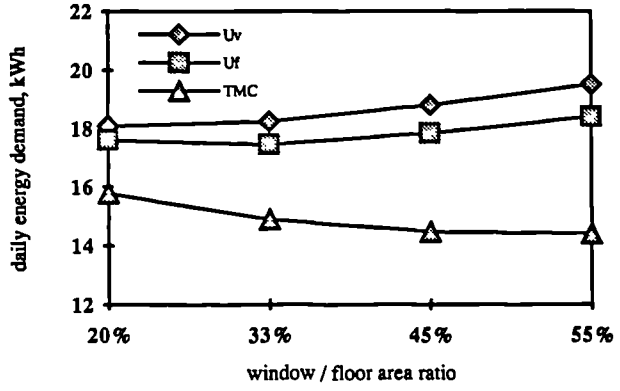

Figure 2.4

Variation of the daily energy demand as the window area is varied (traditional low-insulated, single glazed room on a sunny winter's day).

Although the thermal models of glazing did not influence the actual trends in daily and annual energy demand as the window type was changed, they did have a marked impact on the energy saving predictions. For example, the predicted annual energy savings due to replacing single glazing with double glazing varied from 39% for a fixed (U_f) value specification to 26% for a TMC specification (compare Fig. 2.2). For changes from double glazing to low-emittance glazing the savings were 21% and 14% for the U_f and TMC specifications respectively.

The observed differences can be fully explained by considering the fundamental differences between the TMC and the U-value models and the likely thermo-physical effects which these will have (see IR 1). The differences are mainly caused by the approximate treatment of the internal longwave radiation transfer in the U-value models. These use a combined surface coefficient which does not take account on the actual temperature differences between the internal surfaces and the glazing. It is these temperature differences which control the radiative energy transport to the window. Instead, in the U-value models, the heat loss is driven by the temperature difference between the zone air node and the glazing. The TMC model treats the convective and radiative components separately and calculates the radiative

heat flow by considering the actual temperature differences between the internal surfaces and the glazing.

The impact of the internal convective heat transfer coefficient could not be tested, since it was only explicitly modelled by one specification (TMC). However, the high impact of the external surface convection coefficient (see above), which has a comparable thermal effect on the heat transfer through windows, suggest that the internal coefficients will also have a big impact.

2.2.6 Discussion

The variabilities in energy demand and energy saving predictions due to varying window type or window area, which were indicated by previous inter-program comparisons, were confirmed and explained by the different thermal models of glazing. This study casts significant doubt on the credibility of a simple U-value model for glazings, even for typically glazed domestic scale rooms. The error potential increased with the glazing area, which indicates that highly glazed spaces will be particularly sensitive to the thermal models of glazing.

Since this study explained many of the inter-program variations, which were obtained during the Applicability Study 1 work at DMU, the results of this study were considered within the executive summary of Applicability Study 1 (Lomas 1992).

2.3 COMPARISON OF THERMAL MODELS OF GLAZING AND INTERNAL SOLAR DISTRIBUTION MODELS FOR HIGHLY GLAZED SPACES

2.3.1 Introduction

The previous study (section 2.2) examined different thermal models of glazing in connection with a simply glazed test room. The glazing areas corresponded to those used for typically glazed domestic scale rooms. Since the study indicated that the influence of the models was highly dependent on the area of the glazing, it was felt to be important to study the thermal models in connection with highly glazed spaces, for example with conservatories.

However, the thermal behaviour of a highly glazed space depends not only on the heat transport through the window, but also on the amount of transmitted solar radiation and its internal distribution (see section 1.2). The programs studied (ESP, SERI-RES, HTB2, TRNSYS) used similar approaches for the radiation transfer through the glazing (at least for clear vertical glazing without shading devices). However the programs had different input requirements, and used different models, for the internal solar distribution. Therefore, this second study concentrated mainly on the issues of thermal models of glazing and internal solar distribution models.

Many of the current DSMs require the user to input the relative amounts of sun absorbed by the various interior surfaces of a direct-gain room (e.g. ESP, HTB2, SERI-RES). However, little information is available in the literature to help program users to determine them. Normally, the user has to make (more or less accurate) assumptions. In the case of highly glazed spaces (e.g. conservatories), in which the internal solar radiation split depends highly on the time-of-day, day-of-year, and geographical location, the definition of appropriate values is difficult. The internal distribution of the diffuse radiation, the distribution of radiation reflected from internal surfaces, the radiation backloss, the re-transmission and interzonal radiation transfer etc., are usually calculated implicitly by the DSM. However, the calculation models are normally simplified approximations. To illustrate these points, it is useful to consider the solar distribution models used by the programs ESP, HTB2 and SERI-RES (see also Parand and Lomas 1988). Their models illustrate the diversity of approaches used by the current generation of DSMs.

- In ESP the user can specify three different surfaces to receive direct radiation (through all windows). Using the program module ESP-INS a time dependent variation of three surfaces is possible to account for a moving sunpatch. ESP then apportions the transmitted radiation to those surfaces according to their area weighting. It also calculates the internal distribution of the diffuse radiation, the reflected direct radiation, the interzonal radiation transfer and radiation backloss. Radiation re-transmission to the outside is not considered.
- In HTB2 the user can appoint an unlimited number of surfaces to receive direct radiation and the proportion of the incoming radiation received by each one. The selection must be made for every window and it can be time-scheduled. HTB2 calculates the amount of radiation reflected from the defined internal surfaces, adds this reflected radiation to the incomming diffuse radiation, and then distributes the total using area-weighting around all the internal surfaces. Radiation re-transmission and backloss are not considered. Interzonal radiation transfer can be approximately modelled by assigning direct radiation to internal surfaces in an adjacent zone.
- SERI-RES does not distinguish between direct and diffuse radiation once it enters the zone. The distribution of direct, diffuse and reflected radiation can be specified by the user or calculated internally using an area weighting algorithm. It is not possible to schedule the fraction absorbed by each surface as a function of time, so it is not possible to account for a moving sunpatch.

The foregoing considerations led to the decision to investigate the effect of internal solar distribution in highly glazed spaces in more detail. Since it had already been decided to investigate the effect of thermal models of glazing, the study considered both issues.

2.3.2 The building description

A typical UK domestic scale living-room (of the type used in the previous study, section 2.2) and an attached single glazed conservatory with a typical shape was chosen for the study (Fig. 2.5). To meet the requirements for a passive solar design and to enhance the sensitivity of the heating demands to solar energy gains, the living-room had an advanced highly-insulated and heavy-weight construction (average U-value = 0.3 W/m²K), continuous heating (to a heating set-point of 21°C) and a low infiltration rate (of 0.35 ach).

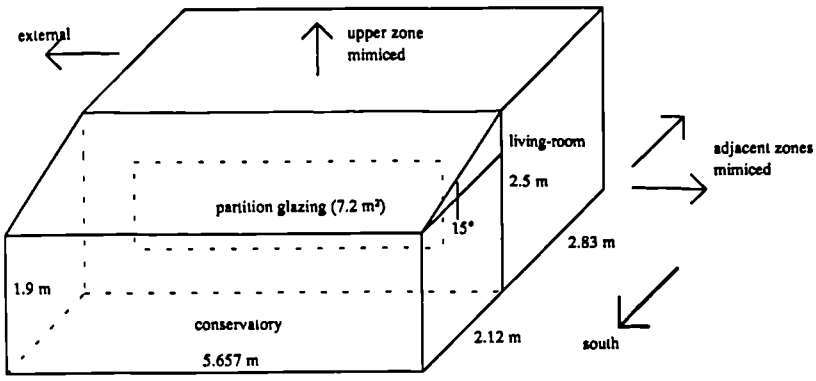

Figure 2.5:

Two-zone module of a typical UK domestic scale living-room and attached conservatory.

The basic conservatory had a rectangular shape (12 m² floor area), and was unheated and not ventilated. It was connected to the living-room by a partition wall with a double glazed window which was half the size of the partition area. There was no interzonal air-flow and the whole building structure was south orientated. For more detailed description see Appendix A.2.

By changing the building design systematically the different reactions of the programs could be examined. The following parameters were varied:

(i) the partition window area (none - 0 m², half - 7 m², fully glazed -14 m²);
(ii) the conservatory glazing type (single, double, low-emittance);
(iii) the partition window glazing type (single, double);
(iv) the conservatory floor area (0 m² - no cons., 6 m², 12 m², 18 m²);
(v) the air-flow between the two zones (0 m³/h, 14 m³/h, 80 m³/h, 200 m³/h); and
(vi) the orientation (south, east, west).

All the variations were studied for three different UK (Kew, London) weather conditions: a cloudy winter's day, a sunny winter's day, and a sunny summer's day (Appendix B). The study concentrated on the influence of the design variations on the heating energy demand of the living-room, and on the peak air temperatures in the conservatory (see IR2).

2.3.3 Alternative algorithms

The programs ESP and HTB2 were used for the study and the following alternative thermal models of the glazings were examined.

(i) The variable U-value approach of ESP (U_v); and

(ii) the rigorous transparent multi-layer construction (TMC) approach of ESP and HTB2.

These have been fully explained in section 2.2.

Two possible internal shortwave radiation distribution models were studied in association with the thermal models of glazing. Since neither of the programs (ESP or HTB2) calculated the internal direct radiation distribution (in the conservatory), and since the User Manuals gave little guidance on appropriate values to use, approximate assumptions were necessary.

(i) In the first approach, all the direct radiation was assigned to the conservatory floor (no interzonal radiation transfer). The diffuse radiation and the reflected direct radiation was distributed among all the internal conservatory surfaces in an area weighted manner. This approach was chosen, since for nearly all locations, seasons and times of day a great portion of the solar radiation will strike the conservatory floor. This model was given the symbol (_f).

(ii) In the second approach, the radiation was distributed in an area weighted way between the conservatory floor, the partition (common) wall, the partition (common) window, and (in the case of HTB2 to consider interzonal radiation transfer) to the adjacent living-room floor (Fig. 2.6). The diffuse radiation and the reflected direct radiation was distributed among all the internal surfaces.

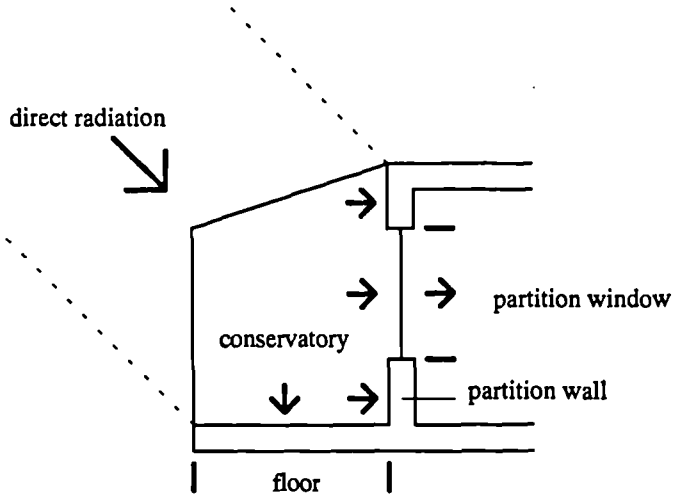

Figure 2.6:
Internal solar distribution in the conservatory and adjacent space.

This radiation distribution was chosen, because it represents approximately the situation at noon, which is the time of the highest radiation intensity. Since ESP permits

the definition of just three internal surfaces to receive direct radiation, the radiation split was limited to three components. This model was given the symbol (_tr).

Both models differ in their treatment of interzonal radiation transfer, it is not modelled by the first (_f) approach, but is approximately considered by the second (_tr) approach. The second model also has a more detailed solar distribution in the conservatory.

A third model was introduced later for a single study to investigate the particular effect of the solar distribution within one space (only for HTB2).

(iii) The radiation was distributed between the conservatory floor, the partition (common) wall and partition (common) window using an area weighting algorithm. The diffuse radiation and the reflected direct radiation was distributed among all internal surfaces. This model was given the symbol (_d).

All three approaches for the solar distribution are approximate models with the following limitations.

- The solar distribution split is fixed (the dependency of internal distribution on the sun position is neglected).
- Re-transmission of the direct radiation is not considered.
- The programs predict the distribution of the diffuse radiation based on an approximate area-weighting algorithm; the accurate geometrical relations (view factors) are neglected.
- Only the first reflection of the direct radiation is considered (higher-order reflections are neglected).

The programs ESP and HTB2 were comparable provided they both had distribution models (_f) or (_tr). However, two main differences could not be avoided.

- ESP considers the backloss of diffuse reflected radiation, while HTB2 distributes the reflected radiation around all the internal surfaces. In neither model is radiation lost to the outside.
- ESP calculates the interzonal radiation transfer internally and considers the direct- as well as the diffuse- interzonal radiation transmission. For HTB2, the portion of interzonal transmitted direct radiation can be specified by the user, however, diffuse interzonal transmission can not be modelled.

It is worth noting, that ESP offers a more detailed time-dependent treatment of solar distribution (ESP-INS), however, there are program limitations, which diminish its application for conservatories. This limitations are discussed in detail in Chapter 8 (section 8.2).

2.3.4 Predicted differences between the thermal models of glazing

As in the previous study (section 2.2), the different window modelling techniques influenced the results in a significant manner. However, the inconsistencies were now much more pronounced. There were not only clear disagreements in the absolute values of energy demand and internal temperature, but also in the predicted design trends. This is important, since in building design applications, DSMs are used primarily to guide the user towards an optimum solution.

Different trends occurred for the heating energy demand of the room (and the peak air temperature in the conservatory) as the conservatory glazing type (Fig. 2.7), the partition window area (Fig. 2.8) and the partition window type were varied. For example, on a sunny winter's day ESP_TMC_tr produced the lowest energy demand for a single glazed conservatory, while ESP_U_v_tr predicted nearly no differences as the conservatory window type changed. HTB2_TMC_tr predicted the lowest energy demand for low-emittance conservatory glazing (Fig. 2.7).

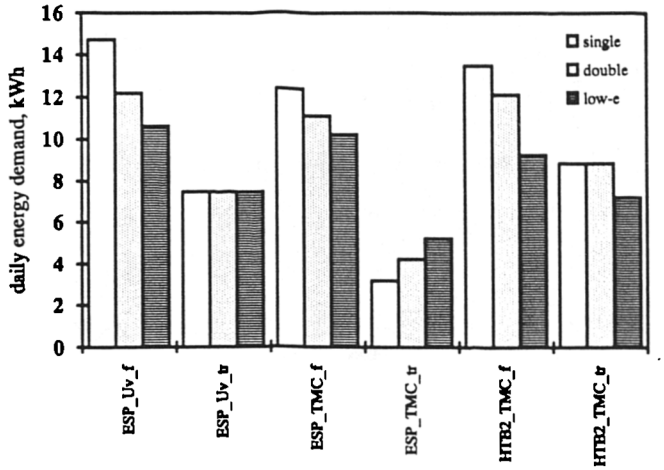

Figure 2.7:

Variation of the daily heating energy demand of the room on a sunny winter's day as the conservatory window type is varied.

2.3.5 Predicted differences between the solar distribution models

As expected, the simulation results were very sensitive to the different solar distribution approaches. The trends predicted by the simplified approach (_f), which did not consider interzonal radiation transfer, differed in most cases from the trends predicted by the detailed approach (_tr). For example, on a sunny winter's day the detailed approach (_tr) indicated the lowest energy demand for a large partition window (14 m²), whereas the simplified approach (_f) calculated the lowest energy demand for a total opaque partition (0 m²; no partition window) (Fig. 2.8).

The absolute energy demand predictions for the large partition window (14 m² in Fig. 2.8) varied from 2 kWh to 17 kWh depending on the solar distribution model used. This is a very large variation.

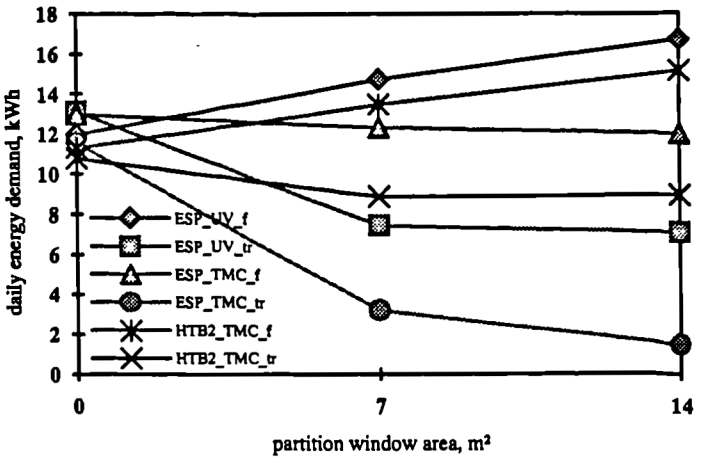

Figure 2.8:

Variation of the daily heating energy demand of the room on a sunny winter's day as the partition window area is varied.

The daily energy demand of the base-case building with the attached conservatory was also compared with an arrangement in which the external wall had a double glazed 7 m² external window and no conservatory (case "no cons" in Fig. 2.9). Thus, the impact of a conservatory on the energy demand of the room (to which it is attached) could be studied. The different solar distribution models predicted quite different outcomes. While the detailed models (_tr) indicated a lower energy demand for the living-room with conservatory, the simplified models (_f) indicated an energy increase (Fig. 2.9)!

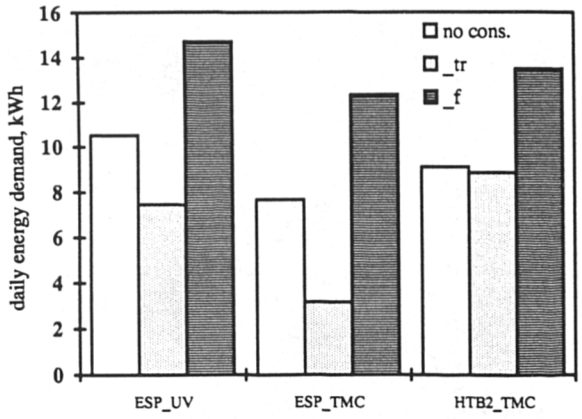

Figure 2.9:

Daily heating energy demand of a living-room with and without a conservatory on a sunny winter's day. The case "no cons." describes the living-room without a conservatory but with a double glazed, 7m² external window. The cases "_f" and "_tr" represent different solar distribution approaches for the living-room with the conservatory.

For all the buildings on clear days (sunny winter's or sunny summer's days) the predicted variabilities in peak conservatory temperatures due to the different solar distribution models were pronounced. Irrespective of the building variation, the differences were more than 10%. On a sunny winter's day the predicted peak temperatures in the single glazed conservatory varied by about 7 K between 21°C (ESP_U_v_tr) and 28°C (ESP_U_v_f). The total variation, due to different programs, thermal models of glazing and different solar distribution models was 9 K (Fig. 2.10).

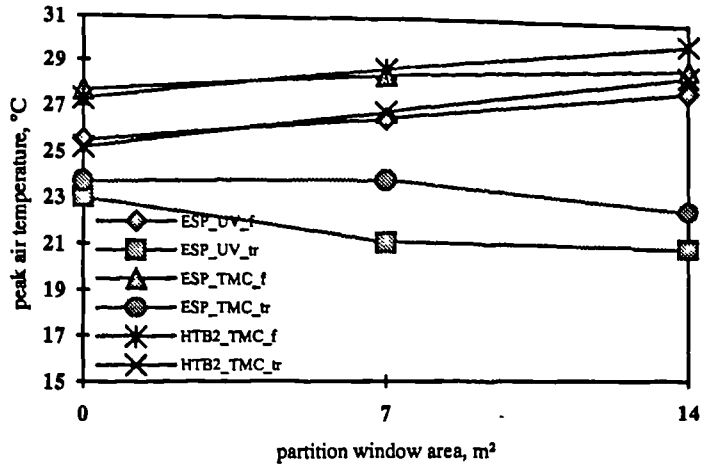

Figure 2.10:

Variation of the peak air temperatures in the single glazed conservatory on a sunny winter's day as the partition window area is varied.

The solar distribution methods (_f and _tr) differed in the modelling of the interzonal radiation transfer and the solar distribution in the conservatory (section 2.3.3). It was therefore not possible to attribute the predicted variabilities to one of these aspects. In a single study the thermal consequences of the solar radiation split within one zone was therefore investigated. An additional solar distribution model was introduced (_d) which considered the same radiation split in the conservatory as the (_tr) model, but no interzonal radiation transfer. In this study the predicted room energy demands (Fig. 2.11) were compared for different partition window areas.

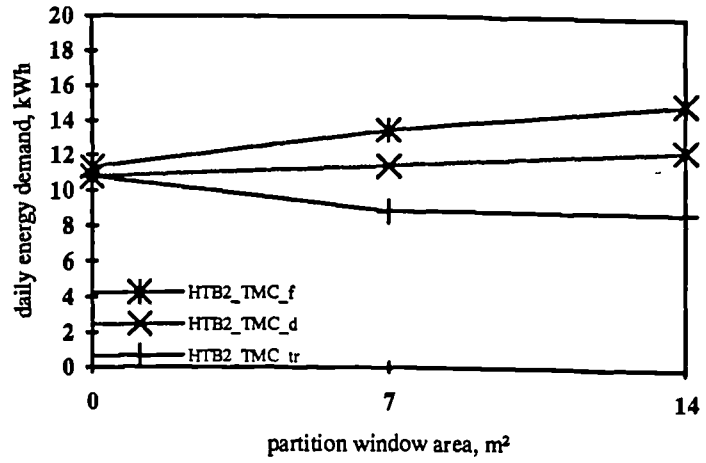

Figure 2.11:

Variation of the daily heating energy demand in the room on a sunny winter's day as the partition window area is varied. The model (_d) describes a detailed solar distribution within the conservatory, but without interzonal radiation transfer.

The trend produced by the (_d) method lies approximately mid-way between the trends for the other two methods (Fig. 2.11). It was therefore concluded, that both effects (interzonal radiation transfer and radiation split) have similar effects on the predicted heating demand of the room.

2.3.6 Predicted differences between the DSMs

Generally, ESP and HTB2 produced similar design trends for the same thermal model of glazing (TMC) and solar distribution model. One exception, however, was for the daily energy demand as the conservatory window type was varied (Fig. 2.7). Here, the

HTB2_tmc_tr specification indicated a minimum energy demand for low-emittance glazing, whereas ESP_tmc_tr indicated a minimum energy demand for single glazing. These differences can only be explained by second order differences in the algorithms for solar distribution and thermal glazing modelling. It is probable, that these include difference in: the diffuse interzonal radiation transfer; the distribution and backloss of diffuse radiation; and the treatment of internal reflections. The TMC glazing models differ mainly in their treatment of the internal and external surface convection coefficients. This is also likely to have a big impact on predictions.

2.3.7 Discussion of solar distribution models

The sensitivity of the predicted energy demands and peak conservatory temperatures to the solar distribution models was pronounced. The programs produced not only marked variations in the absolute predictions, but serious differences in the trends for important design aspects of the building. The predicted differences were mainly attributed to the interzonal radiation transfer and the radiation split within the conservatory.

However, other aspects, such as the treatment of the diffuse radiation, internal reflections and radiation backloss, were also felt to be important. The programs used, ESP and HTB2, considered these aspects only approximately.

(i) The radiation splits within the conservatory were crude approximations and treated as being fixed. The position of the sunpatch as a function of time was not considered. This also affects the calculated interzonal radiation transfer between the conservatory and the adjacent room.

(ii) None of the programs accurately considered the problem of radiation loss (by retransmission of the direct beam or backloss of reflected radiation). However, it is probable that radiation loss is very important when a conservatory (or other highly glazed spaces) is modelled.

Thus, credible design conclusions for a test building with a conservatory cannot be derived from the DSMs used.

The above considerations clearly demonstrate the need of more accurate solar distribution models if highly glazed spaces are to be simulate. These could also be useful for investigation the particular effect of interzonal radiation transfer and radiation loss more closely (see Chapter 8).

2.4 COMPARISON OF SOLAR MODELS OF GLAZING

The forgoing studies demonstrated the differences and weaknesses in the thermal models of glazing and internal solar distribution models in the DSMs. In the first study, the impact of the window algorithms was mainly attributed to their thermal effect and therefore to their effect on the heat loss. However, the solar radiation energy transport through a window is also important. In fact, the solar radiation energy transport can become a predominant issue, especially as glazing areas and the levels of insulation in the opaque elements increases.

As noted in section 2.3.1, the programs ESP, HTB2 and SERI-RES use quite similar approaches for the direct (and to a certain extent diffuse) radiation transfer through clear glazings. An investigation has shown that the predicted direct transmittance values of a 4 mm glass pane (considering different incidence angles of radiation), and therefore the predicted radiation energy flows through the glass pane, were nearly the same for all three programs. In addition, the predicted transmittance values and energy flows agreed very well with exact analytically obtained values (Parand and Lomas 1988).

It was assumed, that the exact treatment of the radiation transfer by DSMs was limited to clear glass and direct radiation only. There were obviously big differences in the treatment diffuse radiation, special (tinted or coated) glazing, and glazings with shading devices. This was felt to be important in the passive solar design of dwellings where low-emittance glazing is used to reduce the heat loss through the large glazed areas. Coated or tinted solar control glazings, as well as shading devices, are increasingly popular in commercial buildings, atria and conservatories. It was also felt, that the importance of diffuse radiation increases as the glazing areas increase.

The programs ESP, HTB2 and SERI-RES were reviewed to identify the main weaknesses in their solar models of glazing, with a special focus on their modelling capabilities for special glazings and shading devices. In addition, the treatment of solar radiation energy gains in simplified, quasi-stationary (empirical), calculation models (BREDEM (Anderson et al. 1985); ASHRAE Handbook 1981; CIBSE Guide 1986; WärmeschutzVO, 1993; DIN 4108, 1981; DIN 4701, 1983; VDI 2078, 1977) was also studied.

It should be noted that the review and improvement of quasi-stationary models was not planned at the beginning of the project (see section 1.4). But work on these models was useful, since the improvements made to the solar models of glazing (which resulted in an improvement of glazing properties) could also be transferable to quasi-stationary calculations. Besides, as an alternative to detailed simulations, quasi-stationary calculation models are often used to assess the performance of highly glazed spaces.

As a result of the theoretical review, the following areas of weakness were recognised.

2.4.1 Diffuse radiation transfer

While DSMs often use complex anisotropic sky models to calculate the diffuse radiation incident on external glazings, they treat the diffuse radiation transfer through the glazings very roughly. Normally, the value of the direct transmittance at an average incidence angle of about 60° is recommended as the diffuse transmittance (ASHRAE 1981). This value results from theoretical investigations of the radiation conditions on vertical glazing and considers the transmission behaviour of clear glass under isotropic sky conditions (Hottel and Woertz 1942). In the case of non-vertical windows, real sky conditions, or special (coated or tinted) glazing the corresponding value is generally unknown and the simplified assumption leads to inaccuracies.

SERI-RES calculates the diffuse transmittance using an equivalent incidence angle of 60° as recommended by ASHRAE, ESP uses 51° and HTB2 leaves the definition to the user (but no recommendations are given).

The diffuse transmittance of clear double glazing (2 × 6 mm clear glass panes) for an equivalent incidence angle of 60° (as used by SERI-RES) is about 0.48. The corresponding value for an equivalent incidence angle of 51° (as used by ESP) is about 0.54. Thus, the diffuse radiation energy flow through the glazing, as predicted by SERI-RES and ESP, differs by more than 10%.

Simple calculations can show that the inaccuracy in the predicted radiation energy flow through a glazing, due to a mistake in the diffuse transmittance of 10%, is comparable to the heat flow through a traditional wall in winter! For example, a 10% error in the transmission of diffuse radiation with an intensity of 200 W/m² produces an error in the calculated energy flow of 20 W/m². This corresponds to the energy flow through a wall with an U-value of 1 W/m²K when the temperature difference between inside and outside is 20 K. Such an error may not be important in modestly glazed spaces (where glazing areas are small in comparison to the total space envelope). However, it is certainly important in highly glazed spaces, (where the glazed areas can be much larger than the opaque areas).

It is probable, that the thermal conditions in a highly glazed space on cloudy days depends mainly on the amount of diffuse radiation energy entering the space. Thus, any inaccuracy in the prediction of the diffuse radiation transfer will lead directly to inaccurate simulation results. Since more accurate values for the diffuse transmittance were not available at the beginning of this work, the thermal consequences of the simplified treatments could not be investigated. This was done as part of the new model development process (Chapter 4).

2.4.2 Radiation transfer through special glazing

DSMs normally consider the direct radiation transfer through glazings very accurately because this phenomenon is known to have a big influence on thermal performance. Simple

(quasi-stationary) models may need one characterising value for the transmittance and absorptance of the radiation, but DSMs normally use the incidence angle dependent values.

ESP and HTB2 rely on the program user to supply the incidence angle dependent transmittance and absorptance properties for each window. In the case of clear glazing these values are either well known or can be easily calculated (based on the Fresnel equations) (DIN 1349, 1972). For special glazing however (coated low-emittance glazing, sun-reflective solar control glazing, absorbing tinted glazing) these values are normally unknown. SERI-RES generates the incidence angle dependent glazing properties internally based on the refraction and extinction indices of the glazings (a similar approach is used by TRNSYS). However, the calculation is limited to only four glazing layers, all of which must have the same properties. In addition, the calculation is only valid for clear glazing.

If the angle dependent properties of clear glazing are assumed to be true for special glazing, the radiation transfer is described quite accurately up to an incidence angle of about 40°, but for higher incidence angles - which is the normal case in Europe - the assumption may only be a rough approximation. This was inferred from the incidence angle dependent transmittance curve shapes for special glazing presented by Tschegg et al. (1984).

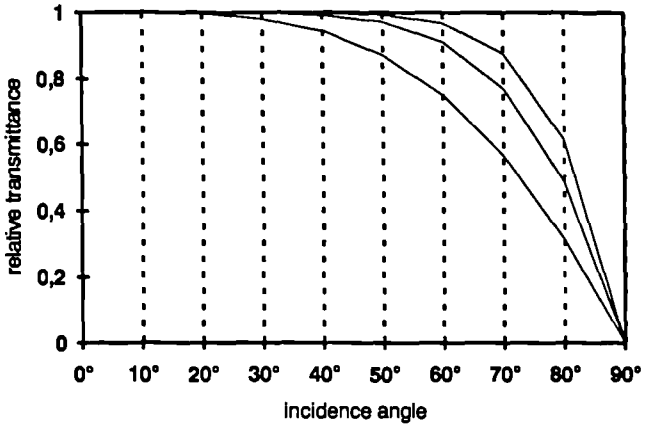

Figure 2.12:

Incidence angle dependent relative transmittance curve shapes of special glazings presented by Tschegg et al. (1984). The curves are not related to particular glazing types. The relative transmittance is the ratio between an actual transmittance value at a particular angle of incidence and the transmittance at normal incidence.

The assumption that conventional properties apply to special glazings is likely to lead to inaccurate predictions of heating and cooling power, energy demands and internal temperatures.

2.4.3 Total solar energy transmittance

Most window producers present fixed total solar energy transmittance values in the same way as fixed U-values are often quoted for glazings. These are used in some DSMs (e.g. ZB-SIMULAP) or in quasi-stationary calculations of cooling or heating demands (e.g. ASHRAE Handbook 1981; CIBSE Guide 1986 etc.). They are widely used in many international standards. However, the total solar energy transmittance in particular, is not a fixed property but highly dependent on the time and season. There is also a dependency on the

location, orientation and the inclination of the window surface. These aspects are generally neglected (DIN 67507, 1980). Since the total solar energy transmittance also depends on the specific transmittance characteristic of the glazing, there is a high dependency on the glazing type (which is particularly important for special glazing). To improve the calculation possibilities it was felt to be important to produce new effective window statements, which consider the time-dependent changes of the properties using an appropriate averaging method.

2.4.4 The radiation transfer through slat-type blinds

The most effective way to reduce the solar load on windows is to intercept direct radiation from the sun using internal or external sunshades. External and internal slat-type blinds (such as venetian blinds) are the most frequently used sun protection devices.

While there are well known calculation methods for the shading effects of frames, side fines, overhang and obstructions (sky line) (Rodriguez et al. 1988; Rodriguez and Alvarez 1991) which are implemented in many programs (ESP, HTB2, SERIRES) there are no calculation principles for external or internal slat-type blinds. There is also no possibility of simulating blind systems dynamically. SERI-RES offers the possibility to define shading factors, which may be scheduled hour-by-hour. ESP and HTB2 permit the definition and scheduling of glazing properties, which can be used to implicitly consider the time-dependent solar shading effect of blinds. But, unfortunately, these quantities are generally unknown.

The available fixed standard shading factors (ASHRAE Handbook 1981; CIBSE-Guide 1986; DIN 4108, 1981; VDI 2078, 1977) do not take account of specific blind systems or locations. Moreover, they do not distinguish between the net-reductions in the different radiation components (transmitted or absorbed, direct or diffuse). These are usually needed by DSMs. These problems lead to a very unsatisfactory situation in the case of highly glazed spaces with slat-type blinds, since the inside climate depends fundamentally on the amount of solar radiation entering the room.

2.5 MODELLING OF TEMPERATURE STRATIFICATION AND VENTILATION IN HIGHLY GLAZED SPACES

Till now, the discussion of model weaknesses in predicting the thermal performance of highly glazed spaces has concentrated on issues of window modelling and solar radiation gains. However, there are other modelling problems, which can be neglected for typical modestly glazed buildings, but which gain importance, when highly glazed spaces are to be simulate.

- **Temperature stratification** is frequently encountered in high glazed halls or in other tall spaces, where warm air rises to the roof space. Stratification could also be estab-

lished in small highly glazed spaces like conservatories (Hofmann 1981). However, there are little or no statements found in the literature, which defined the quantity of stratification for certain situations or explained the thermal impact of stratification on heating (or cooling) load predictions or on comfort assessments. Since stratification depends on the air-flow within one space, the problem of modelling stratification leads to the modelling of air-flow.

- Highly glazed spaces are often cooled by using **natural ventilation** to solve or reduce overheating problems. When DSMs are used to design a cooling system for halls of considerable height (like glazed atria), the modelling of displacement ventilation (natural ventilation based on the stack effect) is known to be an important issue (Borresen and Harsem 1991).
- The solar pre-heated air of conservatories (or atria) can be used to ventilate the parent building, which is called "solar pre-heating of ventilation air" (SPV). This problem requires the simulation of **interzonal air-flow** (see Baker 1985).

In short, single studies the possibility of modelling temperature stratification and ventilation was investigated. This was done with the programs ESP, using the existing air-flow calculation possibilities of ESP-AIR (now called ESP-MFS, mass flow solver), and with HTB2, which permits the parting of a room into a number of fictitious air-spaces. It proved possible to consider forced ventilation effects, like wind-driven air-flow, stack effect (forced convection) or mechanical ventilation. Within these calculations temperature stratification in highly glazed rooms (high atria or conservatory) can be considered (see also McLean 1988; Hensen 1991; Hensen et al. 1991). It is also possible to model interzonal air-flow. In contrast, convection, based on temperature differences within one room, cannot be modelled. The buoyant flows depend on the interaction of many complex boundary conditions and can mathematically only be solved within special computational fluid dynamic programs (CFD). In small spaces with low air-flow rates, e.g. domestic conservatories in winter, the temperature stratification depends mainly on free convection and cannot therefore be considered in today's DSMs.

2.6 IDENTIFIED AREAS OF WEAKNESS

The following four areas of weakness in DSMs for predicting the thermal environment in highly glazed spaces were identified by inter-model comparisons and a theoretical review of existing modelling capabilities. They were felt to be the main issues for further investigations, development of new algorithms, and model implementations.

(i) **Thermal models of glazing** (modelling of heat transfer through glazing)

The weakness of simplified U-value models for windows has been shown. However, since more rigorous transparent multi-layer construction approaches are already available in state of the art DSMs, further improvements are mainly necessary in the area of internal and external convective surface coefficients; external longwave (infrared) radiation energy losses and detailed calculations of the energy transport through air cavities.

(ii) **Solar models of glazing** (modelling of solar energy gains)

The solar radiation transport through windows is normally considered very accurately. However there are modelling weaknesses in the following areas:
- the transmittance and absorptance of diffuse radiation;
- glazing transmission properties for special (coated or tinted glazing);
- models of internal and external slat-type blinds; and
- the total solar energy transmittance used by simpler calculation models.

(iii) **Internal solar distribution**

The methods used for solar distribution within DSMs are quite different. Although general statements about modelling capabilities are difficult to make, the following important modelling aspects were found to be neglected or not fully developed:
- the dependence of the solar distribution on the sun-position and therefore on time and season;
- the immediate re-transmission of direct and diffuse radiation to the outside;
- interzonal radiation transfer of direct and diffuse radiation;
- the backloss of reflected radiation to the outside;
- considerations of internal multi-reflections (higher-order reflections); and
- accurate considerations of geometric conditions (view factors).

(iv) **Temperature stratification and natural convection (buoyant air-flow)**

The problem of temperature stratification is closely related to the problem of air-flow within one space. Although some DSMs permit the separation of one zone in more than one air-space, the air-flow due to natural (buoyant) convection cannot be explicitly modelled.

CHAPTER 3

DEVELOPMENT AND TESTING OF NEW ALGORITHMS

3.1 FOCUS OF WORK

The previous Chapter indicated the key aspects for further investigations, development of new algorithms and model implementations. These were summarised in four groups: (i) the thermal glazing models; (ii) the solar glazing models; (iii) the internal solar distribution; and (iv) temperature stratification and natural convection. It was impossible for one worker to cover the complete range of these problems within the available resources. It was therefore necessary to decide, which problems were of most importance and best suited for investigations in this research. This led to the decision to focus on all aspects of the shortwave radiation transfer into the room and its distribution to internal surfaces or adjacent spaces (aspects (ii) and (iii)).

The decision was based on the following considerations.

- In Chapter 2, the weakness of modelling window conduction has been attributed to the inaccuracies in the surface coefficients. The surface coefficients were shown to be primarily important with poorly-insulation (single) glazing. The influence of the surface coefficients on the calculated heat transfer through double or heat-protective (low-emittance) glazing was shown to be less important. Today, in many countries strong heat-protection standards prescribe highly-insulation glazings for buildings. For example, the future German building regulations (WärmeschutzVO 1993) will prescribe for glazing U-values lower than 1.9 W/m²K. The prescribed insulation standard for glazing will increase as the glazing area increases. Therefore, it was concluded, that the improvement of surface coefficients should not be object of this work, since it is not of primary importance in predictions produced for modern, high-insulated, highly glazed spaces. Furthermore, studies elsewhere have shown that internal surface coefficients have a small impact on peak air temperatures and thermal comfort in typical domestic scale buildings (Lomas and Mardaljevic 1990).
- While the surface coefficients lose importance as the insulation standard of a building increases, the solar radiation energy gains through the windows become more important. In modern high-insulated buildings, where U-values lower than 0.3 W/m²K are typical, the solar heat gains have a large impact on the thermal conditions of a room. Any inaccuracy in the calculated solar heat gains directly influences the predictions of

heating energy demands and internal temperatures. Since the insulation standard of buildings is likely to increase, the significance of solar radiation aspects will also increase.

- The aspects of shortwave radiation can be improved by a rigorous application of known physical theory. Because of available resources there was a preference for theoretically orientated rather than experimentally based work. This also excluded empirical investigations of internal and external convection coefficients, measurements of convection in air cavities and experimental examinations of temperature stratification and air movement. These aspects are objects of a great deal of effort at other places (Linden et al. 1990; Khalifa and Marshall 1990).
- Any theoretical consideration of air movement or convection coefficients would lead to work, which would require a fundamental study of air flow algorithms. This would lead away from the central theme of highly glazed spaces.
- All aspects of shortwave radiation within buildings can be calculated separately in standalone computer modules or in pre-processing programs, which produce the input values for DSMs. The calculation need not necessarily be fully integrated into the thermal simulation. Standalone computer modules offer the big advantage, that they can be used in connection with any DSM. The benefits of the improved calculation models would not therefore be restricted to one single DSM. The work would therefore have the widest possible applicability.

The different aspects of solar glazing models and solar distribution were divided into five main problem areas and each is treated in separate Chapters.

1. Diffuse radiation transfer (Chapter 4).
2. Radiation transfer through special glazing (Chapter 5).
3. Total solar energy transmittance (Chapter 6).
4. Radiation transfer through slat-type blinds (Chapter 7).
5. Internal solar radiation distribution (Chapter 8).

The sequence of the Chapters is not determined by their relative importance, but rather by the sequence which permits the clearest explanation of these interrelated studies.

3.2 PROGRAMS FOR MODEL IMPLEMENTATIONS

As indicated in the previous section, the improvement of shortwave radiation aspects can be done by standalone computer modules or by pre-processing programs. These will produce the input values for DSMs. This is especially important, since the choice of the best DSM for model implementations and model improvements is difficult. Considering the quick de-

velopments in the area of computer technology, it is impossible to make predictions regarding future DSMs. There is no doubt that their appearance will be quite different and that their power, and their features on offer, will be much larger than at present. Since it is not yet clear, which of todays DSMs will be developed further and therefore of future interest, it seems to be much more appropriate to realise program implementations which are independent of a specific DSM. In addition, there is a general move towards object oriented programs (energy kernel system (see Clark and Maver 1991)), and modular programs (e.g. TRNSYS (Klein et al. 1988)), in which different elements are linked to create whole systems. Standalone pre-processing programs will be usable by the (modular) programs of the future.

It was decided to realise the different aspects of solar glazing transmission in separate modules within one pre-processing program, which was later called GLSIM (GLazing SIMulator). The solar distribution problem was also realised in a standalone computer module, which was called SUNSIM (SUN SIMulator).

In principle, these modules can be linked to any DSM. In this work, however, it was not possible to make links to various DSMs for the following reasons.

(i) Since DSMs differ considerably in their input structure and the level of detail of the needed data, the production of universally valid input data was impossible. It was therefore necessary to find appropriate solutions, which meet the requirement of a wider range of DSMs. In extreme cases, the concentration on the need of one DSM appeared to be necessary.

(ii) The coupling of the solar distribution module SUNSIM with the thermal processor required a specific interface, which could not be achieved without modifications of the connected DSM.

The testing and demonstration of model consequences and the application of the improved models on the investigation of highly glazed spaces required only one DSM to be used. To choose the DSM which is best suitable for code modification and to demonstrate the links different program source codes were studied. This led to the decision to focus on the program HTB2 (Lewis and Alexander 1985), which was developed at the Welsh school of Architecture in Cardiff. The decision was based on the following considerations.

- HTB2 was developed as a research tool rather than a design tool. It can operate at very small time-steps and its source code can easily be modified (e.g. there are five special ziproutines for user alterations and extensions). HTB2 has been written in a modular format in which each sub-system has been isolated and localised in specific subroutines. In addition, the programming has been made as explicit as possible to enable the internal operation to be easily understood. It is well documented both internally and in the man-

ual. The suitability of HTB2 for model implementation and modification has been clearly shown on the basis of side-studies conducted during this work (Pfrommer 1994a).

- HTB2 treats glazing as a transparent multi-layered constructions (TMC), which was shown in section 2.2 to be an important feature.
- HTB2 relies on the program user to supply the incidence angle dependent transmittance and absorptance values for each individual window (i.e. these are not calculated internally). In addition, the transmittance and absorptance values for diffuse radiation are specified explicitly (they are not calculated internally assuming the same values for direct radiation at a particular angle). This simplifies any link to a pre-processing program, which calculates these values.
- In HTB2 the user can appoint an unlimited number of internal surfaces to receive direct radiation. Moreover, the internal radiation splitting can be time-scheduled. HTB2 is therefore suitable for modelling very detailed time-varying internal solar radiation distributions. Since the distributions can be specified by the user, HTB2 is also suitable for comparing different radiation distributions.
- HTB2 permits the division of a room into different air spaces without interruption of the internal longwave (infrared) radiation exchange. It is therefore possible to consider more than one air node in a space. This was not important in this research but for the simulation of temperature stratification (perhaps by other researchers) this is valuable.
- HTB2 was considered within the Applicability Study (Lomas et al. 1989) and the IEA 21C/12B Empirical Validation exercise (Bloomfield et al. 1993). Neither study provided evidence to indicate that HTB2 would be unreliable when used in this research.

HTB2 is a non-geometric, multi-zonal model. A building consists of a series of spaces linked to each other and to the outside by walls, windows and ventilation paths. This building is driven by external climate, by heating systems, operating under control systems, and by incident heat sources. HTB2 is designed for simulating the thermal performance of energy efficient occupied buildings. In order to achieve this, HTB2 provides detailed algorithms for convective and radiant gains and exchanges and a flexible way of specifying operation schedules.

HTB2 is written in a standard language, FORTRAN 77, with a minimum of machine dependent features so that it should be portable between machines with a minimum of modifications. Nevertheless, the basic HTB2 version used within this work was intended for a desk top workstation (UNIX computer system). Therefore, all program development, code modification, validation and application work was done under UNIX. However, the new independent program modules are additionally provided for personal computers (DOS com-

puter systems). It is worth notable, that the latest HTB2 version is also available for personal computers (DOS computer systems) (Alexander 1993).

3.3 VALIDATION AND SENSITIVITY STUDIES

Because the work was theoretically based and aimed at developing separate pre-processing modules, each module was validated, as far as possible, in isolation. Similarly, the impact of apply each module to real design situations was assessed separately. The investigations were done as part of the model development process and are therefore described in the appropriate Chapter.

There are three main evaluation techniques for energy simulation programs (Judkoff 1988). These techniques can be applied to program modules, which deal with only a part of the simulation process:

1) **Empirical Validation** in which calculated results from the program are compared to monitored data from real buildings, or intermediate results from an algorithm or subroutine are compared to laboratory (or field) data.

2) **Analytical Verification** in which the output from a program, subroutine, or algorithm is compared to the result from known analytical solutions. This is applicable to isolated physical mechanisms tested under very simple boundary conditions.

3) **Intermodel Comparisons** in which a program is compared to other programs, which include different, or more detailed physical approaches, or which have been more rigorously validated. A program may also be compared to alternative (or earlier) versions of itself.

Each of these approaches has different strength and weaknesses (Judkoff 1988), which are not discussed here. The model development process required the use of all three methods.

Analytical Verification is the most obvious way of validating separate algorithms or program modules, since the correct analytical solution can often be derived and compared with the program's results. This way the correct implementation of a theory can be tested. This was on principle immediately done during the coding process. The analytical verification work is therefore not always fully described.

Empirical Validation was applied, when comparative measurement values were available. Unfortunately, this was not always the case.

Intermodel Comparisons were rarely possible, since the developed modules were improvements and therefore without comparable counterpart. However, in one case, there were useful comparisons possible with programs, which use different, but comparatively accurate physical approaches for application in a different domain: daylight programs, which use a

rigorous ray tracing calculation technique for solar radiation problems, could be used as references for the radiation transfer through blind systems.

Sensitivity analyses seek to determine the total uncertainty in the model predictions due to the uncertainty in individual internal program algorithms or input parameters. Because the models are so complex, there is no simple (analytical) way of relating output uncertainty to the net-uncertainty of particular algorithms or uncertainties in input parameters. Therefore, all errors must be propagated numerically through the models themselves to establish the total error in the predictions (Lomas and Bowman 1988). The impact of the newly developed algorithms and the newly produced input values was therefore investigated in sensitivity studies using realistic situations. This also led to guidance, about when a more accurate treatment of a phenomenon is necessary, or how big the error potential will be when a simplified approach is used. The effect of the new algorithms were also judged by rerunning some of the simulations undertaken in the previous studies (Chapter 2).

CHAPTER 4

DIFFUSE RADIATION TRANSFER

4.1 INTRODUCTION

It is probable, that the thermal conditions in highly glazed spaces depend significantly on the amount of diffuse radiation entering the space. It has been indicated in Chapter 2 (section 2.4.1) that DSMs use different methods to calculate the diffuse radiation transfer through glazings. Therefore, this Chapter investigates the diffuse radiation transfer through glazings in detail.

The diffuse radiation onto a plane consists of the radiation from the sky, ground and surroundings. Each radiation portion has a different average incidence angle and intensity. Its transmittance through glazings depends on its incidence angle. The ratio of the total diffuse transmitted radiation energy to the total incident diffuse radiation energy describes the diffuse transmittance τ_f. Similarly, the ratio of the total absorbed diffuse radiation and the total incident diffuse radiation describes the diffuse absorptance α_f. Often the diffuse transmittance is presented in terms of the equivalent incidence angle θ_f, such that, for the particular glazing system τ_f is equal to the transmittance of direct radiation at an incidence angle of θ_f. The following important factors affect the transmission of diffuse radiation into a room:

(i) the distribution of the sky radiation;

(ii) the ground reflected diffuse radiation;

(iii) the location, orientation and inclination angle of the window; and

(iv) the relationship between the incidence angle and the transmission or absorption for the particular glazing system.

DSMs usually provide different algorithms to calculate the diffuse radiation energy incidence on inclined surfaces from measured data of horizontal insolation. More simple programs use isotropic sky models (ISO), which assume that the diffuse insolation is uniformly spread over the sky vault. However, many programs use complex anisotropic sky models to take account of the detailed luminance distribution over the sky vault. There are different anisotropic sky models available, for example Klucher's model (used by ESP), which treats the diffuse insolation as the sum of a circumsolar term (which is added to the direct radiation) and an isotropic term (ISO), or Hay's sky model (used by SERI-RES), which approximately considers clear and CIE-overcast sky conditions (see Hogan and Loxsom

1981). All formulations are empirical simplifications, which permit a quick calculation during the simulation run.

Although DSMs seek to calculate the radiation energy incidence on inclined surfaces very accurately, they estimate the diffuse radiation transfer through glazings very roughly. No program could be found, which considers aspects of sky radiation distribution in the prediction of the diffuse radiation transmittance or absorptance. For example, SERI-RES uses the value of the direct transmittance for an equivalent incidence angle of 60°, ESP uses 51° and HTB2 leaves the definition of the diffuse transmittance and absorptance values to the user. Normally, the value of the direct transmittance for an equivalent incidence angle of about 60° is recommended (ASHRAE 1981). This value results from theoretical investigations of the radiation conditions on clear glass under hemispherical isotropic sky conditions (Hottel and Woertz 1942). Since this value does not distinguish between the sky and ground diffuse components, it only reflects the symmetric diffuse radiation situation on vertical or horizontal surfaces (and isotropic sky conditions). In the cases of inclined windows (not vertical and not horizontal), real day sky conditions, or special coated or tinted glazing the corresponding value is generally unknown and the simplified assumption leads to inaccuracies.

More rigorous investigations have been conducted previously. These emphasised the weakness of the conventional approach and introduced more detailed treatments.

- Tschegg et al. (1984) presented a simplified formulation, which relates the diffuse transmittance to the incidence angle dependent transmittance curve of the direct radiation. The curve defining the relationship between incidence angle θ and the direct transmittance $\tau(\theta)$ is described as follows

  (4.1) $$\tau(\theta) = \tau^n * \left[1 - (1 - \cos\theta)^\kappa\right]$$

  where τ^n is the transmittance for normal incidence. Thus, the angular dependence of transmittance is described by an empirical constant κ, which usually lies between 2 and 5. The hemispherical diffuse transmittance τ_f is given by

  (4.2) $$\tau_f = \tau^n * \frac{\kappa * (\kappa + 3)}{(\kappa + 1) * (\kappa + 2)}$$

- A similar formulation was used by Rubin (1982) to represent the hemispherical diffuse transmittance for special coated or tinted glazings. The incidence angle dependent transmittance is defined by

  (4.3) $$\tau(\theta) = c_0 + c_1 * \cos\theta + c_2 * \cos^2\theta + c_3 \cos^3\theta$$

  where c_0, c_1 etc. are the empirical coefficients, which describe a certain curve shape. The hemispherical diffuse transmittance can be calculated from,

(4.4) $$\tau_f = c_0 + \frac{2}{3}c_1 + \frac{1}{2}c_2 + \frac{2}{5}c_3$$

In both formulations described above, the transmission behaviour of different glazing systems can be approximately considered. However, both formulations are limited to the isotropic sky conditions (ISO) and the affect of surface inclination is not considered.

- The diffuse transmittance on inclined (flat plate collector) glazing was investigated by Brandemuehl and Beckmann (1979). They studied diffuse radiation incident on inclined planes, and derived a solution, based on the inclination angle η of the collector cover and the angular distribution of incident isotropic (ISO) diffuse radiation. They presented simple quadratic correlations which describe closely the analytical solutions for collector-cover systems, whose refractive indices lie between 1.34 and 1.526 and which had internal absorption extinction lengths of less than 0.0524. The equations distinguish between the sky and ground radiation components. They relate the inclination angle of the surface η to the equivalent beam radiation incidence angles $\theta_{f,gr}$ (for diffuse ground radiation) and $\theta_{f,sky}$ (diffuse sky radiation):

  (4.5a) $$\theta_{f,gr} = 90° - 0.5788\eta + 0.002693\eta^2$$

  (4.5b) $$\theta_{f,sky} = 59.68° - 0.1388\eta + 0.001497\eta^2$$

  Unfortunately, the limits of the refractive and extinction coefficients excludes typical window float glass panes. These usually have extinction coefficients of more than 0.02 1/mm and so the extinction length (product of extinction and thickness) for a 6 mm glass pane is more than 0.12, which is clearly above the limiting value of 0.0524.

The actual approaches for the diffuse radiation transfer do either neglect the dependency of the diffuse transmission on the surface inclination (since they do not distinguish between a sky and ground radiation component), or the specific incidence angle dependent transmission behaviour of the glazing. None of the models considered real day sky and ground luminance distributions. Therefore, an improved calculation model has been developed, which considers all these aspects. It was intended as a pre-processing model which predicts the necessary glazing properties for diffuse radiation. The following sections deal with the theory, the application and the thermal consequences of the new approach.

4.2 THEORY OF DIFFUSE RADIATION TRANSFER

To calculate the diffuse radiation energy incidence on inclined surfaces, DSMs use istropic (ISO) or simplified anisotropic sky models (e.g. Klutcher's or Hay's model), which permit a quick, approximate, calculation during the thermal simulation run (no time consuming numerical procedures are necessary). The diffuse sky models are normally based on measured

values of horizontal irradiation. The inaccuracy in the predicted radiation incidence increases as the inclination angle (i.e. the angle between the surface normal and a vertical plane) of the surfaces increases (Hogan and Loxsom 1981). It is greatest for vertical surfaces, but it is very small for low inclinations.

Although, an accurate calculation of the radiation transfer through glazings cannot correct any inaccuracies in the predicted radiation energy incidence onto an inclined surface, it was decided to calculate the radiation transfer through glazings as accurately as possible. The use of accurate transfer properties, even in association with inaccurately predicted radiation intensities, will produce more accurate results. Calculation time was not critical, since the new computer model was intended to be a pre-processing module. Since numerical calculations were possible, the three-dimensional radiation conditions of the sky could be considered.

As described in section 4.1, the diffuse radiation onto a plane consists of the different radiation portions from the sky, ground and surroundings. Every radiation portion has a different incidence angle and intensity. The relation between the total diffuse transmitted radiation energy to the total incident radiation describes the diffuse transmittance τ_f. Similarly, the relation between the total absorbed radiation to the total incident radiation describes the diffuse absorptance α_f. The values implicitly take account on the incidence angle dependency of the glazing properties and on the change of the radiation intensities due to the irradiation distribution. The diffuse transmittance τ_f is calculated as follows,

$$\tau_f = \frac{\int_{\omega} L_p * \cos(\theta) * \tau(\theta) * d\omega}{\int_{\omega} L_p * \cos(\theta) * d\omega} \qquad (4.6)$$

where $\tau(\theta)$ is the transmittance for beam radiation, θ the incidence angle, L_p the radiance of a certain sky or ground point and ω the spatial integration angle. The diffuse absorptance α_f is calculated by replacing $\tau(\theta)$ with $\alpha(\theta)$ in equation (4.6). Radiance is measured in terms of radiation intensities (W/m^2sr) and is analogous to luminance (cd/m^2) when light is being considered. This is appropriate, since the standardised relative distributions of light in the sky are also valid for radiation (DIN 5034, 1983).

In anisotropic sky models the radiance L_p is not a constant value but varies relative to the sun or, in other models, the zenith. It also depends on the sun height and therefore on the time of day. However, for the prediction of the diffuse radiation transfer properties, the absolute radiance values are unimportant. Instead, normalised radiance distributions (relative to the zenith radiance L_z of one) were considered. These could be derived from the standard CIE clear and overcast sky models of DIN 5034 (1983).

1. The radiance distribution of the **overcast sky** is rotationally-symmetric and independent of the sun position. It is assumed to be brightest at the zenith and decreases from zenith to horizon by a third. The distribution was introduced by Moon and Spencer (1942) and standardised by the CIE (1955) and DIN 5034 (1983). A sky point with the height angle h_p above horizon has a normalised sky radiance L_{sky} of

$$L_{sky} = \frac{1 + 2 * \sin(h_p)}{3} \tag{4.7}$$

The radiance of the ground L_{gr} can be calculated by an analytical integration of the radiation intensities on a horizontal plane (ρ_{gr} is the ground reflectance) (see Aydinli 1981):

$$L_{gr} = \frac{2.45 * \rho_{gr}}{\pi} \tag{4.8}$$

2. The radiance distribution of the **clear sky** is determined by the position of the sun. It shows a maximum brightness around the sun (circumsolar radiation) and near the horizon. There is a minimum brightness in the northern hemisphere opposite the sun. Clear skies are modelled with a complex formulation which considers the sun height h_s, the angle between the zenith and the sky point ε and the angle between the sun position and the sky point μ (all angles in rad) (CIE 1973; DIN 5034, 1983):

$$L_{sky} = \frac{[1 - \exp(-0.32 / \cos\varepsilon)] * [0.856 + 16 * \exp(-3 * \mu) + 0.3 * \cos^2 \mu]}{0.27385 * \{0.856 + 16 * \exp[-3 * (\pi/2 - h_s)] + 0.3 * \cos^2(\pi/2 - h_s)\}} \tag{4.9}$$

The radiance of the ground depends directly on the zenith radiance and on the turbidity of the atmosphere, which is described by the turbidity factor T. The turbidity represents the ratio of the vertical optical thickness of the dull atmosphere to that of the clear atmosphere. The turbidity factor by Linke T_L is standardised in DIN 5034 (1983) (see also Aydinli 1981). The relative ground radiance can be obtained as follows (sun height h_s in deg):

$$L_{gr} = \left(1 + 2 * \frac{\tau_{at,d}}{\tau_{at,a} - \tau_{at,d}}\right) * \frac{\rho_{gr}}{\pi} * \begin{pmatrix} 7.6752 + 0.06196 * h_s - 5.9344 * 10^{-4} * h_s^2 \\ -1.6018 * 10^{-4} * h_s^3 + 3.8082 * 10^{-6} * h_s^4 \\ -3.3126 * 10^{-8} * h_s^5 + 1.0343 * 10^{-10} * h_s^6 \end{pmatrix} \tag{4.10}$$

where:

$$\tau_{at,d} = \exp\left[\frac{-T_L * \exp(H/8)}{0.9 + 9.4 * \sin(h_s)}\right] \tag{4.11}$$

and:

$$\tau_{at,a} = (0.506 - 1.0788*10^{-2}*T_L)*\begin{pmatrix} 1.294 + 2.4417*10^{-2}*h_s - 3.973*10^{-4}*h_s^2 \\ +3.8034*10^{-6}*h_s^3 - 2.2145*10^{-8}*h_s^4 \\ +5.8332*10^{-11}*h_s^5 \end{pmatrix} \quad (4.12)$$

$\tau_{at,d}$ is the transmittance of the Raleigh-atmosphere for direct radiation and $\tau_{at,a}$ is the total transmittance of the atmosphere inclusive the absorption in the air (Schulze 1970); H is the height above sea level in km.

Thus, the normalised sky radiance distributions L_{sky} for overcast and clear skies and the corresponding radiance of the ground L_{gr} can be derived from parameters, which are either known (height above sea level H), or which can be easily estimated (turbidity T_L) or calculated (sun height h_s). When the radiance L_p of a certain sky or ground point in equation (4.6) is replaced by the radiances L_{sky} or L_{gr}, the diffuse transmittance for the corresponding sky models can be obtained.

Both sky models were considered within a new computer module GLSIM-DIF, which calculates diffuse transmittance and absorptance values using equation (4.6). Since the integrals could not be solved analytically, a numerical solution technique was applied. Therefore, the sky (and ground) vault was divided into slices with a constant radius and integrated along the slice angle ξ and height angle ζ (Fig. 4.1 and 4.2).

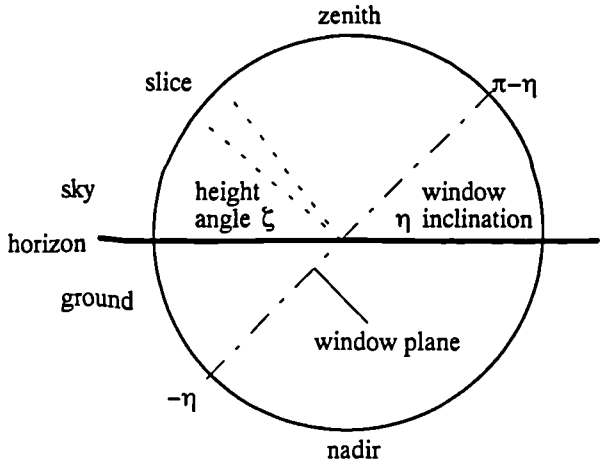

Figure 4.1:

Cross-section through sky and ground vault.

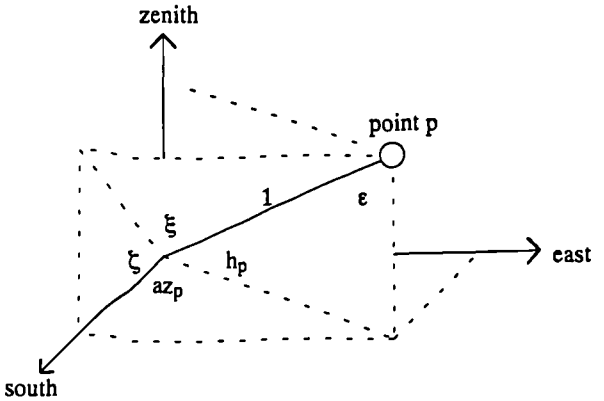

Figure 4.2:

Coordinates and angles used to integrate the irradiation from the sky and ground vaults.

Noting that $d\omega = \sin(\xi) \cdot d\xi \cdot d\zeta$ and that the integrals are calculated by numerical summations, equation (4.6) becomes:

$$\tau_f = \frac{\sum_{\zeta}\sum_{\xi} L_p * \cos(\theta) * \sin(\xi) * \tau(\theta) * \Delta\xi * \Delta\zeta}{\sum_{\zeta}\sum_{\xi} L_p * \cos(\theta) * \sin(\xi) * \Delta\xi * \Delta\zeta} \tag{4.13}$$

The integration limits for the slice angle ξ are constantly 0 and π. The height angle ζ is to consider for the sky and ground vault separately. The integration limits for ζ vary with the inclination angle of the window η (Fig. 4.1).

$$\tau_f = \frac{\sum_{-\eta}^{0}\sum_{0}^{\pi} L_{gr} * \cos(\theta) * \sin(\xi) * \tau(\theta) * \Delta\xi * \Delta\zeta + \sum_{0}^{\pi-\eta}\sum_{0}^{\pi} L_{sky} * \cos(\theta) * \sin(\xi) * \tau(\theta) * \Delta\xi * \Delta\zeta}{\sum_{-\eta}^{0}\sum_{o}^{\pi} L_{gr} * \cos(\theta) * \sin(\xi) * \Delta\xi * \Delta\zeta + \sum_{0}^{\pi-\eta}\sum_{0}^{\pi} L_{sky} * \cos(\theta) * \sin(\xi) * \Delta\xi * \Delta\zeta} \tag{4.14}$$

The radiances of the sky L_{sky} and ground L_{gr} due to equations (4.7) to (4.12) depend on the angles h_p, ε and μ. These angles can be related to the integration angles ξ and ζ considering the following geometrical conversions (see also Fig. 4.2):

$$h_p = \arcsin\left[\sin(\xi) * \sin(\zeta)\right] \tag{4.15a}$$

$$az_p = \arctan\left[\sin(\xi) * \cos(\zeta) / \cos(\xi)\right] \tag{4.15b}$$

$$\varepsilon = 0.5 * \pi - h_p \tag{4.15c}$$

$$\mu = \arccos\left[\sin(h_s) * \cos(\varepsilon) + \cos(h_s) * \sin(\varepsilon) * \cos\left|az_s - az_p\right|\right] \tag{4.15d}$$

In equations (4.15) h_p is the height angle of a certain sky point above horizon, az_p is its azimuth angle and az_s is the azimuth angle of the sun. The incidence angle θ of a radiation portion is given by equation (4.16):

$$\theta = \arccos\begin{bmatrix} \cos(h_p) * \cos(az_p) * \cos(0.5 * \pi - \eta) * \cos(az_w) + \\ \cos(h_p) * \sin(az_p) * \cos(0.5 * \pi - \eta) * \sin(az_w) + \\ \sin(h_{p)} * \sin(0.5 * \pi - \eta) \end{bmatrix} \tag{4.16}$$

where az_w is the azimuth angle of the window surface. After substituting equations (4.15) and (4.16) into (4.14) the last remaining unknown variable (only needed for clear sky simulations) is the sun height h_s. It is calculated by GLSIM-DIF in consideration of fundamental astronomical relations found in DIN 5034 (1983).

When a window lies in the area of dense buildings (city centre) or in an area with a high horizon (e.g. in a valley), the influence of obstructions on the diffuse radiation transfer can become considerable. Within GLSIM-DIF the problem was solved by changing the integration

limits of the height angle ζ assuming that the radiance of the obstructions corresponds to that of the ground (see also IR3). This is appropriate as ground and buildings often have reflectances of similar amount e.g. 0.2.

The uncertainty in the predicted diffuse glazing transmittance and absorptance values depends on the uncertainties of the sky models used. These were not investigated within this work. The danger of programming errors lie mainly in the complicated trigonometric relations, which were carefully tested using plausibility cheques. These are not described here.

4.3 APPLICATION FOR THERMAL SIMULATIONS

The new program module GLSIM-DIF was developed as a pre-processing program, which produces more accurate diffuse glazing properties. The program predicts the diffuse transmittance and absorptance rather than equivalent incidence angles. The diffuse transmittance and absorptance can be directly used as input values for DSMs. However, there are important differences between the predicted diffuse glazing properties for overcast or clear skies, which require program inputs at different level of detail.

In the following sections, the dependence of diffuse radiation properties on the sky conditions are discussed. To exemplary demonstrate diffuse glazing properties, a clear double glazing system consisting of two 6 mm glass panes (refractive index = 1.52; extinction coefficient = 0.025 1/mm) is used. The glazing has a transmittance for direct normal radiation of 0.627.

4.3.1 Overcast sky conditions

On an overcast day the sky radiance depends only on the height of a sky point above the horizon. It is for all directions the same and the relative relations are independent of the sun position. The diffuse glazing properties are therefore only dependent on the surface inclination and ground reflectance (Fig. 4.3).

The dependence of the diffuse transmittance on the surface inclination is very pronounced. The transmittance varies by 0.07 for clear double glazing (between 0.60 and 0.53, Fig. 4.3), which leads to differences in the predicted diffuse radiation energy flows of more than 10%. The variation of the diffuse absorptance is less important. It is not shown here.

The diffuse transmittance for overcast days can easily be considered by many DSMs, which use one fixed value for the diffuse transmittance (and absorptance). A diagram was produced (by GLSIM-DIF), which shows the equivalent beam radiation incidence angle rather than the diffuse transmittance values (Fig. 4.4). It can be used to derive the diffuse transmittance for different clear glazing systems. It also shows, that the influence of the number of

layers in the glazing is small. The curve for double glazing corresponds to that for triple glazing.

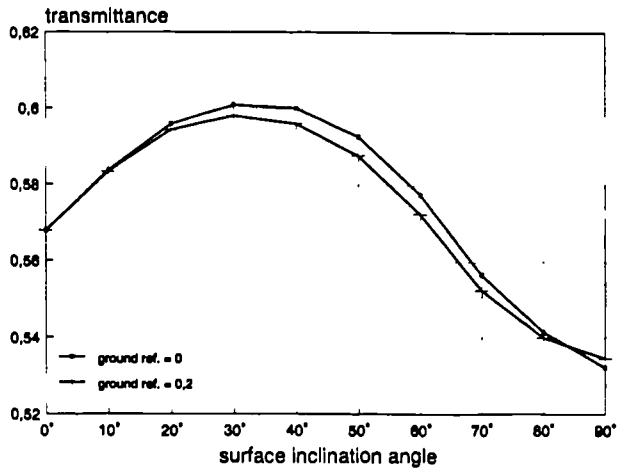

Figure 4.3:

Variation of the diffuse transmittance of clear double glazing on an overcast day as the surface inclination angle (90° - vertical; 0° - horizontal) and ground reflectance is varied. The direct normal transmittance of the glazing is 0.627.

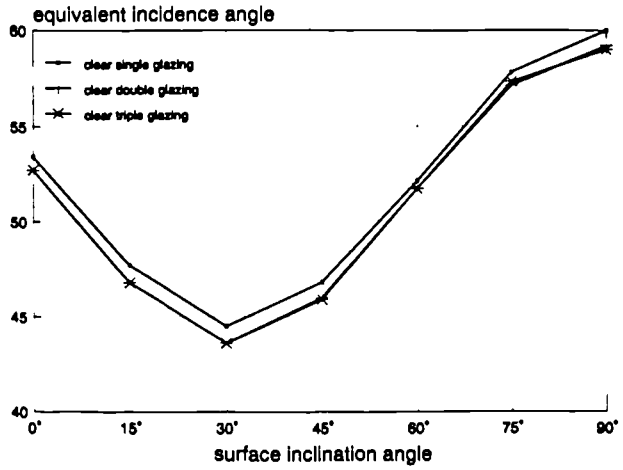

Figure 4.4:

Variation of the equivalent beam radiation incidence angle on an overcast day as the surface inclination angle (90° - vertical; 0° - horizontal) and glazing type is varied (ground reflectance = 0.2).

It is worth noting, that the equivalent incidence angle for the clear glazing systems varied between 44° and 60°, which is for some circumstances very different from the value of 60° recommended by ASHRAE 1981. However, the value for vertical glazings was about 59°, which corresponds well to the recommended value of 60°. Thus, the conventional diffuse radiation treatment seems to represent the diffuse radiation conditions on vertical glazings on overcast days.

The equivalent beam radiation incidence angles for the most important types of special (tinted and coated) glazing and vertical windows are shown in Appendix C (see also Chapter 5). The values vary from 56° to 63° which is considerable. A tilt correction had been introduced, which can be used to approximate the diffuse transmittance for any given inclination angle and glazing type (see Appendix C).

4.3.2 Clear sky conditions

Since the radiance of the clear sky depends on the sun position, the clear sky diffuse radiation properties additionally depend on the time of day (Fig. 4.5). On sunny days, the brightness of the sky is highest near the sun (circumsolar radiation). This leads to an effective incidence angle of the diffuse radiation, which is comparable to that of the direct beam (i.e. the diffuse transmittance of a vertical, south orientated glazing has a maximum at noon, when the solar radiation incidence angle is smallest).

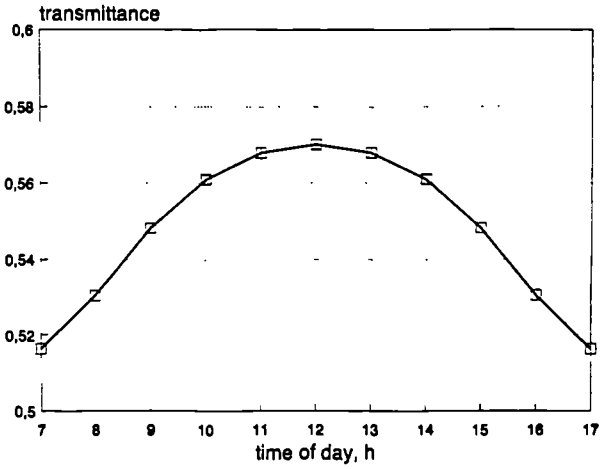

Figure 4.5:

Hourly values for the diffuse transmittance of a vertical clear double glazing on a clear day (location: Kew; date: 21/3; ground reflectance = 0.2). The direct normal transmittance of the glazing is 0.627.

Although some DSMs permit a hourly scheduling of glazing properties (e.g. HTB2), the use of this facility could mean an unpractically high input effort (especially in the case of annual simulations). Further, the incorporation of the numerical solution technique into the thermal simulation would disproportionately increase the simulation time. Therefore, effective diffuse transmittance (and absorptance) values were introduced, which correspond to the solar-energy weighted average of a defined example day. The averaging method considers standard hourly radiation intensities calculated using DIN 5034 (1983). The thermal consequence of this assumption was investigated in a sensitivity study (section 4.4). The effective diffuse transmittance (absorptance) values depend on the window location (inclination, orientation, ground reflectance) and season. In comparison with the yearly swing, the variation of values within one month is less important (Fig. 4.6). For thermal simulations it is therefore possible to consider one example day for each month or even to be satisfied with one example day for each season. The variation between the value at noon (time of the highest diffuse radiation intensity) and the daily effective value is nearly independent of the season and with 0.01 small (Fig. 4.6).

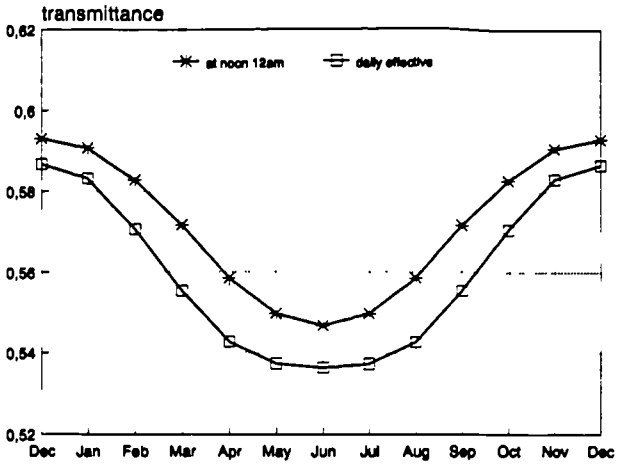

Figure 4.6:

Seasonal variation of the effective diffuse transmittance of clear double glazing for clear example days at Kew (the 21th of every month). The glazing is vertical and south-facing. The ground reflectance is 0.2.

4.3.3 Average sky conditions

Annual simulations require the specification of one value for the diffuse transmittance (and absorptance) on overcast days and, for clear days, either twelve monthly values for the effective diffuse transmittance (and absorptance), or, twelve sets of hourly values for the effective diffuse transmittance (and absorptance). These values must be given for every window separately. During the thermal simulation the DSM must decide whether to use the values for the overcast skies or for the clear skies.

Different algorithms within DSMs require the distinction between clear and overcast sky conditions (e.g. algorithms for external longwave radiation exchange). Therefore, DSMs often consider a cloud-cover (or sky clearance) statement, which is provided by the climate file or calculated internally based on a weighting of the direct and diffuse radiation components. The statement is also used to interpolate between the idealised clear and overcast sky conditions to consider partly-cloudy skies (average skies). For example, ESP uses the following algorithm to calculate the cloud-cover *cc* from the irradiation data in the climate file:

$$cc = 1 - \left(\frac{I_f}{I_d + I_f} \right)^2 \tag{4.17}$$

where I_d and I_f are the direct or diffuse radiation intensities on horizontal respectively.

The cloud-cover statement is suitable to switch from clear to overcast diffuse transmittance (absorptance) values (used for the calculations) or to interpolate between them. The method is simple and easy to implement. It was illustrated using the program HTB2.

The interpolation between clear and overcast sky conditions does only approximately reflect the situation on a partly-cloudy day. The complex sky radiance distribution on a partly-cloudy day excludes a detailed consideration within thermal simulations. The application of a cloud-cover statement to interpolate between clear and overcast sky conditions is only

appropriate for long-term simulations. This approach is similar to statistical methods used for daylight problems, which consider a sun shining probability to take account on changing weather conditions (Aydinli 1981).

It should be noted that DSMs are widely used for the design of heating and cooling systems or for comfort predictions, which requires the simulation of extreme climate conditions (e.g. extremely hot or cold design days). Such calculations normally consider either clear or overcast sky conditions. Hence, for these calculations the improved diffuse glazing properties can be used without having problems due to changing weather conditions. Various DSMs can therefore take advantage of the improved properties without any modification to the program structure.

4.4 SENSITIVITY OF PREDICTIONS TO DIFFUSE GLAZING PROPERTIES

4.4.1 Building description

The thermal consequences of using the improved diffuse glazing properties rather than conventional values, was investigated by studying the thermal performance of the simple direct-gain test room used in previous studies (Appendix A.1, see also Chapter 2). The test room corresponded to a typical UK living-room with an advanced highly-insulated and heavy-weight construction (average U-value of 0.3 W/m²K). It was well sealed and had a low infiltration rate of 0.35 ach. A large clear double glazed window of about 14 m² (which corresponded to the total wall area) was adopted. The glazing system consisted of two 6 mm glass panes with a refraction index of 1.52 and an extinction coefficient of 0.03 1/mm. The glazing had a normal transmittance of 0.59. To enhance the sensitivity of the thermal conditions in the room to the diffuse radiation energy gains on sunny days, the orientation was chosen to be north. The room was continuously heated to 21°C or (for cooling energy predictions) cooled to 30°C. The cooling energy demand prediction was added to demonstrate the sensitivity of the algorithms to the predicted performance of commercial buildings, where cooling equipment is often used.

The room was located at Kew near London (UK): latitude = 51.5° North; longitude = 0°. It was unobstructed with respect to the wind and sun (no shading from other buildings was considered).

The study concentrated on the influence of different window inclination angles (0° - horizontal; 30°; 60°; 90° - vertical) on the predicted daily heating energy demand, daily peak air temperatures and daily cooling energy demand. The affect of different glazing types on the diffuse radiation transfer has not been considered within this study. This was done as part of a sensitivity analysis when special glazings were studied (Chapter 5).

For the daily simulations, the six UK design days generated by Loxsom (1985) were used: an overcast day in January; a sunny day in January; an overcast day in April; a sunny day in April; an overcast day in July; a sunny day in July (Appendix B). The design days represent either pure overcast or pure clear sky conditions. Thus, the influence of the different diffuse glazing properties on clear and overcast days could be studied separately. All the results are described in detail elsewhere (IR7).

4.4.2 Programs used

The investigation concentrated on the program HTB2, which was provided with all necessary input and calculation possibilities. These were:

(i) an input of two different diffuse transmittance and absorptance values - one for overcast and one for clear skies (the hourly time-scheduling of these values was already provided by the basic program);

(ii) the calculation of a cloud cover statement using equation (4.17); and

(iii) a routine, which interpolates between the properties for overcast and clear skies weighted by the cloud cover.

Two methods for calculating the diffuse glazing properties have been compared within this study: (a) the conventional approximate treatment; and (b) an improved treatment.

The conventional treatment uses a fixed equivalent direct radiation incidence angle of 60° as recommended by ASHRAE (1981) and as used by the program SERI-RES. The diffuse transmittance of the clear double glazing (for an equivalent incidence angle of 60°) is 0.481. The absorptance at an incidence angle of 60° is 0.341.

The improved treatment considers the influence of window orientation, inclination and sky conditions as calculated by GLSIM-DIF.
For clear sky conditions, two different calculation possibilities were compared:

(i) a rigorous dynamic treatment, which uses hourly values for the diffuse properties; and

(ii) effective daily energy-averaged diffuse properties, (these were only used in a small, subsidiary, study).

4.4.3 Consequences on overcast days

Generally, on overcast days, the diffuse transmittance values predicted by the two diffuse radiation treatments were nearly the same for vertical windows. The diffuse transmittance predicted by GLSIM-DIF was about 0.487 which corresponds to the value for direct transmittance at an incidence angle of about 59°. These values are close to those produced by the conventional treatment: 0.481 or 60° respectively. This good agreement for vertical glazing has already been mentioned in section 4.3.1 (see Fig. 4.4).

For non-vertical windows, GLSIM-DIF calculated the following diffuse transmittance values at an inclination of: 60° - 0.526; at 30° - 0.552; and at 0° - 0.521. These values are clearly higher (by up to 0.071) than the value of 0.481, used in a conventional treatment.

GLSIM-DIF predicted similar diffuse absorptance values of 0.32 for all inclination angles. These were about 0.02 lower than the value used by the conventional treatment (0.34).

Since the diffuse transmittance due to the two different diffuse radiation treatments nearly agreed for vertical windows, the predicted energy demand and peak temperatures were approximately the same. Thus, the conventional treatment correctly represented the diffuse radiation transfer through vertical windows. It should be noted, that this result was obtained for clear double glazing only. It may not necessarily be true for special (tinted or coated) glazings, which have quite different radiation transmission characteristics.

For non-vertical windows and overcast days, the conventional treatment led to an underestimation of the solar gains. Therefore, the improved treatment generally calculated higher temperatures (Fig. 4.7), lower heating energy demands and higher cooling energy demands. The differences were largest for window inclinations of about 30°, they reached more than 15% for the daily heating energy in April (Fig. 4.8) and up to 2 K in the predicted peak temperatures in July (Fig. 4.7). The differences in the predicted peak air temperatures (and energy demands) increased from winter to summer. This may be expected, since the intensity and the duration of solar radiation is greatest in summer.

Clearly, such discrepancies in the predicted heating energy demands or air temperatures, could lead to inaccurate statements about the energy benefits of the glazing or about the thermal comfort in the room. Moreover, this result was obtained for a simple shoe-box type of room. In the case of highly glazed spaces such as conservatories or atria the differences are likely to be even higher.

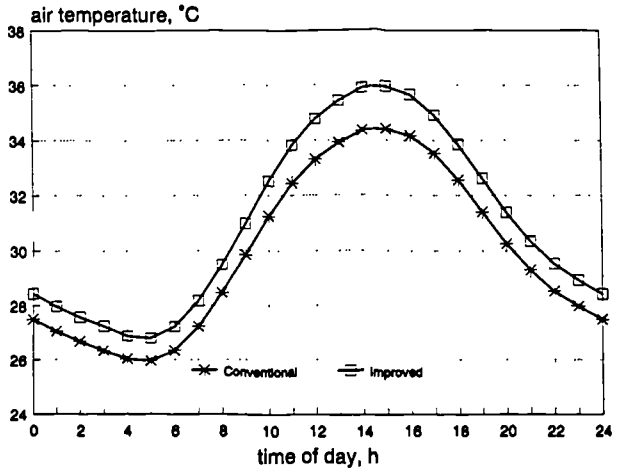

Figure 4.7:

Predicted daily temperature variations for the conventional and improved diffuse radiation treatment on an overcast day in July (window inclination = 30°).

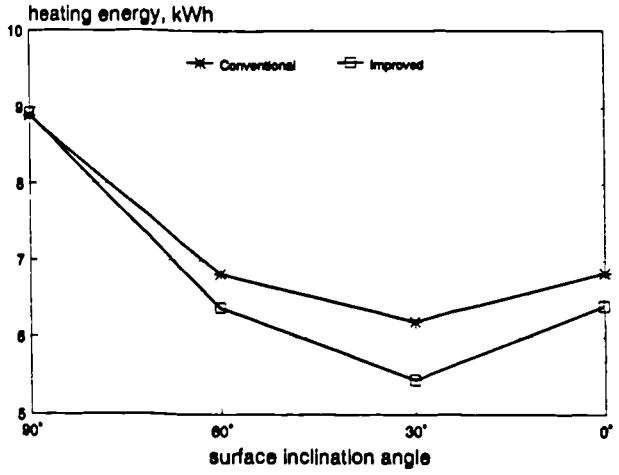

Figure 4.8:

Predicted influence of the window inclination angle on the daily heating energy demand (overcast day in April).

4.4.4 Consequences on sunny days

On a sunny day, the direct beam radiation has more energy than the diffuse radiation. This reduces the sensitivity of the internal thermal conditions to the diffuse radiation. Hence, any inaccuracy in the predicted diffuse energy gains are less important than on overcast days. This was confirmed by auxiliary studies looking at south and west orientated windows. These are not shown here.

The investigation shown here concentrates on north orientated windows, which hardly get any direct radiation. The hourly diffuse transmittance values predicted by GLSIM-DIF (improved treatment) for north-facing windows of varying inclination are summarised in Table 4.1. The highest diffuse transmittance always occurred at 12:00 (noon), the lowest value occurred at about 7am and 5pm (in January at sunrise and sunset).

diffuse transmittance	τ_f in winter (January)		τ_f in spring (April)		τ_f in summer (July)	
inclination angle	highest	lowest	highest	lowest	highest	lowest
90° (vertical)	0.508	0.504	0.500	0.476	0.496	0.480
60°	0.516	0.513	0.502	0.485	0.502	0.483
30°	0.537	0.525	0.543	0.488	0.543	0.501
0° (horizontal)	0.431	0.42	0.486	0.419	0.511	0.420

Table 4.1: Daily variation in the diffuse transmittance of north-facing clear double glazing on clear days as the window inclination angle and season is varied.

The predicted diffuse transmittance values differ by up to ± 0.062 from the value of 0.481 produced by the conventional treatment. The values for vertical windows were close to 0.481 on all the days. (The highest difference was 0.03 at noon in January.) This result is similar to that obtained for overcast days (section 4.4.3).

The predicted diffuse absorptance values were (for all cases) between 0.31 and 0.32. This is 0.02 to 0.03 lower than the value produced by the conventional treatment (0.341).

Generally, the improved model predicted slightly higher solar gains. However, the impact on internal temperatures or cooling energy predictions was small. In July the differences in the predicted cooling energy demand reached 5% for a window inclined at 30° (Fig. 4.9).

The small impact would be expected because the conventional treatment produced diffuse transmittance values which were too low (on average by 0.04), but at the same time generated diffuse absorptance values which were to high (by 0.02 to 0.03). These errors compensate to a certain extend.

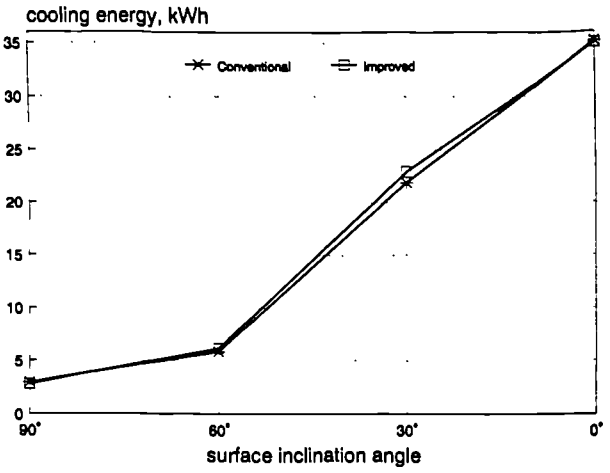

Figure 4.9:

Predicted influence of the window inclination angle on the daily cooling energy demand on a clear day in July (window orientation is north).

In an auxiliary study, the use of daily, rather than hourly, effective diffuse transmittance values was investigated. This study concentrated on the predicted cooling energy demand and peak air temperatures on a clear day in July as the window inclination angle was varied. The cooling energy demands and peak air temperatures predicted by the effective daily values were very close to those predicted by the hourly values. Since the predictions were approximately the same, they are not shown here. Effective daily glazing properties are obviously a good alternative to the very rigorous treatment, which produces a large amount of program input data (8760 values for each window for an annual simulation).

CHAPTER 5

RADIATION TRANSFER THROUGH SPECIAL GLAZING

5.1 INTRODUCTION

Because the direct radiation energy transport into and out of buildings through the glazing is often many times greater than the conductive energy transport through the solid elements, an accurate knowledge of the direct radiation transfer through glazings is essential in order to obtain accurate simulation results. This becomes more important as the levels of insulation in the opaque elements increase, as greater areas of glazing are used, or as the use of special glazings increases (in both domestic and commercial buildings).

It has been shown in Chapter 2 (section 2.4.2) that DSMs normally consider the direct radiation transfer through glazings very accurately because this phenomenon is known to have a big influence on thermal performances. They normally calculate the radiation transfer of the diffuse and direct radiation separately. For the direct radiation the incidence angle dependent transmittance and absorptance values are used. In the case of clear glazing these values are well known and can be easily predicted based on the Fresnel equations (see DIN 1349, 1972). For special glazing however (coated low-emittance, sun-reflective solar control glazing, absorbing tinted glazing) these values are normally unknown. If the angle dependent properties of clear glazing are assumed to be true for special glazing, the radiation transfer is described quite accurately up to an incidence angle of about 40°, but for higher incidence angles - which is the normal case in Europe - the assumption is only a rough approximation (see Fig. 2.12 in section 2.4.2). Unfortunately, manufacturers rarely quote the incidence angle dependent properties of their products.

It was found, that the derivation of more accurate properties for special glazings requires solutions to the following three issues.

(i) A calculation technique is needed, which considers the radiation transfer through thick layers (glass panes) as well as through thin layers (coatings).

(ii) The detailed (wavelength-dependent) optical constants (refractive and extinction indices) of the glass panes and coatings are needed.

(iii) In order to simulate a certain glazing system, the information about the detailed structure of the glazing (and coating) system is needed. For a coating system, the materials, their sequence, and their thickness must be known.

No computer program or calculation technique could be found, which offered an appropriate solution to all three issues.

- The program ESP-WIN (McLean 1981) permits a calculation of the radiation transfer through thin and thick layers. However, at the time of the investigation, the available program version (ESP-WIN V2.1 1988) did not cope correctly with all problem aspects. The calculation of the radiation transfer through thin films was restricted to normal radiation incidence only. For higher incidence angles, the program assumed total reflectance (zero transmittance), which was obviously wrong. In addition, the program offered no help for defining glazing systems, material properties were not provided and the input was complicated and user-unfriendly.
- Rubin (1982) presented a theory (and computer program) which, in principle, can calculate the radiation transfer through thin and thick layers from first principles using the optical constants and thicknesses. However, his thin film analysis concentrated on layers that are described in terms of their overall optical properties (transmittance and reflectance) rather than in terms of optical constants and thicknesses. He assumes, that thin film-coated samples should be described by overall optical properties rather than by their optical constants, since there are large variations in the reported values due to differences in deposition methods and process variables. He used a recursive formulation to derive the incidence angle dependent properties of multi-layered systems from the measured values for single layer systems. His theory for calculating thin layers from first principles is discussed in section 5.3.1.
- An extended database of glazing optical properties had been developed, which stores the properties of special glazing and coatings for normal radiation incidence (Reilly et al. 1992 (IEA Task 12 Subtask A.1)). Programs are available, which calculate the glazing properties for multi-layered glazing systems by considering these values (e.g. Wright and Sullivan 1992 (VISION3)). However, neither the database nor the computer programs consider the incidence angle dependence of the glazing properties.

The basic idea of an improved treatment was to use the producer quoted wavelength dependent transmittance and reflectance values of special glazings (e.g. Vegla 1985; Interpane 1990; Pilkington 1990) to derive the layer sequence and thicknesses of the coating systems. Parametric variations of the thin film materials, layer sequences and thicknesses could be used to adapt the predicted spectral properties to a certain measured characteristic. These could also show the sensitivity of the overall glazing properties to uncertainties in the basic glazing parameters (optical constants, layer thicknesses, materials etc.). A flexible calculation technique appeared to be necessary therefore, which would permit an easy definition of glazing systems and which could be applied to any combination of thick and thin layers.

Within this research work, the program-module GLSIM-FILM had been developed which calculates the wavelength and incidence angle dependent radiation transfer through coated and tinted glazing (see also GLSIM user manual 1994). The solution technique is based on the models of Harbeke (1986), and Heinz (1991), which calculate the radiation transfer properties of multi-layer structures. The models were modified to generate an equivalent application in the domain of window glazing and building simulation. The main feature of the modified model is its applicability to any combination of coatings (thin layers) and substrates (thick layers - in this case glass), without any limitation on the number or sequence of the layers.

This Chapter explains the theoretical basis of GLSIM-FILM and demonstrates its application to produce radiation transfer properties (wavelength and incidence angle dependent transmittance, reflectance and absorptance) of coated and tinted glazing. The validity of the model is demonstrated by comparing its predictions with measurements.

5.2 TYPES OF GLAZING

Modern sun- or heat-protective glazings consist of several glass panes with a combination of metal and/or metal oxide coatings. The coatings in a double glazed system are usually applied to the glass surfaces facing into the cavity.

Glazing systems may be divided into four categories (see also Groth 1977):

(i) glazings with a single pure noble metal coating;
(ii) tinted glass;
(iii) glazings with multi-layer coatings; and
(iv) glazings with single metal oxide coatings.

Noble metal coating is one of the oldest glazing treatment processes. Compared to clear glazings, systems with a noble metal coating have increased absorptance and reflectance in the visible range and a high long-wave reflectance. These glazings therefore reduce solar heat gain and light transmission. The metals used are mostly those with the highest electrical conductivity (copper, silver or gold). The colour of the coated glass is the same as that of the bulk metal. A layer thickness of around 10 nm is sufficient to reduce the emittance to less than 0.1 (Berning 1983). This reduced emittance decreases the U-value of the glass. Thus double glazing with a noble coating can have a U-value similar to that of clear triple glazing (i.e. 1.9 W/m^2K).

Tinted glass is used as the outer pane of the double glazed system. The tinting can produce various colours (e.g. green, grey, bronze). These glazing systems are heat absorbing in the solar radiation range and reduce both the heat and light transmission.

Because noble metal coatings reduce the transmission of visible light, such coatings are often combined with additional dielectric films (usually metal oxides) which selectively raise the transmittance over a chosen waveband. The noble metal may be combined with a single dielectric film or sandwiched between two such films (Gläser 1980, 1990). By the appropriate choice of coating, transmittance can be selectively raised in the range of highest eye sensitivity (550 nm). The reflectance is correspondingly reduced in this region whilst it remains high in the near infra-red range due to the metal layer. Glasses with multi-layered systems can be easily recognised by the pronounced reflection maximum in the near UV-range. This gives the glazing a slightly blue outside appearance (there are also other colour impressions possible). If the coating system is located at the outside of the inner pane, the high absorptance of the coating systems leads to a high secondary heat flow into the room. Such glazings have total solar energy transmittance values of more than 60% and are currently sold as heat-protective glazing.

This Chapter illustrates how GLSIM-FILM can be used for these three types of glazing system when only standard manufactures' data are available.

There are other types of coated glass which use non-metal film, such as single-layer coatings of conductive metal-oxide (tin oxide or indium-tin oxide) for highly transparent heat-protective glazing, or pure dielectric single-layer coatings (e.g. titanium dioxide) for sun-reflective glazing (Berning 1983; Dislich 1983). A homogenous characterisation of these systems is not possible, however, the derivation of the composition from known measured attributes is, in principle, possible. It is shown for one appropriate oxide coating system.

5.3 THEORY OF RADIATION TRANSFER THROUGH COATED GLAZING

5.3.1 Earlier work

The classical calculation approach to thin films handles the lightrays in a recursive way (summation of single lightrays) (e.g. Andres 1965). This approach meets the requirement for fundamental investigations of single films, which are often used as anti-reflective coatings for optical equipment such as spectacles, lenses, objectives etc. However, for multi-layered systems or combinations of films and substrates (glass panes), such a calculation becomes extremely complex.

Rubin (1982) presented a calculation technique for thin films which is based on a matrix multiplication approach. It considers the fundamental physical effects of electromagnetic waves (electric and magnetic field strength) in thin films. The radiation transfer formulation uses one total transfer matrix for every layer. The calculation of the radiation transfer though a layer pile requires the multiplication of a set of transfer matrices. This method is appropriate for any combination of thin films. However, it is not suitable for the calculation

of thick layers (glass panes). In thick layers the radiation transfer is described with the intensities of the transported energy (see section 5.3.2). Energy intensities need the separation of the radiation transfer through the layer interface and through the layer itself. This cannot be provided by total transfer matrices.

For the computer program GLSIM-FILM another possibility was chosen, which is based on the models of Harbeke (1986) and Heinz (1991). These models consider the radiation transfer through layers more rigorously. The solution method uses a matrix multiplication approach in which the effect on the radiation of each interface and of each layer is represented by individual matrices. The *interface matrix* represents the relationship between the amplitudes or intensities of the radiation fields on each side of the interface between two layers. The *layer matrix* describes the attenuation of the radiation as it propagates through a layer. Therefore it becomes possible to consider thin and thick layers with the same matrix multiplication approach. This makes the calculation technique very flexible and fast. In addition, it produces a clear formulation which can be programmed easily and built in by others. It also enables different glazing systems to be quickly modelled on a PC.

This section describes the key points of the theory upon which the computer program GLSIM-FILM is based. By considering the transfer of radiation through both coherent (optically thin) and incoherent (optically thick) layers as well as the effects of interference and absorption, it enables the total reflectance (ρ^T) and total transmittance (τ^T) of any combination of thin and thick layers to be determined. The term "total" means that the net reflectance and transmittance due to all of the layers comprising the glazing are being considered. A more detailed description of the theory is presented elsewhere (IR5; see also Pfrommer et al. 1995a).

5.3.2 Radiation transfer across an interface

In general, when light is incident upon the interface between two optically different materials, part of the light is reflected and part transmitted. If the medium on (what is nominally chosen to be) the outside (o) of the interface has a complex refractive index n'_o and the medium on the inside (i) has a refractive index n'_i, then, for a given wavelength of radiation, Snell's law states that

$$n'_o * \sin(\theta_o) = n'_i * \sin(\theta_i) \tag{5.1}$$

θ_o and θ_i being the angles of incidence and refraction.

For an incident wave of amplitude $\mathcal{E}_o^+$ travelling across an interface from outside to inside (the superscript denotes the direction of propagation), the amplitude reflection coefficient (r) and amplitude transmission coefficient (t) are defined as

$$(5.2) \qquad r_{oi} = \frac{\mathcal{E}_o^-}{\mathcal{E}_o^+} \qquad t_{oi} = \frac{\mathcal{E}_i^+}{\mathcal{E}_o^+}$$

where $\mathcal{E}_o^-$ and $\mathcal{E}_i^+$ are the amplitudes of the reflected and transmitted waves. Similar expressions hold for waves travelling in the opposite direction, for which it can be shown that

$$(5.3) \qquad r_{io} = -r_{oi} \qquad t_{oi} * t_{io} - r_{oi} * r_{io} = 1$$

The reflectance (ρ) and transmittance (τ) of an interface are defined in terms of the incident, reflected and transmitted beam intensities (I):

$$(5.4) \qquad \rho_{oi} = \frac{I_o^-}{I_o^+} \qquad \tau_{oi} = \frac{I_i^+}{I_o^+}$$

Plane-polarized radiation can be regarded as the superposition of two orthogonal plane-polarized waves with zero phase difference, one with the electric field normal to the plane of incidence (S-polarization), the other with the electric field parallel to the plane of incidence (P-polarization). The physical laws governing the reflection and transmission of radiation at an interface are different for each polarization and are given by the following Fresnel equations (DIN 1349, 1972):

$$(5.5) \qquad r_{oi}^S = \frac{n'_o * \cos(\theta_o) - n'_i * \cos(\theta_i)}{n'_o * \cos(\theta_o) + n'_i * \cos(\theta_i)} \qquad r_{oi}^P = \frac{n'_i * \cos(\theta_o) - n'_o * \cos(\theta_i)}{n'_o * \cos(\theta_i) + n'_i * \cos(\theta_o)}$$

$$t_{oi}^S = \frac{2 * n'_o * \cos(\theta_o)}{n'_o * \cos(\theta_o) + n'_i * \cos(\theta_i)} \qquad t_{oi}^P = \frac{2 * n'_o * \cos(\theta_o)}{n'_o * \cos(\theta_i) + n'_i * \cos(\theta_o)}$$

It can be shown that

$$(5.6) \qquad \rho^S = (r^S)^2 \qquad \rho^P = (r^P)^2$$

$$\tau^S = \frac{n'_i * \cos(\theta_i)}{n'_o * \cos(\theta_o)} * (t^S)^2 \qquad \tau^P = \frac{n'_i * \cos(\theta_i)}{n'_o * \cos(\theta_o)} * (t^P)^2$$

When calculating the radiation transfer properties of multi-layer systems (section 5.3.4) the total reflectance of the system (ρ^T) is found by averaging the reflectances determined from the two separate treatments of polarized radiation. The total transmittance (τ^T) is similarly found by taking the mean of the two polarized transmittances.

5.3.3 Radiation transfer through a single absorbing layer

The transmission of radiation through an absorbing material is characterised by the material's complex refractive index n' (Bergmann 1978):

$$n' = n - ik \tag{5.7}$$

The imaginary part of the complex refractive index, the absorption index k, is responsible for the absorption in the layer, the real part n describes the refraction. If a plane-polarized electromagnetic wave of electric field strength $\mathcal{E}$ propagates in the positive x-direction through the medium, then

$$\mathcal{E} = \mathcal{E}_1 * \exp\left[i\omega * \left(t - \frac{x * n'}{c}\right)\right] \tag{5.8}$$

where $\mathcal{E}_1$ is the initial amplitude of the wave, ω the angular frequency, t the time variable and c the speed of light in a vacuum. Substituting for n', equation (5.8) becomes

$$\mathcal{E} = \mathcal{E}_1 * \exp\left[i\omega\left(t - \frac{n * x}{c}\right)\right] * \exp\left[-\frac{\omega * k * x}{c}\right] \tag{5.9}$$

The imaginary part describes the phase of the wave and the real part its spatial attenuation.

To calculate the radiation transmission through an absorbing material it is necessary to distinguish between layers with a thin or thick optical path. A thin layer has a thickness of the order of the wavelength of light or less. The short path-differences between the waves interreflected between the interfaces of a thin layer mean that coherence of the waves is maintained, resulting in interference. The destructive interference which occurs leads to attenuation of the electric fields which manifests itself as absorption. It is therefore appropriate to consider the electric fields when modelling the transfer of radiation through thin layers.

When the thickness of a layer is greater than the coherence length of about 1500 nm disturbances along the path of propagation due to in-homogeneities in the material, disrupt the phases of the waves and destroy coherency. For thick layers it is therefore not possible to describe the radiation in terms of electric field strengths; instead the intensity (I) of the transported energy is used. The resulting reduction of the radiation intensity, referred to as *extinction,* is caused by absorption and scattering.

The attenuation factor (Δ_f) of a thin layer (film-f) relates the initial amplitude $\mathcal{E}_1$ of a wave *within* the layer to its final amplitude $\mathcal{E}_2$ as it propagates between the interfaces. If d is the layer thickness and λ the wavelength, then equation (5.9) leads to the following definition of Δ_f:

$$\Delta_f(d) = \frac{\mathcal{E}_2}{\mathcal{E}_1} = \exp\left[-i\frac{2*\pi}{\lambda}*n*d\right]*\exp\left[-\frac{2*\pi}{\lambda}*k*d\right] \tag{5.10}$$

For a thick layer (substrate-*s*), the attenuation factor (Δ_s) describes the reduction in intensity of the radiation from an initial intensity I_1 to the final intensity I_2 as it traverses the layer. Since intensity is proportional to the square of the wave amplitude,

$$\Delta_s(d) = \frac{I_2}{I_1} = \exp\left[-\frac{4*\pi}{\lambda}*k*d\right] \tag{5.11}$$

5.3.4 Radiation transfer through multiple layers

The propagation of radiation through multi-layer systems is normally represented by a recursive formulation which explicitly models the multiple inter-reflections between and transmissions through the interfaces. This is an appropriate technique for one or two layers, but for a greater number the formulation of the problem and its solution become extremely complicated.

An alternative approach is to calculate the transmission through the multi-layer system using transfer matrices (Harbeke 1986). Each matrix in an ordered sequence of matrix multiplications represents one of two possible transformations of the radiation fields; transformation due to:

(i) transmission across an interface (*interface matrix*);
(ii) transmission through a layer (*layer matrix*).

Polarization, multiple inter-reflections between the interfaces and the effects of wave interference are all accounted for in this model. Each layer can be either thick or thin.

a) The interface matrix

The definition of the interface matrix (*M*) follows from consideration of the boundary conditions at an interface.

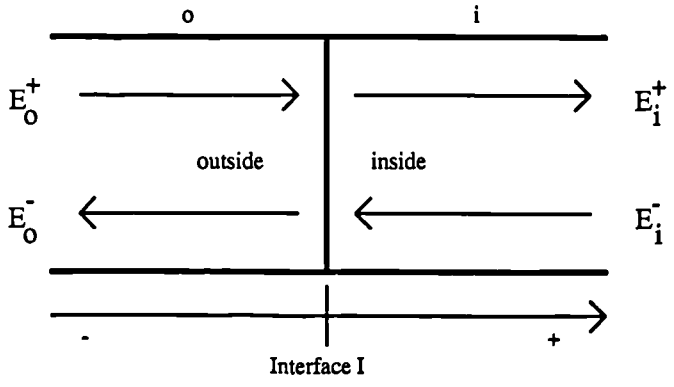

Figure 5.1:
The electric fields at an interface between two layers.

Let E_o^+ and E_i^+ represent the amplitudes of the *net* electric fields propagating towards and away from an interface in the direction from the outside to the inside medium (Fig. 5.1). E is the net field since it arises from the superposition of multiply inter-reflected and transmitted waves. E_o^- and E_i^- are the corresponding *net* electric fields travelling in the reverse direction. E_i^+ is then composed of the transmitted component of E_o^+ and the reflected component of E_i^-, and E_o^- consists of the transmitted component of E_i^- and the reflected component of E_o^+. Equations (5.2) and (5.3) enable this to be expressed mathematically as

(5.12)
$$E_i^+ = t_{oi} * E_o^+ + r_{io} * E_i^-$$
$$E_o^- = t_{io} * E_i^- + r_{oi} * E_o^+$$

or

(5.13)
$$\begin{bmatrix} E_o^+ \\ E_o^- \end{bmatrix} = \begin{bmatrix} \frac{1}{t_{oi}} & \frac{r_{oi}}{t_{oi}} \\ \frac{r_{oi}}{t_{oi}} & \frac{1}{t_{oi}} \end{bmatrix} * \begin{bmatrix} E_i^+ \\ E_i^- \end{bmatrix} = M_{oi}^{(E)} * \begin{bmatrix} E_i^+ \\ E_i^- \end{bmatrix}$$

When transmission across an interface is considered in terms of energy intensities, the following matrix equation is obtained.

(5.14)
$$\begin{bmatrix} I_o^+ \\ I_o^- \end{bmatrix} = \begin{bmatrix} \frac{1}{\tau_{oi}} & -\frac{\rho_{io}}{\tau_{oi}} \\ \frac{\rho_{oi}}{\tau_{oi}} & \tau_{io} - \frac{\rho_{io} * \rho_{oi}}{\tau_{oi}} \end{bmatrix} * \begin{bmatrix} I_i^+ \\ I_i^- \end{bmatrix} = M_{oi}^{(I)} * \begin{bmatrix} I_i^+ \\ I_i^- \end{bmatrix}$$

b) The layer matrix

The layer matrix (N) describes the attenuation of a wave as it traverses the medium *within* a layer. In thin layers (f) one is interested in the attenuation of the electric field strength and in thick layers (s) the attenuation of the intensity.

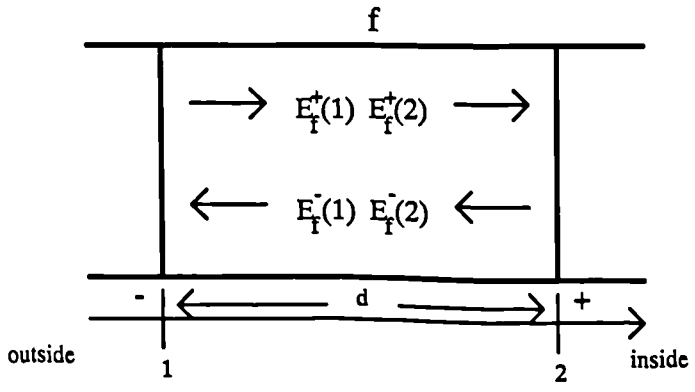

Figure 5.2:

Transmission through a thin absorbing layer of thickness *d*.

When a wave propagates in the positive direction between the interfaces of a thin layer, its initial amplitude at interface '1' $E_f^+(1)$ within the layer is attenuated to, say, $E_f^+(2)$ on reaching the interface '2' (Fig. 5.2). A wave of initial amplitude $E_f^-(2)$ travelling in the opposite direction through the layer is reduced to $E_f^-(1)$. If the layer has thickness d then, from the definition of attenuation factor in equation (5.10),

$$\begin{aligned} E_f^+(2) &= \Delta_f(d) * E_f^+(1) \\ E_f^-(2) &= \Delta_f(-d) * E_f^-(1) \end{aligned} \tag{5.15}$$

or

$$\begin{bmatrix} E_f^+(1) \\ E_f^-(1) \end{bmatrix} = \begin{bmatrix} 1 & 0 \\ \Delta_f(d) & \\ 0 & \Delta_f(d) \end{bmatrix} * \begin{bmatrix} E_f^+(2) \\ E_f^-(2) \end{bmatrix} = N_f^{(E)} * \begin{bmatrix} E_f^+(2) \\ E_f^-(2) \end{bmatrix} \tag{5.16}$$

For thick layers the layer matrix is similar, except that intensities rather than electric field strengths are considered.

$$\begin{bmatrix} I_s^+(1) \\ I_s^-(1) \end{bmatrix} = \begin{bmatrix} 1 & 0 \\ \Delta_s(d) & \\ 0 & \Delta_s(d) \end{bmatrix} * \begin{bmatrix} I_s^+(2) \\ I_s^-(2) \end{bmatrix} = N_s^{(I)} * \begin{bmatrix} I_s^+(2) \\ I_s^-(2) \end{bmatrix} \tag{5.17}$$

c) Matrix multiplication

The following equation set represents the transformation of the electric fields by a thin layer (f) sandwiched between a pair of outer (o) and inner (i) media (e.g. both air):

$$\begin{bmatrix} E_o^+ \\ E_o^- \end{bmatrix} = M_{of}^{(E)} * N_f^{(E)} * M_{fi}^{(E)} * \begin{bmatrix} E_i^+ \\ E_i^- \end{bmatrix} \tag{5.18}$$

In this multiplication of three matrices, the first and third being interface matrices, the second a layer matrix.

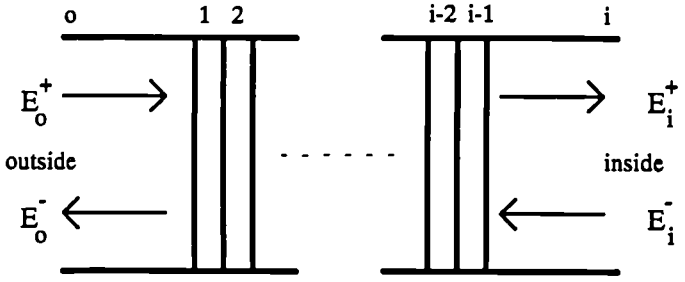

Figure 5.3:
The electric fields at the outer and inner interfaces of a multiple thin layer structure.

A system composed of a greater number of thin layers, say layers 1,2,...,q, sandwiched between media o and i (Fig. 5.3) would result in the transformation

$$(5.19)\quad \begin{bmatrix} E_o^+ \\ E_o^- \end{bmatrix} = M_{o1}^{(E)} * N_1^{(E)} * M_{12}^{(E)} * N_2^{(E)} * \cdots * N_{q-1}^{(E)} * M_{q-1,q}^{(E)} * N_q^{(E)} * M_{qi}^{(E)} * \begin{bmatrix} E_i^+ \\ E_i^- \end{bmatrix}$$

One can use equation (5.19) to obtain the total amplitude reflection and transmission coefficients R_{oi} and T_{oi} of the multiple thin layer structure. This follows by considering the surrounding media o and i to be of infinite thickness so that there is no net reflected wave in medium i incident upon the inner interface (i.e. $E_i^- = 0$). By setting E_o^+ to 1, equation (5.19) becomes

$$(5.20)\quad \begin{bmatrix} 1 \\ R_{oi} \end{bmatrix} = M_{o1}^{(E)} * N_1^{(E)} * M_{12}^{(E)} * N_2^{(E)} * \cdots * N_{q-1}^{(E)} * M_{q-1,q}^{(E)} * N_q^{(E)} * M_{qi}^{(E)} * \begin{bmatrix} T_{oi} \\ 0 \end{bmatrix}$$

which can be solved for R_{oi} and T_{oi}.

The corresponding equation for a sequence of thick layers is derived in terms of intensities, reflectances and transmittances, namely

$$(5.21)\quad \begin{bmatrix} 1 \\ \rho_{oi}^T \end{bmatrix} = M_{o1}^{(I)} * N_1^{(I)} * M_{12}^{(I)} * N_2^{(I)} * \cdots * N_{q-1}^{(I)} * M_{q-1,q}^{(I)} * N_q^{(I)} * M_{qi}^{(I)} * \begin{bmatrix} \tau_{oi}^T \\ 0 \end{bmatrix}$$

where ρ^T_{oi} and τ^T_{oi}, the variables ultimately being sought, are the total reflectance and transmittance of the structure.

To illustrate the method for calculating the total reflectance and transmittance of a multilayer system composed of both thin and thick layers, consider a single thick layer in air with the outer surface coated in a sequence of thin layers. The first step is to use equation (5.20) to calculate the total amplitude reflection and transmission coefficients (R and T) of the thin layer structure, the outside medium being air, the inner medium the thick layer. Equations (5.6) are then used to convert R and T to ρ^T and τ^T where, in this case, the refractive indices n'_i and n'_o, refer to the thick layer and the adjacent thin layer respectively. The thin layer structure is then treated as an *interface* of the thick layer and the interface matrix $M_{o1}^{(I)}$ formed using ρ^T and τ^T. Substituting $M_{o1}^{(I)}$ into equation (5.21) for $q=1$ yields the total reflection and transmission coefficients of the glazing. This procedure is performed separately for each of the S- and P-polarizations and the corresponding values averaged to give the full reflectance and transmittance.

To determine the spectrum averaged transmittance and reflectance for a particular angle of incidence, a weighted sum (integration) is performed over the desired bandwidth using the solar radiation distribution function (DIN 67507, 1980). The absorptance is obtained by taking the difference of the sum of the reflectance and transmittance from 1. Typically,

GLSIM-FILM would be used to calculate these wavelength dependent properties for normally incident solar radiation.

The flexibility of the above matrix formulation enables the angle dependent transmittances for the complete solar spectrum and for any type of glazing system to be found, provided the properties of the coatings are known.

5.4 MATERIAL PROPERTIES

The basic data necessary for calculating the overall properties of glazing systems are the wavelength dependent material properties (refractive and absorption indices) of the absorption and dielectric coatings (see Landlt-Bornstein 1962; Otter 1961; Palik 1985).

The dielectric coatings are mostly non-absorbing and show a relatively constant refractive index over the total solar spectrum. The refractive index lies between 2.0 and 2.5 depending on the material used (normally metal oxides). The representation of the absorbing low-emittance noble metal films like gold, silver or copper is much more complicated. The optical properties of these coatings are highly dependent on the wavelength of the incident light and on the material used. The refractive and absorption indices differ considerable from the constants of the bulk material and depend also on the film thickness (Pulker 1984). For a few exemplary coatings these dependencies are measured and presented as material values (Landlt-Bornstein 1962; Memarzadeh et al. 1988), but in practise different manufacturing processes can lead to a variation in these properties (possibly even within a single pane). The accuracy with which thin noble metal films can be modelled is limited by these practical considerations. It is important to stress, however, that these difficulties also limit the generality with which the physical measurement of one example sheet of glass can be used as a reference for a certain glazing system.

Investigations using GLSIM-FILM have shown, that the uncertainties in the optical constants of metal and oxide films (as well as of glass panes) clearly influence the wavelength dependent transmittance and absorptance for normal radiation incidence as well as the overall glazing properties. However, the differences rarely influence the curve defining the relationship between the glazing properties and the incidence angle. By knowing the usual producer quoted values for normal incidence, sufficiently accurate incidence angle dependent glazing properties for the use within DSMs can therefore be derived.

The calculation of the radiation transfer through clear and tinted glass also requires a knowledge of the wavelength dependent optical constants (refractive and absorption indices). These constants can be back-calculated from measurements of the spectral transmittance and reflectance at various wavelengths. The calculation considers the application of equation (5.21) on one single glass pane. The resultant equation (5.22) is then inverted to

calculate the basic optical constants n and k of the glass pane (for a given wavelength) from the spectral transmittance τ^{T}_{oi}, and reflectance ρ^{T}_{oi}. The detailed mathematical formulation is not shown here.

$$\begin{bmatrix} 1 \\ \rho^{T}_{oi} \end{bmatrix} = M^{(I)}_{o1} * N^{(I)}_{1} * M^{(I)}_{1i} * \begin{bmatrix} \tau^{T}_{oi} \\ 0 \end{bmatrix} \tag{5.22}$$

The wavelength dependent transmittance and reflectance values are presented in many technical descriptions produced by glazing manufacturers (e.g. Vegla 1985; Interpane 1990; Pilkington 1990).

An extensive database of the most important glass panes (clear, grey, green, bronze), absorbing metal films (gold, silver, copper) and dielectric films (metal oxides, metal sulphides) was created and incorporated within the program GLSIM-FILM. The available data are fully presented in the GLSIM user manual 1994.

5.5 APPLICATION AND VALIDATION

5.5.1 Wavelength dependent properties

The wavelength dependent glazing properties are responsible for the special characteristics of the glazing such as solar radiation and light transmittance, reflectance and colour impression. By varying the materials, their thicknesses and the sequence of coatings, a glazing can be adapted to a desired characteristic. Similarly, by parametric variations, the wavelength dependent properties predicted by GLSIM-FILM can be adapted to a certain measured characteristic. It was valuable to test the validity of the GLSIM-FILM predictions of the wavelength dependent properties. This was done in consideration of measured curves presented by Gläser (1980, 1990); Groth (1977); Dislich (1984); Hutchins (1988) and Vegla (1985). The method of varying parameters proved to be suitable for deriving unknown parameters (normally layer thicknesses and material types) from known measured spectral glazing properties.

As an example, the results of one study is shown here: the predicted transmittance and reflectance values of the coated double glazing system Eliotherm Cosmos® are compared with measured values presented in Vegla (1985) (Fig. 5.4). The glazing consists of clear glass panes with a thickness of 2 x 6 mm (normal transmittance = 0.4). The coating system was assumed to be a typical example of multi-layer systems with selective qualities. In this case, the interference layers are designed to minimise reflection in the visible light range and permit a maximum transmission at a wavelength of 550 nm. This is the best case for a high light transmittance. The reflection maximum at 380 nm (which is caused by an interference

effect in the protective layer) is very pronounced (Fig. 5.4) and gives the glazing a slightly blue outside appearance.

The best results were achieved by the following coating system (from outside to inside):

metal oxide (n = 2.3)	31 nm	(adhesive layer between glass and silver);
silver	17 nm;	and
metal oxide (n = 2.3)	47 nm	(protective layer between silver and air).

For the silver layer the optical constants of the bulk material were used.

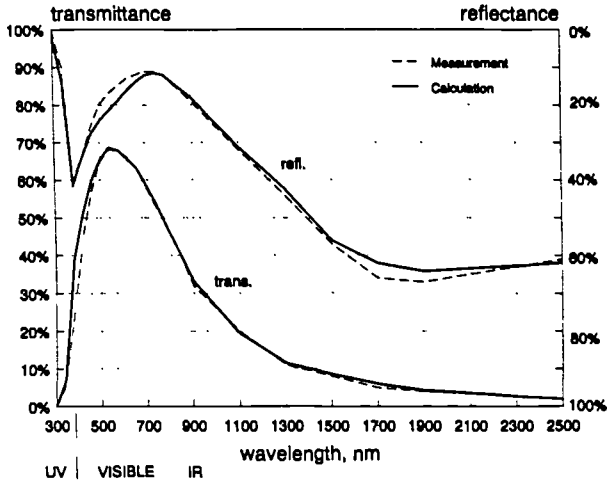

Figure 5.4:

Comparison of the calculated spectral radiation properties τ, ρ of the coated glazing Eliotherm Cosmos® with measurement values. The coating system consists of one silver and two metal oxide layers located on the inside of the outer pane.

5.5.2 The incidence angle dependent properties

A common problem when modelling glazings with coating systems is that the thickness of the layers and the optical constants of the individual films are needed. However, a special investigation showed that uncertainties in layer thicknesses and the choice of material *(optical constants) rarely influenced the curve defining the* relationship between the transmittance and absorptance and the solar incidence angle, provided a plausible layer thickness (which can be derived with the methods outlined in sections a) to d) below) and the correct layer type (noble metal or dielectric coating) was used.

It was found that most glazing systems could be divided into one of four groups:

(i) systems with single noble metal coatings;

(ii) glazings with multi-layered coating systems consisting of noble metal and dielectric coatings (usually metal oxides);

(iii) glazings with tinted glass panes; and

(iv) glazings with pure dielectric (oxide) coatings.

For each group, characteristic relationships existed between the angle of light incidence and the transmission properties. By knowing the usual (producer quoted) total transmittance

and reflectance for normal incidence and the characteristic incidence angle dependence of the glazing group the incidence angle dependence of the individual glazing system could be derived. The different relationships are presented in detail in the following sections (see also Pfrommer et al. 1993a).

To describe the shape of the transmittance versus incident angle curves, the relative (normalised) transmittance representation of Krochmann et al. (1992) has been used. The relative transmittance is simply the ratio of the transmittance at any given angle of incidence to the transmittance at normal incidence. All relative transmittance curves therefore vary from 1 (at 0° incidence) to 0 (at 90° incidence). The absolute transmittance is found by multiplying the relative transmittance values by the known, usually published, transmittance at normal (0°) incidence.

It should be noted, that the same method can also be used to describe other glazing properties: e.g. the relative absorptance and reflectance of the direct radiation (as calculated by GLSIM-FILM) or the relative transmittance, reflectance, and absorptance of the diffuse radiation (as calculated by GLSIM-DIF (Chapter 4)). The relative transmittance and absorptance values for most current glazing systems are presented in Appendix C. Since the transmittance is the most important glazing property, the discussion in the following sections concentrates on the relative transmittance.

It was useful to evaluate the calculated incidence angle dependent properties by comparing them with measurement values. However, all the available measured values are published with the reservation that there exists a high (but not defined) measurement uncertainty. Furthermore, the measured glazing systems were usually not described in detail. The comparisons presented here must be regarded with these limitations in mind. The large differences between the measured values quoted in different sources is a clear demonstration that more confident measurement values are needed for a thorough validation.

a) Pure noble metal coatings

The transmittance, absorptance and reflectance properties of glazings with noble metal coatings vary with the layer thickness, material type and the wavelength of light (Section 5.4). Sensitivity analyses using GLSIM-FILM have shown, however, that the angle dependent solar radiation transmittance properties are relatively insensitive to the precise values of the refractive and absorption indices, provided they are chosen from within the plausible ranges. Although the bulk optical constants (refractive and absorption indices) of different noble metal materials (Ag, Au, Co) differ considerably, all materials produced nearly the same relative transmittance curve. In addition, an investigation showed, that there was almost no difference in the predicted relative transmittance curve, if the optical constants of

the bulk metal were replaced by more accurately measured values (measured by Memarzadeh et al. (1988) as a function of the film thickness) for thin films.

Because, the normal transmittance depends almost entirely on the layer thickness (and to a limited extent, on the metal used), knowing the normal transmittance, which is usually quoted by manufacturers, the layer thickness can be estimated from Fig. 5.5, and hence the angle dependent curves can be predicted by GLSIM-FILM (Fig. 5.6). The metal used can be estimated from the known colour of the glass but it has little impact on the predicted curve (Fig. 5.6).

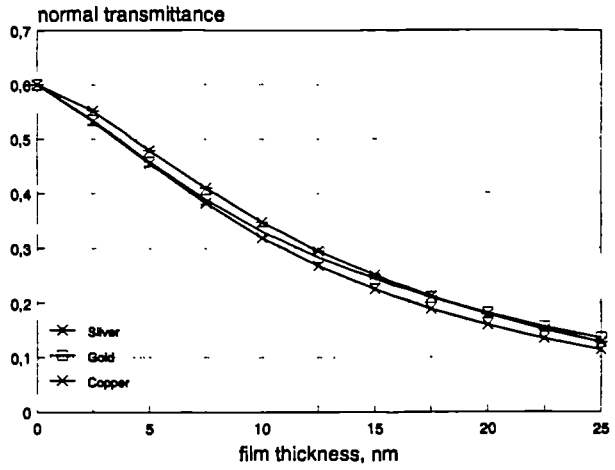

Figure 5.5:

Measured transmittance at normal incidence against film thickness of double glazings with single noble metal coatings.

The predicted relative transmittance curves for various thicknesses of noble metal layer lie above the corresponding curve for clear float glass (Fig. 5.6). However, the normal transmittance is less because the noble metal is present. For example, for clear double glazing the normal transmittance τ is about 0.6. By comparison, the values for the same system with 5 nm or 10 nm metal coatings are 0.48 and 0.33 respectively. Usually the absolute transmittance of the coated glazing at each angle of incidence is also less.

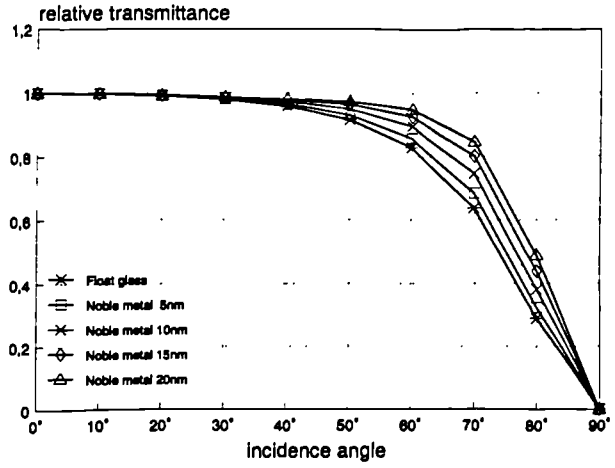

Figure 5.6:

Calculated relative transmittances of double glazing with a single noble metal coating of various thicknesses.

Once the film thickness is known and an estimate has been made of the metal type GLSIM-FILM will also produce angle dependent absorptance (and reflectance) curves. As said before, here, and in the discussions about other glazing systems only the more important transmittance values will be shown.

To validate GLSIM-FILM two measured transmittance curves for glazings with noble metal coatings were available. The measured and predicted curves are compared in Fig. 5.7. The measured values for Pilkington SunCool® glass (Pilkington 1988) were graphically presented in a public prospectus (no more informations was given). It was estimated, from the known normal transmittance of 0.16, that the silver coating was about 20 nm thick. Krochmann et al. (1992) quoted in detail the relative transmittance values of a 4 mm thick Infrastop-silber® glass pane. It was indicated that the glazing had a noble metal coating. However, the normal transmittance of the glazing was not given, nor could it be derived from other information sources. It was therefore not possible to determine exactly the noble metal layer thickness. There was however, a large deviation between the measured curve for Infrastop-silber® and the other curves (see Fig. 5.7). It is probable that the differences (and the curious shape of the measured curve) are due to measurement uncertainties.

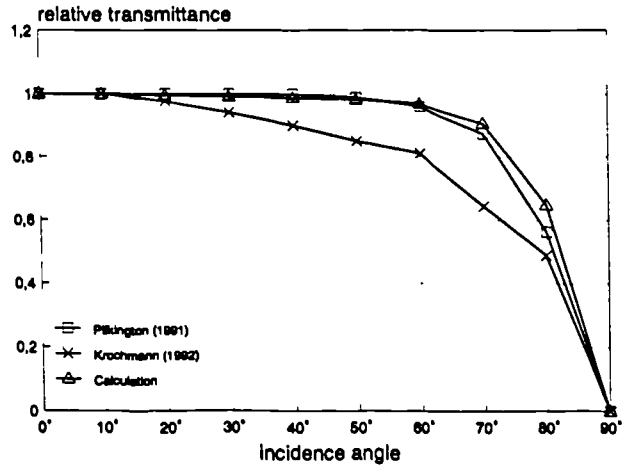

Figure 5.7:

Comparison between the calculated and measured relative transmittance of single noble metal coated glazings.

b) Multi-layer systems

To circumvent the lack of published data describing the materials and layer thicknesses used by manufacturers for multi-layer systems, an extensive examination of two- and three-layer coating systems was undertaken to establish the relationship between the incidence angle dependent transmittance curve of a coating system and its construction. The material and film thickness of each component were varied and the corresponding relative transmittance curves compared. Changes were made to the material of the noble metal film (Ag, Au, Co); the material of the metal oxide films (n between 2.0 and 2.5); the thickness of the noble metal films (10 - 20 nm) and the thickness of the metal oxide films (0 - 35 nm for the adhe-

sion layer and 20 - 50 nm for the protective layer). It was found that the relative transmittance values changed by less than ± 2%. Therefore, the investigation led to the simple result that all multi-layer coating systems, irrespective of the material and film thicknesses, had virtually the same relative transmittance curves. This is because the curve shape is determined entirely by the interface between the highly absorbing noble metal layer and the adjacent highly refractive dielectric layer. The individual values of the absorption and refractive indices are inconsequential. If there is a dielectric protective layer above the noble metal film, the adhesion layer between the glass and noble metal also has no influence on the curve shape.

The location of the layer system also has an insignificant influence on the transmission. The layers may be at the inside of the outer pane or at the outside of the inner pane. The location of the coating will influence the absorptance in each layer and this could be important when modelling the detailed thermal effect of the glazing. The curve shape which is appropriate for all multi-layer systems is shown in Fig. 5.8.

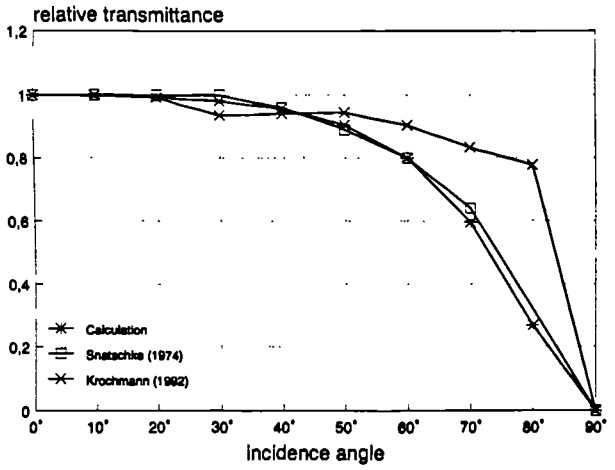

Figure 5.8:

Comparison between the calculated and measured relative transmittance of glazings with a multi-layer coating.

For comparisons purposes two different measurement curves were available. The measured values from Snatzke and Künzel (1974) relate to Infrastop-auresin® double glazing which was indicated by Gläser (1990) to be a three layer system (dielectric/ noble metal/ dielectric). In addition, Gläser published the wavelength dependent properties (transmittance and reflectance) of the glazing. These were also shown in a producers' prospectus (Flachglas AG 1975). The measured and calculated curves of Infrastop-auresin® are in close agreement (Fig. 5.8).

In contrast, the measured curve from Krochmann et al. (1992) for Infrastop-grün® 6 mm single glazing deviates highly from both the other curves. Infrastop-grün® was indicated by Krochmann et al. to be a metal oxide coated glazing. The coating system was assumed to be multi-layered (dielectric and noble metal films), because of the low-emittance quality quoted by the producer (Flachglas AG) and its green colour appearance, which is typical for additional dielectric (metal oxide) coatings; no more information was available. The high devia-

tion of the Infrastop-grün® curve from both of the other curves can hardly be explained by the uncertainty in the coating system. Again, measurement uncertainties are much more probable.

c) Heat absorbing glass

To investigate the wavelength dependent properties of heat absorbing glass, the sun-protective glazing Parsol® (Vegla 1985) was used. A comparison with other products (e.g. Pilkington 1988) showed that different types of glass with the same colour have similar wavelength dependent properties. Similarly, different types of glass of the same colour have nearly the same incidence angle dependent relative transmittance curves. Therefore the colour of a glazing can be used as a guide to derive the relative transmittance curve of a certain absorbing glass.

Unlike noble metal coatings, the relative transmittance curve of clear glazing is now the upper limit. That means, compared with clear glass, tinted glazing has a reduced relative transmittance (Fig. 5.9).

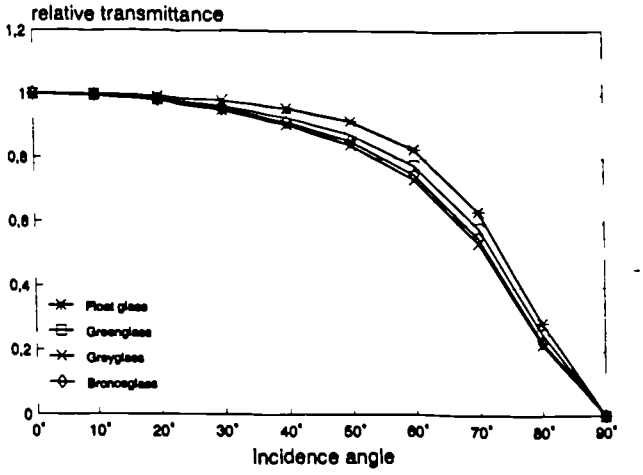

Figure 5.9:

Relative transmittance of double glazing with an absorbing (tinted) outer pane and its dependency on the colouration.

To validate the predicted transmittance curves for heat absorbing glasses, measured curves for green glass from Krochmann et al. (1992) and Snatzke and Künzel (1974) were used. The measured glass by Krochmann et al. was indicated as Parsol green® (Vegla 1985). The exact green glazing type measured by Snatschke and Künzel was not given. However, as indicated before, the relative transmittance curves only depend on the colour of the glazing, which for both glazings was the same (green). The calculated and measured curves are compared in Fig. 5.10.

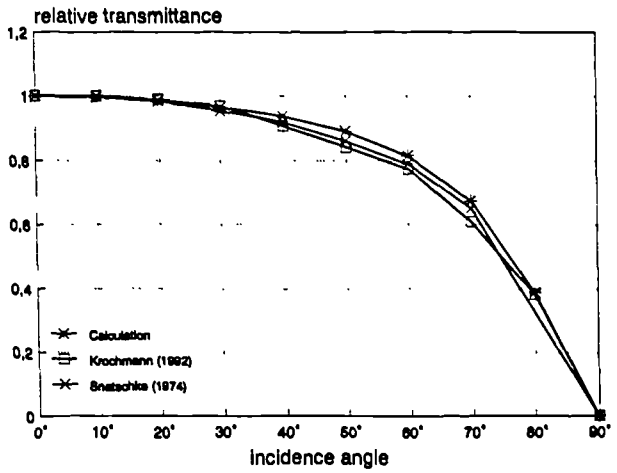

Figure 5.10:

Comparison between the calculated and measured transmittance of absorbing green glass.

d) Dielectric single coatings

The most simple coating systems, which are used to reduce or enhance reflectance in the visible light range, are single dielectric coatings. A homogenous characterisation of these systems, as presented for the previous glazing types, is not possible. One solution to finding the thickness of a single dielectric coating and the material used is to look at the wavelength dependent glazing properties for normal incidence. These properties are often published by the producers (see section 5.5.1).

By considering the physics of light in thin films (interference effects) the following formulations can be derived (j is the order of the reflectance extreme (0, 1, 2, 3, ...))

(5.23) For a maximum in the reflectance curve: $2*d*n = (j+0.5)*\lambda$

(5.24) For a minimum in the reflectance curve: $2*d*n = (j+1)*\lambda$

Noting that the refractive index of a dielectric coating is relatively insensitive to the wavelength, these equations can be used to predict the product of layer thickness and refractive index ($d\times n$) from the curve showing the variation of reflectance and transmittance with the wavelength of light. Again, inaccuracies in the material values and layer thicknesses are fairly inconsequential because the incidence angle dependent characteristics of the coating are relatively insensitive to the precise definition of the optical properties.

As an example, the predicted and measured curves for the sun-protective glazing Calorex AO® are compared (Figs. 5.11 and 5.12). This glazing consists of a single 6 mm pane coated on both sides with titanium dioxide using a dipping process (Dislich 1984). The wavelength dependent properties of the glazing were presented by Dislich as well as by the producer (Schott 1982) (Fig. 5.11). In this case the refractive index was approximately known (2.3 for titanium dioxide, see Memarzadeh et al. 1988). By considering the maximum in the reflectance curve, which occurs at a wavelength of about 550 nm, and by using

2.3 for the refractive index, equation (5.23) produces a layer thickness of about 60 nm. Using this thickness for the coatings on both sides of the glass pane (and a refractive index of 2.3), the wavelength dependent transmittance and reflectance curves predicted by GLSIM-FILM closely reproduced the values measured at the other wavelengths (Fig. 5.11).

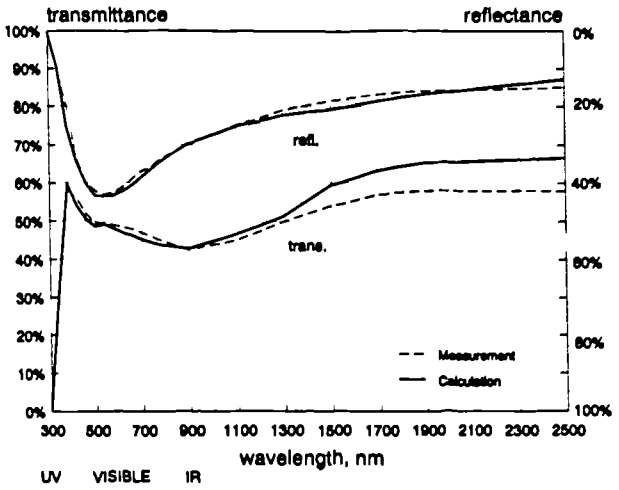

Figure 5.11:

Comparison of the calculated spectral radiation properties τ and ρ for the coated single glazing Calorex A0® with the measurement values. The glass pane is coated on both sides with titanium dioxide.

The relative transmittance curves predicted by GLSIM-FILM and measured values by Krochmann (1992) for Calorex A0® are compared in Figure 5.12.

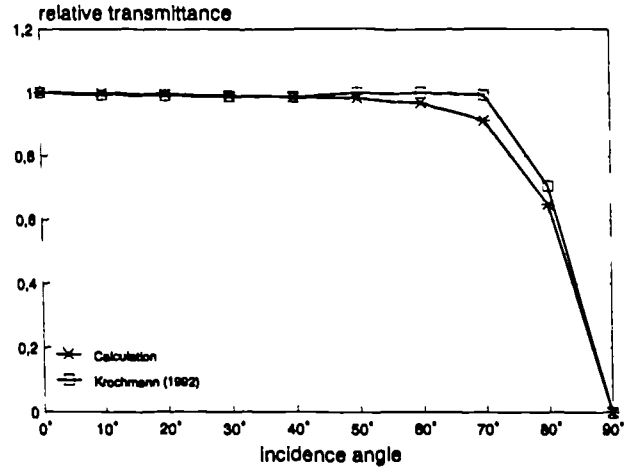

Figure 5.12:

Comparison between the calculated and measured relative transmittance of the sun-protective glazing Calorex AO®. The coating system consists of one metal oxide layer on each side of the pane.

This glazing has an extremely high relative transmittance right up to an incidence angle of 70°. Calculation of the transmission properties of this glazing by assuming it to be clear float glass would be very inaccurate (see Fig. 5.6 or 5.9). For example, at the incidence angle of 70° it would yield a relative transmittance which was approximately 60% of the measured value.

e) Other glazing systems

Most glazing systems fall into one of the four categories given in Sections a) to d) above, and their incidence angle dependent transmittance curves can be calculated using the meth-

ods outlined. A lack of data about the glass and the coating system often precludes predictions being made for other glazing systems. However, GLSIM is able to simulate them.

5.6 SENSITIVITY OF PREDICTIONS TO THE PROPERTIES OF SPECIAL GLAZING

The thermal consequences of using the improved glazing properties rather than conventional Fresnel-based values, was investigated by studying the thermal performance of the commercial building used in IEA Annex 21 work (IEA Task 12 & 21 C, Kataja and Kalema 1992). For the thermal simulations, the program HTB2 was used. HTB2 considers the angular-dependency of the incident radiation by using ten values of transmittance and absorptance for the incidence angles 0° to 90° (step is 10°) which must be specified by the user for every window separately. Similarly, the transmittance and absorptance for the diffuse radiation must be defined. Hence, HTB2 leaves the choice of an appropriate glazing transmission model to the user.

5.6.1 Calculation methods used

Two methods for calculating the incidence angle dependent glazing properties have been compared within this study (see also Pfrommer et al. 1994b; IR9):

(i) conventional approximate method

The conventional method for calculating the incidence angle dependent glazing properties of clear glazing uses a recursive calculation (ray-tracing technique) of the multi-reflected, absorbed and transmitted lightrays in a glass pane based on the Fresnel-equations (DIN 1349, 1972). These calculated incidence angle dependent characteristics are transferred to special glazing (coated or tinted glazing) by using the known (manufacturer quoted) values for normal incidence.

For the diffuse transmittance the values of the direct transmittance for an equivalent incidence angle of 60° were taken (see Chapter 4).

(ii) improved method

The improved method uses the new computer program GLSIM-FILM to calculate the detailed incidence angle dependent transmittance and absorptance values.

The diffuse transmittance are calculated by the new computer program GLSIM-DIF, as introduced in Chapter 4.

5.6.2 The glazings studied

The selection of an appropriate glazing system is one of the key decisions which must be made when designing a commercial building. Clear double glazing often leads to high cooling loads in highly glazed offices, so sun-protective glazing is often preferred. To show the importance of more accurate consideration of glazing properties, four different glazing types, including different types of heat-protective glazing were studied (IR9), the results for just two glazings are shown here:

heat absorbing grey glass (Antisun grey® (Pilkington 1988)); and
non-absorbing, sun reflective glass (Calorex A0® (Schott 1984)).

These glazings have the same conventional (producer quoted) energy related properties: U-value (2.9 W/m²K); and total solar energy transmittance (0.48). (Note, the total solar energy transmittance includes both the directly transmitted radiation and the absorbed radiation, which is transported to the inside by convection and long-wave radiation (secondary heat flow)). Differences occur in the light transmittance and the colour appearance. Because the energy related properties of the glazings are the same, there would be no reason to choose between one or the other when considering such issues as imposed heating or cooling loads, energy demands, peak temperatures etc.

Heat absorbing glass gets its sun-protective quality by its high heat absorbing ability. Such systems are usually double glazed, consisting of an outer coloured pane and an inner clear pane. The particular glass studied, Pilkington's Antisun grey®, had two 6 mm panes. Compared to the conventional method, the detailed calculation produces lower transmittance values for all angles of incidence (Fig. 5.13). The improved method gives a calculated transmittance of the diffuse radiation of 0.278 which is equal to the direct transmittance at 55°. The diffuse absorptance is 0.587.

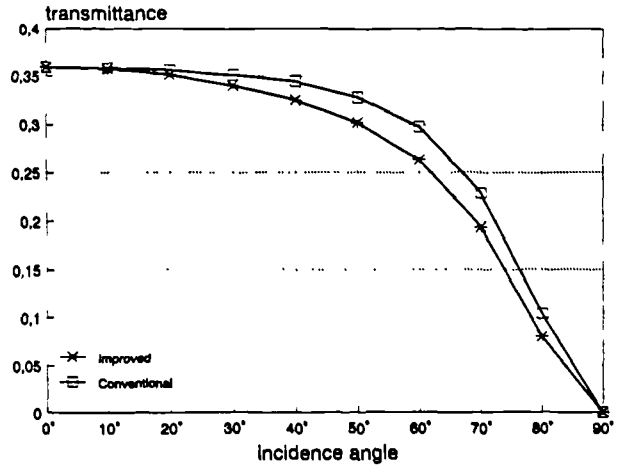

Figure 5.13:

Incidence angle dependent transmittance of Antisun grey®; conventional and improved calculation method.

As an example for non-absorbing sun-protective glazing, the sun-reflective glass Calorex A0 of Schott has been chosen. The glass is coated on both sides with Titanium dioxide films

using a dipping process and is regarded as one of the classic examples of this type of product (Dislich 1984). The light transmittance is 0.5, which is relatively high, and the colour appearance is neutral. When compared with the conventional transmittance values the improved method produces transmittance values which are higher for all angles of incidence (Fig. 5.14). The improved method gives a calculated transmittance of the diffuse radiation of 0.399 which is equal to the direct transmittance at 63°. The diffuse absorptance is 0.243.

The transmittance curve of Calorex A0 is almost horizontal up to high incidence angles and then decreases quickly. In the practically important range (between 50° and 80°) there is a high relative transmittance. Heat absorbing glasses, in this case Antisun grey, have relative transmittance curves which lie considerably below the curve for clear glass. The comparison clearly demonstrates that the relative transmittance curve of special glazing can differ significantly from the curve for clear glazing (section 5.5) even though this approach is often used when modelling special glazings. It also shows that the improved method will calculate higher radiation gains for Calorex A0 than the conventional method, whilst it will calculate lower radiation gains for Antisun grey.

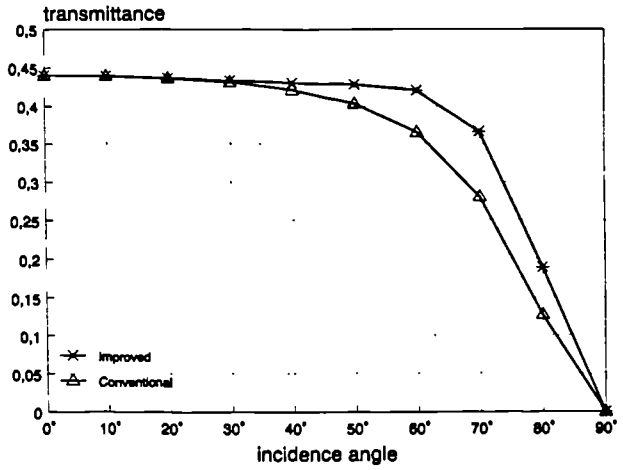

Figure 5.14:

Incidence angle dependent transmittance of Calorex A0®; conventional and improved calculation method.

5.6.3 Commercial building description

In these sensitivity studies, the conventional treatment of the glazing properties is compared with the improved treatment. The studies are based on a commercial building similar to that being used by the IEA Annex 21 and Task 12 model evaluation groups (Kataja and Kalema 1992). In the first study, the clear double glazing used in the IEA work was replaced by different types of special glazing.

The test module is assumed to be in the middle of a multi-storey block. It consisted of two rooms with a corridor between them. The corridor was separated from the office rooms by an internal wall and a door. The area of the window on each external wall was 2.52 m². The windows were orientated to face North-South. The basic building descriptions are given in

Appendix A.3 (more detailed information about the building is given by Kataja and Kalema 1992).

The basic IEA building had: an extremely high ventilation rate (2.47 ach in the daytime); high internal lighting heat gains (500 W in every room); and a relatively small window size (2.52 m²). All three aspects reduce the influence of solar radiation on the inside climate. In commercial buildings with less ventilation, lower casual heat gains, and bigger windows, the impact of the energy transmission through the glazing will be greater. Therefore, any inaccuracies in the glazing properties will have a greater impact.

To produce a building which was more sensitive to glazing properties, three changes were made to the basic IEA building description:

(i) the lighting system was switched off;
(ii) the day-time ventilation rate was reduced to a constant 0.41 ach; and
(iii) the areas of the window were increased to 8.1 m² (i.e. the total external wall area).

In the IEA work, the weather conditions of Denver (USA), which has very hot, sunny summers and very cold, clear winters, were used. To study the impact of the glazing models in more moderate climates, all the simulations were repeated using the more cloudy, overcast weather of Kew, UK (Appendix B).

5.6.4 Effect of the improved method

For both climates and both buildings, the annual heating and cooling energy predicted by HTB2 and the conventional glazing properties, were compared with the corresponding values predicted by HTB2 and the GLSIM-FILM pre-processor (Figures 5.15 to 5.18). Additionally, the maximum cooling powers predicted on a hot, sunny summer day in Kew, UK were compared (Fig. 5.19). Only the results for the south-facing office, which was most sensitive to the glazing models, are shown here.

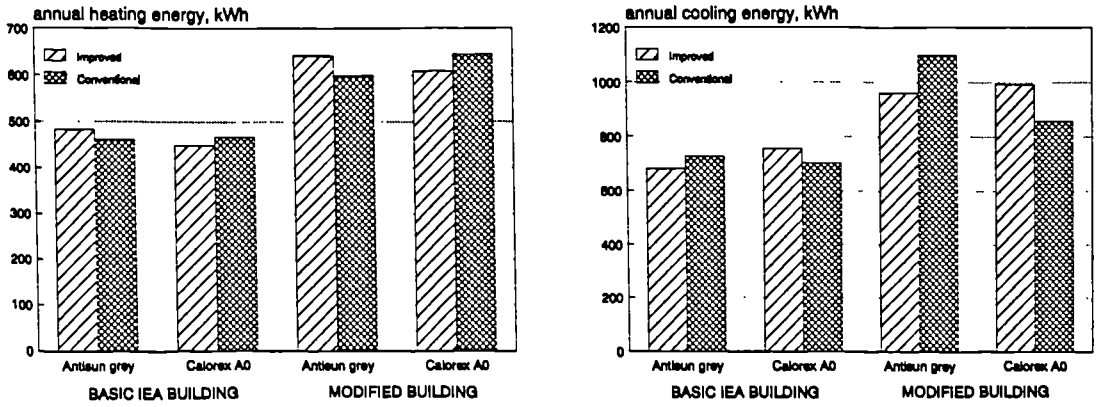

Figure 5.15 and 5.16 Annual heating and cooling energy demands in the south office (basic IEA and modified building description) for Denver.

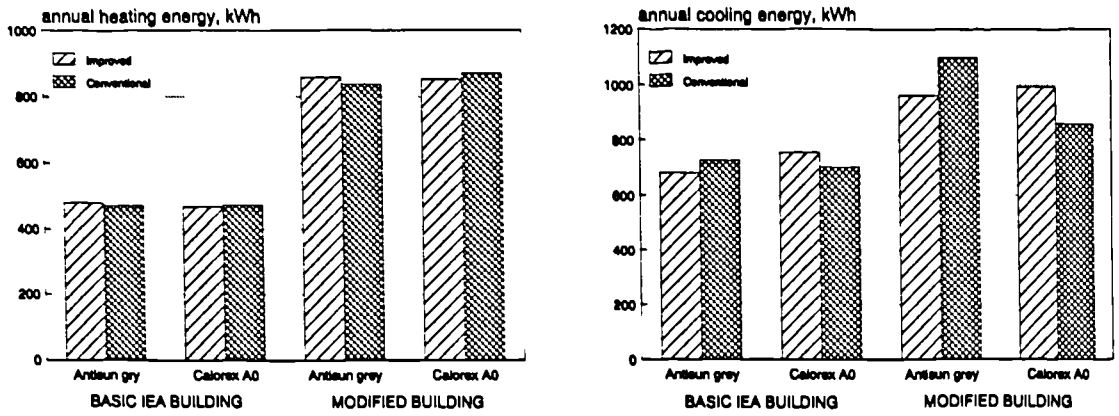

Figure 5.17 and 5.18 Annual heating and cooling energy demands in the south office (basic IEA and modified building description) for Kew.

The errors arising from the use of the conventional calculations, rather than the improved method, may be positive or negative. For Antisun grey, the incidence angle dependent transmittance values of the conventional method lie above the corresponding improved values (Fig. 5.13), hence, the cooling energy demands are over-predicted and the heating energy demands are under-predicted. For Calorex A0 the conventional values lie below the improved transmittance values (Fig. 5.14), so the cooling energy demand is too low and the heating energy demand is too high.

The percentage errors in the heating energy demands are greater for Denver than for Kew, however, the percentage errors in the cooling energy demands are greater for Kew (although the absolute differences are higher for Denver). Generally, the predicted errors in the cooling energy demands are much higher than the errors in the heating energy demands. This may be expected because the intensity, incidence angle, (and at Kew the duration) of the solar radiation, is greatest when cooling is needed. Thus any differences in the glazing models will be exacerbated. For Kew the cooling energy demand error reaches 19% in the case of the modified building compared with 11% for the basic IEA building. The highest error in the heating energy demands was 7% for the modified building located in Denver.

When the simulation results are used for design purposes the decision concerning the best glazing type may be influenced by the calculation method used for the glazing. Looking at the cooling energy demands for the basic IEA building, the improved calculation method leads to a clear preference of Antisun grey since it requires 74 kWh less than Calorex A0 in Denver or 30 kWh at Kew. On the other hand, the conventional method recommends the opposite since it produces 24 kWh more for Antisun grey than for Calorex A0 in Denver or 13 kWh more in Kew. When a design decision is based on the heating energy demands, the improved method recommends Calorex A0 in favour of Antisun grey (33 kWh lower heating demand for Denver and 11 kWh for Kew), while the conventional method again suggests the opposite (6 kWh more heating demand for Denver, 4 kWh for Kew).

The modified building description led to the same conclusions but bigger differences. For example, the predicted difference between the improved and conventional method for the annual cooling energy demands in Denver is 137 kWh for Antisun grey and 133 kWh for Calorex A0.

For Antisun grey, the conventional method over-estimates the maximum cooling power on a hot, sunny summer day in Kew by about 5% (basic IEA building description) and 9% (modified building description) (Fig. 5.19). For Calorex A0 it under-estimates the cooling power by about the same amounts, which could lead to an under-sizing of the cooling equipment. Because the necessary heating power is determined by very cold ambient conditions without significant solar gains (typically at cloudy days or during the night) it is largely unaffected by the glazing calculation methods.

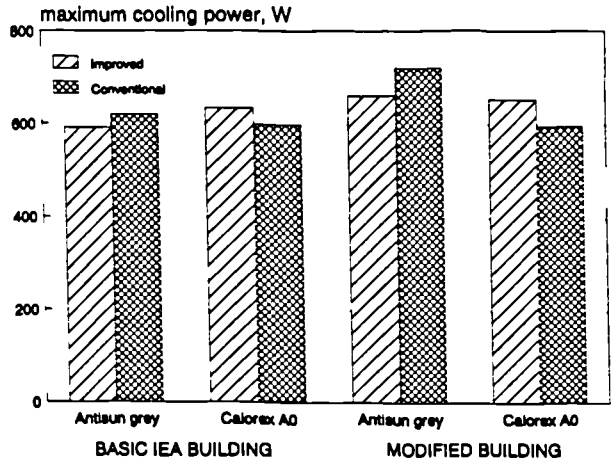

Figure 5.19:

Maximum cooling power in the south office at a hot, sunny summer day (basic IEA and modified building description) in Kew.

It is clear for the above results that thermal simulation programs, such as SERI-RES (Palmiter and Wheeling 1983) or TRNSYS (Klein et al. 1988), which internally calculate the transmission properties of glazing systems using the Fresnel equations and a recursive formulation for multi-layered systems (valid for combinations of clear glass panes), may produce inaccurate predictions. Such programs could therefore lead to incorrect design decisions being made for buildings with special tinted or coated glazings.

CHAPTER 6

TOTAL SOLAR ENERGY TRANSMITTANCE

6.1 INTRODUCTION

The most important glazing property for clear and special glazing is the total solar energy transmittance (see Chapter 2, section 2.4.3). It is widely used in quasi-stationary calculations of cooling or heating energy demands or cooling and heating power (BREDEM (Anderson et al. 1985); ASHRAE Handbook 1981; CIBSE Guide 1986; WärmeschutzVO 1993; DIN 4108, 1981; ISO 9164, 1992; DIN 4701, 1983; VDI 2078, 1977). It is also used in some DSMs. For example, the program ZB-SIMULAP (Zimmermann and Becker 1992) uses total solar energy transmittance values to calculate the solar heat gains. In addition, the simplified U-value approach of windows in ESP (Clark and McLean 1988) requires the definition of total solar energy transmittance values.

The total solar energy transmittance represents the ratio of the total transmitted energy to the total incident global radiation. It considers the radiation which is directly transmitted as well as the absorbed radiation, which heats the panes and is then radiated and convected as a secondary heat flow into the room. The total solar energy transmittance and the heat transfer coefficient (U-value) are both fundamental energy related properties which completely describe the thermal impact of the glazing. DIN 67507 (1980) defines the total solar energy transmittance as a fixed value considering normally incident radiation only. Many international glass producers use this method for describing of their products (e.g. Pilkington 1988). It is calculated as follows:

$$\tau^n_{tot} = \tau^n_d + fr * \alpha^n_d \qquad (6.1)$$

where τ^n_{tot} is the total solar energy transmittance, τ^n_d is the direct transmittance for normal incidence, α^n_d is the absorptance for normal incidence and *fr is* the fraction of secondary heat directed inwards using the *normal* exterior and interior surface resistances in the CIBSE-Guide (1986) and DIN 67507 (1980).

In practise, of course, the incidence angle of the solar radiation is not fixed; it varies with the sun position and is therefore highly dependent on the geographical location and the time of day. For vertical surfaces the incidence angle is usually greater than 40°, normal incidence rarely happens. Since the energy transport through glazing decreases as the incidence angle of the radiation increases (see Chapter 4 and 5) the total solar energy transmittance

for normal radiation incidence is higher than that which is found in practise. Thus, if the value for normal incidence is used in thermal energy calculations the heat gains through the glazing will be overestimated.

This detailed investigation of total solar energy transmittance values was inspired by the new German heat protection law (WärmeschutzVO 1993) for buildings, in which solar energy gains are a predominant issue. The first draft of the law used typical total solar energy transmittance values for normal radiation incidence. Since these values over-estimate the solar gains, the heating energy demand of a building was underpredicted. Moreover, since highly insulated buildings are particularly sensitive to solar energy gains, the total solar energy transmittance values has a significant impact on the overall assessment of a building, in particular, on the selection of appropriate glazing areas and glazing types.

To get a better representation of the total solar energy transmittance, the new calculation models described in Chapters 4 and 5 were extended to predict 'effective window properties'. A computer module GLSIM-TOT was created, which calculates the total amount of radiation entering a space by using hourly irradiation data (of the type found in the climate files of DSMs). The calculation considers, of course, the accurate incidence angle dependent glazing properties for the direct and diffuse radiation at each hour. Thus, the new effective (time averaged) values implicitly take account of the incidence angle dependency of the radiation transfer and the change of radiation intensity. The values depend on the location, orientation and inclination of the window surface and on the special transmission behaviour of the glazing system (which is particularly important for special glazing).

The following sections deal with the theory of the new computer module GLSIM-TOT and demonstrate how the newly predicted effective total solar energy transmittance values affect the thermal assessment of glazing systems.

6.2 THEORY OF TOTAL SOLAR ENERGY TRANSMITTANCE

The effective total solar energy transmittance τ^{e}_{tot} describes the relationship between the transmitted solar energy E_{in} and the total incident radiation energy E_{on}, which consist of a direct radiation portion E_d and of a diffuse radiation portion E_f. The calculation, on which the computer module GLSIM-TOT is based, considers the incidence angle dependent transmittance and absorptance (τ_d and α_d) of the direct radiation (Chapter 5) and the diffuse transmittance and absorptance (τ_f and α_f) (Chapter 4).

$$\tau^{e}_{tot} = \frac{E_{in}}{E_{on}} = \frac{\Sigma\left(E_d*(\tau_d+\alpha_d*fr)+E_f*(\tau_f+\alpha_f*fr)\right)}{\Sigma\left(E_d+E_f\right)} \tag{6.2}$$

The direct and diffuse radiation energies E_d and E_f are calculated on a hourly basis using the irradiation data in a climate file (of that type used by DSMs). The intensity and incidence angle of the direct radiation on inclined surfaces is obtained using the theory in DIN 5034 (1983). Generally, it is possible to calculate τ^{e}_{tot} for any time-period. However, the investigations, which are shown here, concentrated on monthly values τ^{m}_{tot} and on annual values τ^{a}_{tot}.

In (6.2) *fr* is the fraction of secondary heat flow which is directed inwards. It can be calculated from the thermal properties of a glazing (*U*-value; internal and external surface heat transfer coefficients β_i and β_o; thermal resistance of the glazing Λ and the ratio of radiation absorbed in the inner pane to the total absorbed radiation (absorptance-split) sp_i (DIN 67507, 1980)):

(6.3) $$fr = \frac{\beta_i}{\beta_i + \beta_o}$$ for single glazing;

(6.4) $$fr = \frac{U}{\beta_o} + \frac{sp_i * U}{\Lambda}$$ for double glazing.

Often the exact absorptance-split of double (or triple) glazing is unknown. However, assuming that the absorptance-split is largely independent of the incidence angle, *fr* can be calculated from the glazing properties for normal incidence (which are usually known) by rearranging equation (6.1):

(6.5) $$fr = \frac{\tau^{n}_{tot} - \tau^{n}_{d}}{\alpha^{n}_{d}}$$

6.3 EFFECTIVE TOTAL SOLAR ENERGY TRANSMITTANCE OF CLEAR GLAZING

As described in section 6.1 the total solar energy transmittance is not fixed, but depends on the orientation and inclination of a window surface; it also depends on the sun position, which leads to a seasonal and geographical variation of the values. Therefore, a parametric study was conducted to investigate the seasonal variations in τ^{m}_{tot} as the window orientation and inclination of glazings is varied. The study concentrated on the German weather conditions of North-Württemberg (Appendix B), since the main aim was to improve German laws and standards. However, a special investigation showed that the trends produced by British weather data were similar.

The highest seasonal swing in τ^{m}_{tot} occurred for south orientated glazing (Fig. 6.1). For a typical (2×6 mm) clear double glazing (refraction = 1.52; extinction coefficient = 0.03 1/mm; normal transmittance = 0.61), τ^{m}_{tot} was 0.65 in winter and reduced to lower than 0.54

in summer. North orientated glazing had a smaller seasonal swing: while τ_{tot}^{m} was about 0.60 during the winter season (Oct. - Mar.), it decreased to 0.56 in summer (June/July). West orientated glazings showed the opposite behaviour: in winter τ_{tot}^{m} was 0.575 whilst it was higher in summer (τ_{tot}^{m} = 0.62). It was assumed that east orientated glazings were similar to west orientated glazings.

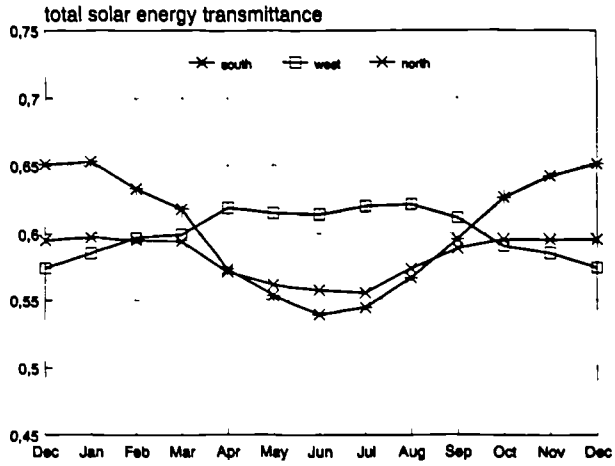

Figure 6.1:

Effective monthly total solar energy transmittance values for south, north and west orientated vertical windows. The glazing consists of 2×6 mm clear glass.

Tilted glazings often occur in south orientated highly-glazed spaces, which are designed for high solar gains (e.g. conservatories), or in the roofs of atria and glazed halls. They are also found in the roofs of modestly glazed spaces. Effective total solar energy transmittance values for tilted glazings are demonstrated in Fig. 6.2.

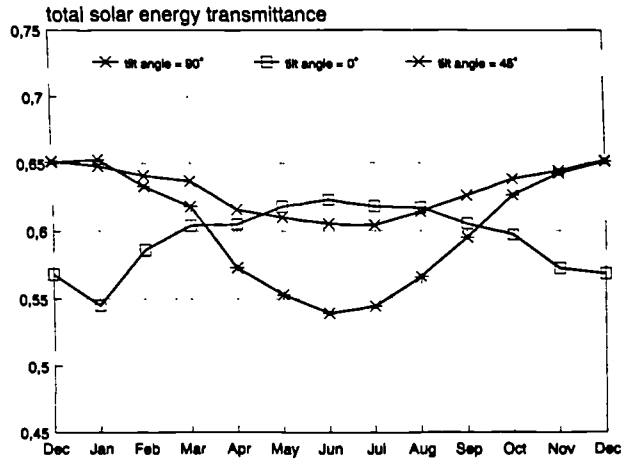

Figure 6.2:

Effective monthly total solar energy transmittance values for south orientated windows as the inclination angle of the glazing is varied: 90° (vertical); 45°; 0° (horizontal). The glazing consists of 2×6 mm clear glass.

The highest solar gains occur in winter for a vertical and 45° tilted window (0.65), while at that time τ_{tot}^{m} is around 0.56 for horizontal glazing. In summer the trends are reversed: τ_{tot}^{m} reduces to 0.54 for the vertical glazing (0.60 for 45° tilt), while the horizontal glazing transmits more radiation (0.63).

These results clearly demonstrate, that the standard total solar energy transmittance for clear double glazing of 0.8 (DIN 4108 (1981), part 2, table 4) is too high. Similarly, the

more accurately calculated value for normally radiation τ^{n}_{tot} found in DIN 67507 (1980) are also too high: a value of about 0.72 for clear double glazing is not found in practise. Compared to this, an approximation of $0.85 \times \tau^{n}_{tot}$ leads to a value (0.60 for the 2×6 mm double glazing), which is the value about which the monthly values of τ^{m}_{tot} oscillated, with a variation of about ± 5%.

The reduction factor of 0.85 was first proposed by CEN TC 129/WG 9 (draft 1993) members. It was confirmed by the investigation discussed here (see also Pfrommer et al. 1993b). This investigation led to a new formulation for the solar gain calculations in the German heat protection law (WärmeschutzVO 1993), which implicitly includes a reduction factor of 0.85. In addition, the factor was accepted for the new DIN 4108 (1993) standard.

6.4 EFFECTIVE TOTAL SOLAR ENERGY TRANSMITTANCE OF SPECIAL GLAZING

Whilst the shape of the incidence angle dependent relative transmittance curve is nearly the same for all clear glazing systems, it differs considerably for special glazing (Chapter 5, section 5.5.2). For example, metal-oxide or noble metal coated glazings maintain high relative transmittance as the solar radiation incidence angle increases above 40°, whilst the transmittance of tinted glazing is reduced even for low incidence angles. Therefore, it is inappropriate to describe these systems by applying a fixed effective reduction factor to the total solar energy transmittance at normal incidence; which was the method adopted for clear glazing (section 6.3). Instead, the effective annual total solar energy transmittance values τ^{a}_{tot} are used to demonstrate the differences of these systems more realistically. These values implicitly take account on the known incidence angle dependent transmission characteristics of the glazing system.

To demonstrate the consequences of this new approach for special glazings, the two glazings used in section 5.6 are compared. The glazing systems were:

heat absorbing grey glass (Antisun grey® (Pilkington 1988)); and
non absorbing, sun-reflective glass (Calorex A0® (Schott 1982)).

These glazings have the same conventional (producer quoted) energy related properties: U-value (2.9 W/m²K) and total solar energy transmittance (0.48). Differences occur in the light transmittance and the colour appearance. Because the energy related properties of the glazings are the same, there would be no reason to choose between one or the other when considering such issues as imposed heating or cooling loads, energy demands, peak temperatures, etc.

The incidence angle dependent total solar energy transmittance curves of both glazing systems are demonstrated in Figure 6.3. These values were calculated at each angle of incidence using the following equation

(6.6) $$\tau_{tot} = \tau_d + fr * \alpha_d$$

where *fr* was obtained using equation 6.5. Both τ_d and α_d are calculated by GLSIM-FILM. For normal incidence, both glazings show the same total solar energy transmittance (0.48) as quoted by the manufacturers. For higher incidence angles, Calorex A0 has a total solar energy transmittance curve which lies considerably above the curve for Antisun grey.

Using GLSIM-TOT, the effective annual total solar energy transmittance τ^a_{tot} for a vertical, south orientated glazing located in Denver (USA) or Kew (UK), as used in the sensitivity analysis of section 5.6, becomes 0.40 for Antisun grey and 0.44 for Calorex A0. In this instance there are only small differences due to the different locations and weather conditions. It should be noted however, that τ^a_{tot} values actually depend on the geographical location (latitude) (and on the particular climate conditions). The latitudes of Denver (40°N) and Kew (51.5°N) are not too different. More work is needed to investigate the dependence of these values on the latitude and climate.

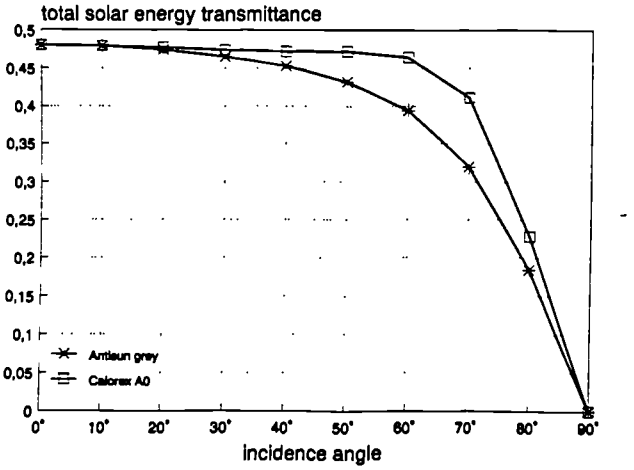

Figure 6.3:

Incidence angle dependent total solar energy transmittance of Calorex A0 and Antisun grey glazing systems.

In section 5.6 the thermal consequences of both glazings on the predicted environmental conditions in a commercial buildings were discussed. Comparing the simulation results with the producer quoted U-values and total solar energy transmittance values, it was clear, that the conventional classification of the glazing systems did not represent the thermal consequences of the glazings correctly. The simulation results showed significant differences between the glazings, while the energy related glazing properties indicate that the thermal impact will be similar (same total solar energy transmittance, same U-value).

As described above, the effective annual total solar energy transmittance values were calculated as 0.40 for Antisun grey and 0.44 for Calorex A0 whilst the conventional values for

both were 0.48. The higher effective total solar energy transmittance of Calorex A0 points to higher solar radiation gains which would result in higher cooling energy demands and lower heating energy demands. This was in fact the case (Fig. 5.15 - 5.18). The lower value corresponding to Antisun grey demonstrates reduced solar energy gains which causes higher heating energy demands and lower cooling energy demands. Because the effective annual total solar energy transmittance reflects the thermal consequence of the glazing more realistically it appears to be a valuable parameter upon which to make design decisions.

As described above, the reduction factor of 0.85 to τ^{n}_{tot} as considered in the WärmeschutzVO (1993) and DIN 4108 (1993) is only adequate for clear glazing systems. It does not reflect the special incidence angle dependent transmittance characteristic of special glazings. Therefore, the introduction of effective annual total solar energy transmittance values τ^{a}_{tot}, which could be listed for the most important glazing systems (as it is already common for U-values or τ^{n}_{tot}) could further improve the characterisation of special glazings. In addition, by indicating effective values, the glazing producers would give valuable informations to the customers enabling them to predict the thermal consequences of special glazings more accurately.

CHAPTER 7

RADIATION TRANSFER THROUGH SLAT-TYPE BLINDS

7.1 INTRODUCTION

Shading is important to reduce the risk of overheating in highly glazed spaces. It has been indicated in Chapter 2 (section 2.4.4) that DSMs use simplified calculation methods for shading effects which may lead to inaccurate simulation results for highly glazed spaces. This Chapter deals with the current calculation practices and introduces a new, improved calculation model for slat-type blinds.

The most effective way to reduce the solar load through windows is to intercept direct radiation from the sun using external sunshades, e.g. roof overhangs, vertical or horizontal architectural projections, obstructions, awnings, horizontal panels, venetian blinds or louvers. Internal shading devices are also used to protect occupants from direct solar radiation. External and internal slat-type sunshades are the most current sun protection devices. Movable louvers can adapt in response to the illumination conditions. The slat surfaces reflect and absorb direct sunlight. At the same time, the space between the slats guarantees the transmission of diffuse sunlight, which does not evoke uncomfortable illumination, but contributes to lighting a room. In the following, the term "blind" always means a slat-type internal or external sunshade.

While there are well known calculation methods for the shading impact of frames, side fins, overhangs and obstructions (sky line) (Rodriguez et al. 1988; Rodriguez and Alvarez 1991) which are implemented in many programs (ESP; SERI-RES; HTB2) there are no calculation principles for slat-type blinds. There is no possibility of simulating blind systems dynamically. Some programs offer crude methods of defining time-fixed shading factors (e.g. SERI-RES). ESP and HTB2 permit the scheduling of glazing properties, which can be used to implicitly consider the time-dependent solar shading effect of blinds. Unfortunately, the fixed or time-scheduled values are generally unknown. It should be noted, that ESP also permits the scheduling of the thermal resistance of glazing/blind systems, which is useful for considering the thermal effects of blinds and shutters.

Time-fixed standard shading factors are published which relate either to the total solar energy transmittance (DIN 4108, 1981; see Chapter 6), or to the solar gains through a reference glass pane (ASHRAE Handbook 1981; VDI 2078, 1977). Sometimes total solar en-

ergy transmittance values of a combination of glass and blind systems are presented (CIBSE-Guide 1986).

- DIN 4108 (1981) gives just two reduction ("z") factors for venetian blind systems (0.5 for internal blinds and 0.3 for external blinds).
- VDI 2078 (1977) distinguishes between three reduction ("b") factors; which depend on the location of the blinds (external; between the glass panes; internal). These values are indicated to be valid for blinds with 45° inclined slats (no more information).
- The total solar energy transmittance values in the CIBSE-Guide (1986) distinguish between the colour of the slats (dark or light) the geometry (horizontal or vertical slats) and the location (internal or external). The slat inclination angle for horizontal slats is indicated to be 45° (downwards).
- The ASHRAE Handbook (1981) presents shading coefficients ("SC") for internal venetian blinds which depend on the glazing system and the colour of the slats (medium; light). For external slats, shading coefficients for six groups of blinds and different profile angles (see section 7.2) are given.

Some blind producers seek to demonstrate the optical quantities of their products more precisely:

- Hunter Douglas (1979) presented shading factors, which were measures at a sun radiation incidence angle of 45°. These values distinguish between the colour of the slats (white; grey; dark), the inclination angle of the slats (45°; 80°) and the blind location (external; internal).
- Pilkington (1992) presented a detailed investigation of opaque, as well as of translucent blinds in connection with different glazing systems. The total solar energy transmittance values given distinguish between the glazing type, the colour of the slats (white; pastel; dark), the slat inclination angle (closed; 60°; 45°) and the slat material (opaque; translucent). The values were calculated for a fixed sun radiation incidence angle, which was always normal to the slat surface.

None of the given values meet the requirements for the use within DSMs, which usually need the net-reductions of the different radiation components (transmitted or absorbed; direct or diffuse). In addition, none of the published values considered the time-dependent changing of the shading factors as the beam radiation incidence angle varies (no time-scheduling).

Just one presentation of shading factors was found to be useful for DSMs. Pilkington (1988) demonstrated the direct beam incidence angle dependent transmittance values of several glazing and blind systems. These values are suitable as input data for ESP or HTB2.

However, the corresponding blind systems were not described in detail, the calculation or measurement methods were not documented and no range of uncertainty was given.

These problems lead to a very unsatisfactory situation in the case of highly glazed spaces, in which the inside climate depends fundamentally on the amount of solar radiation entering the room. A new program module GLSIM-BLIND was therefore created, which calculates the detailed radiation transfer through glazing and blind systems. It can produce the necessary input values for DSMs to either simulate blind systems accurately at each simulation time-step (by specifying the incidence angle dependent properties of the blind and glazing or by scheduling the shading factors) or to simulate blinds approximately using simplified daily effective shading factors for the different radiation components. In addition, the program calculates effective total solar transmittance values or effective shading factors, which can be used in quasi-stationary calculation models of cooling and heating loads or for more simple DSMs such as SERI-RES. The predicted values are comparable with the currently available properties in ASHRAE Handbook 1981; CIBSE-Guide 1986; DIN 4108, 1981 and VDI 2078, 1977.

The rigorous mathematical formulation of the complex radiation path through glazing/blind systems allows any arrangement of blinds with horizontal slats to be simulated. The algorithms can also be used to investigate, compare and optimise blind arrangements during the early design states of a building. For many applications, the ideal blind adjustment shades the direct beam while it permits the transmission of a great portion of diffuse radiation to illuminate the space. Thus, the program can be used to find the ideal slat inclination angle.

The following sections deal with the basic calculation principles, and the application and verification of the new calculation model (see also Pfrommer et al. 1995b). A more detailed description of the theory is given in Appendix D (or in IR6).

7.2 THEORY OF RADIATION TRANSFER THROUGH BLINDS

The theory upon which the computer module GLSIM-BLIND is based, was developed to facilitate quick calculations during a thermal simulation run. The algorithms were originally intended for implementation directly into the thermal processor. Therefore, analytical solutions were preferred before time-intensive numerical procedures or ray-tracing techniques. Although the algorithms were finally realised in a pre-processing program, they are nevertheless appropriate for implementation directly into a thermal processor. The clarity afforded by the analytical formulations enables different blind systems to be quickly solved on a PC. This is an important feature when various blind systems are to be compared, or when one blind system is to be optimised to produce desired shading characteristics. GLSIM-

BLIND also offers a cost-effective route to generating a database of blind properties which could be used by DSMs.

At the start of the work, there were nearly no useful references available. All algorithms in GLSIM-BLIND were developed by considering the fundamental geometrical and physical relations of light in blind and glazing structures. However, the political changes in Germany (and eastern Europe) in the early 90s gave access to research work in the eastern countries. Interesting investigations of blinds were found to have been done at the technical University of Dresden (see Löber 1974; Rudolph 1978). There are many similarities between the work conducted in Dresden and the new algorithms developed for GLSIM-BLIND. In fact, the formulation of the basic calculation principles are more or less identical although the mathematical solutions are quite different. Unfortunately, it has not been possible to make detailed comparisons between the two approaches.

The radiation transmission through slat-type blinds was divided into four different radiation paths (see also Rudolph 1978):

(i) the unshaded transmission of the direct beam (direct transmittance);

(ii) the direct-reflected beam at the slat surfaces (direct-reflected transmittance)
The reflectance may be pure diffuse, pure specular (metallic) or any combination between both;

(iii) the unshaded transmission of the diffuse radiation (diffuse transmittance); and

(iv) the reflected diffuse radiation at the slat surfaces (diffuse-reflected transmittance).

The calculation considers the inter-reflections between the slats and between the glass panes and the slats. The incidence angle dependent transmittance through a glazing behind a blind (external device) is treated by considering the true or effective incidence angle of both the directly received radiation and the radiation reflected from the slats. The effect of curved slats is approximately considered.

The following sections concentrate on the calculation principles of the different radiation portions. The basic symbols used to describe blind systems are demonstrated in Fig. 7.1. Since the slats are assumed to be of infinite length, the spatial blind geometry is reduced to two dimensions. The slat geometry is fully described by the slat width (*sw*) the slat distance (*sd*) and the slat inclination angle (*si*). Usually the slat width corresponds approximately to the slat distance. This is called a *regular* blind geometry.

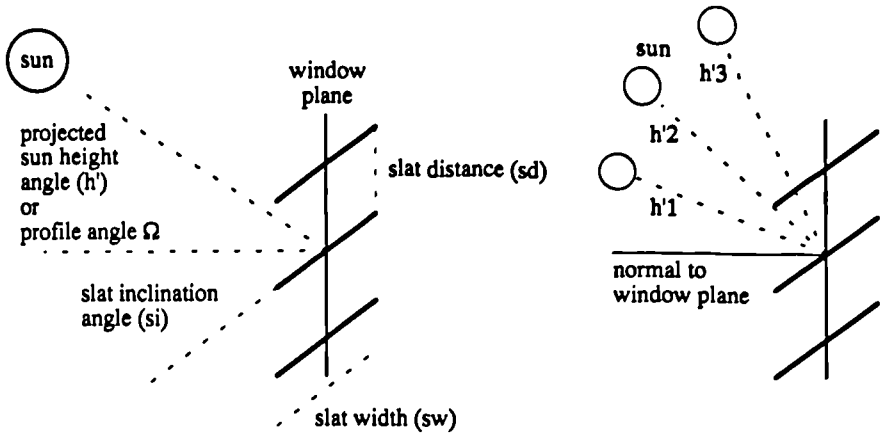

Figure 7.1: Basic symbols and angles used to describe the blind systems. The right Figure demonstrates the projected sun height angles (h'1 - h'3) for different illumination situations.

The ability of horizontal panels or slats to intercept the direct component of solar radiation depends on their geometry and on the projected (effective) sun height angle h'. The projected sun height angle h' determines the effective incidence angle of the direct beam radiation onto the slat surfaces. It is defined as the angular difference between a plane normal to the window and a plane tilted about a horizontal axis in the plane of the window until it includes the sun. It can be calculated from the real sun height angle h_s as follows,

$$h' = \arctan\left(\frac{\sin(h_s)}{\cos(az_s - az_w)*\cos(h_s)}\right) - 90° + \eta \tag{7.1}$$

where az_s is the azimuth angle of the sun, az_w the azimuth angle of the window and η the inclination angle of the window (0° for horizontal).

The corresponding angle, which determines the effective incidence angle of a diffuse radiation portion from a certain sky (or ground) point, is called the profile angle Ω. (For vertical south-facing surfaces, Ω corresponds to ζ, see Fig. 4.2.) If the sky (or ground) vault is cut into slices, all sky (or ground) points on the same slice surface have fortunately the same height projection (profile angle). It is therefore possible to reduce the two-dimensional integration of diffuse radiation portions (along a height and a slice angle) to a one-dimensional integration along the profile angle Ω (Fig. 7.2).

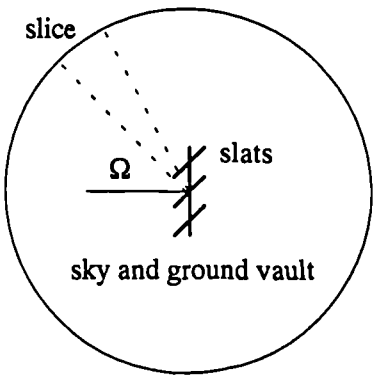

Figure 7.2:

Cross-section through the sky and ground vault. The slice surface area corresponds to that area on the sky or ground vault which lies between two curves with constant projected height (or profile) angles.

7.2.1 Direct transmittance

One portion of the direct radiation is shaded by the slats, the other portion enters the room through the unshaded open space between the slats. The direct transmittance τ_d^b (the superscript *b* denotes blinds) is simply the ratio between the unshaded space and the total space between the slats,

$$(7.2) \quad \tau_d^b = 1 - \frac{sh}{sd} = 1 - sw * \frac{\sin(h' - si)}{\sin(90° - h') * sd} = 1 - (sw * \sin(si) - sw * \cos(si) * \tan(h')) / sd$$

where *sh* is the shaded area, *sd* the slat distance, *sw* the slat width, and *h'* the projected sun height angle (Fig. 7.3).

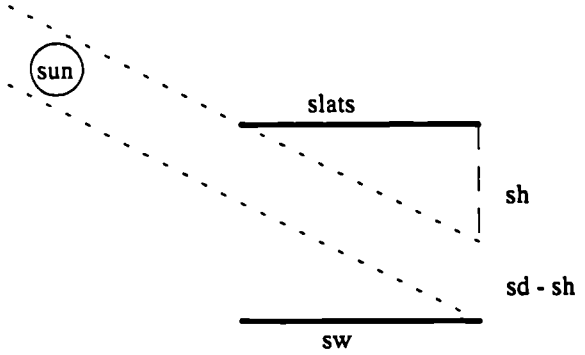

Figure 7.3:

Relationship between sunposition and slat geometry to illustrate the shading of direct solar radiation.

7.2.2. Direct-reflected transmittance

The direct-reflected radiation consists of two parts: a direct-to-diffuse reflected radiation portion τ_{df}^b and a specular-reflected radiation portion τ_{ds}^b. The relation between both components depends on the slat material and is defined by the shining factor σ of the material. The shining factor becomes 1 for pure diffuse reflection or 0 for ideal specular reflection. Shining factors for different materials were measured by Ward (1992) (Table 7.1).

rolled brass:	0.23	enamel finished metal:	0.83
rolled aluminium:	0.32	Latex paint:	0.9
lightly brushed alum.:	0.44	plastic laminate:	0.9
glossy grey paper:	0.78		

Table 7.1: Shining factors, after *Ward (1992)*.

The calculation of the direct-to-diffuse reflected radiation considers the multi-reflections between the slats up to the second reflection. This is an appropriate approximation since the radiation portion remaining after the second reflection is very low. The error in this radiation path was found to be lower than 5% for light slats (reflectance, $\rho = 0.6$) or lower than 1% for dark slats ($\rho = 0.2$). The direct-to-diffuse reflected radiation is given by

$$(7.3) \quad \tau_{df}^b = (\rho * f_1 + \rho^2 * f_2 * f_3) * (1 - \tau_d^b)$$

where ρ is the slat reflectance and f_1 is the view factor between the illuminated slat area and the inside, f_2 is between the illuminated slat area and the upper slat and f_3 is between the upper slat and the inside. These view factors were approximated based on an approach which correctly represents the radiation emittance of infinitely small illuminated areas. The approach has a maximum error of 4% (compared to the rigorous numerically predicted value), when the total slat width is illuminated. The term $(1 - \tau_d^b)$ defines the absorbed or reflected direct radiation component. The total direct absorptance α_{df}^b can be obtained by summation of all the absorbed radiation portions (see Appendix D.3.1).

The calculation model for the specular-reflected radiation portion uses a rigorous analytical solution with no approximations. It considers all higher-order reflections. The specular-reflected radiation normally consists of different portions Po_i, which are reflected with a different number of inter-reflections nr_i:

$$\tau_{ds}^b = \sum_i \rho^{nr_i} * Po_i \tag{7.4}$$

The number of inter-reflections, nr_i, is calculated by considering different geometrical situations (with and without radiation backloss) using fundamental geometrical relations (Fig. 7.4). Again the total direct absorptance corresponds to the sum of each the radiation absorbed at each reflection (Appendix D.3.2).

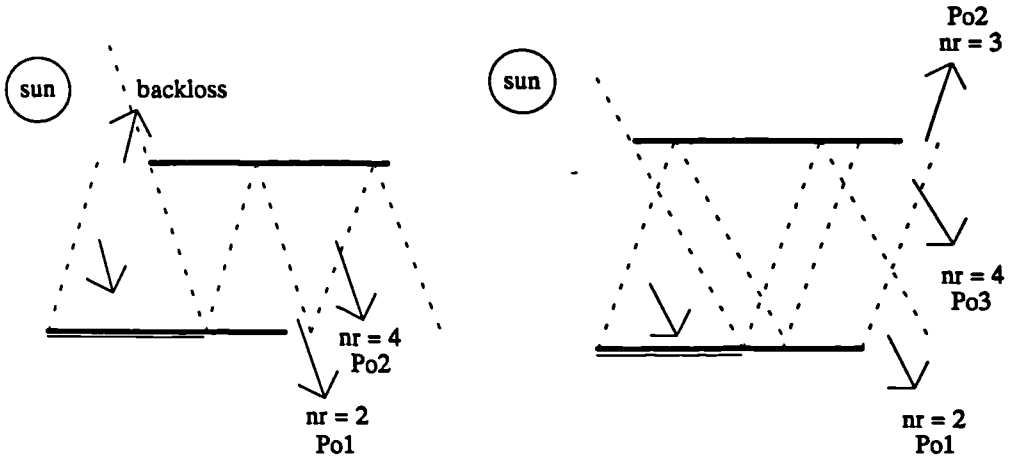

Figure 7.4: Specular inter-reflections of direct radiation between slat surfaces.

7.2.3 Diffuse transmittance

The diffuse radiation on a surface consists of a portion from the sky and a portion from the ground (see Chapter 4). In Chapter 4, the accurate consideration of radiance distributions were found to be primarily important for overcast days, whilst the distribution was largely irrelevant for clear days. Since blind calculations are mainly interesting for clear days, the

assumption that the sky is isotropic seems to be justified. Others have used this approach for this type of calculation (see Rudolph 1978).

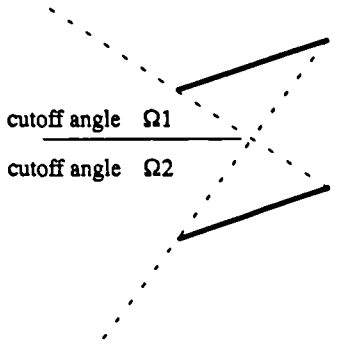

Figure 7.5:

Geometrical presentation of the cutoff angles. Any radiation from above the cutoff angle Ω1 and below the cutoff angle Ω2 is totally shaded.

The unreflected diffuse radiation enters the room through the open space between the slats, which is defined by the cutoff angles $\Omega 1$ and $\Omega 2$ (Fig. 7.5). These depend on the slat geometry and slat inclination angle (si). The diffuse transmittance τ_f^b follows by integrating the radiation from each slice of the sky (or ground) across the vault between the cutoff angles. The net-transmittance $\tau(\Omega)$ of the diffuse radiation from each slice is calculated in a similar way to the direct transmittance $\tau_d^b(h')$ (see section 7.2.1). Here, the projected sun height angle h' is substituted by the profile angle Ω of a certain sky (or ground) slice. When Ω is the integration angle, $\tau(\Omega)$ the diffuse transmittance of radiation from a slice and L the radiance of the sky (or ground), the formulation becomes,

$$\tau_f^b = \frac{\int_{\Omega 1}^{\Omega 2} L * \cos(\Omega) * \tau(\Omega) * d\Omega}{\int_{-90°}^{90°} L * \cos(\Omega) * d\Omega} \tag{7.5a}$$

$$\tau(\Omega) = 1 - (sw * \sin(si) - sw * \cos(si) * \tan(\Omega)) / sd \tag{7.5b}$$

For isotropic sky and ground radiance distributions the integrals can be solved analytically. Since the calculation distinguishes between sky and ground radiation, it must be executed for both components separately.

7.2.4 Diffuse-reflected transmittance

The reflectance of the diffuse radiation on the slat surfaces is either diffuse, specular or any combination of these. The calculation of the specular reflectance needs numerical solution techniques. These were not considered within the basic version of GLSIM-BLIND (but added to a later version of the program). For an analytical solution, the reflectance of the diffuse radiation on the slat surfaces was assumed to be purely diffuse. Thus, the calculation of the reflected radiation from each slice is similar to the calculation of the direct-to-diffuse reflection calculation (section 7.2.2). Here, the projected sun height angle h' is substituted

by the profile angle Ω of a certain sky (or ground) point. The diffuse-reflected transmittance τ_{ff}^{b} is obtained by considering the inter-reflections of each diffuse radiation portion and the corresponding view factors *f* up to the second reflection.

$$\tau_{ff}^{b} = \frac{\int_{-90}^{90} L * \cos(\Omega) * (1 - \tau(\Omega)) * (\rho * f_1(\Omega) + \rho^2 * f_2(\Omega) * f_3) * d\Omega}{\int_{-90}^{90} L * \cos(\Omega) * d\Omega} \tag{7.6a}$$

$$1 - \tau(\Omega) = (sw * \sin(si) - sw * \cos(si) * \tan(\Omega)) / sd \tag{7.6b}$$

Again, the integration must be split into different parts, which consider either ground or sky radiation slices. In (7.6a) the view factors f_1 and f_2 depend on the illuminated width of the slats (*isw*), which again depends on the profile angle Ω of the radiation slice. To get an analytical solution, a simplified assumption was adopted, which uses either half or total illumination of the slats. Half illumination is assigned to all radiation portions from the sky (or ground) vault above or below the cutoff angles, which is approximately the energy-weighted average. Total illumination actually occurs for all radiation slices with a profile angle lying between the cutoff angles. The error of the total transmittance due to this simplification was found to be lower than 1%. For the diffuse absorptance see Appendix D.5.

7.2.5 Curved slats

In GLSIM-BLIND curved slats are treated as surface-slices of a cylinder. The curvature of the slat is described by the radius of the cylinder. The influence of curved slats on the transmittance of the different radiation components was considered as follows.

- The direct transmittance is reduced by an additional shadow due to the slat curvature. A correction is introduced which represents the additional shadow correctly (no approximation). It is calculated from first principles dependent on the sun location and the exact blind geometry.
- The influence of the slat curvature on the direct-to-diffuse transmittance is approximately considered by a correction of the view factors. For flat slats the error in the view factors due to the simplifications was found to be lower than 4% (compared with the rigorously calculated values; see section 7.2.2). Since the rigorous view factor for curved slats is difficult to obtain, the error was not investigated. However, it is probable that the uncertainty is similar to that of flat slats.
- To avoid numerical calculations, the effect of slat curvature on the diffuse transmittance as well as on the specular-reflected direct transmittance was neglected.

- The influence of the slat curvature on the diffuse-reflected transmittance is approximately considered by a correction to the view factors (similar to the correction used for the direct-to-diffuse transmittance.

An investigation showed that the influence of slat curvature decreases as the radius of curvature increases. For normal blind geometries (slat radius of curvature > slat width) the influence was negligibly small (Fig. 7.6). In most cases the approximation of slats as being flat appears to be justified. If, nevertheless, the slat curvature is considered, the error due to simplifications in the treatment of curved slats will be marginal. However, for highly curved slats (slat radius of curvature < slat width) the influence of the slat curve may be important.

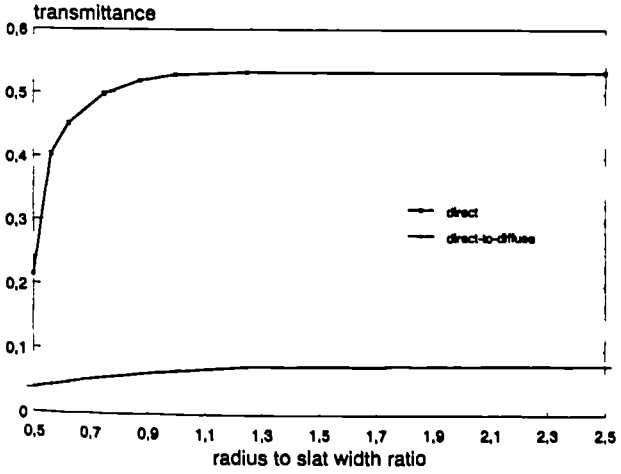

Figure 7.6:

Variation of the direct transmittance and direct-to-diffuse transmittances of a vertical blind with horizontal (*si* = 0°) slats as the ratio of the radius to slat width is varied (2.0 means that the radius is twice the slat width). The projected sun height angle is 25°, which leads to a certain direct transmitted radiation portion.

7.2.6 Interaction between blind and glazing

Interactions between the blind and the glazings occur in two ways:

- by multi-reflections between glass panes and slats; and
- by the effect of blinds on the beam direction, which modifies the angle at which solar radiation strikes the glass panes.

The multi-reflections between the blind and the glazing are considered by using a recursive row of calculation steps up to the second reflection. An investigation showed that the error due to neglecting of the third or higher order reflections was, in most cases, lower than 1%. When 'o' is the external layer (glass or blind) and 'i' the internal layer (glass or blind) in principle the calculation row follows by,

$$(7.7) \quad \tau^{o+i} = \tau^{o} * \tau^{i} + \tau^{o} * \rho^{i} * \rho^{o} * \tau^{i}$$

where τ are the blind or glazing transmittance components for direct, diffuse or direct-to-diffuse radiation and ρ the blind or glazing reflectance components for direct, diffuse or direct-to-diffuse radiation.

The primary radiation ray (first order transmittance) is calculated by considering the true incidence angle of the radiation onto the glass panes behind external blinds. For specularly reflected direct beam radiation, the incidence angle can be calculated easily from simple geometrical considerations (see Appendix D.7.1). For diffuse radiation (direct-to-diffuse; diffuse; diffuse-reflected) it is necessary to predict equivalent diffuse radiation incidence angles and hence diffuse glazing transmittance values (Fig. 7.7). These must be calculated for each diffuse radiation path:

(i) the effective glazing transmittance for direct-to-diffuse reflected radiation τ^g_{df};
(ii) the effective glazing transmittance for the diffuse-reflected radiation τ^g_{ff}; and
(iii) the effective glazing transmittance for the unreflected diffuse radiation τ^g_f.

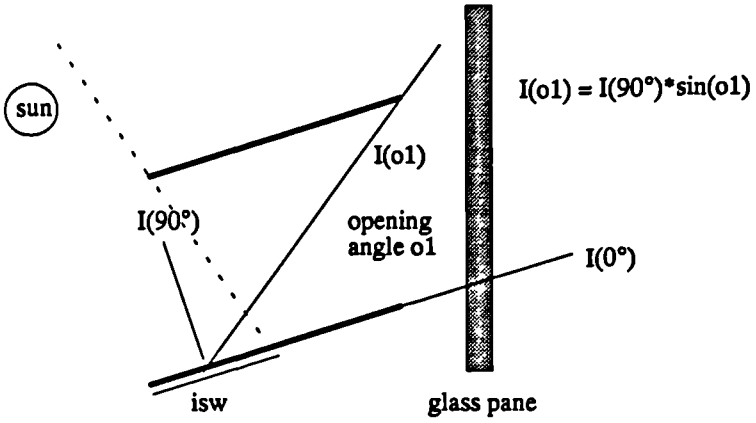

Figure 7.7: Incidence of diffuse-reflected radiation onto a glass pane at the inner side of external blinds.

The Law-of-Lambert states that the radiation intensities above an ideal diffuse shining (reflecting) surface decrease with the sine of the emittance angle. Thus, the effective diffuse transmittance τ^g for the glass pane behind a diffusing slat surface is given by,

$$\tau^g = \frac{\int_0^{o1} \sin(\Omega) * \tau^g_d(\Omega - si) * d\Omega}{\int_0^{o1} \sin(\Omega) * d\Omega} \qquad (7.8)$$

where τ^g_d is the direct radiation glazing transmittance for incidence angle (Ω - si) and *o1* is the opening angle, within which the reflected radiation reaches the glass pane.

The effective glazing transmittance τ^g_{df} for direct-to-diffuse reflected radiation is obtained from equation (7.8) by considering the actual illuminated slat width (*isw*). The calculation of the effective glazing transmittance τ^g_{ff} for the diffuse-reflected radiation is similar, however the illuminated slat width always corresponds to the total slat width (*isw* = *sw*). In addition, in the case of diffuse-reflected radiation both sides of the slats are illuminated simultane-

ously. It is therefore necessary to consider two different opening angles, one from the lower slat and one from the upper slat (see Appendix D.7.1).

The calculation of the effective glazing transmittance for the unreflected diffuse radiation $\tau_f^{\downarrow}$ is more complicate. The diffuse radiation coming from the sky (or ground) between the cutoff angles, is not reflected by the slat surfaces (Fig. 7.8). Thus, the direction of the radiation is not changed. The distribution of the unreflected diffuse radiation at the inner side of external blinds must therefore retain its usual three-dimensional character. The calculation is shown in Appendix D.7.1 (see also Chapter 4).

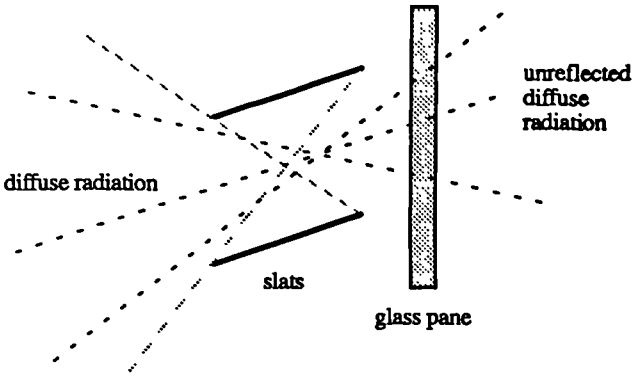

Figure 7.8:

Transmittance of unreflected diffuse radiation through a glass pane at the inner side of external blinds.

Since the incidence angle dependent glazing transmittance is usually given as a series of discrete values for each incidence angle (e.g. 10 values for 0° - 90° as used by HTB2) the integrals (e.g. in equation 7.8) can not be solved analytically, instead numerical summations become necessary. These are the only numerical procedures in the basic version of GLSIM-BLIND. However, the simple numerical summations can be solved quickly. In addition, the glazing properties for diffuse radiation stay the same over the whole simulation period. They are therefore calculated only once at the beginning of the program run.

Generally, the significance of the effective radiation incidence angle should not be under-estimated. As an example, consider a situation where a 'regular' blind (slat width = slat distance; slat reflectance = 0.5) is located at the outer side of a horizontal clear double (2×6 mm) glazing (normal transmittance = 0.6; diffuse transmittance on overcast days = 0.52). The projected sun height angle is 0°, hence, the sun beam strikes the window normally. The effective transmittance for the direct-to-diffuse reflected radiation decreased from 0.55 to 0.1 as the slat inclination angle increased from 0° to 80° (Fig. 7.9). For the unreflected diffuse radiation, the effective glazing transmittance due to the slat inclination angle decreased from 0.56 to 0.43. In contrast, the variation of the effective glazing transmittance for the diffuse-reflected radiation was found to be very small.

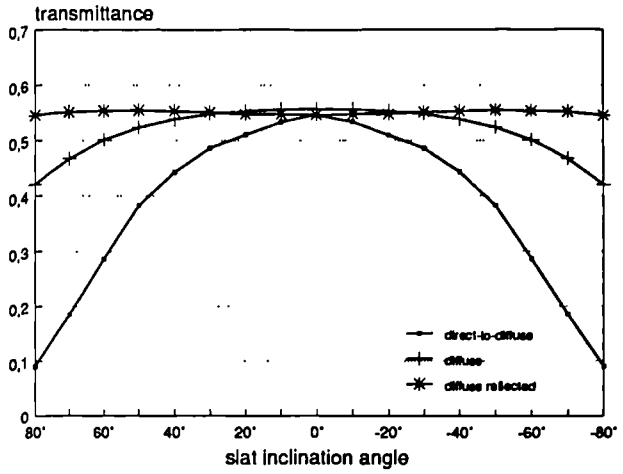

Figure 7.9:

Variation of the effective glazing transmittance values for a horizontal window (no influence of the ground) as the slat inclination angle (*si*) is varied. The projected sun height angle is 0°, hence, the sun beam strikes the window normally. The glazing consists of two clear glass panes (direct normal transmittance = 0.6).

7.3 APPLICATION FOR SIMULATIONS

The theory was implemented in the program module GLSIM-BLIND, which produces shading factors at three different levels of abstraction and accuracy. The most accurate option permits a dynamic treatment of the blinds. For this purpose, the incidence angle dependent transmittance and absorptance of a glazing/blind system are produced for use as inputs to DSMs. Secondly, effective daily glazing/blind properties are generated by considering the standard clear sky conditions on an example day. Thirdly, at the simplest level, the program can calculate the radiation transfer through glazing/blind systems by considering the irradiation data in a climate file. This method leads to an annual effective shading factor. The following sections describe the principles of all three calculation methods, and different applications (blind optimisation; ranking of systems etc.) are discussed.

The theory (sections 7.3.1, 7.3.2 and 7.3.3) concentrates on external blinds. Modifications appropriate to internal blinds are discussed later (section 7.3.4). In addition, one section deals with the modelling of different blind control methods (section 7.3.5).

7.3.1 Dynamic treatment

The ability of slats to intercept solar radiation is highly dependent on the sun position and therefore on the time of day, season and geographical location (latitude). An accurate simulation of the hourly thermal conditions in a shaded space requires the time-dependent glazing/blind properties (dynamic blind treatment) to be considered. As described above, the new calculation technique was originally intended for implementation in the thermal processor (e.g. in HTB2), however, to make the program independent of a specific DSM the theory was finally realised as a pre-processing module (GLSIM-BLIND). Nevertheless, a dynamic treatment of blind/glazing systems, based on input values rather than implicit calcula-

tions, is still possible. Authors of DSMs could use the theory outlined here to integrate blind/glazing calculations within their program.

Many DSMs use incidence angle dependent transmittance and absorptance values to calculate the radiation transfer through glazing (e.g. HTB2 or ESP). By knowing the corresponding values for a glazing with a shading system, the impact of the shading system can be accurately simulated. No modifications or implementations to the DSM are necessary. Therefore GLSIM-BLIND calculates the relationship between the direct radiation transmittance properties (which depend on the projected sun height angle h') and the incidence angle of the direct beam radiation onto the window plane.

Since every incidence angle of the direct beam radiation onto a window plane occurs twice a day (generally once in the morning and once in the evening), there are always two sets of values given (see Fig. 7.10). The first set is valid from sunrise to the time with the lowest incidence angle (e.g. half past three in Fig. 7.10); the second set is valid till sunset. For south orientated windows the situation is symmetric, hence, both sets are corresponding.

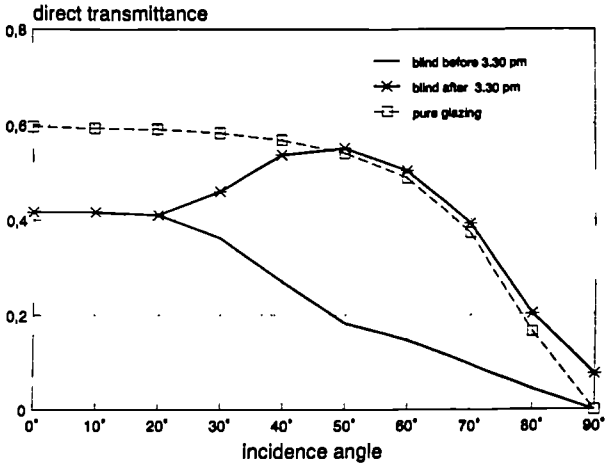

Figure 7.10:

Beam radiation incidence angle dependent transmittance values for a pure clear double glazing (direct normal transmittance = 0.6) and the glazing with external horizontal slats (slat reflectance = 0.5; slat width = slat distance) at Kew. The orientation of the window is south-west. The date is 21/3.

The values depend on the date and the geographical latitude of the site. When the local time does not correspond to the local sun time, the geographical longitude is also important. For annual simulations, the values for example days can be scheduled. Since the variation within one month is insignificant, it is possible to use one example day for each month (e.g. the 15th day) or even to be satisfied with one example day for each season (see also section 7.6.1).

Since the calculation of the diffuse radiation transfer through blinds uses an isotropic sky model (ISO), the diffuse transmittance and absorptance values are independent of the time of day, date, season or location. In addition, the values can be used for clear, as well as for overcast days. The diffuse transmittance (and absorptance) through a glazing/blind system is easily specified by changing the diffuse transmittance (and absorptance) of the glazing used by the DSM. (This can normally be done through the standard user interface).

GLSIM-BLIND also produces incidence angle dependent direct-to-diffuse transmittance values. Unfortunately, DSMs do not often permit the specification of these values. To consider the thermal effect of the direct-to-diffuse transmitted radiation in an approximate way, the incidence angle dependent direct-to-diffuse transmittance values can be added to the incidence angle dependent direct transmittance values.

7.3.2 Daily effective properties

For simpler DSMs, and for quasi-stationary calculation models of daily heating or cooling loads, values which express the daily influence of blinds are needed. In addition, these daily values can be used to find the best blind arrangement or the best slat inclination angle for a chosen day. Therefore, daily effective glazing/blind properties were introduced, which correspond to the daily average transmittance and absorptance values weighted by the incident radiation energy. The calculation considers the direct and diffuse radiation intensities on a window at each hour using a method similar to the one in DIN 5034 (1983) (standard clear sky conditions). The resulting effective properties distinguish between the direct and diffuse-, as well as between the transmitted and absorbed-, radiation components. They therefore meet the requirement of the most DSMs.

The following direct radiation glazing/blind properties are predicted:

- effective direct transmittance of glazing/blind system
- effective direct absorptance of the glazing,
- effective direct absorptance of internal blinds (= 0 for external blinds)

The calculated direct radiation transmittance and absorptance values depend on the date and geographical location of the site but, because the calculation considers standard clear sky conditions, the values are independent of a particular climate.

The variation of the values within one month is insignificant. Therefore, it is possible to use the values for each month or even to be satisfied with the values for each season (see section 7.6.2). Since the calculation of the diffuse radiation transfer through blinds uses an isotropic sky model (ISO), these values are independent of the time of day, date, season and location. In addition, the values are used for clear, as well as for overcast days. The following diffuse radiation glazing/blind properties are predicted:

- diffuse transmittance of glazing/blind system
- diffuse absorptance of the glazing
- diffuse absorptance of internal blinds (= 0 for external blinds)

Until this point, the glazing and the blind have been treated together and described by combined radiation transfer properties (transmittance or absorptance values). Often, however, the pure shading effect of a blind system (without the glazing) is required. (Shading factors

are often used to express the extra shading effect of a shading device when added to a certain existing glazing.) Therefore, effective blind reduction (shading) factors were introduced which are (approximately) independent of the glazing system.

The effective reduction values are given by the ratio of the total daily transmitted radiation energy of a glazing with blinds (g+b) to the total daily transmitted radiation energy of the same glazing without blinds (g):

- reduction factor of the direct radiation transmittance $RFtd = \frac{Etd^{g+b}}{Etd^{g}}$
- reduction factor of the diffuse radiation transmittance $RFtf = \frac{Etf^{g+b}}{Etf^{g}}$
- reduction factor of the direct absorptance $RFad = \frac{Ead^{g+b}}{Ead^{g}}$
- reduction factor of the diffuse absorptance $RFaf = \frac{Eaf^{g+b}}{Eaf^{g}}$

where *Etd* is the total daily transmitted direct radiation energy and *Etf* the corresponding diffuse radiation energy. *Ead* is the total daily direct radiation which is absorbed in the glazing and *Eaf* the diffuse radiation energy absorbed.

As noted before, GLSIM-BLIND can be used to investigate, compare and optimise blind arrangements during the design stage of a building. This is especially important when fixed blind devices are planned. Often the best slat inclination angle is required. For many applications, the ideal blind adjustment shades the direct beam radiation whilst enabling the transmission of as much diffuse radiation as possible to illuminate the space. Sometimes movable slats are considered. Because the position of the sun changes continually it is usually impracticable to keep the slats in the most efficient position at all times. Therefore, it is common practise to make an initial setting and then leave the slats unchanged until the sun is off the façade.

Considering either the case of fixed slats, or assuming that the slats are adjusted only once a day, it is interesting to compare the effective daily transmission properties.

The method of detecting the best slat inclination angle is demonstrated for a vertical glazing/blind system on the 21th of March (Fig. 7.11): In this case, the highest radiation transmission occurs when the slats are inclined upwards with an inclination angle of about 40°. To reduce the transmittance of the direct beam radiation effectively, the slat inclination angle must be reduced. Because the diffuse transmittance decreases slowly as the slat inclination angle decreases, the direct beam can be intercepted without the total lost of the diffuse radiation. When a direct transmittance of about 20% (in March) is admitted the best slat inclination angle would be 0° (horizontal slats).

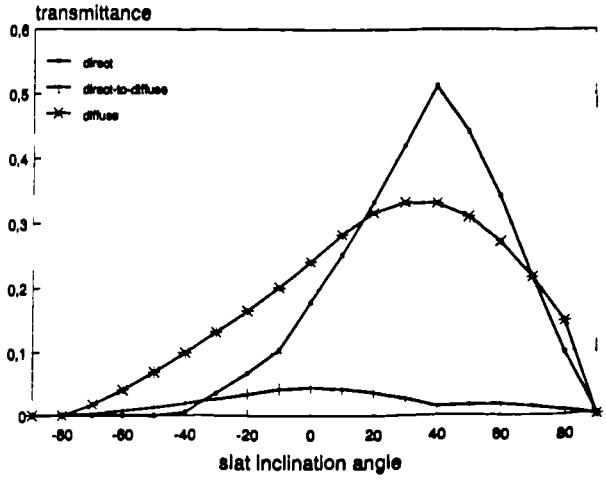

Figure 7.11:

Daily effective transmittance values on 21/3 for a vertical, south-facing clear double glazing system (direct normal transmittance = 0.6) with external slats (slat reflectance = 0.5; slat width = slat distance) at Kew (ground reflectance = 0.2) as the slat inclination angle (*si*) (positive = inclined upwards) is varied.

7.3.3 Annual (monthly) effective properties

Most quasi-stationary calculation models of cooling and heating loads (CIBSE-Guide 1986; DIN 4108, 1981; VDI 2078, 1977 etc.) need one single value of the total solar energy transmittance (Chapter 6) or one single shading factor. As described in section 7.1, most available statements about blind systems are formulated in this way. These single values can also be used to quickly compare the shading effect of different blind systems. They can be useful for classifying or ranking different systems. In addition, such values meet the requirement of simple thermal programs, which do not distinguish between the net-reduction in the direct or diffuse, transmitted or absorbed, radiation components (e.g. SERI-RES). Therefore, GLSIM-BLIND was extended to calculate annual (or monthly) effective blind properties, which correspond to the energy weighted average for the whole year (or month).

The calculation uses the hourly irradiation data in a climate file. The values are therefore location specific. The effective annual solar energy transmittance τ^{a}_{tot} describes the relationship between the annual transmitted solar energy E_{in} and the total incident radiation energy E_{on}:

$$\tau^{a}_{tot} = \frac{E_{in}}{E_{on}} = \frac{\Sigma\left(E_d * (\tau^{T}_{d} + \tau^{T}_{df} + \alpha^{T,b}_{d} + \alpha^{T,g}_{d} * fr) + E_f * (\tau^{T}_{f} + \alpha^{T,b}_{f} + \alpha^{T}_{f} * fr)\right)}{\Sigma\left(E_d + E_f\right)} \tag{7.9}$$

Equation (7.9) corresponds to equation (6.2) in Chapter 6, which was used to obtain the effective total solar energy transmittance of pure glazing systems. However, here the hourly transmittance and absorptance data of the glazing and blind system are considered (see Appendix D.7.2): direct (diffuse) transmittance τ^{T}_{d} (τ^{T}_{f}); direct-to-diffuse transmittance τ^{T}_{df}; di-

rect (diffuse) absorptance of internal blinds $\alpha_d^{T,b}\left(\alpha_f^{T,b}\right)$; direct (diffuse) absorptance of the glazing $\alpha_d^{T,g}\left(\alpha_f^{T,g}\right)$.

The effective annual reduction in the total radiation transmitted to the space (the shading factor) is defined as the ratio of the effective annual total solar energy transmittance of the glazing/blind system to the effective annual total solar energy transmittance of the pure glazing system. This value corresponds to the "z-factor" defined in DIN 4108 (1981).

$$z = \frac{\tau_{tot}^{a}\,(blind\,/\,glazing\,system)}{\tau_{tot}^{a}\,(pure\,glazing\,system)} \tag{7.10}$$

To study the seasonal variation of the total solar energy transmittance, the monthly effective values τ_{tot}^{m} of a vertical, south-facing clear double glazing (normal total solar energy transmittance = 0.72) with internal or external horizontal slats were calculated (Fig. 7.12). The corresponding monthly total solar energy transmittance values of the pure glazing without blind have already been discussed in Chapter 6 (see also Fig. 6.1 and Fig. 6.2). For external blinds, the predicted effective z-factors were in summer 0.41 and in winter 0.77. Both of these are higher than the standard value of 0.3 (DIN 4108, 1981). For internal blinds, the values become 0.89 in summer, or 0.92 in winter. These are both much higher than the standard value of 0.5 (DIN 4108, 1981). Clearly, the predicted values are only valid for one certain glazing/blind system and location, while the standard values seek to represent all systems. Nevertheless, the results clearly show that the standard values must be used with considerable caution.

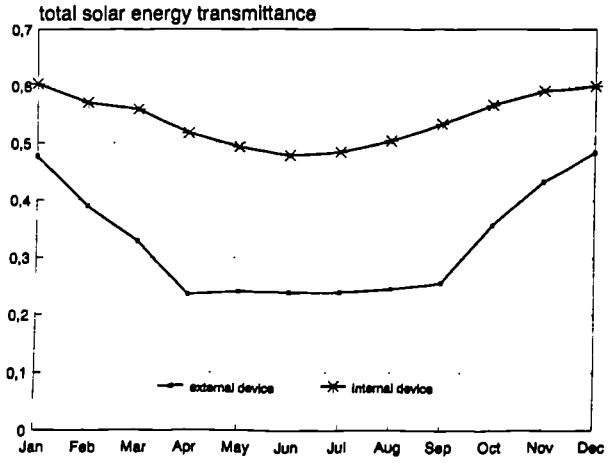

Figure 7.12:

Effective monthly solar energy transmittance of a vertical, south-facing double glazing system (normal total solar energy transmittance = 0.72) with internal and external horizontal slats (slat reflectance = 0.5; slat width = slat distance) for North Württemberg (Germany) climate conditions (ground reflectance = 0.2).

It should be noted, that the values for internal blinds (shown in Fig. 7.12) do not consider any secondary thermal effect which the blinds may have, e.g. the ventilation, longwave radiation or conduction energy transport to the outside (see following section).

7.3.4 Modelling of internal blinds

The theory (outlined in sections 7.3.1, 7.3.2 and 7.3.3) can be used to model external as well as internal blinds. However, for internal blinds some additional modifications must be considered.

Since the absorbed radiation energy of external blinds is lost to the ambient air, it is not necessary to calculate the (incidence angle dependent or daily effective) direct or diffuse absorptance values of external blinds. In contrast, the radiation energy absorbed by internal blinds contributes to the heat gain to the space. Thus, the (incidence angle dependent or daily effective) direct or diffuse absorptance values of internal blinds are important.

For internal blinds it is also important to decide how to assign the absorbed radiation (in the internal blinds) to the space. Since the surface area of the slats is very high, while the thermal mass of the slats is very low, the heat storage of the slats, and therefore their transient (non-stationary) effects is minimal. Any absorbed radiation energy is quickly lost to the surroundings. Two simplifications seem to be appropriate.

(i) The (incidence angle dependent or daily effective) direct or diffuse absorptance values of internal slats are given as input values to the DSM. The direct and diffuse radiation energy absorbed by internal blinds is then directly (without any time-delay) assigned to the air in the space by a (new) program subroutine. New model implementations are therefore necessary.

(ii) Alternatively, the direct and diffuse radiation energy absorbed by internal blinds is simply added to the direct or diffuse transmitted radiation, which is then distributed among the internal room surfaces (internal solar distribution). Thus, the absorptance of internal blinds can be considered in a way which does not require new program implementations.

The first method treats the heat loss from the slat surfaces as being purely convective. This appears to be a realistic assumption, since the air flow around the slats is emphasised (free convection due to temperature differences), whilst the longwave radiation (infra-red) heat losses are reduced (the slat surfaces often lie flat, which reduces the radiation connection with the surroundings). The second treatment however assumes a purely radiative energy gain to the room surfaces. Therefore, the radiation absorbed by the slats is assigned to an unrealistically high thermal mass (wall material). This may introduce an unrealistically long time delay into the heat gain to the air. Both models were implemented within HTB2 and compared in a sensitivity analysis (section 7.5).

Neither treatment of internal blinds considers any thermal effects, which the blinds may have on the energy transport to the outside. Often, the air gap between the glass and the internal blinds is ventilated with outside air, which increases the shading effect of the blinds. How-

ever, issues of ventilation and conduction are treated separately by DSMs in the simulation of temperatures and energy flows. Only shortwave radiation processes are considered in this work. It would be an interesting task to try and model the thermal effects of internal blinds. This could be an objective of future work.

7.3.5 Modelling of blind control

One important advantage of (non-fixed) slat-type blinds is that they can easily be adapted:

(i) by lifting them up (which totally removes the shading) or lowering them down (for full shading); or

(ii) by rotation of the slats.

Both methods of blind adjustment need controls, which are either manual (user dependent) or automatic. In detailed simulations of moving blinds the control regimen must be considered. This can be done as follows.

- Movable blinds are normally only brought down (by automatic or manual control) when uncomfortable direct illumination occurs. For example, they are unlikely to be used on overcast days. This interrupted use of movable blinds can be modelled by limiting the times when shading factors are applied to certain solar radiation situations (e.g. for direct radiation intensities above a certain level). As an illustration, this form of control was realised in the source code of HTB2.

- The modelling of rotating slats is much more difficult. With manual control, the exact slat inclination angle is generally unknown. However, it is plausible to assume that the blind will be (at least in a statistical way) ideally adjusted. The ideal slat inclination angle cuts off the (unreflected) direct beam radiation, while it enables as much diffuse radiation to enter the space as possible. Because the position of the sun changes continually it is impracticable to keep the slats continually in the most efficient position and it is customary to make an initial setting and then leave the blind unchanged until the sun is off the façade. Considering adjustment once a day, the ideal slat inclination angle can be found by using the slat optimisation method outlined in section 7.3.2 (looking at the daily effective blind properties). For annual simulations, the glazing/blind properties for monthly or seasonal example days can be scheduled.

  Automatic slat control is able to continuously produce the ideal slat inclination angle. The ideal slat inclination angle at a certain time of day corresponds to the maximum cutoff angle, which completely eliminates the direct beam radiation (see Fig. 7.5). It can be calculated as follows,

(7.11) $$sd*\sin(90°-h') = sw*\sin(h'-si)$$

For the special case of a regular blind geometry (slat distance = slat width) equation (7.11) reduces to:

(7.12) $si = 2*h' - 90°$

These formulations were realised within the latest version of GLSIM-BLIND to calculate either the incidence angle dependent or effective properties of glazing/blind systems with this form of automatic control.

It should be noted, that DSMs are often used to simulate the internal temperatures or cooling loads on a single extremely hot design-day. For these simulations, the seasonal variation of the ideal slat inclination angle, as well as the consideration of movable blinds, is unimportant.

7.4 VALIDATION OF THE CALCULATION MODELS OF BLINDS

Verification was mainly done using analytical investigations during the model development process. Inter-model comparisons were however possible by using programs which use a different (ray-tracing) technique to calculate the radiation transfer through glazing/blind systems (Furler 1990; Diegmann 1991; RADIANCE). In Diegmann (1991) measured data are also presented, but this was the only empirical validation that was possible. Clearly, further data to evaluate the software would be useful. This could be from full-scale field measurements, or from models placed outside or in artificial sky conditions.

7.4.1 Empirical and inter-model tests of diffuse transmission

Diegmann (1991) presented a computer program which calculates the radiation transfer through inclined slat structures using a ray-tracing technique (here named DIEG91). The program was tested against measured values for one blind system at different slat inclination angles. The comparison was limited to the 'hemispherical' (without ground reflected radiation or for horizontal surfaces respectively) diffuse radiation transfer through a blind without any glazing. The measured and simulated sky conditions were isotropic (ISO).

The blind geometry was regular (slat distance = slat width) and the slats were smooth. The upper slat surface was coated with a metal (mirror) film, so the reflectance at this surface was purely specular (shining factor = 0, see section 7.2.2). The lower slat surface was white (reflectance 0.9) and purely diffusing (shining factor = 1). Since it is not possible to define different slat surfaces in GLSIM-BLIND, an average shining factor of 0.5 was adopted. (It should be noted, that for the hemispherical diffuse transmittance, the statements 'upper' or 'lower' are irrelevant).

The measured and calculated (by DIEG91 and GLSIM-BLIND) diffuse transmittance values as the slat inclination angle varies are compared in Fig. 7.13. The values calculated by GLSIM-BLIND were found to be in close agreement with the measured values. In addition, GLSIM-BLIND reproduced the measured values better than DIEG91. For high slat inclination angles (> 60°), GLSIM-BLIND produced nearly identical values, while DIEG91 generated differences of more than 100%.

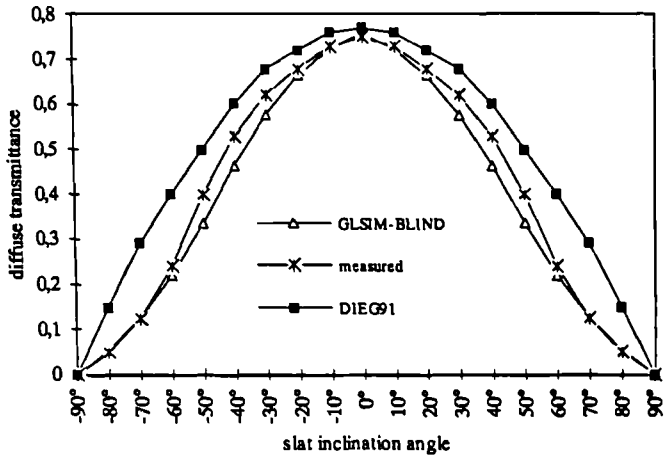

Figure 7.13:

Variation in the hemispherical diffuse transmittance (for isotropic sky conditions) of a horizontal blind system as the slat inclination angle is varied (slat reflectance = 0.9; slat distance = slat width, shining factor = 0.5).

The level of agreement is particularly pleasing because:

(i) the greatest uncertainty, and the most simplifications (e.g. in view factors) exist in the algorithms for the reflected radiation;

(ii) the extremely light coloured slats will exacerbate any calculation error;

(iii) a simplified assumption for the reflectance at the slat surfaces was adopted (shining factor = 0.5);

(iii) the calculation of diffuse radiation transmittance is more complex than the calculation of direct radiation transfer.

7.4.2 Inter-model verification of direct and diffuse radiation

Voss (1992) presented results for the radiation transfer through blinds (without glazing), which were based on calculations done by Furler (1990). Unfortunately, the basic principles of the computer program (here named FURL90) were not given. In addition, the precise reference to Furlers work was not given.

The blind system investigated was similar to that used by Diegmann 1991. The slats were extremely light coloured (reflectance = 0.9), flat, and regular (slat width = slat distance). The slats were horizontal (inclination angle = 0°), but the axis of the blind was inclined at an angle of 90° (vertical). Thus, the ground reflected diffuse radiation component (ground reflectance = 0.2) was considered.

For this blind system the diffuse radiation transmittance as well as the direct radiation transmittance for different projected sun height angles (h') (Fig. 7.14) was studied. The diffuse as well as the direct radiation transmittance values were calculated for either purely diffusing slats (shining factor = 1) or for purely specular slats (shining factor = 0).

a) Purely specular slats

For purely specular slats the programs FURL90 and GLSIM-BLIND predicted the same direct transmittance values at all projected sun height angles (Fig. 7.14). The diffuse transmittance was calculated to be 0.92 by FURL90, and 0.91 by GLSIM-BLIND.

Such close agreements may be expected, since the direct transmitted radiation (section 7.2.1) and specular-reflected radiation (7.2.2) can be reproduced without any simplifying assumptions. Although the simulation principle of FURL90 is unknown, the agreements give confidence in the GLSIM-BLIND program.

b) Purely diffusing slats

For the purely diffuse slats the programs produced direct transmittance values which differed by between 0.05 and 0.1 (Fig. 7.14). However, the predicted trends in the direct transmittance as the projected sun height angle varied, were similar for both programs. The break in the curve at a projected sun height angle of 45°, which corresponds to the slat cutoff angle (Fig. 7.5), is reproduced by both programs.

The diffuse transmittance was calculated by FURL90 to be 0.65, while GLSIM-BLIND yielded a slightly lower value (0.60).

The differences in the predictions may be caused by simplifying assumptions in one or both of the programs (view factors, multi-reflections). An exact explanation is not possible.

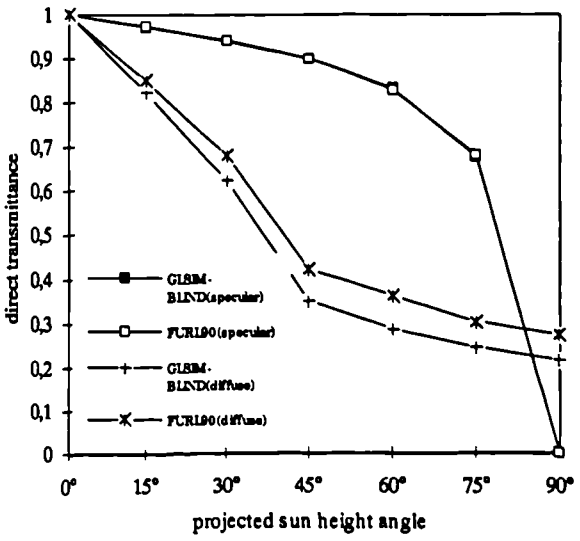

Figure 7.14:

Variation in the direct transmittance of a vertical blind system as the projected sun height angle (h') varied. The blind had regular horizontal slats (reflectance = 0.5).

7.4.3 Inter-model tests of diffuse transmittance with glazing

The validation has, so far, concentrated on blind systems without any glazing, so interactions between the glazing and the blinds has not been tested. Therefore, another validation study was undertaken which concentrated on a clear single glass pane (thickness = 6 mm) with internal or external horizontal flat slats (the slat reflectance was 0.5 and purely diffusing; the slat width equalled the slat distance). The blind/glazing system was not inclined (no ground reflected radiation) and the sky conditions were isotropic (ISO).

The predicted (hemispherical) diffuse transmittance values by GLSIM-BLIND were compared with those predicted by RADIANCE (Ward 1989). RADIANCE uses a ray-tracing technique to simulate the lighting characteristics and luminance levels in buildings. Most important is its ability to accurately account for both diffuse and specular inter-reflection in complicated spaces and system structures. It therefore considers in detail the radiation transfer through transparent materials and sunshades.

For external blinds GLSIM-BLIND predicted a diffuse transmittance of 0.408, while RADIANCE predicted 0.393. For internal blinds, the results of both programs were nearly identical (0.383 for GLSIM-BLIND and 0.385 for RADIANCE). The differences for external blinds may be attributed to the approximate assumptions used by GLSIM-BLIND to calculate the effective incidence angle of the diffuse radiation onto the internal glass pane.

7.5 SENSITIVITY OF PREDICTIONS TO BLIND CALCULATION METHODS

7.5.1 Blind models used

An investigation examined the thermal consequences of using different blind/glazing models. The investigation concentrated on the program HTB2, which was provided with all the necessary inputs and calculation possibilities. Three alternative calculation methods were studied.

- A rigorous dynamic treatment (see section 7.3.1) with the radiation absorbed by internal blinds assigned directly to the zone air using a solar-to-air number.
- By assigning daily effective properties (see section 7.3.2) with, in most cases, the radiation absorbed by internal blinds assigned directly to the zone air. The thermal consequences of adding the internal absorbed radiation to the transmitted radiation portion (simplified case) was investigated in a single study.
- By using annual effective properties (see section 7.3.3) with the radiation absorbed by internal blinds implicitly added to the transmitted energy. (The pre-calculation of the annual effective properties used the same climate data as used for the other methods.)

7.5.2 Building description

To predict the influence of the different blind models on the environmental conditions in a room, the simple direct gain test room used in previous studies (see Chapters 2 and 4) was used (Appendix A.1). This corresponded to a typical UK living-room with an advanced highly-insulated and heavy-weight construction (average U-value of 0.3 W/m²K). To exaggerate the thermal influence of the glazing, a large vertical clear double glazed (2×6 mm) window of about 14 m² (which corresponded to the total south wall) and a low infiltration rate of 0.35 ach was adopted. The room was continuously heated to 21°C.

The room was located at Kew near London (UK) (latitude = 51.5° North; longitude = 0°). It was unobstructed with respect to the wind and sun (no shading from other buildings was considered).

The room was studied for different window orientations (south; south-west; west; north-west; or north) and for January and July sunny design days (Appendix B). These represent the lowest and highest sun positions. The blinds used had a regular geometry (slat width = slat distance), a medium colour (reflectance = 0.5) and a shining aluminium surface (shining factor = 0.5). The basic room had external horizontal slats (slat inclination = 0°). Within different studies the location of the blind (external; internal) and the slat inclination angle (0° (horizontal); -30° (downwards)) were varied.

Predictions of hourly or peak air temperatures and daily heating energy demand (in January) were examined. The results are described in detail elsewhere (IR7).

7.5.3 Consequence of dynamic treatment

The shading effect of external horizontal slats increases as the incidence angle (or projected sun height angle h') of the direct radiation increases. Thus shading is greater in summer than it is in winter. A dynamic blind treatment should reproduce the seasonal variation of the shading effect correctly. Therefore, the thermal consequence of horizontal slats were studied for a sunny day in both January (low shading) or in July (high shading).

The predicted inside temperatures in the shaded, south orientated room in January clearly exceeded the heating setpoint of 21°C. The predicted peak air temperature was more than 30°C (dynamic treatment; Fig. 7.15), while the outside air temperature was lower than 5°C. (The peak air temperature in the same room without the blind was just 3 K higher, i.e. 33°C). Therefore, the peak inside temperature is mainly determined by the strong solar energy gains and the shading effect of the blind system is small.

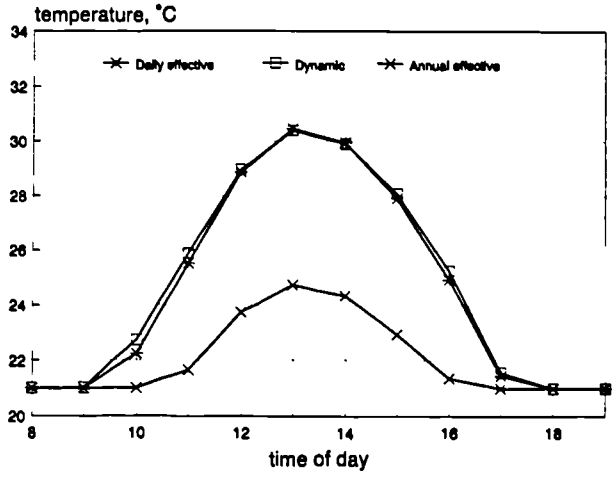

Figure 7.15:

Influence of different blind calculation treatments on predicted hourly air temperatures in a south-facing room with external horizontal slats in January.

Although the outside temperatures, the intensity and the duration of solar irradiation were greater in July, the predicted inside temperatures in the south orientated room (Fig. 7.16) were similar to those for January. The peak air temperature in the same room without blinds was 48°C. This result confirms the strong shading effect of the blind system in summer.

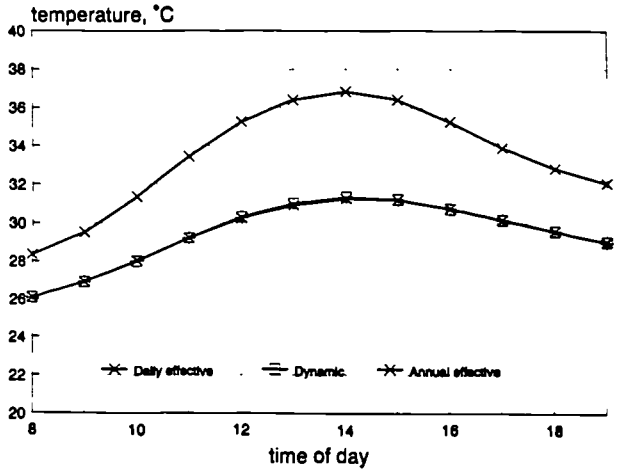

Figure 7.16:

Influence of different blind calculation treatments on predicted hourly air temperatures in a south-facing room with external horizontal slats in July.

This simple comparison demonstrates the marked influence of the shading effect of a blind system on the predicted thermal conditions in rooms. It also demonstrates that the seasonal variation of the shading effect is important. The dynamic blind treatment can reproduce these seasonal changes.

7.5.4 Consequence of daily properties

For south orientations the predicted internal temperatures when the daily effective properties were used agreed very closely with those predicted when the rigorous dynamic treatment was used. The predicted differences in the hourly temperatures for external slats in January (Fig 7.15) and July (Fig. 7.16) were less than 1%. (The agreement was independent of the season. This may be expected, since the daily effective properties implicitly consider the seasonal situation.)

When different slat inclination angles were used, the peak January temperatures predicted using the two approaches also differed by less than 1% (Fig. 7.17).

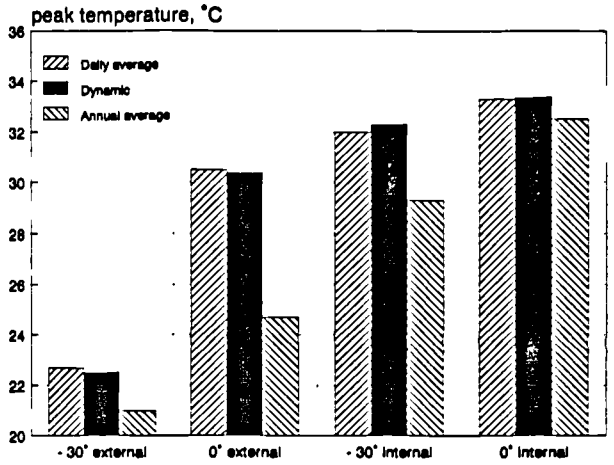

Figure 7.17:

Influence of different blind calculation treatments on the predicted peak air temperatures in a south-facing room in January. Different slat inclinations and blind positions are shown.

For east or west orientated windows the daily effective properties led to inaccuracies. There were errors in the absolute temperatures as well as in the times of which the highest temperature occurred. For example, consider the case of external blinds. The predicted peak temperature for a west orientated window was 41°C and it occurred at about 6pm using the dynamic treatment; by comparison, the value was 39°C and occurred at about 5pm when the daily properties were used (Fig. 7.18). In the evening, both curves were shifted by about one hour.

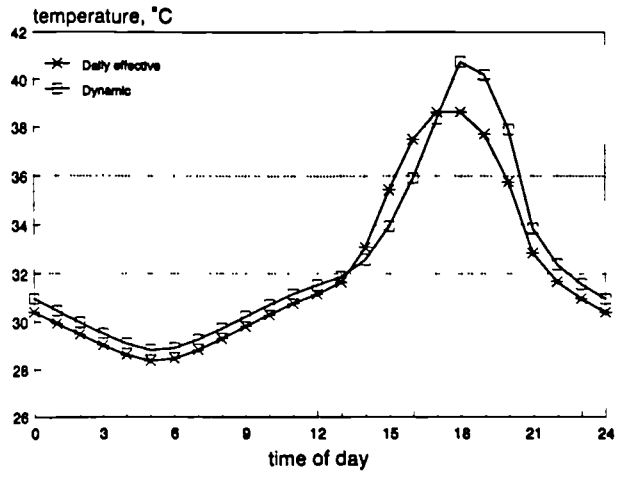

Figure 7.18:

Influence of different blind calculation treatments on the predicted hourly air temperatures in a west-facing room with external horizontal slats in January.

It would appear that, for detailed investigations of the hourly temperature variations in east or west orientated rooms, the rigorous dynamic blind treatment, which correctly represents the interaction of the sun location and the blinds, should be used. For south orientations, the use of daily effective properties seems sufficient.

7.5.5 Consequence of annual properties

The annual average properties generally led to an overestimate of the shading effect of external blinds in winter and to an underestimate in summer. For example, with south-facing blinds the underestimate in winter in the peak temperature was 6 K (Fig. 7.15) and the overestimate in summer was also 6 K (Fig. 7.16). The error decreased as the orientation changed from south to north (Fig. 7.19). It was very low for north orientation, where the influence of the incidence angle dependent direct beam radiation is small.

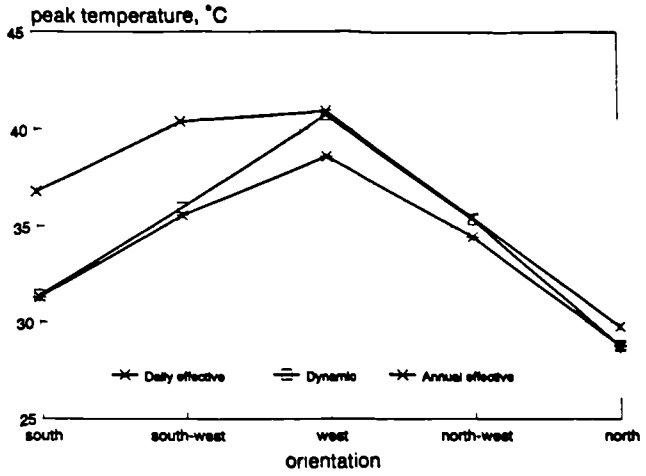

Figure 7.19:

Influence of different blind calculation treatments on the predicted peak air temperatures in January due to changing the orientation of a blind with external horizontal slats.

The agreement was better for internal blinds than it was for external devices (Fig. 7.17). This phenomenon can be explained by the particular shading impact of internal blinds, which is approximately independent on the sun location (and season) (e.g. Fig. 7.12). This arises because a reduction in the transmitted radiation due to shading is partly compensated by an increase in the absorbed radiation which then appears as heat in the room.

As a conclusion, it seems that the annual shading factors are unsuitable for detailed investigations of the environmental conditions (internal temperatures, heating demands in winter, cooling demands in summer, and heating or cooling loads) in rooms with externally shaded south-facing windows. They may however be useful for comparing or ranking different blind systems, or for quick, but approximate, thermal calculations.

7.5.6 Consequence of internal absorbed radiation treatment

The absorbed radiation of internal blinds may be assigned directly to the zone air (base-case) or added to the transmitted radiation, which is distributed among the room surfaces (simplified method). The latter possibility correctly considers the energy magnitudes, but may lead to a changed thermal interaction with the room environment. Both methods can be used in connection with a rigorous dynamic blind treatment, or with effective blind properties. Here, the thermal consequences of both assumptions were tested using daily effective blind properties. The investigation was limited to sunny weather conditions in January.

Generally, the simplified method produced higher peak temperatures and lower heating energy demands than the base-case treatment. In highly glazed and highly-insulated spaces, the utilisation of solar energy is better when it is assigned to a high thermal mass (insulated wall surfaces) rather than to the air. (This may be because the thermal resistance between the air and the window is lower than the thermal resistance between the wall surfaces and the window. The heat losses through the walls are low. When the absorbed radiation is assigned to the air, the heat losses through the window are increased). This may be different in traditionally-insulated rooms with small glazing areas.

For an internal blind with slats inclined downwards by -30°, the differences were about 2 K in peak temperatures (Fig. 7.20). The predicted heating energy demand was about 6 kWh for the simplified case, while the base-case method yielded about 10 kWh. The difference in heating energy demand was therefore more than 30%.

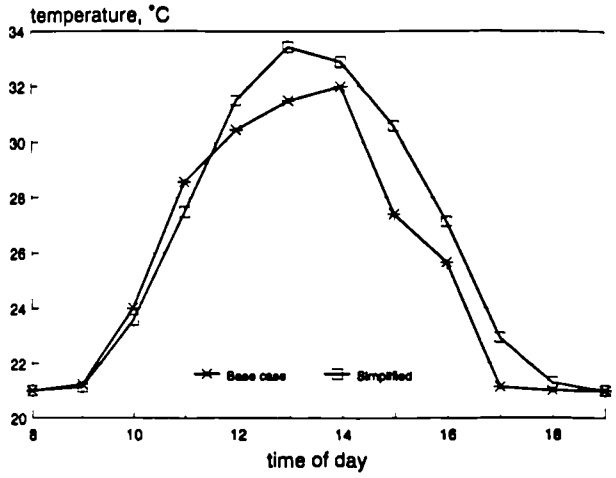

Figure 7.20:

Influence of the treatment of the energy absorbed by internal blinds on the predicted hourly temperatures in a south-facing room in January (-30° inclined slats)

The results demonstrate, that the treatment of the internal absorbed radiation energy may influence the predicted environmental conditions in buildings. A rigorous solar-to-air statement is preferred to a simplified treatment, in which the absorbed radiation is added to the radiation incident on internal surfaces.

7.6 DISCUSSION

In section 7.3 three approaches to modelling blinds (dynamic treatment, daily effective properties, annual effective properties) were introduced. None of the treatments require the implementation of new algorithms in the thermal processor. The different glazing/blind properties produced by GLSIM-BLIND can be directly used as input values for DSMs. The treatments differ in the level of detail (section 7.3), accuracy (section 7.5) and in the number of necessary input values.

In section 7.5 the three approaches to model blinds were tested using daily simulations. In daily simulations, the (incidence angle dependent or daily effective) transmittance and absorptance values need not to be scheduled. Therefore, the number of input values was small. The input for all three approaches could be done easily without modifications to the HTB2 input structure, and without the help of computer facilities (to automatically create the input files).

However, in long-term simulations (e.g. annual simulations) a daily, monthly or seasonal scheduling of the input values becomes necessary. The following sections discuss the different blind modelling methods in the context of long-term (e.g. annual) simulations. In addition, the possibility of creating and using databases for blind properties is discussed.

7.6.1 Dynamic blind treatment

When the dynamic treatment of blinds is used for annual simulations, the scheduling of the daily curves of transmittance and absorptance versus incidence angle is necessary. Since the variations of the curves within one month are small, it is only necessary to schedule one typical day per month (e.g. the 15th day). Nevertheless, the accuracy can be increased, if more than one day per month is considered. These values must be calculated and specified for each window type in the building. In this context, the window type changes if the orientation, window inclination angle, glazing type or blind type change.

Thus, for annual simulations using HTB2 it is necessary to input 10 transmittance values (one for each 10° increment in the incidence angle between 0° and 90°) and 10 corresponding values of absorptance for each month; a total of 240 values. (For windows which are not south orientated, two sets of values for transmittance and absorptance must be specified for each day, thus, the number of values increases to 480.) In programs such as ESP where values are only needed for 5 angles between 0° and 90°, the data demands are reduced.

Since many programs allow the time-scheduling of input properties (e.g. HTB2 and ESP) the specification of the transmission data is often straight forward. However, the input cannot be readily prepared without the help of a computer program. Hence, a routine was added to GLSIM-BLIND which produces the necessary input file in the format needed by HTB2 (a similar routine could be written for other programs).

It is also possible to simulate a blind/glazing system by scheduling the hourly values of transmittance and absorptance (instead of the incidence angle dependent values for one day). However, since most programs (e.g. HTB2 and ESP) do not accept hourly values of transmittance and absorptance, this method requires modifications to the input structure of the DSM.

It should be noted that none of the treatments (hourly values, or incidence angle dependent values for one or more days) increases the thermal simulation time. In addition, the pre-simulation time of GLSIM-BLIND is insignificant.

7.6.2 Daily effective properties

The daily effective property (daily shading coefficient) approach produces one value of direct transmittance and one value of direct absorptance for each day. Since the variations within one month are small, it is possible to use the values for one example day to represent a month. Nevertheless, the accuracy can be increased, if more than one day per month is considered. The diffuse transmittance and absorptance values are independent of the date and season.

For the annual simulation of one glazing/blind system, the input of at least 12 values of direct transmittance and 12 values of direct absorptance, one value of diffuse transmittance, and one value of diffuse absorptance is necessary (26 values altogether). Hence, the data needed are (relatively) low and need not necessarily be automated. Considering that the calculation accuracy using daily effective properties for south-facing windows is comparable with that of using the rigorous dynamic blind treatment (see section 7.5.4) the use of effective properties appears to be the most practical option for such windows. For east and west orientated windows the daily effective properties lead to inaccuracies.

It should be noted however, that this option requires a DSM to accept the input of daily shading factors (or effective properties). If a DSM does not allow the definition of shading factors (e.g. HTB2; ESP) new program implementations become necessary.

7.6.3 Annual effective properties

The annual shading coefficient approach produces only one annual shading factor which can be easily used for thermal simulations. However, the calculation accuracy is limited (see section 7.5.5). Annual shading factors appear to be unsuitable for detailed thermal simulations of internal temperatures, daily heating or cooling load and annual heating or cooling demands in rooms with externally shaded, southerly-facing windows.

Since the annual effective shading factors consider the specific features of a blind/glazing system (location, orientation, blind geometry etc.) more accurately than the common standard values (DIN 4108, 1981; CIBSE-Guide 1986 etc.) (see section 7.3.3), the new effective shading factors are likely to be an improvement on these methods. This was not, however, investigated in detail.

7.6.4 Database of glazing/blind properties

The incidence angle dependent (section 7.3.1) and daily effective (section 7.3.2) glazing/blind properties depend on the location of the site (latitude; ground reflectance), the location of the window (orientation; inclination angle) and the particular glazing/blind system characteristics (glazing type; blind type; slat inclination angle etc.). The annual effective glazing/blind properties (section 7.3.3) also depend on the local climate conditions (climate file).

The influence of geographical location (latitude) on the glazing/blind properties was not investigated in detail. This could be an objective of future work. However, one investigation showed that there was nearly no differences between the values for South-Germany (latitude about 48° North) and the values for London (latitude about 51.5° North). Thus, the values could be reasonably constant across middle Europe.

In contrast, the dependence of glazing/blind properties on the window location and on particular system characteristics was found to be significant. Therefore, a database should consider different window orientations, inclination angles, glazing types, blind geometries, slat inclination angles, slat surfaces (colour, shining) etc. Thus, a database would contain a huge number of different systems, all of which must be considered for different (at least 12 monthly) example days. The plausibility of such a database has not been tested. This could also be an objective of future work.

It should be noted, that a database of annual effective shading factors for many different systems has been created (Semen 1994) by using the program GLSIM-BLIND. The database was created to provide more accurate shading factors for use in simplified thermal calculations. The data were based on German climate conditions.

CHAPTER 8

INTERNAL SOLAR RADIATION DISTRIBUTION

8.1 INTRODUCTION

It has been indicated in Chapter 2 (section 2.3) that the thermal behaviour of a glazed space depends on the amount of transmitted solar radiation and its internal distribution. Solar energy, which enters the room through large glazing areas, is distributed around internal surfaces (sun-patching), absorbed, transmitted to the outside (re-transmission), reflected onto other internal surfaces or back to the outside (backloss) or transmitted through internal glazings into adjacent spaces (interzonal radiation transfer) (Fig. 8.1). In a modestly glazed room radiation backloss is small, interzonal radiation transfer happens rarely, solar distributions can be easily determined, and finally, the overall solar energy gains are limited. These are the reasons why DSMs use simplified shortwave radiation processes. In highly glazed spaces, such as conservatories, these processes can be important.

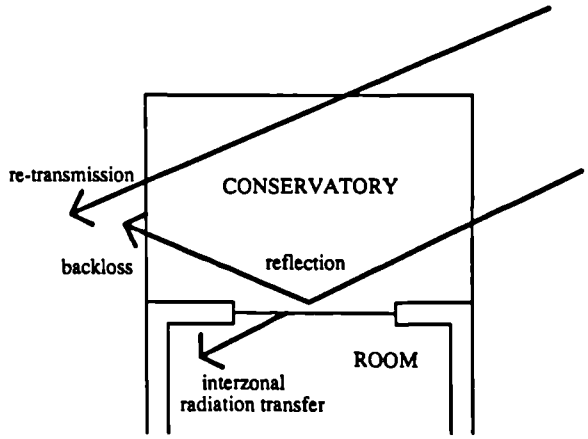

Figure 8.1:

Plan view of a conservatory with attached room to illustrate radiation re-transmission, backloss and interzonal radiation transfer.

An important weakness of the current solar distribution models within DSMs is, that the programs require the user to input the relative amounts of sun received by the various interior surfaces (see section 2.3). They do not usually provide program modules to calculate this. Guidelines exist (e.g. Niles 1984), which can be used to derive these figures for simple (traditional) room shapes with small windows, but these guidelines are not suitable for highly glazed spaces.

Moreover, DSMs normally assume the radiation split to be fixed over the whole simulation period (since time-scheduling is often not possible or it too must be determined by the user). But in highly glazed spaces, the solar distribution is highly dependent on the time of day and

season. In addition, the diffuse radiation distribution in the space, inter-reflections, radiation backloss and interzonal radiation transfer is calculated only approximately. None of the reviewed DSMs could model the immediate loss of direct radiation (re-transmission).

The thermal consequences of using different, simplified internal shortwave distribution models (as typically used within DSMs) has been investigated already (section 2.3). The impact of the models on the predicted internal temperatures in a conservatory and on the energy demand of an adjoining living-room were investigated.

The different simplified solar distribution models produced marked variations in the absolute predictions which would lead to the wrong assessment of the internal temperatures and comfort conditions in the conservatory. The modelling method also affected the design trends, most notably, whether, by attaching a conservatory, the heating energy demand of the attached building would increase or decrease. Since the solar distribution models in the DSMs used in the study were only crude approximations, credible design conclusions for the test building with the conservatory could not be derived. The study did however demonstrated the importance of using detailed solar radiation distributions in the conservatory, especially when there was interzonal radiation transfer. In addition, in highly glazed spaces the treatment of radiation backloss, diffuse radiation, and internal reflections was felt to be important. It was concluded that there was a need of more detailed solar distribution models.

8.2 EXISTING DETAILED SOLAR DISTRIBUTION MODELS

In a first step towards solving the solar distribution problem, existing more detailed solar distribution programs were reviewed. Two computer programs ESP-INS (Clark and McLean 1988) and ATRIA (Chuard 1992) produce detailed internal solar radiation splits as a function of time and can therefore be used as pre-processors for DSMs. In addition, one program the TRNSYS sunspace model (Beckman and Parsons 1980) was examined, which derives detailed time-dependent solar distributions during the simulation. The ability of these programs for simulating highly glazed spaces and for connection to other DSMs was studied.

- ESP-INS predicts the time-series insolation of internal zone surfaces (opaque or transparent), caused by direct solar radiation penetrating through windows. The computations are performed only for the day in the user-specified month which corresponds to the condition of average solar declination. The consideration of more than on month (e.g. for annual simulations) is possible. The insolation profiles can be transferred, automatically, to a zone insolation database for subsequent access.

As noted in section 2.3, the applicability of ESP-INS for modelling highly glazed spaces is limited. The program version ESP-INS 6.20a, which was available at the beginning of this work, could not treat more than 3 insolated surfaces at any one time. Unfortunately, the number of simultaneously insolated surfaces in highly glazed spaces is usually higher. Secondly, when windows were treated as multi-layer constructions (TMCs) the ability to use the insolation data files, and therefore to consider time-changing solar distributions, was lost. In Chapter 2, it was indicated that the modelling of windows as multi-layer constructions (TMCs) was important. These problems have already been recognised by the program developers and suggested as future improvements to ESP (Strachan 1990). Other fundamental weaknesses of ESP-INS are that: it does not consider the re-transmission of direct radiation; and it leaves the calculation of diffuse radiation distribution, internal reflections and view factors to the main thermal processor ESP-BPS (building and plant simulation system), which treats these operations only approximately. The fact that ESP-INS only deals with part of the solar radiation distribution problem (direct sun-patching) diminishes its value for a wider range of DSMs.

- The IEA task 12 work group developed a solar distribution program (ATRIA), which calculates the internal solar radiation split for each hour of example days (Chuard 1992). Unfortunately, the program can only deal with simple rectangular room shapes (shoebox), which is insufficient for simulating complex highly glazed spaces.
- Similarly, the TRNSYS (Klein et al. 1981) attached sunspace model can only be used for certain room shapes. In addition, the solar distribution method used assumes simplified geometrical condition for determining the sun-patching, and interzonal radiation transfer is not considered (Beckman and Parsons 1980). The program was originally developed for use in connection with the TRNSYS building processor. An application for other DSMs appears to be difficult.

None of these thermal models were felt to be suitable for the rigorous simulation of highly glazed spaces. Since the relative distribution of light and solar radiation in a room is approximately the same, another possibility was to use existing daylighting programs to predict internal solar radiation distributions. All that is needed is the hourly proportion of transmitted direct and diffuse radiation received by each surface on sample days. Thus, the usefulness of the daylight programs SUPERLITE (Wilde 1985) and RADIANCE (Ward 1989) as solar pre-processors for DSMs were investigated. This investigation identified the following problems.

- Daylight programs predict the internal light (radiation) distribution for certain fixed clear or overcast sky conditions. However, DSMs need the dynamic solar distribution for each hour of day. The repeated use of daylight programs for each hour of the day would be very time consuming (especially when the ray-tracing program RADIANCE is used).

- Daylight programs calculate the detailed lighting levels on internal surfaces, while DSMs usually need one value for the received radiation by each surface. Therefore, an additional conversion of lighting levels into single values of solar radiation energy would be necessary.
- The available version of SUPERLITE (1.0) could not treat complex room shapes and interzonal radiation transfer.

It was concluded that the daylight programs can not readily produce the input values, which are necessary for DSMs to simulate solar radiation distribution in highly glazed spaces. The development of a special linkage between daylight programs and DSMs was felt to be difficult.

Elsewhere, effort is being expended to combine daylight programs and DSMs. The new linkage SUPERLINK (Erhorn and Szerman 1993, 1994) connects the daylight programs SUPERLITE and RADIANCE with different DSMs. However, the linkage concentrates on the effect of daylight levels in rooms on the predicted lighting energy demands. It does not provide the accurate solar distribution for the thermal processor. The newly developed module TRNSYS-LIGHT (Dietrich 1994) offers similar possibilities for the thermal processor of TRNSYS. It should be noted, that these programs were not available at the starting of this work and that their detailed calculation principles were unknown.

Because appropriate solar distribution programs for modelling complex highly glazed spaces were not available, a new geometric solar distribution program (called SUNSIM) was created. It considers all the important aspects such as: dynamic (time-changing) internal radiation distribution; re-transmission; backloss; interzonal radiation transfer etc. It produces the hourly absorbed radiation energy quantities for all internal surfaces for the whole simulation period, rather than the relative radiation splits (as calculated by ESP-INS). In this way, the solar processing is totally separated from the thermal processing.

The pre-simulation module SUNSIM is independent of a particular DSM. For demonstration and testing purposes a new interface was created, which allows its connection with HTB2.

The following sections deal with the most important calculation principles of SUNSIM, they illustrate its ability to calculate solar distribution, interzonal radiation transfer, radiation re-transmission, and backloss in highly glazed spaces. A sensitivity analysis concentrates on the thermal effects of these aspects on the environmental conditions of a room with an attached conservatory. A detailed description of the SUNSIM input structure is enclosed to IR10 or given in the SUNSIM user manual.

8.3 OPERATION OF SUNSIM

8.3.1 Geometry

The solar distribution program SUNSIM can model one room, which is enclosed by any number of opaque or transparent planes. Adjacent zones are not modelled. Partition windows to adjacent rooms must be defined as opaque planes (the method of modelling interzonal radiation transfer is discussed in section 8.3.4).

To simplify the definition of certain room geometries, a pre-processing program GEOSIM was created which permits the automatic digitising of the room geometry. The user only has to specify the building type and the basic geometrical information about the length, depth and height of the room. Currently it is possible to process six different building types: rectangular room with flat roof (shoe-box); hipped roof; gable roof; pent roof; barrel roof; or a round room with dome roof (Fig. 8.2).

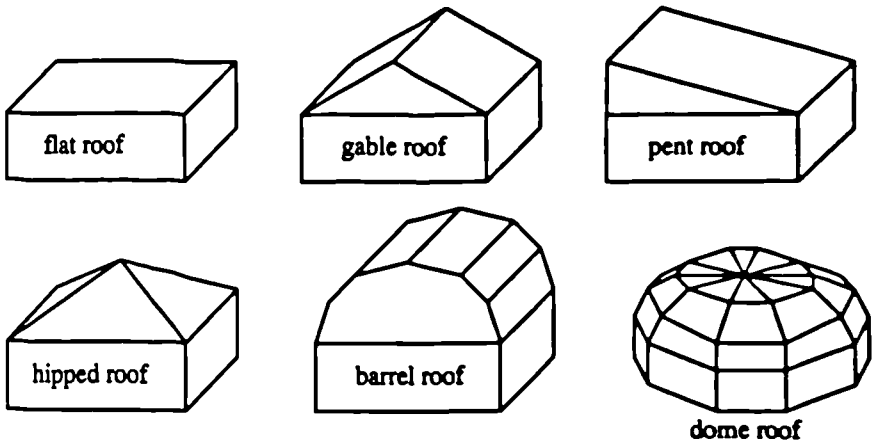

Figure 8.2: Possible room and roof shapes used by the solar distribution program SUNSIM.

The planes which define the space are divided by meshes into part-planes (grids) (Fig. 8.3). These part-planes are either opaque or, to model windows, transparent. The calculation accuracy and the calculation time increases with the grid density.

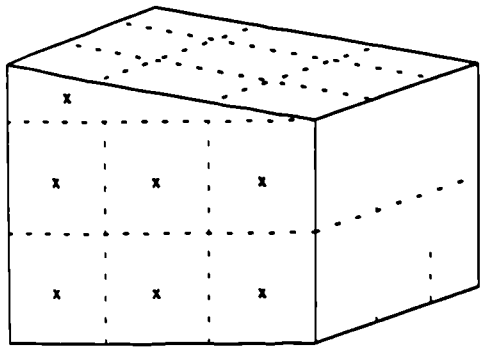

Figure 8.3:

Illustration of the sub-division of planes by meshes to produce part-planes.

All the planes and part-planes of the zone are mathematically described with the coordinates of their 4 corner points. (In the case of triangular surfaces, the fourth point is set to zero). The information about the room shape is stored in a file (termed *part.def*). It is used by

SUNSIM to track the solar radiation round the space (section 8.3.2) and to produce the view factors between the part-planes (section 8.3.3).

It should be noted, that SUNSIM can deal with any convex room shape and any number of opaque and transparent planes (part-planes). The number of possible room shapes could therefore be extended by replacing the graphical interface GEOSIM by a sophisticated CAD computer program, which generates these room shapes. This could be an objective of future work.

8.3.2 Theory of solar tracking

To determine the amount of beam radiation striking a particular part-plane at a certain time requires the intersection of the sun's rays with the interior part-planes to be determined. This can be done for any time by calculating the vector projection of the sun beam through the centre point of the transparent part-plane onto the internal part-plane. The transmitted radiation power through one part-plane is assigned to exactly one internal part-plane (Fig. 8.4). The part-planes to which the solar radiation is 'patched' can be either opaque or transparent, they can bound another room or separate the zone from ambient conditions.

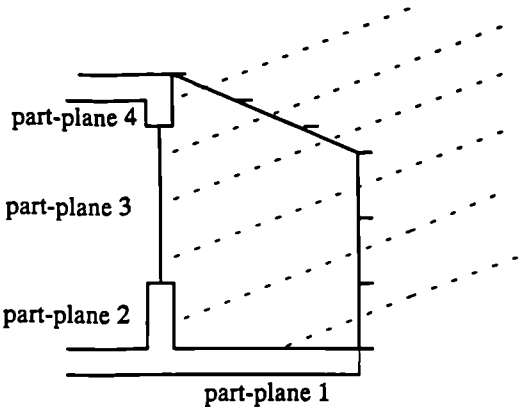

Figure 8.4:

Cross-section through a conservatory with attached room to illustrate the passage of sun beams through the external part-planes onto internal part-planes.

When the internal part-plane receiving the radiation is a transparent external element the re-transmission of the beam to the outside is considered. The reflected radiation at each part-plane is distributed among all internal part-planes by considering very accurate view factors. A matrix solution method permits a mathematically complete simulation of all multi-reflections without any limitation on the amount of reflection. The backloss of reflected radiation is also considered.

The direct normal, and the global horizontal, radiation intensities (as used by HTB2) are taken from a user specified climate file. It is also possible to use direct and diffuse horizontal radiation as provided by many other climate files. The direct and diffuse radiation intensities onto inclined surfaces (and the incidence angle of the direct radiation onto the surfaces) is then calculated assuming standard isotropic (ISO) sky and ground models (DIN 5034, 1983).

When the outside plane or part-plane is a transparent element (with the area A_1) the transmitted direct radiation (Q_{d1}) is obtained by:

(8.1) $$Q_{d1} = \tau_{d1}(\theta) * A_1 * I_{d0}$$

The diffuse radiation (Q_{f1}) is given by:

(8.2) $$Q_{f1} = \tau_{f1} * A_1 * (I_{gr} + I_{sky})$$

In these equations, θ is the incidence angle of the direct beam radiation, τ_d and τ_f are the transmittance for the incidence angle dependent direct radiation and diffuse radiation respectively, and I_{d0} is the direct radiation intensity normal to the surface. I_{gr} and I_{sky} are the sky and ground diffuse radiation intensities on the part-plane respectively.

A vector projection of the sun beam through the middle point of part-plane (say 1) yields the number of the illuminated internal part-plane (say 2) and the incidence angle of the beam according to the internal part-plane (ψ) (see Fig. 8.4). When α_{f2} is the diffuse absorptance of part-plane 2, the absorbed radiation Q_{ab2} in part-plane 2 results as follows:

(8.3) $$Q_{ab2} = \alpha_{f2} * Q_{d1}$$

When the internal part-plane is opaque, the direct reflected radiation portion Q_{ref2} is obtained by,

(8.4) $$Q_{ref2} = (1 - \alpha_{f2}) * Q_{d1}$$

When the internal part-plane is transparent, the direct incidence angle dependent re-transmitted (and absorbed) radiation must be considered:

(8.5) $$Q_{ref2} = (1 - \alpha_2(\psi) - \tau_2(\psi)) * Q_{d1}$$

The incidence angle dependent transmittance ($\tau(\theta)$ and $\tau(\psi)$) and absorptance ($\alpha(\psi)$) values (10 values of transmittance and absorptance for incidence angles from 0° to 90°; see Chapter 5) as well as the diffuse transmittance (τ_f) and absorptance (α_f) for clear and overcast skies (see Chapter 4) must be input by the program user.

The reflectance ρ at internal part-planes is treated as purely diffuse. The total radiation emitted from a transparent part-plane 2 (Q_{e2}) consists of the direct-to-diffuse reflected radiation Q_{ref2} and a transmitted diffuse radiation component Q_{f2} (Fig. 8.5). For opaque part-planes the transmitted diffuse radiation component is omitted.

(8.6) $$Q_{e2} = Q_{f2} + Q_{ref2}$$

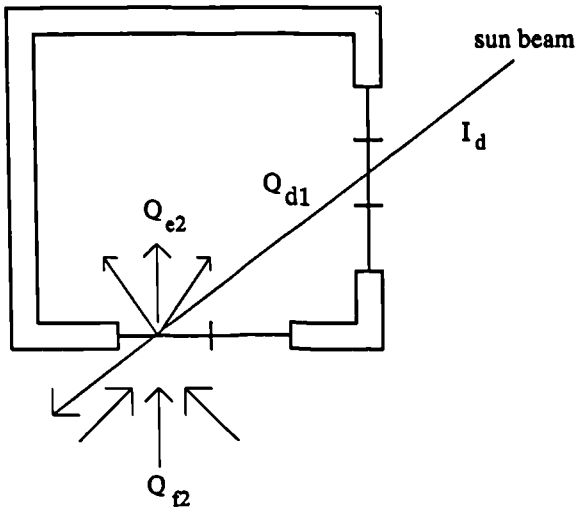

Figure 8.5:

Plan view of a room with two transparent sides to illustrate the total diffuse radiation emitted from a transparent part-plane.

The emitted radiation Q_{e2} is than distributed among all internal part-planes weighted by the view factors f (see section 8.3.3). The total diffuse radiation portion Q_{2j}, which is transported from part-plane 2 to any internal part-plane j is calculated as follows:

(8.7) $$Q_{2j} = f_{2j} * Q_{e2} + f_{2j} * \rho_2 * Q_2$$

where Q_2 is the total (reflected) diffuse radiation, which was arrived at part-plane 2 from all the other internal part-planes and ρ_2 is the diffuse reflectance, which considers the backloss of the radiation ($\rho_2 = 1 - \alpha_{f2} - \tau_{f2}$).

The total radiation Q_j onto any internal part-plane j can be obtained by,

(8.8) $$Q_j = \sum_{k=1}^{n} f_{kj} * Q_{ek} + f_{kj} * \rho_k * Q_k$$

where n is the total number of internal part-planes.

This can also be written as one line in a linear equation system. The left side contains the known quantities and the right side defines the unknowns.

(8.9) $$f_{1j} * Q_{e1} + f_{2j} * Q_{e2} + \cdots + f_{nj} Q_{en} = Q_j - f_{1j} * \rho_1 * Q_1 - f_{2j} * \rho_2 * Q_2 - \cdots - f_{nj} * \rho_n * Q_n$$

For example, three part-planes lead to an equation system with 3 lines and 3 unknowns,

(8.10) $$\begin{bmatrix} f_{21} * Q_{e2} + f_{31} * Q_{e3} \\ f_{12} * Q_{e1} + f_{32} * Q_{e3} \\ f_{13} * Q_{e1} + f_{23} * Q_{e2} \end{bmatrix} = \begin{bmatrix} 1 & -f_{21}\rho_2 & -f_{31}\rho_3 \\ 1 & -f_{12}\rho_1 & -f_{32}\rho_3 \\ 1 & -f_{13}\rho_1 & -f_{23}\rho_2 \end{bmatrix} * \begin{bmatrix} Q_1 \\ Q_2 \\ Q_3 \end{bmatrix}$$

For n part-planes, the corresponding equation system has n lines and n unknowns. The equation system is solved by a matrix solution method (Gauss-Seidel algorithm). The resultant radiation portions Q_j describe the total amount of diffuse radiation, which is assigned to

the part-planes. The total amount of absorbed diffuse radiation Q_{abj} follows by multiplication with the surface absorptance.

(8.11) $$Q_{abj} = \alpha_{jj} * Q_j$$

This energy portion is added to the direct absorbed radiation (equation (8.3)) and stored for every part-plane and simulation hour in a file (termed *greenh.aks*).

8.3.3 View factors

A view factor f_{12} is defined to be the relation of the radiation portion transmitted from area A_1 to area A_2 to the total radiation emitted from area A_1,

(8.12) $$f_{12} = \frac{1}{\pi * A_1} * \int_{A_1} \int_{A_2} \frac{\cos(\varphi_1) * \cos(\varphi_2)}{di^2} * dA_2 * dA_1$$

where *di* is the distance between the areas A_1 and A_2; φ_1 and φ_2 are, respectively, the emittance angle and incidence angle of the radiation (defined in relation to the surface normal vectors).

There are a lot of analytical solutions to this problem for simple geometrical arrangements (e.g. parallel surfaces; perpendicular surfaces). More complex arrangements need a numerical prediction.

Current numerical methods divide a surface into small part-planes and calculate the view factor for every part plane as follows (see also VDI Wärmeatlas 1988):

(8.13) $$f_{12} = \frac{\cos(\varphi_1) * \cos(\varphi_2)}{di^2 * \pi} * A_2$$

A precondition of this calculation technique is that the distance *di* between the surfaces is at least 5 times the diameter of the areas A. The reason of this limitation is the acceptance, that the areas A are infinitely small and that the radiation emittance is hemispherical. Edge and corner situations do not comply with this requirement.

To predict the exact view factors between all the part-planes, another more accurate calculation approach was chosen. It is based on a graphical representation of view factors found in the VDI Wärmeatlas (1988) and has the following advantages:

- much more accurate view factors are calculated when *di* is small;
- the calculation is totally independent of the surface area shapes;
- the requirement $\sum f_{12} = 1$ (sum of all view factors equal 1) is always fulfilled, even when there are inaccuracies in single values.

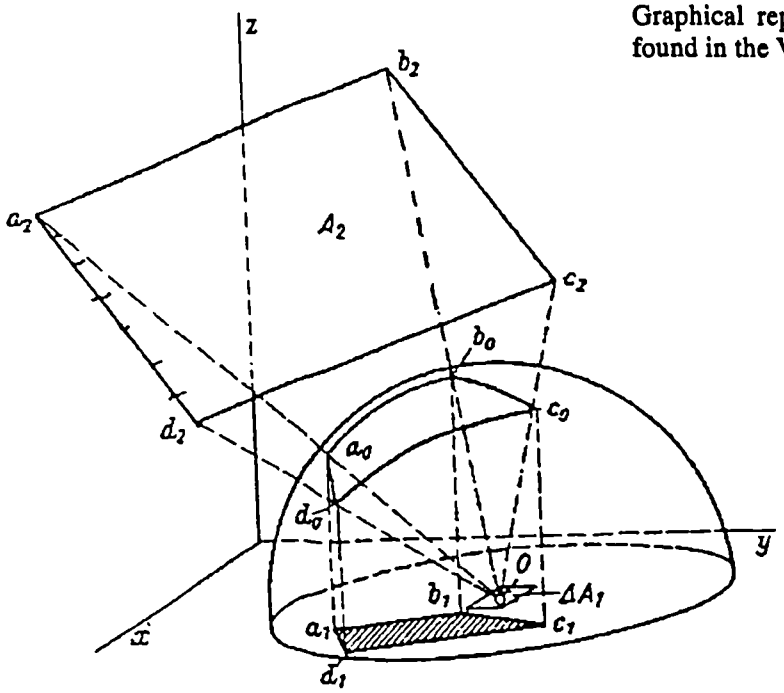

Figure 8.6:

Graphical representation of view factors found in the VDI Wärmeatlas (1988).

A half vault is conducted above area ΔA_1, with the radius 1, and intersecting the x,y-plane. The view factor between the area ΔA_1 and A_2 then corresponds to the ratio between the projected area A (a_1; b_1; c_1; d_1) and the area of the circle (π).

(8.14) $$f_{12} = A / \pi$$

A numerical transformation of the graphical representation was used which calculates the area A (a_1; b_1; c_1; d_1) by vector projection (see Küster 1992).

8.3.4 Interzonal radiation transfer

When an illuminated internal part-plane is a transparent partition to an adjacent room, a part of the incident radiation is transmitted into the adjacent room. Since SUNSIM is a one-zone model, the radiation path into the adjacent room (and the distribution in the adjacent room) is not simulated. Instead, the distribution of interzonal transferred radiation is left to the main processor.

In SUNSIM, partition windows are defined as opaque surfaces with an absorptance, which corresponds to the sum of the diffuse absorptance α_f and the diffuse transmittance τ_f.

(8.15) $$\alpha'_f = \alpha_f + \tau_f$$

Thus, the absorbed radiation ($\dot{Q}'_{ab}$) stored in the transfer file (*greenh.aks*) includes the absorbed radiation as well as the transmitted radiation to the adjacent room. In the thermal processor both radiation portions are separated using a weighting function:

(8.16) The absorbed radiation: $$\dot{Q}_{ab} = \dot{Q}'_{ab} * \frac{\alpha_f}{\alpha_f + \tau_f}$$

(8.17) The transmitted radiation: $$\dot{Q}_{tr} = \dot{Q}'_{ab} * \frac{\tau_f}{\alpha_f + \tau_f}$$

The transmitted radiation to the adjacent room is treated as being purely diffuse. The transmitted radiation power $\dot{Q}_{tr}$ is distributed among all internal surfaces using an area and absorptance weighting algorithm. This is the original HTB2 algorithm for internal diffuse radiation distribution.

(8.18) $$\dot{Q}_j = \dot{Q}_{tr} * \frac{\alpha_j * A_j}{\sum_n \alpha_n A_n}$$

A_j and α_j are the area and the absorptance of surface j, while n is the total number of internal surfaces.

The exact geometrical information of the sunpath (correct sun patching) is neglected. More precise calculations may be possible and could be the objective of further improvements. However, as long as the adjacent space is not highly glazed just like the highly glazed zone, the error due to the used simplification is marginal.

8.4 INTERACTION WITH THE THERMAL PROCESSOR

The solar distribution module SUNSIM is an independent pre-processing program. It uses the weather data (which will subsequently be used by the DSM) to calculate the transmitted solar radiation which is absorbed by each internal surface at each hour. The resultant file (*greenh.aks*) contains the absorbed radiation for every room surface and simulation hour. This file is used by the thermal processor during the simulation along with the usual weather file. The interface definition file (termed *greenh.dat*) contains all the necessary information to connect the module with the main program (Fig. 8.7).

Figure 8.7: Interaction between SUNSIM and the connected DSM.

It was intended that SUNSIM would calculate the solar distribution in one (highly glazed) zone in a complex multi-zone building. This zone was termed *greenhouse zone*. Although it is also possible to pre-calculate conventional rooms (with small window surfaces), SUNSIM is most useful for highly glazed spaces such as greenhouses and conservatories. An accurate calculation of the solar distribution is usually only necessary in highly glazed spaces, where radiation re-transmission, radiation backloss, and interzonal radiation transfer, are important (see section 8.1). Since SUNSIM only produces the solar distribution for one particular (highly glazed) zone, it does not replace the solar distribution routine of the DSM.

The greenhouse zone can be attached to the building (such as conservatories) or it can be totally embedded (like many atria). There may be more than one neighbouring zone with partition windows into the greenhouse zone (Fig. 8.8).

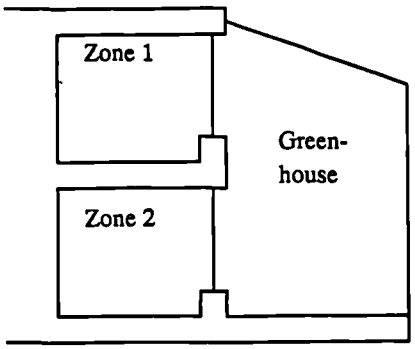

Figures 8.8:
Illustration of a greenhouse with two adjacent zones.

The greenhouse is included as a zone when the normal thermal simulations are undertaken. The use of the module SUNSIM does not compromise the normal operation of the DSM. Because of this, the DSM is used to calculate the radiation absorbed by the external wall surfaces and by the external glazings (of the greenhouse zone) (Fig. 8.9). It should be noted that both of these aspects can be accurately calculated by thermal models and need not, therefore, be part of the solar pre-simulation (SUNSIM).

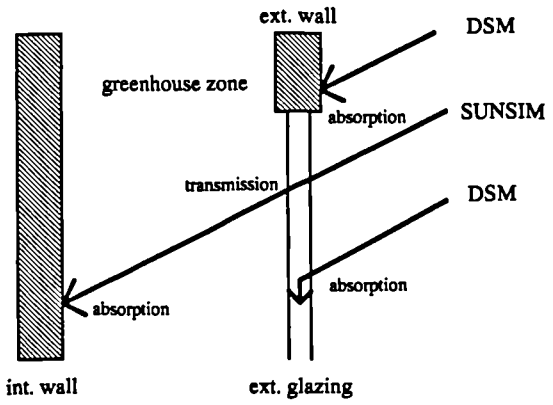

Figure 8.9:
Illustration of the radiation absorbed by internal elements (as calculated by SUNSIM) and external elements (as calculated by the DSM).

Since the thermal simulation is totally separated from the shortwave processing, the greenhouse zone can be subdivided to fictitious air spaces to simulate air flow and temperature stratification (Fig. 8.10). Many DSMs, which internally calculate aspects of solar radiation

distribution (e.g. ESP), cannot accurately calculate the shortwave radiation transfer through the fictitious surfaces between the air layers.

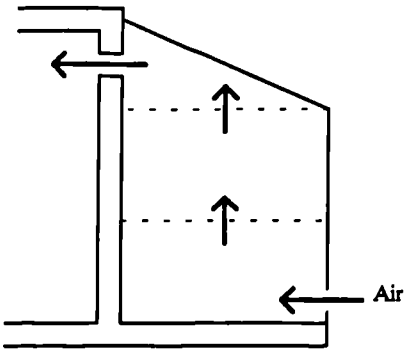

Figure 8.10:

Sub-division of a greenhouse zone into fictitious air spaces to simulate air flow and temperature stratification.

Coupling the solar distribution module SUNSIM with the DSM, requires a specific interface which means modifications are needed to the DSM. The following changes are necessary.

- The part-planes used by SUNSIM must be assigned to the surfaces (walls, windows etc.) used by the DSM. In the case of partition window planes, the part-planes must be assigned to the corresponding adjacent zone. The necessary information is stored in the interface definition file *greenh.dat.*
- During the thermal simulation a new routine reads the transfer file *greenh.aks* and assigns the absorbed radiation values to the corresponding surfaces (walls, windows etc.). These values replace the absorbed radiation values, which are calculated by the DSM using its original (native) solar distribution algorithms. (It is possible to slightly reduce simulation time, when the original solar distribution algorithms of the DSM are switched off).

The program HTB2 was modified to permit its interaction with SUNSIM. The new HTB2 version, which includes the SUNSIM interface, was called HTBSOL.

8.5 VALIDATION OF SUNSIM

Since SUNSIM is a purely geometrical model, which does not use any empirical relations (except those of the standard sky models) the validation was restricted to a code debugging task. This was done using analytical evaluation methods. The correct reproduction of the sky model was tested by inter-model comparisons with HTB2.

8.5.1 Inter-model comparison

An investigation was conducted, which compared the internal absorbed radiation energy in a conservatory (of the type used for the sensitivity analyses; section 8.6) predicted by SUNSIM and HTB2.

When the SUNSIM calculation process of re-transmission and radiation backloss is switched off, the transmitted radiation energy is totally absorbed by the space elements (Q_{abj}). Thus, the total amount of absorbed radiation in the space predicted by SUNSIM should agree with that predicted by HTB2 (or any other DSM), which only considers internal radiation absorption.

(8.19) $$\sum_i Q_{ab_i}(SUNSIM) = \sum_i Q_{ab_i}(HTB2)$$

With such a comparison the following short-wave calculation principles and algorithms can be tested:

- **sun position** (latitude, sun declaration, equation of time, solar altitude, solar azimuth, hour angle, angle of incidence)
- **modelling of diffuse radiation** (sky radiation, ground reflected radiation)
- **surface location** (orientation, inclination, area)
- **transmission through windows** (incidence angle dependent direct transmittance, diffuse transmittance)
- **timing convention** (simulation start time, time in climate file, stop time)

The investigation yielded nearly identical values for the internal absorbed radiation for both calculation models (Fig. 8.11). This was a very encouraging result, since both programs use different algorithms for the calculation of the sun position, surface location and window transmittance. It should be noted that SUNSIM and HTB2 use the same isotropic (ISO) sky model.

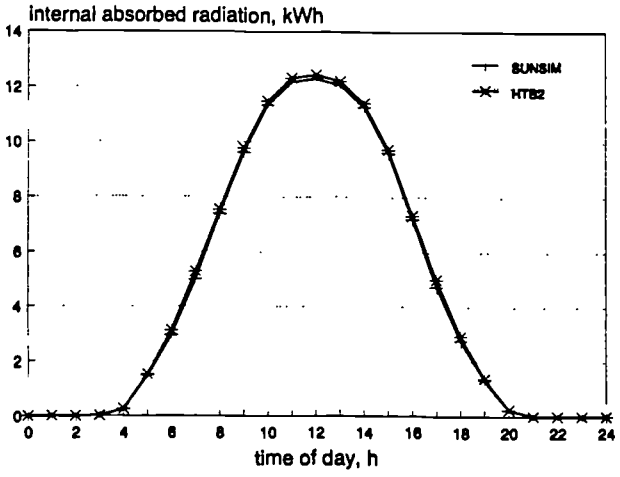

Figure 8.11:

Total internal absorbed radiation in the conservatory on a UK sunny summer's day.

8.5.2 Analytical verification

- To validate the vector projection of the sun beam onto internal surfaces the SUNSIM predictions were compared against graphically determined solar distributions. Different

geometrical arrangements were tested. In all cases, corresponding results were obtained from the two methods.

- To validate the calculation of internal reflections the values for the total radiation absorbed by internal surfaces for different geometrical arrangements, were compared with values, which were predicted using a different, recursive calculation method. The agreement was good.
- The numerical calculation of the view factors was tested against analytical values for simple geometrical arrangements. In this way, the error potential (especially for edge and corner situations) could be assessed. As a result, the error in the view factors were found to be very low (lower than 5% for normal geometrical relations). For extreme corner situations (distance about the same as surface diameter, see section 8.3.3) a maximum error of 35% was found. This is much lower than the error of 120%, obtained by the conventional calculation method (equation (8.13)).

8.6 SENSITIVITY OF PREDICTIONS TO INTERNAL RADIATION DISTRIBUTION MODELS

A previous investigation looked at a two-zone arrangement in which a typical UK living-room was attached to a conservatory (section 2.3). The study examined the effect of using simplified internal solar distribution models on the predicted daily energy demand of the living-room and the daily peak air temperatures in the conservatory. The simplified solar distribution models corresponded to those typically used by DSMs.

This study demonstrated the importance of modelling the dynamic solar radiation distribution in the conservatory, especially when there was interzonal radiation transfer. In addition, in highly glazed spaces, radiation re-transmission and backloss, the treatment of the diffuse radiation and the modelling of internal reflections were felt to be important. The solar distribution models, used in that study, treated these aspects only approximately. Since there was no accurate reference model available, it was not possible to quantify the error introduced by the simplified modelling assumptions. Using SUNSIM, with its improved treatment of internal solar distribution, it is now possible to undertake such quantifications.

The previous sensitivity analysis (section 2.3) was repeated using SUNSIM. The differences in the predictions produced by SUNSIM and the simplified models (used in the previous study) is a measure of the accuracy of the simplified models. All the variations were studied for a UK sunny winter's day (Appendix B), which was shown in the previous study (section 2.3) to produced significant differences in predictions (section 8.6.3).

In addition, using SUNSIM, it is possible to investigate the thermal effects of different solar distribution issues (such as interzonal radiation transfer or radiation loss). This was studied

by conducting annual simulations using weather data of Kew (UK) (section 8.6.4). All the results are described in detail in IR11.

8.6.1 Building description

The basic building description corresponded to that used in the pervious study (section 2.3): a two zone model of a typical UK living-room and a single glazed conservatory with a typical shape (Appendix A.2) (Fig. 8.12). To comply with the requirements for a passive solar design and to enhance the sensitivity of the heating demand to solar energy gains, the living-room was highly insulated (average U-value = 0.3 W/m²K). It was continuously heated (to a set-point of 21°C) and had a low infiltration rate of 0.3 ach. The conservatory had a rectangular shape (floor area = 12 m²) and was not heated. It was connected to the living-room by a partition wall and a partition window, which was half the size of the partition area (7.07 m²) and double glazed. The conservatory was south orientated.

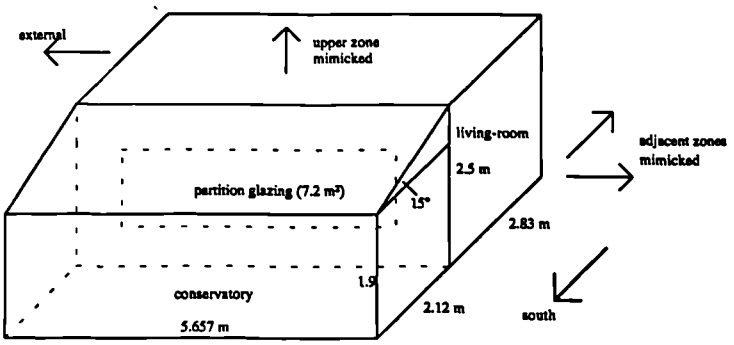

Figure 8.12:

Two zone model of a typical UK living-room with attached conservatory.

The study examined the influence of different partition window areas (none - 0 m²; half - 7.07 m²; completely glazed -14.14 m²) on the predicted heating energy demand of the adjacent living-room and on the peak air temperatures in the conservatory. The partition window size is of primary importance when interzonal radiation transfer is modelled (see section 2.3).

For the daily simulations (section 8.6.3) the conservatory was not ventilated. However, to model the conservatory performance more realistically (especially in summer), ventilation was introduced for the annual simulations. In these simulations, the conservatory was ventilated with a basic infiltration rate of 0.35 ach, which was increased to 10 ach when the conservatory temperature exceeded 27°C. The increased infiltration rate was assumed to mimic the opening of windows in the conservatory. Interzonal air flow between the living-room and the conservatory was not modelled.

8.6.2 Solar distribution models used

The study concentrated on the programs HTB2 and HTBSOL (HTB2 linked with SUNSIM). The use of the same thermal processor for all comparisons is advantages, since it

prevents differences arising due to changes in other algorithms. The following HTB2 and HTBSOL solar distribution models were considered for the daily simulations (see also section 2.3).

(i) The original HTB2, with all radiation directed to the floor, called **HTB2_f.**

All direct radiation was assigned to the conservatory floor. The diffuse radiation and the reflected direct radiation was distributed among all internal conservatory surfaces. There was no interzonal radiation transfer, radiation re-transmission or backloss.

(ii) The original HTB2 with a fixed user-specified solar distribution, called **HTB2_d.**

All the direct radiation was distributed between the conservatory floor, the partition (common) wall and the partition (common) window using an area weighting algorithm. The diffuse radiation and the reflected direct radiation was distributed among all the internal conservatory surfaces. There was no interzonal radiation transfer, radiation re-transmission or backloss.

(iii) The original HTB2 with a fixed user-specified solar distribution, including interzonal radiation transfer, called **HTB2_tr.**

All the direct radiation was distributed between the conservatory floor, the partition (common) wall, the partition (common) window and the adjacent living-room floor (to consider interzonal radiation transfer) using an area weighting algorithm. The diffuse radiation and the reflected direct radiation was distributed among all internal surfaces. There was no radiation re-transmission or backloss.

(iv) Dynamic solar distribution predicted by SUNSIM linked to the HTB2 thermal simulation program, called **HTBSOL.**

All complex time-varying radiation distribution mechanisms in the rooms and adjacent spaces were considered (including interzonal radiation transfer, re-transmission and backloss).

To investigate the particular effects of radiation loss and interzonal radiation transfer in more detail, two additional solar distribution models were introduced. These were used for the annual simulations only.

(v) Dynamic solar distribution predicted by SUNSIM and the HTB2 thermal simulation program, but with *no loss* of radiation in the conservatory, called **HTBSOL_nl**

All the complex radiation distribution effects in the rooms and adjacent spaces were considered. However, the SUNSIM features for predicting radiation re-transmission and backloss were switched off.

(vi) Dynamic solar distribution predicted by SUNSIM and the HTB2 thermal simulation program, but with *no* interzonal radiation transfer, called **HTBSOL_nz**.

All the complex radiation distribution effects in the rooms and the adjacent spaces were considered except that the SUNSIM feature for predicting interzonal radiation transfer was switched off (the partition window was treated as opaque).

8.6.3 Consequences of using a rigorous treatment (HTBSOL)

The dependency of the heating energy demands of the adjacent living-room on the partition window area has already been studied (see Fig. 2.8 in section 2.3). The investigation was repeated but additionally the results of the detailed solar distribution model HTBSOL were considered.

On the sunny winter's day, the detailed model (HTBSOL) produced (for all partition window areas) lower heating energy demands than all the other models (Fig. 8.13). Of the simplified models (HTB2_f; HTB2_d; HTB2_tr) the best agreement with HTBSOL was achieved by HTB2_tr, which roughly modelled the radiation distribution in the conservatory and the interzonal radiation transfer. However, while HTBSOL predicted that the room would demand about 6 kWh heating energy for a 14.14 m² partition window, HTB2_tr predicted 9 kWh, which was about 30% higher. The crudest algorithm (HTB2_f) produced 15 kWh, which was more than 200% to high!

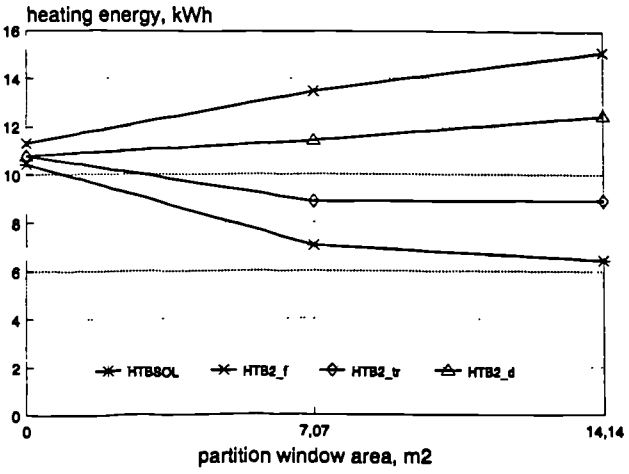

Figure 8.13:

Variation of the room heating energy demand on a sunny winter's day as the partition window area is varied.

It is worth noting that those models which did not consider any interzonal radiation transfer (HTB2_f and HTB2_d) produced the wrong result trend: while HTBSOL and HTB2_tr predicted decreasing energy demands as the partition window area was increased (from 0 m² to 7.07 m²), the models HTB2_f and HTB2_d indicated the opposite trend. This confirms the conclusion drawn in section 2.3 that the accurate treatment of interzonal radiation transfer is crucial for attached conservatories are to be simulated reliably.

The trends in peak air temperatures as the partition window area varied were also discussed in section 2.3 (Fig. 2.10). Again, the investigation was repeated with the detailed solar distribution model, HTBSOL, included. On the sunny winter's day, HTBSOL predicted peak conservatory temperatures which were, irrespective of the partition window area, more than 3 K lower than the temperatures predicted by the simplified models (HTB2_f; HTB2_d; HTB2_tr) (Fig. 8.14). The differences were greatest for the largest (14.14 m²) partition window: while HTBSOL produced a peak temperature of about 21°C, the simplest distribution model (HTB2_f) predicted 30°C! The best agreement with the HTBSOL predictions was achieved by using HTB2_tr (26°C), even this result was 5 K to high.

HTBSOL yielded decreasing peak temperatures as the partition window area was increased, whilst the simplified algorithms produced the opposite trend (Fig. 8.14). The trend generated by HTB2_tr, which considered a fixed interzonal radiation transfer, lies between the results from HTBSOL and those of the other models.

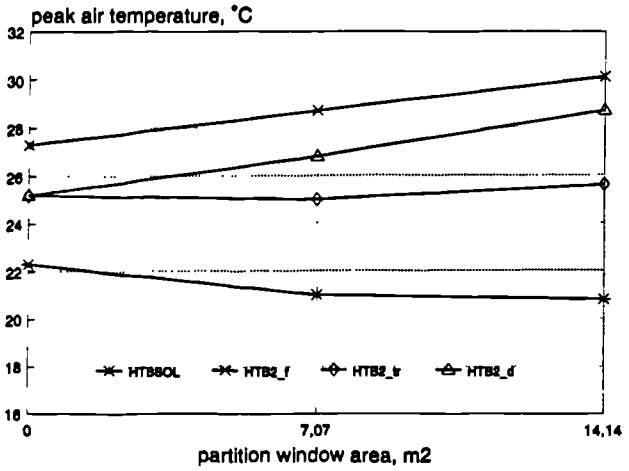

Figure 8.14:

Variation of the conservatory peak air temperatures on a sunny winter's day as the partition window area is varied.

The HTBSOL solutions, which are a result of the modelling of solar distributions can be taken as a benchmark against which to compare other simplified treatments (as adopted in most DSMs). The simplifications can cause errors which can make it impossible to make credible estimates of the impact of a conservatory on space heating energy demands of the attached dwelling. Similarly, the studies have shown that they may seriously undermine any attempt to estimate the thermal comfort and period of habitability of the space. In both cases, for the particular day chosen, the simplifications lead to results which give a pessimistic view of conservatory performance.

8.6.4 Consequences of interzonal radiation transfer and radiation loss

The differences in the result trends between the models which considered interzonal radiation transfer (HTBSOL and HTB2_tr) and those which did not (HTB2_f and HTB2_d) suggest that interzonal radiation modelling is particular important (Fig. 8.13 and 8.14).

However, since other aspects of the models also differed, the particular effect of interzonal radiation transfer (or any other aspect such as radiation loss) could not be demonstrated.

To investigate the particular effect of interzonal radiation transfer and radiation loss in more detail, an additional study was conducted using HTBSOL and two other models: HTBSOL_nz and HTBSOL_nl. These two models differed only in the modelling of interzonal radiation transfer or radiation loss respectively (see section 8.6.2). By comparing the predicted conservatory temperatures and the heating energy demands (of the adjacent room) with or without interzonal radiation transfer and with or without radiation loss, the significance of these individual simplifications can be quantified. Many DSMs neglect interzonal radiation transfer and radiation loss (or treat both of them very approximately).

To assess the influence of the different solar distribution models in more realistic situations, the heating energy demand of the adjacent room and the conservatory temperatures were studied using annual simulations. Again, the partition window area was varied.

a) Consequences of interzonal radiation transfer

The trend in the annual heating energy demand, as the partition window area was varied, predicted by HTBSOL_nz, which did not consider interzonal radiation transfer, differed from the trend predicted by HTBSOL. The lowest annual heating energy demand calculated by HTBSOL (1500 kWh) was for a 7.07 m² window, whereas HTBSOL_nz produced a minimum demand (of 1800 kWh) for a total opaque partition (0 m² in Fig. 8.15). The annual energy demand for the large window (14.14 m² in Fig. 8.15) was predicted, by HTBSOL, to be 1700 kWh, whereas HTBSOL_nz produced 2200 kWh. Clearly, such discrepancies would lead to quite different perceptions about the influence of the partition window area on the energy demand of the building.

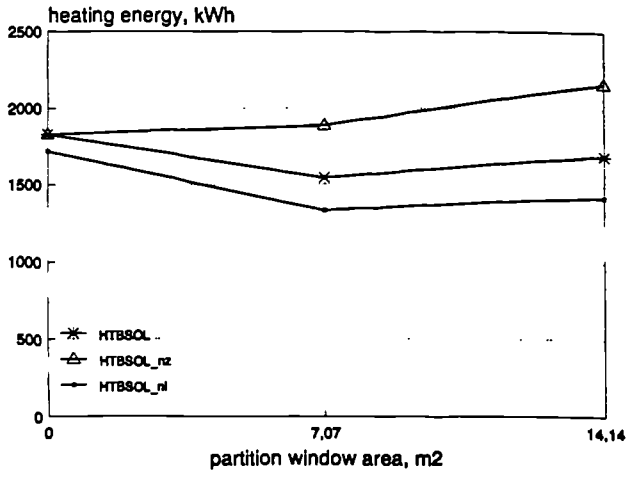

Figure 8.15

Variation of the annual heating energy demand (of the adjacent room) as the partition window area is varied.

Design decisions based on the occurrence of overheating are likely to be based on the total number of hours in a year for which the temperature exceeds a particular level. For conser-

vatory air temperatures, it was observed (Fig. 8.16) that, irrespective of the level chosen, HTBSOL produced lower totals than HTBSOL_nz (without interzonal radiation transfer).

Taking an air temperature of 30°C as being indicative of overheating, the predicted trends in hours of overheating caused by varying the partition window area disagreed (Fig. 8.17). While HTBSOL predicted the least overheating for a large partition window (14.14 m²), HTBSOL_nz indicated that partition window area had nearly no influence. These results are in qualitative agreement with those from the single-day studies. (Compare the results for HTBSOL and HTB2_tr in Figs. 8.13 and 8.14 with those in Figs. 8.15 and 8.17 respectively).

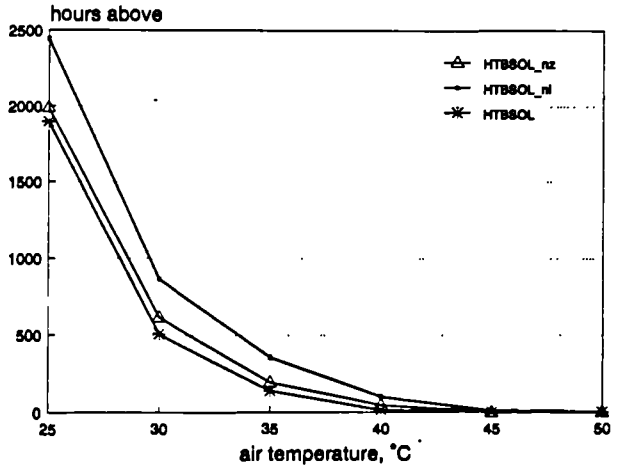

Figure 8.16

Annual occurrence of excessive air temperatures in the conservatory.

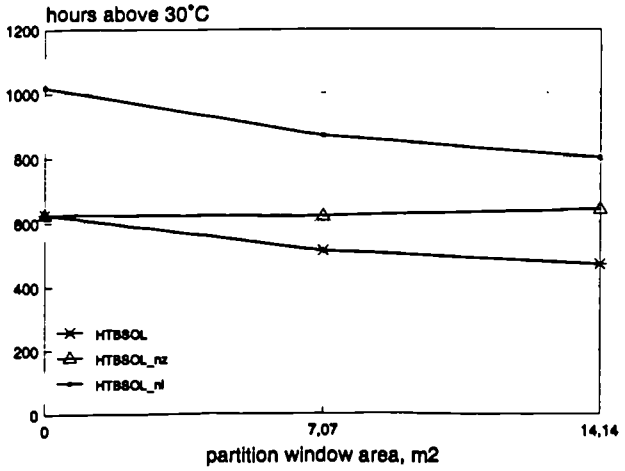

Figure 8.17

Annual occurrence of air temperatures in the conservatory exceeding 30°C as the partition window area is varied.

The result differences produced by HTBSOL and HTBSOL_nz clearly demonstrated that the interzonal radiation transfer is an important aspect which can have marked impact on the predicted temperatures in conservatories and energy demands of adjacent spaces. The neglect of interzonal radiation transfer (as is often done in current DSMs) can lead to the wrong assessment of the best partition glazing area between a conservatory and an adjacent

space. An accurate modelling of interzonal radiation transfer is also likely to be important in other highly glazed spaces, such as atria.

b) Consequence of radiation re-transmission and backloss

Since none of the models used in the previous study (section 2.3) appropriately considered radiation loss (re-transmission of direct radiation or backloss of diffuse radiation), the impact of these aspects could not be investigated. The above investigation compared the predictions of HTBSOL, which rigorously considered radiation loss, with HTBSOL_nl, which did not.

The two models predicted similar trends for the variation of heating energy demands and conservatory temperatures as the partition window area was varied. However, irrespective of the partition window area, HTBSOL_nl predicted annual heating energy demands which were about 200 kWh (10-15%) to low (Fig. 8.15). More significantly, the annual number of hours for which the conservatory air temperature exceeded 30°C was about 400 hours (60-80%) to high (Fig. 8.17). Such discrepancies in absolute temperature predictions clearly demonstrated, that reliable comfort assessments based on DSM predictions in highly glazed spaces are only possible, when radiation loss is carefully considered.

It should be noted, that these results were obtained for a dark coloured conservatory (surface absorptances was 0.8) which leads to a small radiation loss (mainly caused by radiation re-transmission). The radiation energy loss of medium or light coloured conservatories is much more pronounced, and so the thermal consequences of backloss modelling will be even greater.

The effect of radiation loss modelling has been estimated using solar distribution models which are quite sophisticated. Most DSMs use a much cruder treatment of these issues and so, as the results above suggest, the errors involved may be very large. It is valuable therefore, to try and generate effective solar-lost values which modellers may use to improve the performance of existing (crude) DSMs. Therefore, in a first step, SUNSIM was used to generate solar-lost factors for conservatories. The radiation loss was found to be highly dependent on: the time of day; the season; and the conservatory design. For Kew (UK) climate conditions, the solar-lost factors reached 70%. It was concluded that more work is needed to derive appropriate solar-lost factors for typical highly glazed spaces. This could be an objective of future work.

8.7 PRACTICAL ASPECTS OF USING SUNSIM

As noted before, SUNSIM is independent of a particular DSM. Modellers could use it to simulate the internal solar distribution in one particular zone. (An accurate calculation of

internal solar distribution is mainly necessary in buildings with highly glazed spaces such as greenhouses and conservatories.) If a building consists of more than one space with glazing (which is the usual case) the internal solar distribution of the remaining building must be calculated by the DSM. Therefore, SUNSIM can not totally replace the solar distribution algorithms of the DSM.

Coupling the solar distribution module SUNSIM with the DSM requires a specific interface, which can not be achieved without modifications to the DSM (section 8.4). This interface must ensure that the values of the internal absorbed radiation calculated by the DSM are replaced by the pre-calculated values. The problem lies mainly in the correct assignment of the absorbed radiation values to the different surfaces of the room (as defined by the DSM). Since DSMs use different internal numerical descriptions of room geometries and surfaces, a unified interface can not be developed. In addition, the difficulty of creating such an interface will be highly dependent on the DSM.

SUNSIM was basically intended for UNIX workstations. However, it can also be used on a PC. The pre-calculation time of SUNSIM depends on the number of part-planes and, of course, on the computer used. Since SUNSIM uses numerical procedures, the calculation time is relatively long. It was found that HTB2 with SUNSIM attached (called HTBSOL) took about twice as long to simulate a highly glazed space as HTB2 did in its native code.

The solar distribution calculated by SUNSIM depend only on the geometry of the highly glazed zone, the geographical location (latitude) and the climate conditions. Therefore, if a user wanted to simulate different building designs (without changing the highly glazed space) he would only have to calculate the solar distribution once.

At the moment, SUNSIM is a simple pre-processor. It would, however, be possible to integrate SUNSIM into the core of a DSM so that solar distributions are calculated in step with the thermal calculations. This has not been tested. However, the advantage of saving simulation time (by reusing the pre-simulated solar distributions) would be lost.

Finally, it would be possible to modify SUNSIM so that it calculates the amount of radiation falling on each surface as a function of the sky radiation (e.g. global horizontal irradiation and diffuse horizontal irradiation). The pre-processed file would then contain two values for each part-plane and hour: (i) the proportion of direct transmitted radiation to go to the part-plane directly and/or by reflection from other surfaces; and (ii) the fraction of diffuse radiation to go to the part-plane. Such values would then be usable by any climate data. However the latitude would have to remain the same. This could be an objective of future work.

CHAPTER 9

APPLICATION OF IMPROVED MODELLING METHODS TO THE STUDY OF CONSERVATORY DESIGNS

9.1 INTRODUCTION

The application of all the new simulation aspects (glazing and blind modelling, solar distribution) leads to a more authentic prediction of the environmental conditions in highly glazed spaces than was possible before. In this Chapter the new modelling possibilities are used to produce widely applicable information about conservatories, e.g. their design, their energy saving potential as a passive solar systems, and their internal comfort conditions.

Many previous design guidelines for highly glazed spaces were derived from DSM predictions. For example, the program SERI-RES was used in the UK Department of Energy's Passive Solar Design Program (PSP) to study the effect of glazing types; glazing areas; glazing orientations and conservatories on the energy demand of passive solar dwellings (Yannis 1994). Also in the PSP the program ESP was used to predict the energy demand of commercial atria (BDP 1991). The program FRED (Penz 1983) was used by Baker (1985) to study the energy demand of dwellings with conservatories or the temperatures in conservatories respectively. Other studies were also based on DSM simulations (e.g. Hauser 1984, 1986), however, the used DSM was not stated in the publications. In addition, design guidelines for highly glazed spaces were also derived from simplified quasi-stationary calculations (e.g. Balcomb et al. 1983 (Passive Solar Design Handbook); Nikolic 1983 (TÜV Rheinland); Chu and Oreszczyn 1991).

However, the sensitivity studies conducted within this work have indicated that the approximate methods used to model glazings and internal solar distribution, solar shading etc. can severely compromise the accuracy of DSM predictions, especially when highly glazed spaces are modelled.

- The best glazing type of conservatories, partition glazing type and partition glazing area etc. was shown to be dependent on the used internal solar distribution or thermal glazing model when considering such issues as conservatory peak temperatures or heating energy demands of the adjacent space (Chapter 2).
- The important question if conservatories can reduce the heating energy demand of adjoining rooms was shown to be dependent on the detail of simulation internal solar distribution (Chapter 2).

- The predicted room temperatures and heating energy (cooling energy) demands of typical domestic scale rooms were shown to be highly sensitive to the calculation model of solar energy gains (solar transmission through glazings). These are often treated approximately, especially, when special coated or tinted glazings or slat-type blinds are simulated (Chapter 4 - 7). In conservatories or atria, in which the inside climate depends fundamentally on the amount of solar radiation entering the room, the uncertainty due to simplified solar glazing models are likely to be even more pronounced (this was not investigated in particular).
- The heating energy demand of the adjacent space to an conservatory was very sensitive to the interzonal radiation transfer into the space, which is modelled by most DSMs only approximately (Chapter 8).
- Reliable comfort assessments based on DSM predictions in conservatories were only possible, when radiation loss was carefully considered (Chapter 8).

It was concluded that design studies of highly glazed spaces such as atria and conservatories based on current DSM predictions (which do not appropriately consider the above modelling aspects) must be treated with caution. However, the application of all the new simulation improvements (glazing and blind modelling, solar distribution) leads to a more authentic prediction of environmental conditions in highly glazed spaces than was possible before. It was therefore decided to use the new modelling possibilities to produce widely applicable information about the design of highly glazed spaces, their energy saving potential as passive solar systems and their internal comfort conditions. This study concentrated on conservatories, rather than on atria or glazed halls. The choice was based on the following considerations.

- There is a wide interest of conservatories as fuel saving, passive solar features in the UK (UK Passive Solar Design Program). Conservatories are popular retrofits to existing houses in the UK (and in other countries such as Germany).
- Various studies were conducted on conservatory design. But the main massages, design guidelines and recommendations for conservatories do highly differ (see section 9.3).
- The performance of conservatories depends strongly on the solar radiation process treated within this work. In atria and glazed halls other issues such as ventilation are also highly important, however, these were not particularly object of this work.

The conservatory design study investigated the influence of design variations on the usability, on the impact of conservatories on the energy demand of adjacent buildings and on summer-overheating for typical conservatories in connection with different parent building arrangements. It concentrated on unheated conservatories, however, the effect of heating a

conservatory was also considered. Other important aspects of the building physics such as lighting, moisture transfer, ventilation etc. were not detailed studied but considered within the discussion of conservatory design guidelines. However, building aspects of architecture, construction, building materials, pleasantness and economy could not be considered within this study.

9.2 CONSERVATORY ORIGINS AND CURRENT PRACTICES

Historically, a conservatory was used like a greenhouse for growing temperature sensitive (tropical) plants which could not survive without protection. For example, in the 17th century, citrus fruits were produced widely in northern Europe in solar-heated orangeries. Conservatories were heated to protect the plants from cold temperatures in winter.

In the mid 20th century the falling price of glass made conservatories affordable and they became a popular feature of domestic buildings. After the oil price rises of the early 1970s, there was a growing interest in passive solar design of UK dwellings (and commercial buildings). The aim was to make greater use of the renewable energy source, the sun, to provide heating. As a result, conservatories were widely recommended as passive solar systems, and so conservatories are seen as a valuable 'passive solar feature' for domestic scale buildings. Moreover, they were seen by some as a pre-requisite for passive-solar dwellings. Indeed, they were used as a visible outward statement that a house was energy conscious, consider, for example, the Energy World dwellings in Milton Keynes, UK.

However, conservatories cannot be meant purely as solar collectors to save heating energy. Their capital cost could hardly be justified on that basis alone. They are intermediate spaces between indoors and outdoors, with their own climate and character and can be occupied. A recent survey (Oreszczyn 1992) found that the majority of conservatories are used as habitable spaces for much of the year. The survey suggests that conservatories are predominately built to provide extra living-space. The main design objective is to create a space that is pleasant and usable for as much of the year as possible. Therefore, the habit of heating such spaces is increasing. But a heated sunspace could hardly still be termed a conservatory, for it is used like a living-room not like a greenhouse. It has an artificial environment rather than a natural environment which responds the external climate conditions.

Here, the word "conservatory" describes a space which is physically separated from outdoors, mainly by glazed surfaces and has, in particular, a glazed roof. It is not mechanically heated or cooled and usually adjoins a heated indoor space. The British Building Regulations (1985) define a conservatory as an unheated structure with a transparent or translucent roof, which is exempted from building restrictions. There are no provisions for heated conservatories in the Building Regulations (see Chu and Oreszczyn 1991). In Germany,

heated conservatories are regulated such as conventional living-space (WärmeschutzVO 1993). Since they usually can not comply the requirements, heated conservatories are not allowed.

Conservatories can take a variety of shapes and relate to the parent building in a number of different ways. The size of a conservatory, the orientations and type of its glazing and its relationship to the parent building are the major factors which determine the thermal environment and amenity offered by the space and the potential energy savings for the parent building.

The energy savings result from the following effects.

- The conservatory acts as a buffer zone reducing conductive heat losses through partition walls and windows. For example, a double glazed conservatory in connection with a double glazed partition window (set in a small or highly-insulated partition wall) basically corresponds to a quadruple glazing, for which the surface area of the two outer panes is greatly increased.
- The conservatory captures solar radiation like a solar collector. Compared to a simple external window, a conservatory offers an increased surface area for collecting solar energy. Due to the solar radiation gains, the air temperatures in the conservatory are raised. This reduces the conductive heat losses from the living-space into the conservatory.
- The solar radiation captured by the conservatory can be used to pre-heat air before it enters the parent building. This solar pre-heated ventilation (SPV) strategy reduces the heat losses associated with ventilation.
- When solar gains make the conservatory warmer than the parent building, the building air can be heated by circulating it through the conservatory. This can be termed 'recirculating air heating'. But recirculating air heating is only significant when the conservatory temperature is much higher than room temperature. This occurs infrequently in the heating season in Northern Europe. This makes recirculating air heating relatively unimportant in this regions.
- In summer a conservatory can be used to ventilate (cool) the parent building. The increased buoyancy of the air in the conservatory (due to its high temperature) can generate a stack effect. This can be used to pull air through the building into the conservatory and out through the conservatory roof. Thus, using the conservatory as a motor for ventilation, the energy demand for mechanical ventilation may be reduced.

Although it is currently assumed that unheated conservatories can reduce the heating energy demand of adjacent buildings, conservatories are hardly economic without considering the improvement of the home amenity. Conservatories are unlikely to be adopted solely for

their energy saving contribution. Hence, the time-of-usability becomes a very important question. It is reasonable, however, to examine the cost-effectiveness of any marginal investments made to make a conservatory a more effective fuel saver.

As described above, the classical conservatory is not heated or cooled. However, when designing conservatories one must always be the aware that they may be heated in the future. A questionnaire of conservatory owners showed that the majority of users heat their conservatory more or less frequently (Oreszczyn 1992). It is estimated, that 50% of the conservatories built every year in the UK are fully heated as living-spaces (Chu and Oreszczyn 1991). Indeed, modern conservatories are currently marketed as heated spaces. Therefore, every design criterion for unheated conservatories should also consider the possibility that the space will be heated.

9.3 REVIEW OF PREVIOUS CONSERVATORY DESIGN STUDIES

To derive the most important design questions for further examination, different conservatory design studies were reviewed. Their design guidelines were compared to highlight diverging views. Clearly, the sources reviewed could only be a small selection of all the investigations into conservatory design. However, the example studies demonstrate the wide range of options on the subject.

Most of the design studies were based either on simplified, quasi-stationary calculations or detailed computer simulations (Balcomb et al. 1983; Baker 1985; Hauser 1984/1986; Nikolic 1983; Chu and Oreszczyn 1991). These studies often try to provide widely applicable design guidance. The limitations of such calculations have already been discussed (section 9.1). Other studies were based around observations made in existing sunspaces (e.g. BINE 1989/1991a/1991b; Erhorn 1989; Ohlwein 1992). These investigations tend to be building specific.

Most of the research has been concerned with the potential energy savings through the use of conservatories as passive solar systems. Less information was found about the thermal comfort in -, and usability of -, conservatories. It should be noted, that all the statements, which are considered here, refer to either UK or German weather conditions. It was assumed that, despite the differences between these climates, general statements about conservatory performances could be compared. The well known Passive Solar Design Handbook (Balcomb et al. 1983) was not considered, since it concentrates on US weather conditions for Albuquerque and Boston. Unfortunately, a precise description of the buildings studied is not always given, neither is the exact location or the weather data used.

The estimated energy savings, due to adding an unheated conservatory to a building, differ markedly between the sources studied.

- Simulation results for a detached house (of modern highly-insulated construction) in Kew (UK) with 110 m^2 floor area and an attached conservatory (floor areas 8.64 m^2 or 14.4 m^2) were presented in the energy efficient house design guide (Yannis 1994). The energy saving due to the conservatory was indicated to be 900-1000 kWh/year or 25-28% of the dwellings heating requirement. Some 40% of this saving was attributed to solar ventilation pre-heat (SPV). There was no difference between single or double glazed conservatories.

- Baker (1985) concluded, that a single glazed conservatory in Kew (UK) covering an 11.6 m^2 wall on a well-insulated 95 m^2 terraced house reduces the auxiliary heating of the house by about 1000 kWh/year. This will increase to 1400 kWh/year if the conservatory is double glazed. The savings would be mostly achieved by SPV although there would be a small reduction in conductive heat losses.

- Ohlwein (1992) quotes a reduction of the energy demand of dwellings due to adding conservatories of 20% in Germany. These results were obtained by measurements on dwellings with and without conservatory.

- Hauser (1984) indicated an energy saving of 15.7% - 16.7% (about 2000 kWh/year). These values were calculated for a well insulated dwelling (U-values between 0.23 and 0.55 W/m^2K; floor area = 88 m^2) in Essen (Germany) with an attached single glazed conservatory of 24 m^2. The partition area was 28 m^2 and completely double glazed. The calculation approximated the effect of SPV.

- Measurements on two identical dwellings (average U-value = 0.64; floor area = 81.7 m^2) in Rosenheim (Germany), of which one had a double glazed conservatory (floor area 10.6 m^2; partition area 16.3 m^2), indicated a 12% (1670 kWh/year) lower heating energy consumption for the dwelling with the conservatory (SPV was not used) (BINE 1991b).

- Erhorn (1989) presented the result of a two years observation of 25 dwelling's in Germany with passive solar components, 10 had conservatories. The energy saving potential of the conservatories was concluded to be about 10% of the dwellings heating energy demand.

- The energy performance of a house plus conservatory has been modelled by Chu and Oreszczyn (1991) to estimate the potential energy saving of an unheated conservatory and the energy cost of heating a conservatory in the UK. The houses were modelled with varying levels of insulation, corresponding to houses built at different times. It was concluded that, generally, the energy saving derived from an unheated conservatory was "very small" (lower than 2%).

Although the energy saving potential was estimated very differently, most publications agreed on the question of the economic efficiency of a conservatory: a conservatory was considered to be uneconomic without considering the additional amenity benefits it provided (Yannis 1994; Ohlwein 1992; Hauser 1984/1986; Erhorn 1989; Nikolic 1983).

There were a few statements found about the thermal comfort of conservatories or about their time-of-usability.

- Yannis (1994) stated that small or well integrated conservatories in Kew (UK) can maintain mean temperatures that are close to those of indoor spaces for up to eight months a year. With very sunny weather peak temperatures of 30 or 40°C would not be surprising for unprotected conservatories.
- The simulation studies of Baker (1985) showed that a double glazed conservatory in Kew (UK) covering 11.6 m^2 on a well-insulated 95 m^2 terraced house is above 13°C for 1609 hours over seven month heating season - i.e. about 90% of daylight hours, or 30% of total time. A similarly designed single glazed conservatory was shown to be habitable for 1257 hours.
- Hauser (1986) presented the annual number of hours, for which the dry resultant temperature (average of the air temperature and surface temperatures of the enclosure) was above 15°C. It was noted that single glazed south conservatories in Essen (Germany) would be habitable for 3800 h/year, and that this would increase to 5600 h/year when heat protective (low-emittance) glazing is used.
- Measurements in German conservatories showed that comfortable temperatures, between 18°C and 25°C, were obtained for 40% of the day-time, i.e. between 8am and 8pm (BINE 1989).

The following list summarises the conservatory design guidelines, which were given by the different sources. Since it is not possible to discuss all the statements in detail, the list restricts itself to the important design questions, and concentrates on those points for which conflicting, or differing, information was given.

a) The conservatory size

Nikolic (1983) concluded that conservatories are, from the perspective of energy saving, better than 3- or 4- pane glazings. This means that a conservatory acts not only as a thermal buffer, but also effectively as a solar collector. Large glazing areas are therefore favourable for a conservatory. A similar result was presented by Hauser (1986). Yannis (1994) however indicated that small conservatories have energy, cost and comfort advantages. He concluded that the contribution of a conservatory, in terms of energy saving for the parent building, does not increase with its size.

b) The conservatory glazing type

"Very small" differences in the predicted energy demand of parent buildings with single and double glazed conservatories were indicated by Yannis (1994). But Baker (1985) and Hauser (1986) indicated a considerable decrease in the energy demand of the parent building as single glazing (for the conservatory) was replaced by double glazing.

c) The partition glazing type

Nikolic (1983) studied the energy demand of the parent building and the usability of the conservatory. It was found to be better to put the thermal insulation (double glazing) to the outside of the conservatory, while using single glazing for the partition window than the other way round. He admitted, however, that an accurate quantification of the effects would be impossible with the calculation technique used. Hauser (1986) indicated the lowest energy demand of the parent building occurred when highly-insulated glazing (double or low-emittance) was used for the partition window.

d) The partition glazing area

The effect of the partition glazing area on the energy exchange between conservatory and adjoining heated spaces, was found, by Yannis 1994, to be important. However, little indication of the best partition glazing area was found in the literature. In one study measurements on double glazed conservatories indicated that there was a small reduction in the heating energy of the adjoining building, when the partition window (also double glazed) area was large (75% of the partition area) (BINE 1991b).

e) The conservatory orientation

There were many different and contradictory statements on the topic of energy saving and orientation. Hauser (1984) stated that the relative energy saving contribution of a conservatory would be independent on the orientation. In addition, while the lowest absolute energy demand of a building with conservatory would occur for south orientation, the absolute reduction of heating energy due to a conservatory was indicated to be highest for north orientation. These statements were confirmed by measurements of conservatories at different orientations (BINE 1991b). However, Baker (1985), recommended an orientation, which should be "somewhat east of south".

f) Opaque elements

With opaque, highly insulated panels, a conservatory can be shaded and its heat loss can be reduced. Yannis (1994) recommended that the conservatory side walls or roof should be insulated to maintain the conservatory at higher temperatures. Measure-

ments, however, indicated that it is not useful to insulate more than a third of the conservatory roof (BINE 1991b).

g) Summer overheating

Measurements on two conservatories (BINE 1991a) demonstrated that a ventilation rate of 15 1/h - 20 1/h was sufficient to reduce the sunspace temperature to nearly ambient temperatures. Therefore, no additional shading was recommended. Ohlwein (1992) also indicated that extensive ventilation was the most important requirement. In contrast to these findings, most other authors recommended additional shading device, e.g. Yannis (1994) and Hauser (1984).

h) Integrated conservatories

Hauser (1984) recommended that it is advantageous to integrate a conservatory into a house plan as far as possible. This was confirmed by Yannis (1994), however, he noted that great care would be required "in attempting to estimate savings in such cases since a house plan developed around a conservatory is unlikely to retain such a form without the conservatory".

9.4 TERMINOLOGY FOR COMPARISONS

It was necessary to define a few simple parameters which would adequately reflect the internal comfort conditions in conservatories. Similarly, the impact of a conservatory on the heating energy demand of the space to which it is attached had to be expressed clearly. Unfortunately, an uniform approach to these issues could not be derived from literature (e.g. see variety of parameters used in section 9.3).

- A conservatory (cons) was defined as usable (habitable) if the temperature was between 15°C and 27°C. It was assumed that, in practise, the temperature could be prevented from exceeding 27°C by adequate ventilation and shading i.e. by occupant intervention. Thus, a temperature over 15°C was used to indicate usabilities.
- A conservatory was defined as being overheated if the temperature exceeded 27°C. This was used in studies to show the likely-hood of overheating when there was no occupant intervention.
- The usability and overheating were evaluated using: (i) the air temperature; and (ii) the dry resultant temperature (average of the air temperature and the surface temperatures). Since the dry resultant temperature did not significantly differ from the air temperatures, only the air temperatures are shown.

- The period of usability was taken to be the fraction of the annual hours of occupancy for which the air exceeds 15°C. (The symbol T>15°C is used for this parameter.) The assumed hours of occupancy were from 7am to 11pm every day of the year; i.e. a total of 365 × 16 = 5840 h/year. This follows the assumptions used in previous work (Lomas et al. 1989).
- The risk of overheating (when there was no occupant intervention) was taken as a fraction of the occupied hours for which the air temperature exceeded 27°C. (The symbol T>27°C is used for this parameter).
- The impact of conservatories on the energy demand is demonstrated by comparing the absolute figures for the annual energy demand of the parent building with the conservatory with the corresponding figures but without the conservatory (or for different conservatory designs). In some cases, the monthly or hourly energy demands are shown as well.
- The annual energy demand of the heated conservatory (heated from 7am to 11pm) was used for comparisons of different heated conservatory arrangements. If heating the conservatory had a marked impact on the energy demand of the parent building, the total heating energy demand of the conservatory and the parent building was considered.

The program HTB2 was used for the simulations, with all the improved calculation modules developed in this research included. Within the Applicability study (Lomas 1992) the Resolution of DSMs was investigated for either single-zone direct-gain living-rooms, or for whole realistic UK dwellings. For absolute annual energy demand predictions, the Resolution of DSMs was found to be around ± 15% for single zone arrangements and ± 10% for whole dwellings. For energy saving predictions (relative figures) a Resolution of ± 5% was derived. The predicted increases (relative figures) in the numbers of hours overheating as the window area and orientation varied were 15% or less.

These Resolutions were taken as guidelines for interpreting the simulation results and simulation result trends. The statements concerning the hours of overheating were assumed to be fairly transferable to the hours of usability, since these are based on a similar method of analysis (the time-of-usability merely refers to the temperatures over 15°C). However, since the quoted Resolutions were valid for the simulation of single-zone direct-gain rooms or realistic dwellings, their transfer to highly glazed spaces such as conservatories has to be done with caution. It may be assumed that the simulation of the more complex climatic conditions in a conservatory leads to higher uncertainties (worse Resolutions).

9.5 DESCRIPTION OF BASE-CASE DWELLING AND CONSERVATORY

9.5.1 Modelling considerations

In a conservatory design study there are many possible ways of modelling the spaces. The conservatory may be attached to a realistic building or to an abstract space. The building may be one, two or more storeys high. It may be a typical domestic building with living spaces or a commercial building with offices. The connected rooms may be totally enclosed in the building or corner rooms. In this conservatory study two different cases were used for the parent buildings attached to the conservatory:

(i) a typical domestic living-space, which considers neighbourhood zones in a non-explicit manner; and

(ii) a realistic multi-zone domestic building.

The investigation of attached conservatories concentrated on the typical domestic living-space. The realistic multi-zone domestic building was mainly used to study integrated (corner or enclosed) conservatories. The choice was based on the following considerations:

- a two-zone arrangement (conservatory and living-space) requires a quick and uncomplicated calculation whilst considering all the complex thermal interactions of realistic rooms;
- the likely-hood of modelling mistakes is reduced for simpler buildings;
- the design of a conservatory has a considerable affect on the heating energy demand of the adjacent room, however, it has an energy impact, which is small in comparison to the total energy demand of the whole house. So, if a whole dwelling is considered, the comparison and evaluation of very small differences in heating energy would be necessary, these could be beyond the Resolution of the DSM.

9.5.2 Parent dwelling

For the adjacent room, the typical UK living-space, used in the previous sensitivity studies (Chapters 2 and 8), was adopted (Fig. 9.1; Appendix A.4). It was a 16 m^2 corner room with an average external U-value of 0.5 W/m^2K. The west and south walls were external and heavy-weight (two layered brick walls). The south wall adjoined the conservatory. Two walls were internal and heavy-weight (one layer of brick), the ceiling was internal and light-weight (two layers of plasterboard). Adjacent zones were imitated using fictitious constructions on North, East and Ceiling. The floor was a concrete slab on the ground.

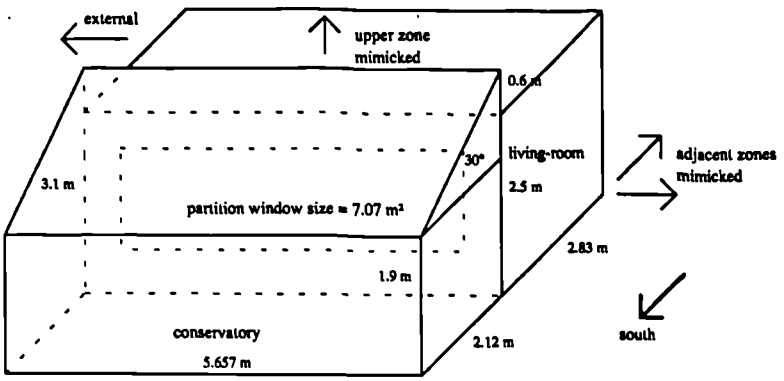

Figure 9.1:

Base-case module of living-room with attached conservatory.

The room was ventilated with external air using a fixed infiltration rate of 1.0 ach. This was increased to 5 ach when the inside air temperature exceeded 27°C. This means, in reality, there must be a ventilation connection between the room and the external air other than through the conservatory. This is usually provided by an additional external window. However, to maximise the sensitivity of the room to the conservatory this additional window was not modelled.

The room was heated to 21°C from 7am to 11pm. During the night there was a 'set-back' to 16°C. The 'set-back' represented the common heating habit in Germany, where most houses have central heating (some houses are heated throughout the night). Although in the UK night-time heating is not typical, it was assumed, that a 'set-back' also represented modern UK central heated dwellings. It was felt, that the 'set-back' was a good compromise between complete night-time heating which is sometimes adopted in Germany and no night-time heating which is common in the UK.

The room had one, south-facing external window with an area of about 7 m² which corresponded to half of the total wall area. The window was double glazed (window curtains were not considered). (The symbol "d" was used for the base-case room with a double glazed external window.) When the room was modelled with an attached conservatory, the external window became a partition window between the living-room and the conservatory.

9.5.3 Conservatory

The base-case conservatory was rectangular and had a floor area of 12 m². It was double glazed and its floor was concrete on the ground. The conservatory window frames were assumed to cover 15% of the whole glazing area. The U-value of the frames always corresponded to that of the glazing. A conservatory shading device was not considered. The reflectance of the internal opaque surfaces was 0.2.

Interzonal air-flow (SPV), between conservatory and living-room, was not considered. SPV requires additional construction measures like ducts and possibly fans and control units. It was assumed that these measures would not be provided in a classic conservatory, which

mainly acts as a solar-heated thermal buffer. The energy saving by using SPV is, however, discussed separately (section 9.10).

The conservatory was ventilated at a rate of 1.0 ach or, when the air temperature exceeded 27°C, 15 ach. The increased (summer) ventilation rate was assumed to represent the typical effect of opening the windows in the conservatory. To get this summer ventilation rate without mechanical ventilation system, the necessary opening area has to be at least 10% of the total external glazing area (see Hauser (1987) and Ohlwein (1992)). The base-case conservatory was not heated. (The symbol "cons" is used for the unheated base-case conservatory attached to the base-case living-room.)

9.6 IMPACT OF LOCATION AND CLIMATE ON CONSERVATORY PERFORMANCE

While the energy demand of common opaque rooms depends mainly on the outside air temperature, the performance of any passive solar system is, in addition, strongly influenced by the solar radiation gains. In particular conservatories show a high sensitivity to outside sky condition (clear or overcast) and wind velocities. Therefore, any statements about the performance of conservatories are strongly dependent on the location and climate of the building.

The design study concentrated on the UK. However, it was important to investigate, whether conclusions about conservatory design, based on a UK climate, could be transferred to other locations and climates.

For the UK the Example Weather Years of Kew, Finningley (near Sheffield) and Glasgow were available (see Appendix B). The weather data of Kew were found to contain some impossibly high solar radiation values for early morning or late evening hours, which are probably caused by mistakes in the data. It was found, that these high solar radiation values had a big impact on the internal climate of conservatories with east- or west-orientated glazings. Since Glasgow had a non-representative northern climate, for the design studies the Example Weather Year of Sheffield was used.

To study the influence of climate three different locations and climates were compared: Sheffield, UK (fin); North-Württemberg, GERMANY (nwb); and Denver, Colorado, USA (dco). To characterise the different climate files, the annual average of the external air temperature, the heating degree-days (to base 15.5°C) and the annual total horizontal irradiation were calculated (Table 9.1). For more information see Appendix B.

Location (code)	Average annual external air temperature, °C	Degree-days to base 15.5°C, Kelvin×days	Total annual horizontal irradiation, kWh/year m²
fin	9.0	3906	878
nwb	9.0	3895	1119
dco	9.7	3829	1832

Table 9.1: Characteristics of the climates studied.

Sheffield represents a moderate climate with low seasonal temperature variations (compare Figure B.2) and relatively frequent overcast conditions (low solar radiation). North-Württemberg has a typical middle European continental climate with cold, clear winters and warm, sunny summers (high solar irradiation). Denver has an extreme continental climate with very cold and clear winters and very sunny summers (solar irradiation is very high).

Three different building arrangements were compared:

- a reference case, with no south-facing surface (i.e. five well insulated opaque surfaces only, no south window, no insolation, heat loss through five surfaces only);
- the base-case living-room (i.e. with 7 m² of double glazed window); and
- the base-case living-room with the base-case conservatory.

The reference case, without a south-facing surface, produced nearly the same annual heating energy demand for Sheffield and North-Württemberg (Fig. 9.2). The addition of a south wall and south window had no consequences in Sheffield. Therefore, the area of double glazing in a well insulated wall appears to be thermally neutral over a year in a Sheffield (and possibly UK) climate. In North-Württemberg the glazed wall led to an increase of 8% in the annual heating energy demand. Therefore, the introduction of glazing is disadvantageous in the German climate. This effect is probably caused by higher outside longwave radiation and convective losses on the window in North-Württemberg due to lower winter temperatures and clearer weather conditions.

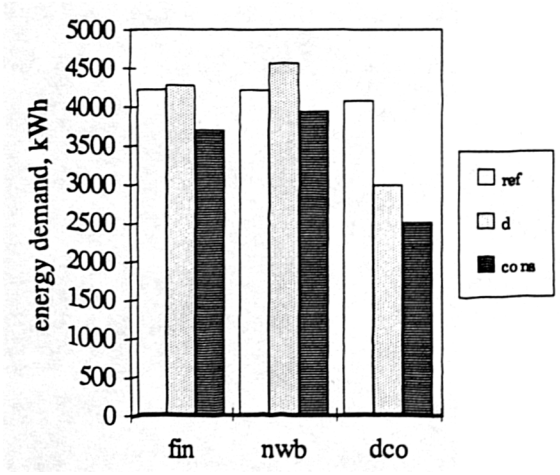

Figure 9.2:

Influence of different locations and climate conditions on the annual heating energy demand of the south-facing living-room with different types of south-facing surfaces (passive solar systems): no south surface (ref); the base-case, double glazed room (d); the base-case, double glazed conservatory (cons).

fin: Sheffield, UK
nwb: North Württemberg, GERMANY
dco: Denver, USA

For Denver the south window produced a significant reduction of the heating energy demand. Because the average outside temperature for Denver (9.7°C) is only slightly higher than for the other climates, this effect can only be due to the very high solar energy gains.

The attachment of the base-case conservatory to the south window yielded the same reduction of the energy demand (13.5%) in Sheffield and North-Württemberg. Therefore, any statements about the effect of conservatories on the annual energy demands of a building should be fairly transferable from one climate to the other. For Denver the energy saving was predicted to be 16%, which is similar to that for both the other climates.

The time-of-usability (T>15°C) of the conservatory in North-Württemberg was 58.4% of the annual occupied hours. It was only slightly higher in Sheffield (61.6%). However, it was significantly higher in Denver (78.6%).

Based on these results, it was assumed, that for moderate or continental middle European climates the thermal behaviour of a conservatory is similar. Therefore, the results of the conservatory design study should be approximately valid for middle Europe and the British Islands. However, it should be noted, that the performance of a conservatory also depends on the heating habit of the adjoining room. However, that was, as already indicated in section 9.5.2, assumed to be similar for modern dwellings in Germany and the UK.

9.7 PERFORMANCE OF BASE-CASE CONSERVATORY

9.7.1 Annual heating energy demand

This section compares the energy saving effect of conservatories (without SPV) and direct-gain passive solar systems. The annual energy demand of the base-case living-room and conservatory was compared with that of a living-room (without conservatory) but with five different external glazings (Table 9.2). Except for the change in glazing type, all other factors of the room were unchanged.

Code	Glazing type	U-value, W/m²K	Normal total solar energy transmittance
s	single	5.4	0.83
d	double	2.9	0.72
t	triple	2.0	0.59
q	quadruple	1.5	0.55
l	low-emittance	1.9	0.62

Table 9.2: Properties of the glazings studied. The low-emittance glazing corresponds to Pilkington Kappafloat (neutral) 74/62®.

These six different passive solar systems were also compared against the reference case (section 9.6), which had no south wall or external glazing.

A single glazed living-room (without conservatory) showed the highest annual energy demand (Fig. 9.3). This was about 17% (710 kWh) higher than that of the reference case without south-facing surface. As noted previously (section 9.6) the double glazed living-room (without conservatory) had nearly the same energy demand as the reference case. Therefore, the net annual energy balance of the glazing is, in this case, virtual zero. All other passive solar measures (triple glazing, quadruple glazing, low-emittance glazing or a conservatory) led to net energy gains. Low-emittance glazing produced the lowest energy demand. This was about 14% (530 kWh) lower than that of the reference case.

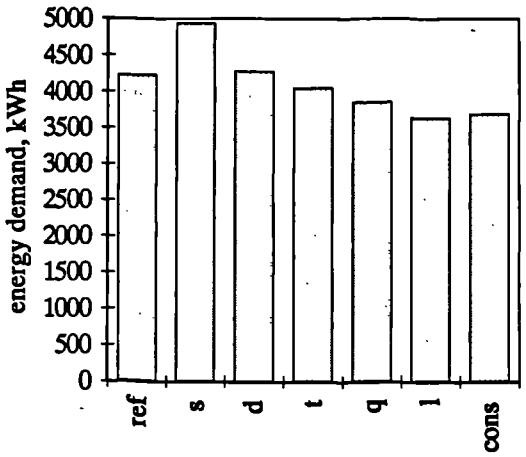

Figure 9.3:

Influence of different types of south-facing external glazing (passive solar systems) on the annual heating energy demand of the living-room.

ref:	no glazing
s:	single glazing
d:	double glazing (base-case room)
t:	triple glazing
q:	quadruple glazing
l:	low-emittance glazing
cons:	base-case conservatory

The attached conservatory reduced the energy demand (of the base-case (double glazed) living-room) by 14% (580 kWh). Thus, this arrangement has roughly the same impact as low-emittance glazing and was marginally better than quadruple glazing (by 4%). The low-emittance glazing, the quadruple glazing and the conservatory produced energy demands which were within 5-6% of each other (i.e. between 3850 kWh and 3640 kWh). Thus, given a Resolution of 5% for this type of predictions they must be taken as being indistinguishable from each other. Compared with a pure double glazed direct-gain space, quadruple glazing, low-emittance glazing and conservatory, offered an energy saving of between 10% - 15% (400 - 600 kWh).

These percentage energy savings were obtained for a south-orientated living-room with an unshaded, double glazed conservatory. The energy benefits of such a conservatory would be much lower when compared to the energy saving of the whole dwelling (see section 9.11). However, if low-emittance (quadruple) glazing was installed on the whole south side of a house, the benefits (compared with double glazing) would still be 10% - 15% (of course, a similar saving would be achieved, if a conservatory would cover the whole south side of a house). In practise, therefore, passive-solar house designs are likely to be basically direct-gain designs (low-emittance glazing is much cheaper than a conservatory). However, it should be noted that unheated conservatories offer extra living-space (at least for a limited

time) without an increase in the energy demand (compared to simple direct-gain designs using low-emittance (quadruple) glazing).

To study the seasonal energy benefits of the conservatory, the monthly energy demand of the double glazed living-room (case "d") and the room with a conservatory (case "cons"), were compared (Fig. 9.4). The conservatory produced a reduced heating demand during every month of the year. The percentage monthly energy reductions varied between 9% in November and 29% in June. The absolute monthly energy reductions varied between 14 kWh/month in July and 90 kWh/month in January.

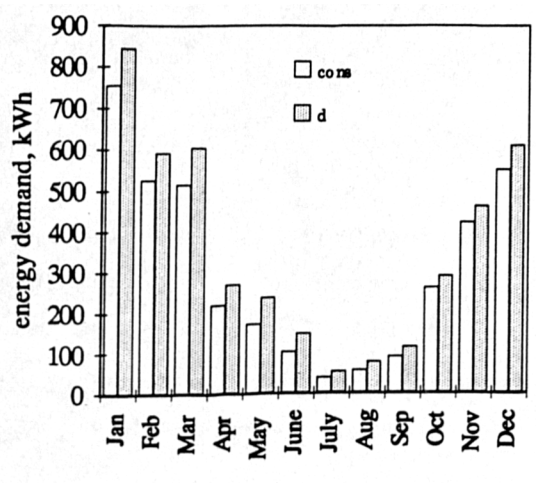

Figure 9.4:

Monthly energy demand of the south-facing living-room with (cons) and without conservatory, but with a double glazed external window (d).

9.7.2 Usability

To study the usefulness of a conservatory, the number of hours in each month exceeded 15°C (T>15°C) in the base-case conservatory (case "cons") were compared with those of the external air (Finningley climate file, case "ext") (Fig. 9.5). During April, May, June and October the external air temperature reached 15°C for about 100 hours per-month during the occupied period (about 20% of the occupied hours). In the conservatory, however, 15°C was exceeded for about 400 hours per month (about 80% of the occupied hours in each month). Hence, during that time, the conservatory was four times more usable than an open-air garden.

During summer-time, the external temperatures are generally higher (up to 350 hours above 15°C). This reduces the apparent benefits of the conservatory.

Whilst there is no possibility of living in the open-air in winter, the conservatory offers 50-100 hours per month during the occupied period, with temperatures higher than 15°C. This is approximately 2 - 3 hours per day on average.

The annual time-of-usability for the base-case conservatory was about 62% of the occupied hours (which is approximately 10 hours per day on average). During that time the average

temperature in the conservatory exceeded the external air temperatures by between 4 K (in winter) and about 11 K (in spring, summer and autumn).

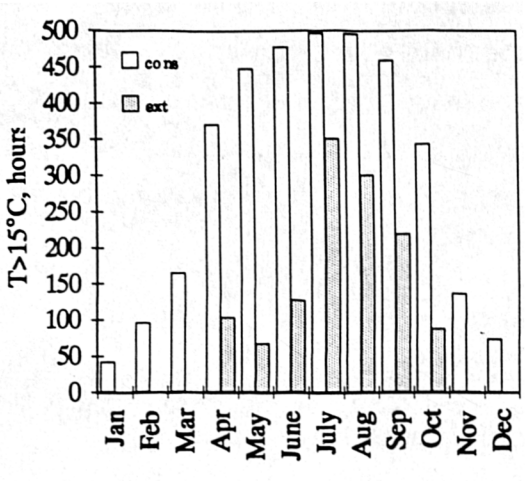

Figure 9.5:

Number of hours in each month for which the external air temperature (ext) and the conservatory air temperature (cons) exceeded 15°C in Sheffield.

It is worth recalling that without adequate ventilation and shading there are likely to be periods of the day within which this conservatory will be overheated (see section 9.4). In the base-case conservatory the annual time of overheating (T > 27°C) was about 9% of the occupied hours (which is approximately one and a half hours per day on average). Thus, these figures of usability given here assume that adequate ventilation and shading features are incorporated.

9.7.3 Heating the conservatory

Since conservatories are mainly used as an extension of the living-space, occupants tend to heat such spaces. By heating of a conservatory temperatures can be kept above a chosen value, which increases the time-of-usability. Heating may also be used to protect temperature sensitive plants.

To study the influence of restricted heating on the energy demand of the base-case conservatory and time-of-usability, the conservatory heating setpoint was varied between 0°C and 21°C, where "0°C" means that the conservatory was unheated (i.e. the base-case). This heating was restricted to the occupied period, i.e. between 7am and 11pm. (It was assumed, that conservatories are very unlikely to be heated throughout the night, when they are not occupied.) To recognise the fact that plants may need continuous heating, a second series of simulations were undertaken using round-the-clock heating in the conservatory.

For both heating regimes, the energy demand of the conservatory increased exponentially as the heating setpoint was increased (Fig. 9.6). For a 10°C set-point the annual energy demand was about 600 kWh for the 16 hour heating regimen. Although there were only eight additional heating hours, the energy demand for the continuous heating was approximately twice as much as for the partly-heating (1100 kWh).

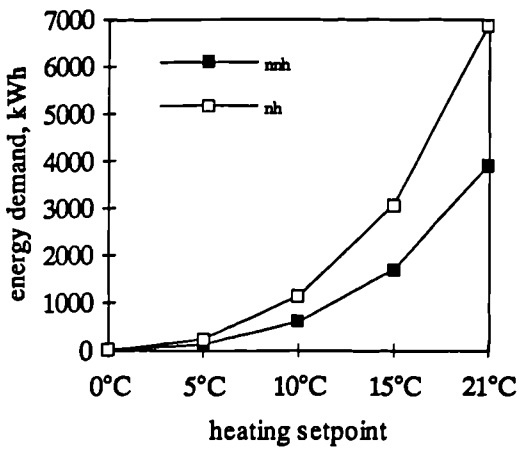

Figure 9.6:

Influence of the heating setpoint on the annual energy demand of the heated base-case conservatory.

nnh: no nighttime heating
nh: 24h continuous heating

For a 21°C set-point, the energy demand of the continuously-heated conservatory (6360 kWh) clearly exceeded the energy demand of the well-insulated adjacent living-room (4280 kWh; see case "d" in Fig. 9.3). In comparison, the partly-heated conservatory has a lower energy demand (3900 kWh) than the living-room. However, when the energy demand is compared as a fraction of floor area, the partly-heated conservatory (325 kWh/m²) has an higher energy demand than the living-room (268 kWh/m²). It should be noted that the energy demand of the partly-heated conservatory clearly exceeds the requirements of the proposed future German insulation standards (e.g. WärmeschtzVO 1993) which specifies energy levels of 100 kWh/m² or less for domestic living-rooms.

The time-of-usability only marginally increased as the heating setpoint increased (for heating setpoints lower than 15°C). Thus, with a heating setpoint lower than 15°C, the conservatory temperature can hardly be lifted into the comfortable range. The graphical representation of this result is not shown here.

Thus, to extend the habitable living-space (from the energy point of view) it may be better to chose a traditional construction (with insulated opaque walls) instead of planning a conservatory. A typical, double glazed conservatory should be used as a purely unheated, occasionally occupied space. Since occupants tend to heat their conservatory, it is best designed without any heating possibility.

The restricted heating under 10°C is not very energy intensive and may be useful to protect plants. However, restricted heating to a setpoint lower than the comfort temperature does not sufficiently improve the time-of-usability to justify the energy demand. Nighttime heating is very energy intensive and should be avoided as often as possible.

9.8 INFLUENCE OF ATTACHED CONSERVATORY AND DWELLING DESIGN ON PERFORMANCE

9.8.1 Construction of adjacent room

The construction of the living-room influences its heat loss rate and the thermal storage mass. It determines not only the annual heating energy demand, but also the utilisation of solar energy and therefore the benefits of any passive solar system. The insulation level of the base-case design (U-value = 0.5 W/m²K) corresponded to the current standard in the UK and was heavy-weight.

To assess the relationship between the energy saving potential of a conservatory and the insulation level (average U-value) of the parent room, the annual heating energy demand of the base-case room and conservatory (case "cons") was compared with that of the base-case room without the conservatory (case "d") (Fig. 9.7). The average U-value of the living-room was varied from 0.3 W/m²K (advanced high-insulation) to 1.4 W/m²K (traditional low-insulation). The constructions are described in detail in Appendix A.1.

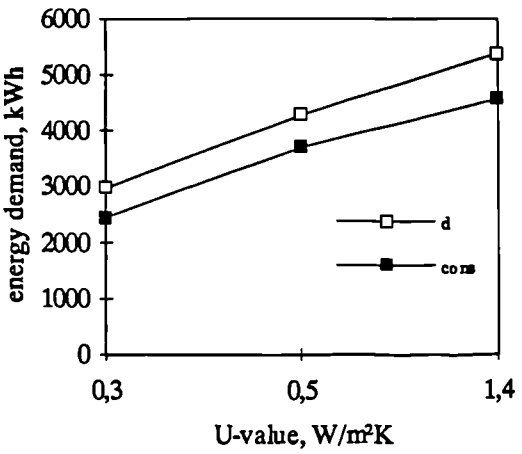

Figure 9.7:

Influence of the average living-room U-value on the annual energy demand of the living-room with conservatory (cons) or without conservatory, but with a double glazed external window (d).

The energy demand decreased by 46% as the average U-value of the living-room was decreased from 1.4 W/m²K to 0.3 W/m²K. In comparison, the reduction in energy demand due to adding a conservatory was always about 500 kWh, i.e. between 13% and 18%. For energy saving purpose, it is therefore much more useful to increase the insulation level of a room, than to add a conservatory.

A one-off study showed, that the energy saving potential of the conservatory (and therefore the utilisation of the solar energy) was still the same, when the heavy-weight floor and walls of the room were replaced by light-weight constructions. Furthermore, the internal temperatures in the conservatory were not affected by the living-room construction.

The studies showed that the energy saving potential, usability and overheating of a conservatory is virtually independent of the insulation levels and storage mass of the adjacent building.

9.8.2 Shading a conservatory (with opaque elements)

The base-case conservatory did not have any shading devices. Although overheating was reduced by increased ventilation rates (15 ach when air temperature was above 27°C), the time of overheating in the conservatory (T > 27°C) was considerable (0.09 or 9%, see section 9.7.2). Higher ventilation rates in summer could further reduce the time of overheating, but they do not offer any protection against discomfort due to solar radiation impinging directly onto people. Direct solar radiation is also likely to damage plants. Therefore, additional shading is important in a south-facing conservatory.

One effective way of shading a conservatory is to install opaque, highly insulated, elements in the conservatory roof or in the side-walls (east/west walls). The chosen panels containing 120 mm of mineral wool (U-value = 0.3 W/m²K) reduced the solar gain in the conservatory and offered better heat insulation. The performance of the base-case conservatory (with and without heating) with different arrangements of opaque panels was investigated.

The annual energy demand of the adjacent room increased as opaque panels were added to the unheated conservatory (Fig. 9.8). The increase was, however, marginal (1%) if they were located in the side walls. An opaque roof increased the energy demand by 16%.

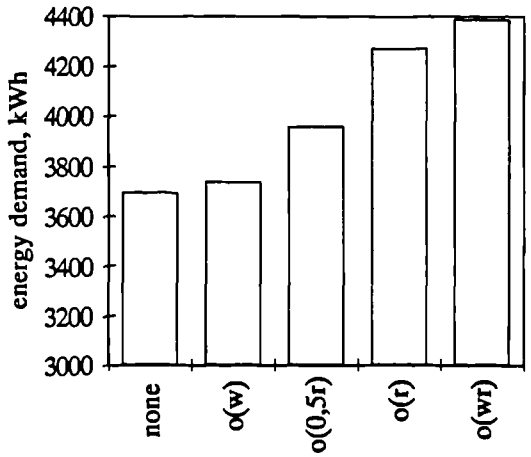

Figure 9.8:

Annual energy demand of the living-room with a double glazed unheated conservatory and different arrangements of opaque panels.

none: base-case without panels
o(w): opaque panels on both side-walls
o(0.5r): panels on half of the roof
o(r): total roof opaque
o(wr): total roof and side-walls opaque

The time-of-usability changed very little as opaque panels were added (Fig. 9.9). The change was greatest in the case of opaque side-walls, for which the usability increased by 0.025 (but this is probably beyond the Resolution of the DSM).

The overheating potential, in the absence of shading, reduced as the opaque panels were added to the roof. With a totally opaque conservatory roof the overheating problem nearly disappeared (Fig. 9.10).

In the case of a conservatory heated to 21°C between 7am and 11pm, the total annual energy demand of the conservatory plus adjacent space, was reduced if opaque panels were added. (The reduction was roughly proportional to the area of glass replaced by insulation.) Of the options studied insulated side-walls led to the greatest reduction (Fig. 9.11).

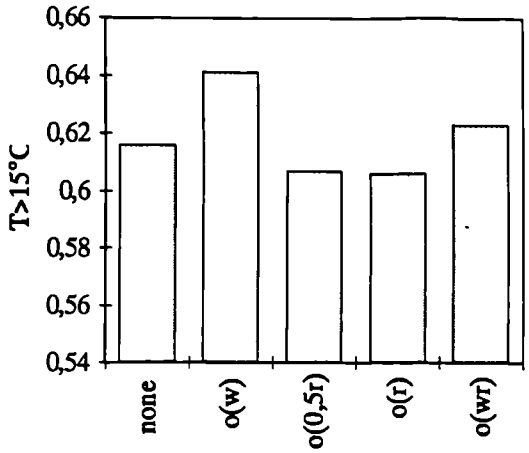

Figure 9.9:

Influence of opaque panels on the relative number of occupied hours (7am - 11pm), for which the conservatory air temperature exceeds 15°C.

(see Fig. 9.8 for key)

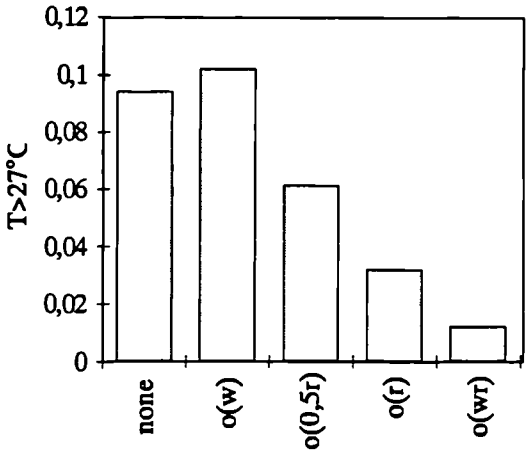

Figure 9.10:

Influence of opaque panels on the relative number of occupied hours (7am - 11pm), for which the conservatory air temperature exceeds 27°C.

(see Fig. 9.8 for key)

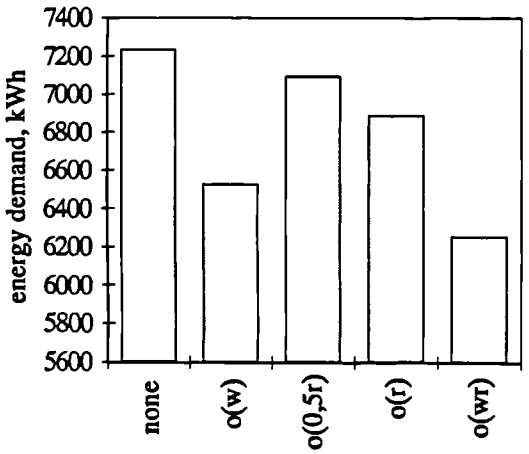

Figure 9.11:

Influence of opaque panels on the total annual heating energy demand of living-room and conservatory, when the conservatory is heated to 21°C (between 7am and 11pm).

(see Fig. 9.8 for key)

Overall considerations show, that opaque side-walls only marginally influence: the heating energy demand of the space attached to the (unheated) conservatory, the time-of-usability and the amount of overheating in the conservatory. They reduce the heating energy demand if the conservatory becomes heated (by about 11%). For terraced houses with conservatories opaque side-walls may also be useful to increase privacy.

Opaque roof elements are effective measures to reduce overheating in a conservatory. Although the covering of the roof had nearly no influence on the time-of-usability (Fig. 9.9), more detailed investigations yielded some comfort advantages for a shaded conservatory. On a clear day (sunny winter's day; see Appendix B) the opaque roof not only reduced the peak temperatures in the conservatory but it increased the temperature level in the evening and at night (Fig. 9.12).

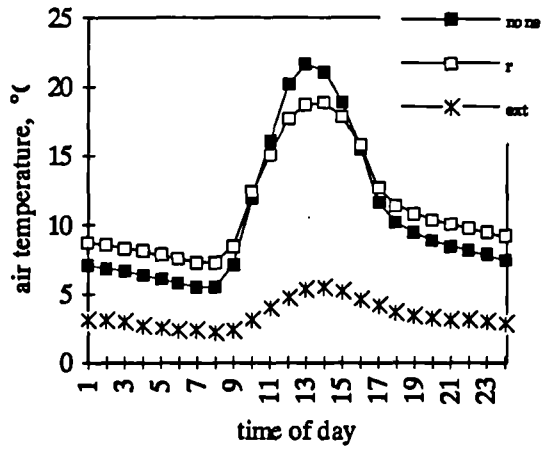

Figure 9.12:

Daily air temperature variation in the conservatory on a sunny winter's day.

none: base-case without panels
r: opaque roof
ext: external air (Sheffield)

However, the opaque roof elements can have an unfavourable influence on the heating energy demand of the adjacent space. The totally opaque conservatory roof shaded the adjacent room from direct radiation over the whole year. Even when only half of the roof was covered by opaque elements, the direct radiation was shaded for most of the year (a few hours in winter excluded). Covering the roof (or part of it) increased the energy demand of the living-room by up to 16% (580 kWh) (Fig. 9.8). Its heating energy demand is similar to that of a simple double glazed direct-gain room (compare case "d" in section 9.7.1). Hence, in this case, the energy benefits of the attached conservatory disappeared completely. For the energy saving potential of an unheated conservatory to be realised, the transfer of radiation across the conservatory into the adjoining living-space is crucial.

An opaque conservatory roof also reduces the lighting level in the adjacent room. This is likely to be unwelcomed since the levels have already been reduced by the conservatory construction. The reduced levels in the conservatory could have a negative effect on the growth of plants. If a high sun protection is wanted, without a considerable rise in the energy demand, movable shading devices, which permit an appropriate and careful adaptation

(e.g. by an automatic control, which brings them down only when high solar radiation is present), are assumed to be favourable.

It should be noted that a conservatory with an opaque roof is not a strictly conservatory in terms of its usual definition (see section 9.2). Moreover, a conservatory, for which five surfaces are opaque (case "wr"), looks more like a conventional living-room with one external window than like a conservatory.

9.8.3 Conservatory and partition glazing type

To study the thermal consequences of the choice of glazing, nine different glazing arrangements were compared. The conservatory had either single glazing, double glazing or had low-emitttance glazing and for each of these options the partition window had either single glazing, double glazing or low-emittance glass (see Fig. 9.13). The glazing properties have been discussed previously (section 9.7.1; Table 9.2).

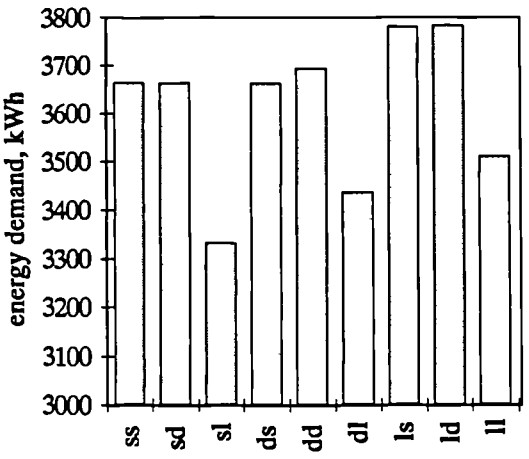

Figure 9.13:

Influence of the partition and conservatory glazing type on the annual energy demand of the living-room with unheated conservatory.

ss:	partition single - conservatory single
sd:	partition single - conservatory double
sl:	partition single - conservatory low-emittance
ds:	partition double - conservatory single
dd:	partition double - conservatory double
dl:	partition double - conservatory low-e.
ls:	partition low e. - conservatory single
ld:	partition low-e. - conservatory double
ll:	partition low-e. - conservatory low-e.

Considering the annual energy demand of the living-room with an unheated conservatory, there was virtually no difference between single or double glazing for the conservatory, or between single and double glazing for the partition (Fig. 9.13). (The small differences which are seen are less than 1% and thus beyond the Resolution of the model).

However, when low-emittance glazing was used, it was better to put this glazing on the outside (conservatory), while keeping the reduction of the interzonal-radiation transfer between living-room and conservatory as small as possible (i.e. by using single glazing). As an example (Fig. 9.13), the energy demand of a single glazed conservatory with a low-emittance partition window (ls) was 12% greater than for a low-emittance glazed conservatory with a single glazed partition window (sl). It increased by 9% when the combination of double glazed partition and low-emittance glazed conservatory (dl) was reversed (ld). The combination with the lower overall insulation, single glazed partition with low-emittance

glazed conservatory (sl), is slightly (5%) better than identical windows (ll). (This may, however, be beyond the model Resolution.)

When the conservatory was heated to 21°C (from 7am to 11pm) the partition glazing type had nearly no influence on the total energy demand of the living-room and conservatory (Fig. 9.14). The annual heating energy demand was determined only by the conservatory glazing type and could be nearly halved by changing from single to low-emittance glazing (i.e. from 9240 kWh to 5040 kWh).

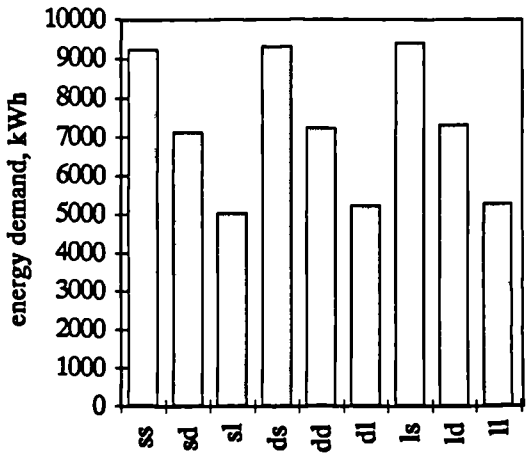

Figure 9.14:

Influence of partition and conservatory glazing type on the annual energy demand of the living-room and conservatory, when the conservatory is heated to 21°C from 7am to 11pm.

(see Fig. 9.13 for key)

The time-of-usability was determined by the conservatory glazing type and independent of the partition glazing type. It increased from 0.53 (of the annual occupied hours) for single glazing to 0.73 for low-emittance glazing (Fig. 9.15). This corresponds to a rise of 1170 hours per year (or about 3 hours per day on average). Conservatory glazing with good insulating properties is crucial if a space is to be used intensively.

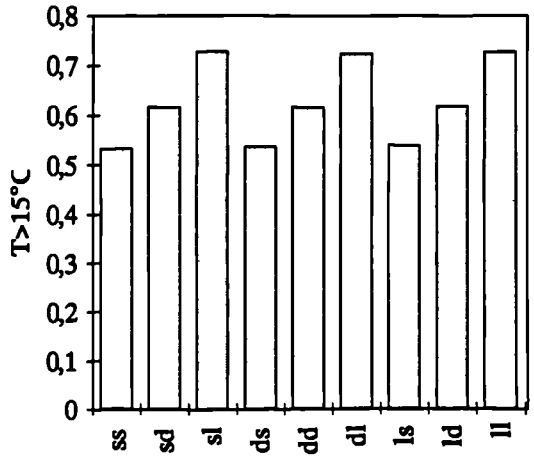

Figure 9.15:

Influence of partition and conservatory glazing type on the relative number of occupied hours (7am - 11pm) for which the conservatory temperature exceeds 15°C.

(see Fig. 9.13 for key)

The time of overheating, in an unshaded conservatory, increased from 0.05 for single glazed conservatories to 0.16 for conservatories with low-emittance glass. Hence, the importance

of having an effective shading device increases as the insulation level of the conservatory glazing increases (Fig. 9.16).

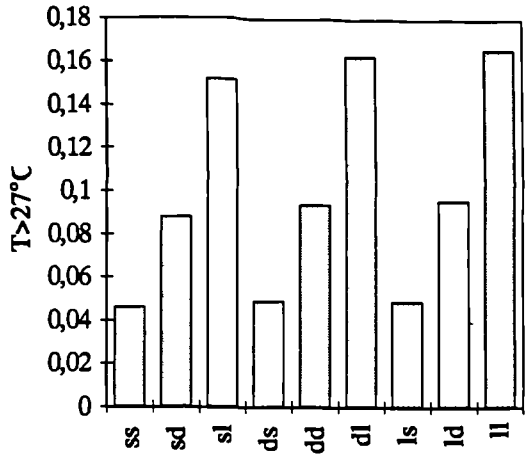

Figure 9.16:

Influence of partition and conservatory glazing type on the relative number of occupied hours (7am - 11pm) for which the conservatory temperature exceeds 27°C.

(see Fig. 9.13 for key)

Generally, heat protection (low-emittance) glazing for the conservatory, leads to the lowest total annual energy demands (with either an unheated conservatory or a heated conservatory) and to the highest time-of-usability. It is worth noting, that insulating glazing (low-emittance and to a lesser extend double) reduces (or even avoids) condensation at the glass surfaces. This would be particularly relevant when a conservatory is used as a greenhouse. In addition, higher surface temperatures (as provided by insulated glazing) increase the thermal comfort of the occupants.

The usability of a conservatory, its energy demand and its tendency to overheating is not influenced by the partition glazing. However, a highly transparent, single glazed, partition slightly reduced the energy demand of the living-room (with unheated conservatory) compared to better insulated partition glazings. It should be added, that highly transparent partition glazings are also favourable concerning the lighting of the adjacent room. (They may be worse concerning the overheating of the adjacent room but this was not investigated.)

9.8.4 Area of partition glazing

Reliable statements of the variation of energy demand with window area are crucial for optimising direct-gain passive solar designs. Similar design questions occur for partition windows, which are surrounded by a conservatory.

To investigate the best glazing size, the external glazing area (living-room without conservatory) and partition glazing area (living-room with conservatory) was varied (no glazing (0 m^2); half wall glazed (7 m^2); completely glazed (14 m^2)). Double glazing was used (see base-case arrangement) for the conservatory glazing as well as for the partition glazing.

For the base-case living-room without conservatory (case "d") the energy demand varied by 9% with the lowest energy demand occurring for a glazing area which was about 7 m^2 (half

of the wall) (Fig. 9.17). When the window was covered by a conservatory (case "cons"), the optimum was shifted towards higher glazing areas (Fig. 9.17). The saving by using 14 m², rather than 0 m², of double glazing was 11%. Similarly, the total energy demand of the living-room with heated conservatory was lowest with the totally glazed (14 m²) partition (Fig. 9.18).

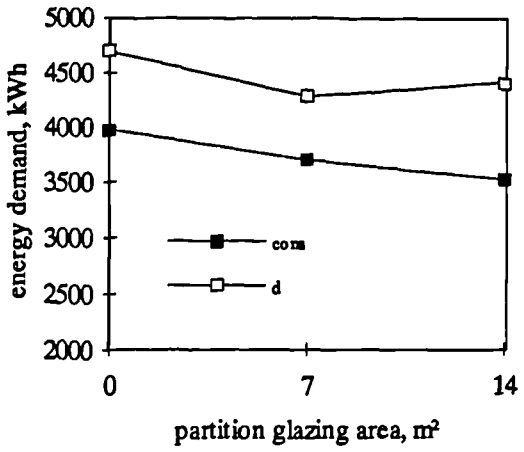

Figure 9.17:

Influence of partition glazing area on the annual heating energy demand of the living-room with or without an unheated conservatory.

cons: double glazed conservatory, base-case
d: double glazed room, no conservatory

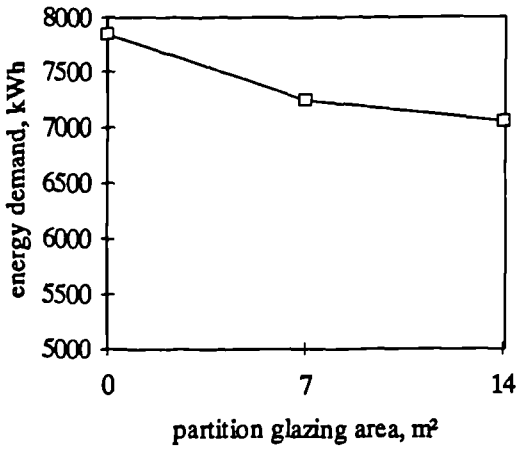

Figure 9.18:

Influence of partition glazing area on the total annual heating energy demand of the living-room and conservatory, when the conservatory is heated to 21°C between 7am and 11pm.

The time-of-usability, as well as the time of overheating were only marginally influenced by the partition window area. The simulation results are not shown here.

From the above statements, it seems preferable to have a big partition window between the conservatory and the adjacent room. In addition, big partition glazing areas improve the lighting of the adjacent space, which is already reduced by the conservatory construction. They also offer an almost unobstructed view into the conservatory, which is often desired by conservatory owners.

However, it is important to consider other issues like the overheating in the adjacent room, which becomes more likely as the partition area increases (this was not investigated in detail). To avoid this possibility, it is important to have some way of ventilating the living-

space with air coming directly from the outside (this is also important to avoid moisture problems in the space, when the conservatory is used as a greenhouse). It is also valuable to have shading devices on the partition windows (curtains or blinds) which occupants can use. When these measures cannot be employed overheating of the adjacent space is likely to be a problem.

9.8.5 Conservatory size

It has been shown in section 9.7.1 that the thermal benefits of adding an unheated conservatory to a double glazed external window are comparable with those obtained when changing from a double glazed external window to a quadruple glazed external window (or to a low-emittance glazed window). This result was obtained for a small (depth = 2.12 m) conservatory with 12 m² floor area (base-case). It was important to investigate, whether this was still true, for conservatories with other dimensions.

The conservatory depth was varied from 1 m to 4.2 m (corresponding to floor areas from 6 m² to 24 m²). Whilst the conservatory depth was varied, the same partition area was kept at about 14 m². The variation in the annual energy demand of the living-room with the unheated conservatory was less than 2% (Fig. 9.19), which is well beyond the Resolution of the DSM. (The unevenness in the results trend could not satisfactorily be explained.)

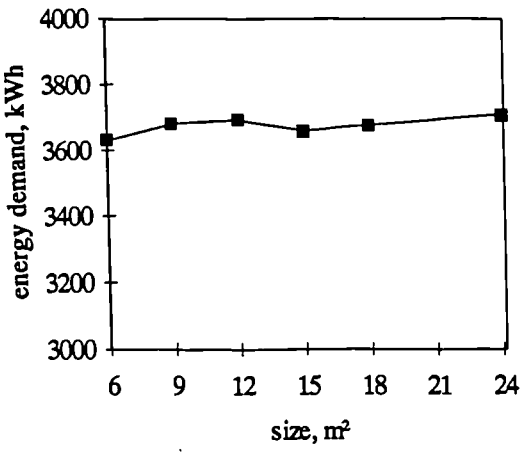

Figure 9.19:

Influence of the conservatory size on the annual energy demand of the living-room with double glazed unheated conservatory.

The time-of-usability decreased only marginally as the size increased (from 0.64 for 6 m² to 0.59 for 24 m², Fig. 9.20), which corresponded to a reduction of 290 hours a year (or lower than one hour per day on average). However, the daily temperature variations on a cold, clear winter's day (Appendix B) showed (Fig. 9.21) that for limited time periods a small conservatory can have considerably higher air temperatures than large conservatories which makes them much more favourable.

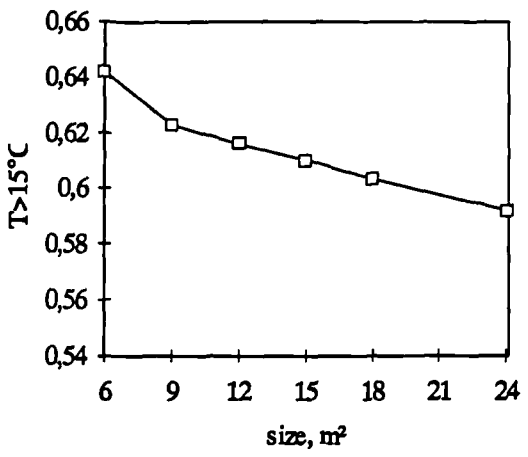

Figure 9.20:

Influence of the conservatory size on the relative number of occupied hours (7am -11pm) for which the conservatory air temperature exceeds 15°C.

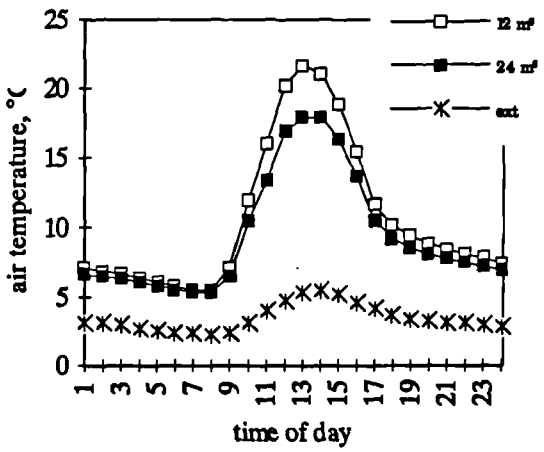

Figure 9.21:

Daily variation of conservatory air temperature on a sunny winter's day for different conservatory sizes.

12 m²: conservatory floor area = 12 m²
24 m²: conservatory floor area = 24 m²
ext: external air (Sheffield)

Size is much more important if the conservatory is heated. The annual heating energy demand of the conservatory (heated to 21°C between 7am and 11pm) more than doubled as the size was increased from 9 m² to 24 m² (Fig. 9.22). When the heating energy demand of the conservatory was related to its size, the relative energy demand decreased with the conservatory size from 497 kWh/m² (for a 6 m² conservatory) to 281 kWh/m² (for a 24 m² conservatory). Compared to the base-case living room (268 kWh/m²; see case "d" in section 9.7.1) a 24 m² conservatory has only a marginally higher heating energy demand. Thus, large heated conservatories appear to be as economic as conventional spaces. However, the following considerations reduce the universality of this conclusion.

(i) The size of the conservatory was increased keeping the same height. If the height had been increased along with the floor area (which is the usual case), the heat losses through glazings would have been increased too. This would have worsen the performance of the conservatory.

(ii) The conservatory was heated between 7am and 11pm, whilst the living-room was heated continuously (with a night set-back). If the heating regime of the living-room was adopted for the conservatory its energy demand would increase (see section 9.7.3).

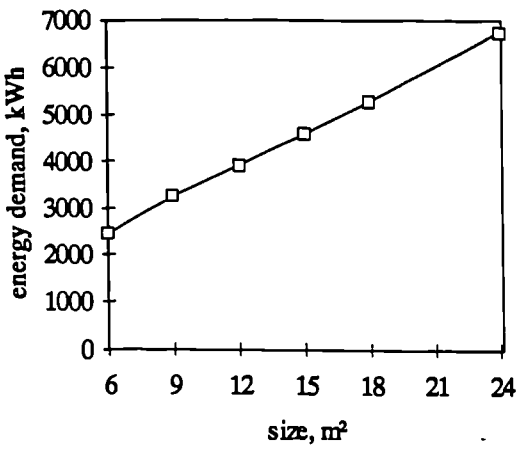

Figure 9.22:

Influence of the conservatory size on the annual heating energy demand of the conservatory, when it is heated to 21°C from 7am to 11pm.

Thus, small unheated conservatories have comfort advantages. Small conservatories also permit steeply sloping roof glazings to be used whilst maintaining enough head rooms at the ends. The size of an unheated conservatory does not affect the energy demand of the adjacent living-room. However, big conservatories may demand less energy (per unit floor area), if occupants choose to heat them.

9.8.6 Conservatory thermal storage mass

The storage mass of the conservatory (mainly the floor) influences the utilisation of the solar energy. To study the influence of the thickness of the concrete floor it was varied from 0 to 15 cm. There was a 5 cm thick insulation layer below the concrete. For these investigations, the storage mass of the partition wall was eliminated by putting the wall insulation on the outside.

The storage mass of the conservatory floor had nearly no influence on the energy demand of the living-room (with unheated conservatory). When the conservatory was heated, there was a very weak minimum in the conservatory heating energy demand for a concrete thickness of about 9 cm. The influence was about 5% which is relatively low and probably beyond the Resolution of the DSM. The results are not shown here.

The time-of-usability had a slight optimum for concrete of thickness 6 to 9 cm (Fig. 9.23). If there was no storage mass in the conservatory the time-of-usability reduced by only about 0.03 (175 hours a year). In comparison with other conservatory design influences (e.g. conservatory glazing type, see section 9.8.3) this effect must be termed as being marginal and beyond the Resolution of DSMs.

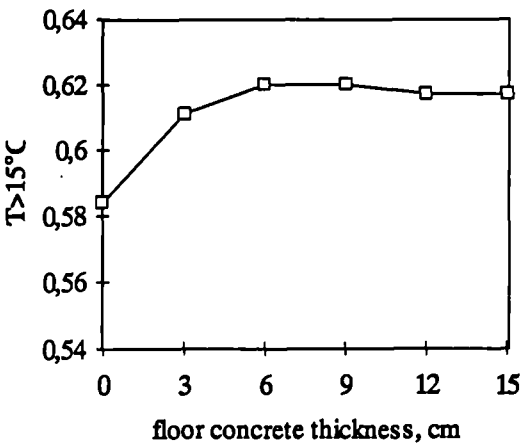

Figure 9.23:

Influence of the thickness of the concrete floor on the relative number of occupied hours (7am - 11pm), for which the conservatory air temperature exceeds 15°C.

Although the influence of the storage mass on the annual figures of the usability were shown to be very small, more detailed investigations, of daily temperature variations, indicated considerable differences. On a clear winter's day a 9 cm thick concrete floor in the conservatory reduced the daily peak temperatures slightly, but more importantly increased the conservatory temperatures in the evening and night (Fig. 9.24). For example, with a 9 cm concrete floor the early evening temperature was 5 K higher than in a conservatory with no storage mass. Thus, whilst the time-of-usability was not improved by adding storage mass, it did improve the protection offered to plants against cold and frosty weather. The energy demand of frost protection heaters may also be reduced by having some mass, but this was not explored. Additional storage elements such as water tanks may also be beneficial but these were not studied either.

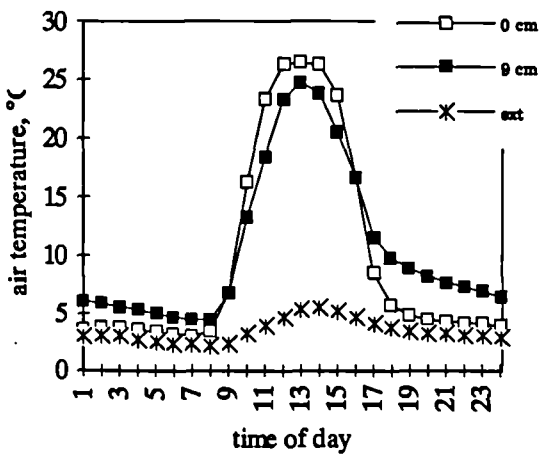

Figure 9.24:

Daily variation of conservatory air temperature on a sunny winter's day for different conservatory concrete floor thicknesses.

0 cm: no concrete floor (no storage mass)
9 cm: concrete floor thickness = 9cm
ext: external air (Sheffield)

A storage mass of about 9 cm in the concrete floor appears to be optimal but extra mass is not detrimental. The surface area of the storage materials also determines the thermal performance of a room. So, in circumstances with opaque side walls, additional mass could be located in these elements.

9.8.7 Surface reflectances

The reflectance of the opaque conservatory elements (mainly the floor and the partition wall) determines the thermal storage, radiation backloss and the interzonal radiation transfer into the adjacent space. For the base-case design a low reflectance (of 0.2) was used. This corresponds to dark colours and a high solar energy absorptance.

To study the influence of surface reflectance on conservatory performance, the surface reflectances of the conservatory floor and partition wall were varied from 0.2 to 0.4 and 0.6.

The influence of the reflectance on the annual heating energy demand of the living-room (with unheated conservatory), was very small (lower than 1%). Similarly, when the conservatory was heated, the total annual energy demand of the conservatory and room increased only slightly (by 5%) as the reflectance was increased. Both these results are probably below the Resolution of the DSM.

The time-of-usability reduced by 0.035 (204 h per year) as the reflectance increased. This reduction is comparable with the effect of storage mass in the conservatory (see previous section).

Only the time of overheating was affected by the surface reflectance. It decreased by a third (from 0.09 to 0.06) as the reflectance increased. This reduction in the overheating does not solve the overheating problem. Shading and ventilation are much more effective at reducing overheating.

As a conclusion, the surface reflectance has only marginal influences on the thermal conditions in the conservatory and adjacent room. The choice of the surface colour is more likely to be dictated by other issues, like aesthetics or the choice of materials. Since the influences were shown to be low, graphical representations of the results are not shown here.

9.8.8 Partition wall-type

In section 9.8.4 it was concluded, that big partition glazing areas between conservatory and living-space are favourable. Therefore, it was evident that the preferred partition wall area will be small. However, if a conservatory is added to an existing older house, the partition wall area between conservatory and living-space may be considerable.

To study the influence of the insulation level of the partition wall the U-value of the (7 m^2 base-case) wall was varied from 0.3 W/m^2K (advanced, highly-insulated) to 1.4 W/m^2K (traditional, poorly-insulated).

It was found that the partition wall U-value had only a small effect on the energy demand of the adjacent room (with an unheated conservatory) and the energy demand of the room with a heated conservatory. The U-value of the partition wall did not influence the time-of-usability of the unheated conservatory.

Since the U-value of the partition wall has only little influence on the operation of the conservatory, it is not an important factor in conservatory design. It may be tempting therefore, to reduce the costs of a new building by reducing the U-value of the area of wall. This should not be taken to extremes however, because a purely insulated partition wall may lead to serious condensation problems at the inner wall surface (especially if the relative humidities in the living-space are high and the conservatory is unheated (see Hauser 1987)). This issue should be considered when the partition wall has a lower insulation level than the other walls of a building.

9.9 ATTACHED NORTH CONSERVATORIES

Investigations of passive solar design (big glazing areas with or without conservatories) generally lead to the conclusion that the best orientation is south or close to south (i.e. the absolute energy demand of a building is lowest when the whole building is south-orientated). However, the energy savings offered by a conservatory may not necessarily be highest for south orientation.

If south glazings are not possible because of the building site (e.g. on north slopes) and if large north-facing glazings are necessary, heating loss reduction through the north glazings becomes very important. This could be achieved by heat-protection glazings (triple -, quadruple -, low-emittance glass) or by attaching a conservatory.

To study the influence of northward orientation on the annual energy demand the base-case room and conservatory were used (section 9.5; Appendix A.4), but this time these faced northwards. For the living-room alone, the glazing types (double, triple, quadruple, low-emittance (see Table 9.2 in section 9.7.1)) were varied as were the glazing areas (no glazing (0 m^2), half glazing (7 m^2), or completely glazed (14 m^2)). With the north-orientated (double glazed) conservatory in place the same range of glazing areas was studied but the partition was double glazed. It is important to stress that the study concentrated on a north room which did not have additional south windows. If those had existed, the utilisation of the solar gains through the north windows would decrease. Therefore, the result trends are only transferable to purely north-orientated rooms, and not to rooms with additional big south-facing windows.

Considering firstly the direct-gain spaces, it is apparent that the annual energy demand increases as the insulation properties of the glazing decrease (Fig. 9.25). With double- and triple- glazing, the energy demand of the (direct-gain) living-room increased considerably with the glazing area (Fig. 9.25). For quadruple glazing, the energy demand stayed nearly the same. With low-emittance glazing the energy demand decreased as the glazing area increased. Thus, the net annual energy loss of the low-emittance glazing was lower than that

of the partition wall (U-value = 0.5 W/m²K). However, the solar energy gains did not completely compensate for the heat losses. (The annual energy demand of a reference case (without either a north wall or north window) was about 4200 kWh. This is lower than the 4400 kWh obtained for the completely glazed external window with low-emittance glazing.)

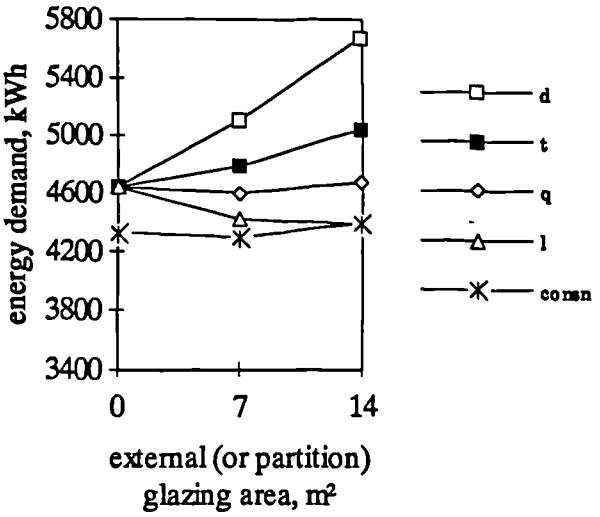

Figure 9.25:

Influence of external (or partition) glazing area on the annual energy demand of a north-facing living-room with different types of external glazings or a double glazed partition window plus conservatory.

d:	double glazed external window
t:	triple glazed external window
q:	quadruple glazed external window
l:	low-e glazed external window
consn:	double glazed unheated conservatory

Irrespective of the glazing area, a north-orientated room with an unheated double glazed conservatory (case "consn") had about 7% lower energy demands, than the same room without a conservatory but with quadruple glazing (case "q") (Fig. 9.25). (For south orientation it was marginally (4%) less, see section 9.7.1). For great partition glazing areas, the energy demand lay in the range of that produced by low-emittance glazing. For small partition glazing areas, the conservatory behaved even better than low-emittance glazing.

Comparing Fig. 9.3 (section 9.7.1) with Fig. 9.25 (for 7 m² glazing) the north-facing options, direct-gain or conservatory, are using between 16% and 18% more energy than the south-facing options (irrespective of the passive solar system type). The energy saved by attaching a conservatory to a north-facing double glazed room was about 16% (800 kWh) (half partition glazed), or 23% (1300 kWh) (total partition glazed). For south orientation the saving was 14% (600 kWh) or 20% (900 kWh) (see Fig. 9.17 in section 9.8.4). The small differences between these two sets of energy saving rates (2% for half partition glazing and 3% for total partition glazing) are beyond the Resolution of the model. It appears therefore, to make little difference to the percentage energy savings whether a conservatory is attached to a south, or a north-facing façade.

If the conservatory was heated to 21°C, the total energy demand decreased by about 5% as the partition glazing size increased (Fig. 9.26). This may be beyond the model Resolution. The heating energy demand of the conservatory was 20-30% higher than for south orientation (compare Fig. 9.18).

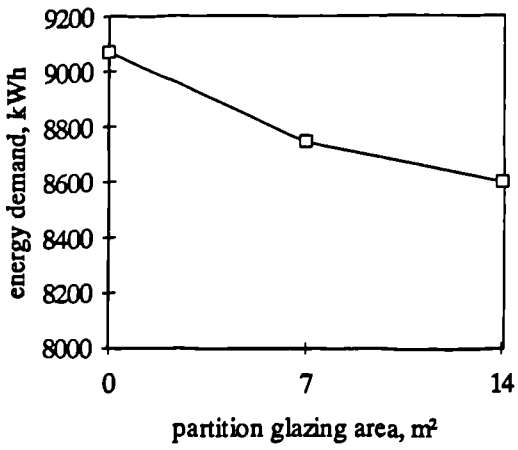

Figure 9.26:

Influence of the partition (external) glazing area on the total annual energy demand of a north-facing living-room with double glazed conservatory, when the conservatory is heated to 21°C from 7am to 11pm.

The time-of-usability of a north conservatory was independent on the partition glazing area and with about 0.52 (3025 annual hours) significantly lower than for south orientation (0.62, 3600 h). The difference of 575 hours corresponds to one and a half hours per day on average. The average temperature in the north conservatory was 2 K lower than for south orientation. It was about 5 K above ambient. The time of overheating in a north conservatory was very small (lower than 0.05).

These results are strictly valid for north conservatories, which are not shaded by the adjacent building. Even when the sun is at the south sky-vault, direct radiation can enter the conservatory through the ceiling or though the side-glazings. In reality this is often not possible because of obstructions. However, an investigation showed, that the influence of the direct radiation on the thermal conditions in north-orientated conservatories is very small. In the worst case, when there is no direct illumination of the conservatory, the time-of-usability was marginally reduced (by 0.03) to 0.49. The heating energy demand of the adjacent room increased slightly by 3%. Neither is significant.

The results show that, when ever possible, it is better to direct glazings towards the south, whilst keeping north glazings as small as possible. However, when there is a large north glazing area, an unheated, double glazed north-facing conservatory will yield about the same percentage energy savings as it would on the south side. Compared with quadruple glazing an unheated, double glazed north-facing conservatory produces bigger energy savings in the adjacent space. The time-of-usability of a north-facing conservatory is clearly lower than for one with a southerly orientation. (It corresponds to that of a south conservatory with single glazing.) However, north-orientated conservatories show very rarely exhibit overheating problems - this may be advantageous for temperature sensitive plants. In addition, it makes its operation very simple and cheap (no costly shading or ventilation devices are necessary).

In choosing the orientation of a conservatory, other issues, like its exposure to wind, should not be neglected. Single glazed conservatories are especially sensitive to wind exposure, since their heat loss depends strongly on the air velocities at the glazing surfaces. Wind protected locations are recommended.

9.10 SOLAR PRE-HEATING OF VENTILATION AIR (SPV)

The preceding studies did not consider any interzonal air flow. The conservatory reduced the heating energy demand of the living-room purely due to its function as a solar heated buffer space. It was therefore reasonable to examine the additional reduction of heating energy demand, when the adjoining room was ventilated with solar pre-heated conservatory air (SPV). The simulations did not consider the detailed air-flow mechanism driven by wind speed or temperature differences (stack effect). Instead, a simplified assessment method based on fixed ventilation rates was used. (For more detailed information about interzonal air flow patterns see, for example, Baker (1985).)

The ventilation heat loss of a space is proportional to the temperature difference between inside and ambient. The advantage of SPV lies in the lower temperature difference between the inside and the conservatory. Hence, the ration between these two temperature differences indicates the energy saving potential of SPV.

The reduction *red(t)* of the temperature difference at any time *t* is defined to be

$$red(t) = \frac{T_{con} - T_o}{T_i - T_o} \tag{9.1}$$

where T_{con} is the conservatory temperature; T_i the inside temperature and T_o the outside (ambient) temperature.

The reduction of the ventilation heat losses at a given time dP_v can be calculated from:

$$dP_v = p * red(t) \tag{9.2}$$

where p is the portion of ventilation air from the conservatory to the total ventilation air quantity. The annual average reduction *red* is the mean of the present reductions during all the heating periods.

To study the dependence of the conservatory temperature on the amount of ventilation rate, the ventilation rate of the base-case conservatory (section 9.5.3) was varied between 0 and 320 m³ per hour (corresponding to conservatory air change rates between 0 and 10.7 ach). As expected, the annual average reduction of the temperature difference decreased as the ventilation rate increased (Fig. 9.27). It was about 0.54, when there is no ventilation, going down to 0.32 for a ventilation rate of 320 m³/h. The reduction of the conservatory tempera-

tures was also reflected in the time-of-usability (Fig. 9.28), which decreased as the ventilation rate increased.

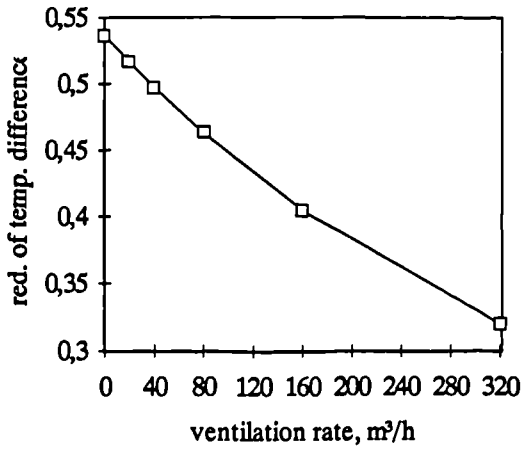

Figure 9.27:

Influence of the conservatory ventilation rate on the annual average reduction of the air temperature difference between the dwelling and the conservatory.

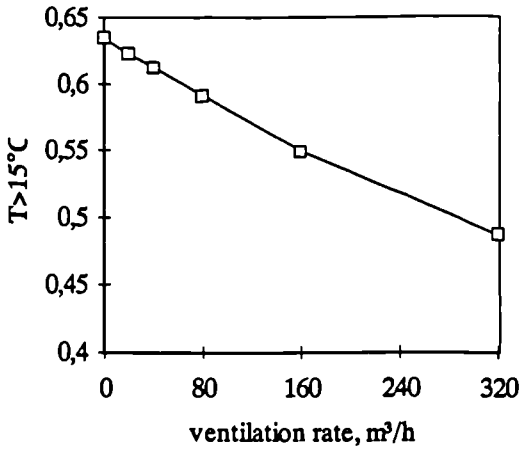

Figure 9.28:

Influence of the rate of solar pre-heat ventilation on the relative number of occupied hours (7am - 11pm) for which the conservatory air temperature exceeds 15°C.

The influence of the reduced conservatory temperatures on the heating energy demand of the room turned out to be lower than 5%.

Thus, in relation to the total energy demand, of a whole building, the additional fabric heat loss (to the conservatory) due to SPV is minimal. The reduction of the ventilation heat losses can therefore be calculated from the reduction of the temperature difference *red* and the portion of ventilation air through the conservatory *p*.

For example, consider a space of 160 m³ (one or more rooms, one-storey high, 62 m² floor area) which is ventilated with an air change rate of 1 ach. If half of the air is taken from the conservatory, this leads to a ventilation rate through the conservatory of 80 m³/h. From Fig. 9.27 the temperature difference is reduced by a factor of 0.46. Hence, by using SPV the ventilation heat losses of the whole dwelling can be reduced by 0.5 * 0.46 = 0.23 (23%). If the ventilation heat loss is about half of the total heat loss for the space (which is a reason-

able assumption for modern highly-insulated dwellings), SPV reduces the total energy demand of the dwelling by about 11%.

For double glazed conservatories the practical reduction of the temperature difference is in a range of 0.4 - 0.5. If all the ventilation air is recovered by the conservatory (the best case) and the ventilation heat loss is half of the total heat loss of the adjoining house, SPV offers an maximum energy saving of between 20% and 25%. This must be regarded as upper limitation.

If SPV can only be used to cover the ventilation of those rooms, which directly adjoin the conservatory, the saving of 20% - 25% refers only to the energy demand of those rooms. In comparison, a conservatory without SPV (acting mainly as a solar heated buffer) reduced the energy demand of the adjoining rooms (with double glazed external windows) by 10% - 15% (section 9.7.1). Thus, the energy benefits by using SPV would be about twice as much as those offered by the buffering effect alone.

It should be noted, that SPV can reduce the energy demand of a whole building by these 20%-25%. However, this is only possible, when all the ventilation air of the whole building is recovered by the conservatory. This is normally only possible, when the conservatory covers many points where air can enter the building. Thus, integrated conservatories are better suitable for SPV than attached conservatories. In comparison, a buffer conservatory reduces the energy demand of a whole dwelling normally by lower than 10% - 15%, possibly down to 2% (see section 9.11.2).

Since the energy saving by using SPV depends directly on the air temperature in the conservatory, it can be further increased by using low-emittance glazing for the conservatory instead of double glazing as used in the base-case. Similarly, double glazing is better than single glazing. (This result contrast with that obtained when the conservatory was acting only as a solar heated buffer space. In that case there was virtually no difference in the energy saving potential of single or double glazed conservatories (see section 9.8.3)). In contrast, the benefits of SPV would clearly be lower in north-orientated conservatories (section 9.9). All the other design options (partition glazing area; conservatory size; thermal mass etc.) only marginally influenced the conservatory air temperatures (see previous sections) and will therefore have little impact on the benefits of using SPV.

9.11 TWO-STOREY BUILDING WITH CONSERVATORIES

9.11.1 Building descriptions

Integrated conservatories have two or more partition walls to the adjoining building. The coupling between the building and conservatory environments is therefore more pro-

nounced. If there are big partition glazing areas, the heat losses from the house into the conservatory will significantly heat the conservatory.

To study the performance of integrated conservatories, two-storey semi-enclosed or corner conservatories with a floor area of 12 m^2, were integrated into a two-storey UK dwelling with a floor area of 60 m^2. In addition, to compare integrated and attached conservatories, a similar dwelling (with a floor area of 72 m^2) was investigated in connection with a two-storey attached conservatory of 12 m^2. The design and operation of the three conservatory and house options are outlined in Table 9.3 (more details are in Appendix A.5).

Construction mode of the dwelling:	heavy-weight, average U-value = 0.5 W/m^2K
Floor of the dwelling and the conservatory:	concrete slab on the ground
Internal storage mass:	10 cm internal concrete partition floor
Floor area of the dwelling:	60 m^2 [72 m^2][1]
Floor area of the conservatory:	12 m^2
Volume of the dwelling:	312 m^3 [374 m^3][1]
Volume of the conservatory:	72.8 m^3 [52 m^3][1]
Volume of the roof-space:	51.9 m^3 [62.3 m^3[1]]
Ventilation rate of the dwelling:	1.0 ach (5.0 ach if inside air temperature > 27°C)
Ventilation rate of the conservatory:	1.0 ach (15.0 ach if inside air temperature > 27°C)
Ventilation of the roof-space:	no
Interzonal air flow (SPV):	no
Heating of the dwelling:	21 °C (7am - 11pm); 16°C (11pm - 7am)
Heating of the conservatory:	no
Heating of the roof-space:	no
Windows of the dwelling:	20.8 m^2 at south wall; 6.24 m^2 at north wall
Partition windows:	50% of the partition wall area
Glazing type of all the windows:	clear double glazing
Frames of all the windows:	15% of window area
Curtains or blinds at all the windows:	no

[1] Values apply to all conservatory types except where square brackets are used to show the different values for the attached conservatory.

Table 9.3 Description of the base-case dwelling and conservatory.

The dwelling was treated as a three-zone arrangement of heated living-space, unheated roof-space and conservatory. It was simply a "blown up" version of the living-room used in the previous sections. Thus, the construction, heating, ventilation and location of the dwelling corresponded to those of the living-room (described in section 9.5.2).

Although the different rooms of the living-space were not explicitly modelled, the internal storage mass was partly modelled by considering a 10 cm thick internal concrete partition floor. The partition walls between the living-space and the conservatory (and the roof-space) had the same construction and insulation level as the external walls.

Apart from the conservatory, there were four large exposed south-facing windows of total area 20.8 m^2 (50% of the south wall) and north-facing windows of 6.24 m^2 (10% of the

north wall). The partition window area (between the heated space and the conservatory) was 50% of the total partition area.

Each conservatory was located at the south side of the building. Their base-case construction, roof-slope (30°), glazing type (double glazed) and ventilation rate (1.0 ach) corresponded to that for the base-case conservatory described in section 9.5.3. Their floors had the same area but measured 4 m by 3 m rather than 5.651 m by 2.12 m. (The symbol "cons" is used for the unheated base-case conservatory attached to the base-case dwelling.) As noted above, three different conservatory types were investigated: attached; semi-enclosed and corner.

The attached conservatory (termed "consa") had a partition wall area of 20.8 m² and contained, therefore, 10.4 m² of double glazing (Fig. 9.29).

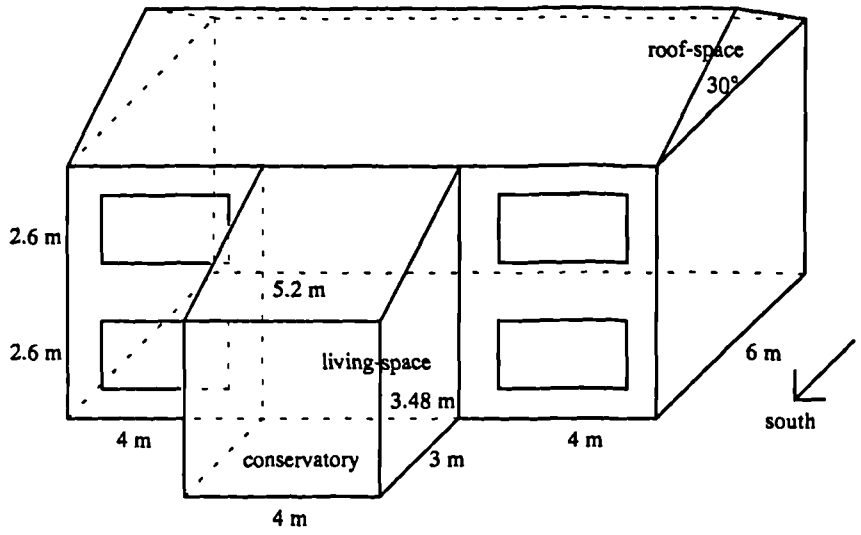

Figure 9.29:
Three-zone dwelling with attached conservatory.

The semi-enclosed conservatory (termed "conse") had three partition walls (of total area 64.11 m²) with the adjoining building. Of this area, 12.11 m² adjoined the roof-space and was separated from it by an opaque wall of standard (external wall) construction, and 52 m² adjoined the living-space and had 26 m² of double glazing. Only the roof and the south-facing surface of the conservatory are exposed to the external climate (Fig. 9.30).

The corner conservatory (termed "consc") had two partition walls (of total area 45.92 m²) with the adjoining building. Of this area, 9.52 m² adjoined the roof-space and was separated from it by an opaque wall of standard (external wall) construction, and 36.4 m² adjoined the living-space and had 18.2 m² of double glazing. The roof, the south-facing surface, and the east-facing surface of the conservatory are exposed to the external climate (Fig. 9.31).

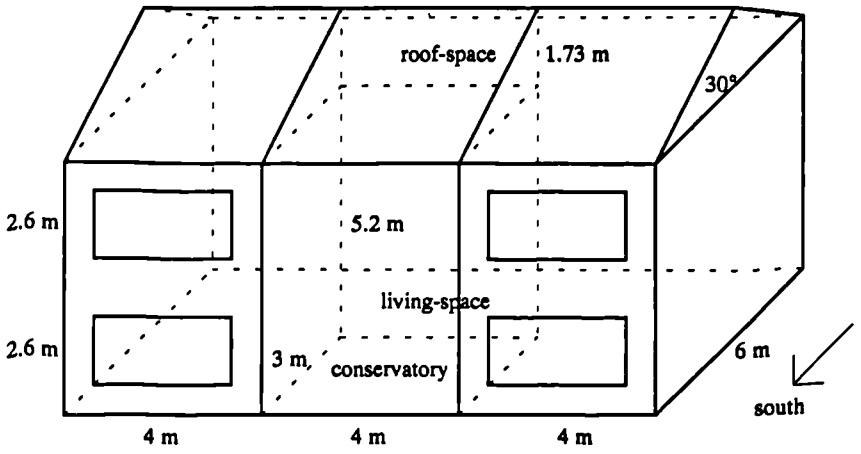

Figure 9.30:

Three-zone dwelling with semi-enclosed conservatory.

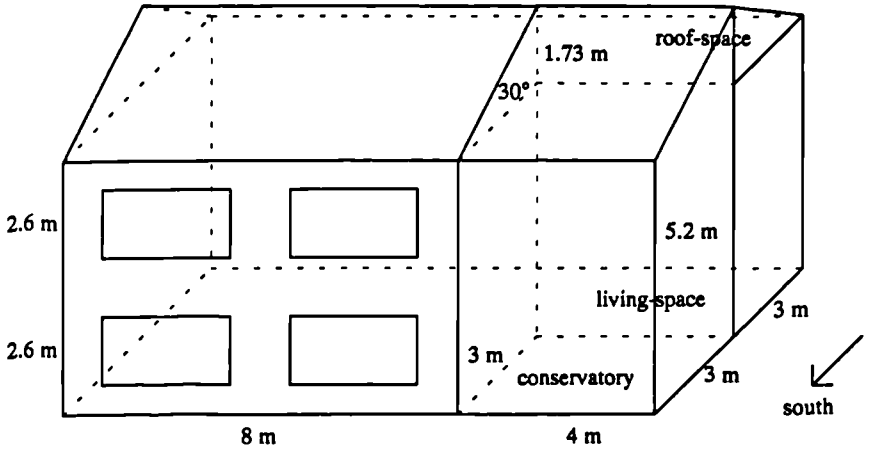

Figure 9.31:

Three-zone dwelling with corner conservatory.

In the base-case the partition as well as the conservatory windows were double glazed. However, the dwellings were also investigated for other, different partition and conservatory glazing types (see Table 9.2 in section 9.7.1).

It is important to note that any statements about the benefits of integrated conservatories should not be compared to the building arrangement without the conservatory, since a house plan developed around a conservatory is unlikely to retain such a form without the conservatory. Instead, for comparison purpose, an arrangement was used in which the integrated conservatory was replaced by a heated living-space. This had the same vertical glazing as the conservatory (in the case of corner conservatories the side glazings are kept) but: an opaque roof; a partition floor between the storeys; and continuous heating with night setback just like the rest of the dwelling. These arrangements were termed "no conse", "no consc", and "no consa" for the enclosed, corner and attached conservatories respectively. Simulations were also undertaken with each of the three conservatories being heated to 21°C from 7am to 11pm ("heated conse", heated consc", and "heated consa" respectively).

9.11.2 Attached conservatory

The adding of a double glazed conservatory to a purely double glazed dwelling reduced the energy demand of the dwelling by 450 kWh, or 2%, from 22030 kWh to 21580 kWh (Fig.

9.32). In section 9.7.1 the energy saving potential of a single-storey double glazed conservatory was 580 kWh, which was 14% of the living-room energy demand. The low relative energy savings obtained here (2%) confirms the assumption made in section 9.5.1 that the energy impact of an attached conservatory is small in comparison to the total energy demand of a whole house.

However, the absolute energy savings of the double-height conservatory attached to a whole dwelling were also (by 130 kWh) lower than those of the single-storey conservatory attached to a living-room. Although this may be a consequence of modelling uncertainties (Resolution), it could also be explained by the following effects:

(i) the two-storey conservatory was narrower and deeper (the length of the common side was only 4 m);
(ii) the proportion of useful solar gains from the conservatory was limited by additional big south windows of the dwelling (see Fig. 9.29);
(iii) the two-storey dwelling shades the conservatory during early morning and late evening hours in spring and autumn.

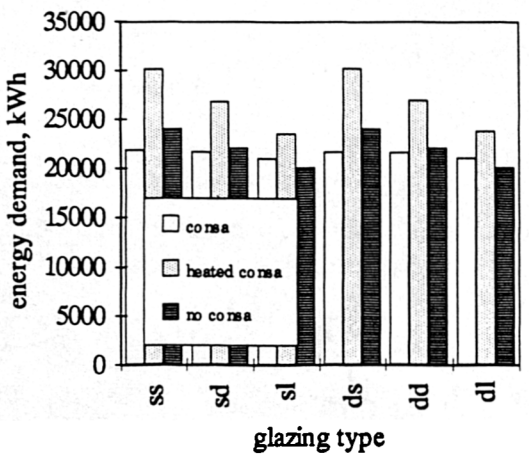

Figure 9.32:

Total annual energy demand of a dwelling with unheated attached conservatory (consa); heated attached conservatory (heated consa) or without conservatory, but with heated living-space (no consa)

ss: partition single - conservatory single
sd: partition single - conservatory double
sl: partition single - conservatory low-emittance
ds: partition double - conservatory single
dd: partition double - conservatory double
dl: partition double - conservatory low-e.

The energy demand of the dwelling with unheated conservatory decreased marginally as the insulation of the external glazing was increased from single to low-emittance glazing by 4% (Fig. 9.32). There were nearly no differences due to different partition window types. This confirms the conclusion of section 9.8.3, that it was more favourable to use low-emittance glazing for the conservatory, while the partition window type was relatively unimportant. Here, the glazing type had only a small impact on the heating energy demand of the adjacent space (about 4%). This was because the influence of an attached conservatory on the total energy demand of a whole dwelling was very low. Infact, all the results are possibly below the Resolution of the DSM.

The energy demand of the dwelling with a heated conservatory (heated to 21°C from 7am to 11pm; case "heated consa") decreased by 21% as the insulation of the external glazing

was increased from single glazing to low-emittance glazing. The strong influence of the conservatory glazing on the heating energy demand of an attached conservatory has already been shown in section 9.8.3. Again, the partition glazing type had little effect.

The trends in the time-of-usability, and in the time of overheating, as the partition and conservatory glazing types changed, were similar to those for the one-storey conservatory (see Fig. 9.15 and Fig. 9.16 in section 9.8.3). The absolute time-of-usability and the absolute time of overheating in the two-storey conservatory were, irrespective of the glazing type, only marginally lower than in the one-storey conservatory of section 9.5.3. (The relative number of occupied hours for which the temperature exceeded 15°C (i.e. the usability) and the number of hours for which the temperature exceeded 27°C (i.e. the overheating) reduced by less than 0.02.) This is probably beyond the Resolution of the model.

9.11.3 Semi-enclosed conservatory

Compared to the dwelling without a conservatory, but with the same external glazing type (case "no conse", see section 9.11.1 for description), an unheated semi-enclosed conservatory always, irrespective of the glazing type, led to reduced total annual energy demands. For example, whilst the dwelling with a double glazed façade instead of a conservatory (case "no conse") had an energy demand of 21690 kWh/year, the dwelling with the unheated double glazed (base-case) conservatory had an energy demand of 18970 kWh/year, which was 12% lower (Fig. 9.33). (The reductions were 8% for low-emittance external glazing and 18% for single external glazing, respectively.)

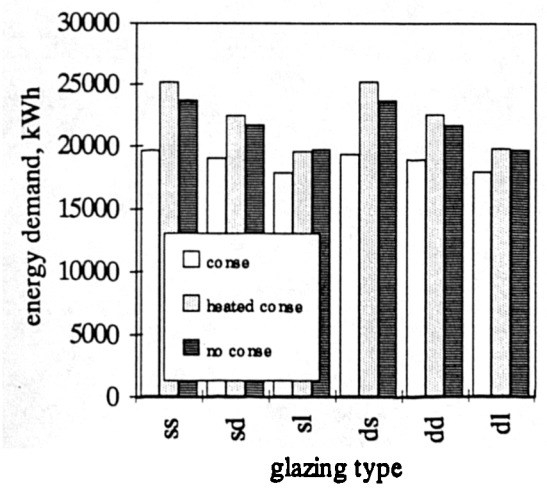

Figure 9.33:

Total annual energy demand of a dwelling with unheated semi-enclosed conservatory (conse); heated semi-enclosed conservatory (heated conse) or without conservatory, but with heated living-space (no conse)

(see Fig 9.32 for key)

The heating energy demand of the case "no conse" was in most cases lower than that of the cases "heated conse" (Fig. 9.33). However, the differences were lower than 5%, and therefore probably below the Resolution of the DSM. In practice, a small energy increase of 5% may be worth it to have a heated conservatory (with glazed ceiling) rather than a typical room with an opaque roof.

The trends for the energy demand of the dwelling with the unheated semi-enclosed conservatory, were very close to those for the attached conservatory (compare Fig. 9.32 and 9.33). However, the differences due to different glazing types were more pronounced. For the unheated semi-enclosed conservatory, the energy demand of the dwelling decreased by 7% as the external conservatory glazing was changed from single to low-emittance glazing (Fig. 9.34). For the attached conservatory the decrease was 4%. The partition window type had little impact on the energy demands (variations lower than 3%).

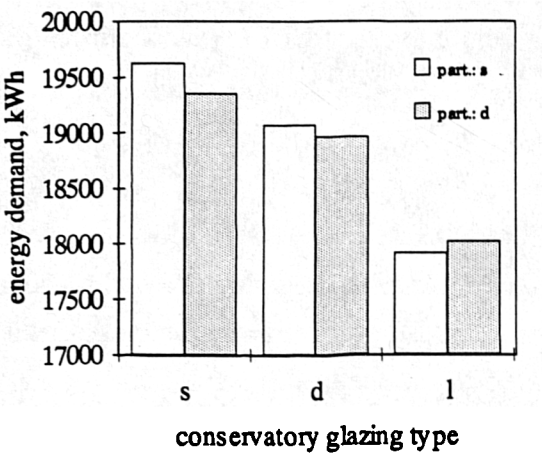

Figure 9.34:

Influence of the conservatory and partition glazing type on the annual energy demand of the dwelling with unheated, semi-enclosed conservatory.

s: single glazing
d: double glazing
l: low-emittance glazing

The total energy demand of the dwelling with the heated conservatory also decreased significantly (by 20%) as the insulation of the external glazing improved from single to low-emittance glazing (Fig. 9.33). Again, the partition glazing was unimportant (variations lower than 1%).

The time-of-usability of the unheated conservatory increased significantly as the insulation of the external window (ceiling) increased, i.e. from 0.61 (for single glazing) to 0.81 (for low-emittance glazing) (Fig. 9.35). This increase corresponds to 1280 hours per year or three and a half hours per day on average. Again, the partition window type had very little impact.

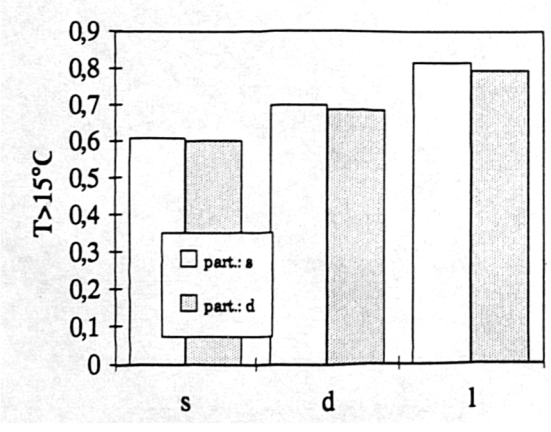

Figure 9.35:

Influence of the conservatory and partition glazing type on the relative number of occupied hours (7am - 11pm), for which the air temperature in the semi-enclosed conservatory exceeds 15°C.

(see Fig. 9.34 for key)

Thus, the external glazing type has a big impact on the energy demands of a dwelling with a (heated or unheated) semi-enclosed conservatory, and the usability of the conservatory, while the influence of the partition glazing type is generally marginal.

When the annual energy demand is compared as a fraction of usable floor area (annual time-of-usability × conservatory floor area + floor area of heated living-space) the dwelling with a single glazed unheated conservatory had an energy demand of 154 kWh/m², while the dwelling without conservatory but with a single glazed façade (case "no conse") had 164 kWh/m². Similarly, the dwelling with a double glazed unheated conservatory had 148 kWh/m², while the dwelling with double glazed facade had 151 kWh/m². The dwelling with a low-emittance glazed unheated conservatory had 140 kWh/m², while the dwelling with low-emittance glazed facade had 137 kWh/m². Hence, with regard to the pure energy demand per m² of usable living-space, there was only a small difference between an unheated semi-enclosed conservatory or a heated living-space (without glazed roof).

The time of overheating in the semi-enclosed conservatory was very low. (It corresponded approximately to that of an attached conservatory with an opaque roof, see section 9.8.2). The value of T>27°C increased from 0.02 to 0.05 as the insulation level of the external glazing was increased. Again, the influence of the partition glazing was low.

9.11.4 Corner conservatory

The result trends concerning energy demand of the dwelling and the time of usabilities of the unheated conservatory as the glazing type was varied were the same as for semi-enclosed conservatories. Similarly the predicted heating energy demands (for unheated or heated conservatory) differed in most cases by less than 5% from those predicted for semi-enclosed conservatories. These results are below the Resolution of the DSM and therefore not discussed in detail here (see section 9.11.5).

It should, however, be noted that the time-of-usability of an unheated corner conservatory was lower than that of a semi-enclosed conservatory. It was 0.55 for single glazing (semi-enclosed conservatory 0.61), 0.63 for double glazing (semi-enclosed conservatory 0.70) or 0.75 for low-emittance glazing (semi-enclosed conservatory 0.81).

9.11.5 Comparison of conservatory performance

To compare the different characteristics of attached and integrated conservatories more clearly, the results of the base-case conservatory (double glazed external glazing and double glazed partition) for all three conservatory types (semi-enclosed; corner; attached) were plotted (Fig. 9.36 and Fig. 9.37).

It can be seen, that the unheated, semi-enclosed conservatory and the unheated, corner conservatory had a similar impact on the energy demand of the adjoining dwelling. The un-

heated, double glazed, corner conservatory reduced the energy demand by 17% (related to a dwelling with south and east glazed façades), while the semi-enclosed conservatory offered an energy saving of 12% (related to a dwelling with purely south glazed façades) (Fig. 9.36). The attached conservatory led to an energy saving of 2%.

The energy demand for heating a conservatory decreased as the integration with the building increased (Fig. 9.36). It decreased by 13% from attached conservatories to corner conservatories and by 5% changing from corner to semi-enclosed conservatories. Thus, compared with attached conservatories, enclosed conservatories are less critical concerning their heating.

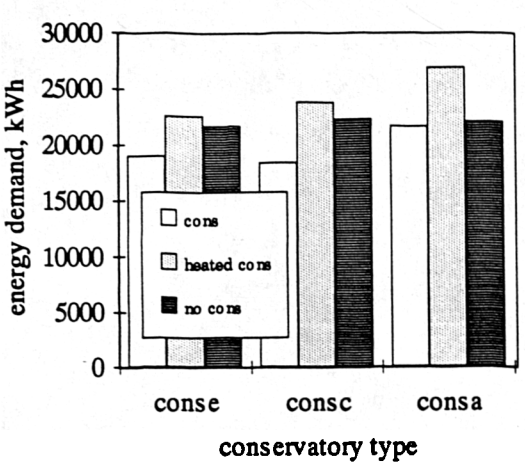

Figure 9.36:

Influence of the conservatory type on the total annual energy demand of a dwelling with an unheated conservatory (cons); heated conservatory (heated cons) or without conservatory, but with heated living-space (no cons).

conse: semi-enclosed conservatory
consc: corner conservatory
consa: attached conservatory

The time-of-usability increased (from a T>15°C value of 0.60 to a value of 0.68) as the integration into the building increased (the external glazing area decreased) (Fig. 9.37). Since the average annual air temperature in the conservatory is higher, integrated conservatories are more effective collectors for use in SPV systems than attached conservatories. Integrated conservatories also border more spaces and thus offer greater potential for ventilating these spaces with pre-heated conservatory air. In addition, the operation of SPV can be more easily achieved without mechanical support (e.g. by fans).

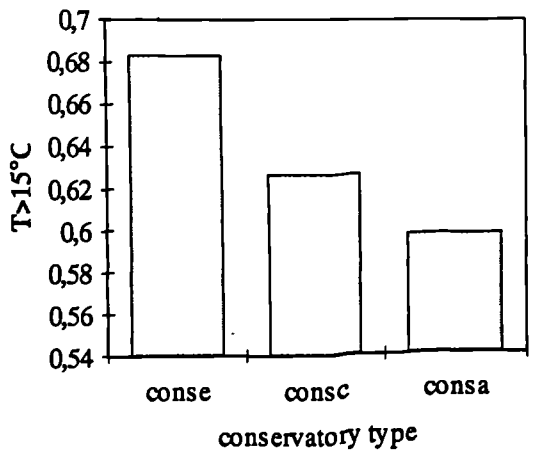

Figure 9.37:

Influence of the conservatory type on the relative number of occupied hours (7am - 11pm), for which the conservatory air temperature exceeds 15°C.

(see Fig. 9.36 for key)

While the unheated attached conservatories increase the usable living-space (at least for a limited time), integrated unheated conservatories reduce the usable living-space. When the energy demand is compared as a fraction of usable floor area (annual time-of-usability × conservatory floor area + floor area of heated living-space) the dwelling with attached (double glazed) conservatory had an energy demand of 143 kWh/m², while the dwelling with (double glazed) semi-enclosed conservatory had 148 kWh/m² (corner conservatory 144 kWh/m²). Hence, with regard to the pure energy demand per m² of usable living-space there was not a great difference between integrated and attached conservatories.

9.12 COMPARISON WITH PREVIOUS RESULTS

In section 9.3 previous conservatory design studies were reviewed and their statements were compared. It is worth trying to compare these statements with the simulation results found in this study (section 9.7 - 9.11).

An attempt has been made to relate the estimated energy savings, due to adding an unheated conservatory to a building, to the building and conservatory types (Table 9.4). Only the investigations, presented in section 9.3, for which the main important building parameters are known, are considered.

Number: Source (and date)	House floor area, m²	Cons. floor area, m²	Partition area, m²	Annual heating energy demand, kWh[1]	SPV	cons. glazing type	Saving, kWh per year	rel. saving %
1: Yannis (1994)	110	8.6	?	3534	yes	double	900 -1000	25 - 28
2: "	110	8.6	?	3534	no	double	530 - 600	15 - 17
3: Baker (1985)	95	?	11.6	6675	yes	single	1000	16
4: "	95	?	11.6	6675	yes	double	1400	21
5: Hauser (1984)	88	24	28	11765	yes	single	2000	16 - 17
6: BINE (1991b)	82	10.6	16.3	13920	no	double	1670	12
7: Section 9.7.1	16	12	14	4280	no	double	580	14
8: Section 9.11.2.	72	12	20.8	22030	no	double	450	2

[1] without conservatory

Table 9.4: Energy saving estimates of attached, unheated conservatories in different sources.

A comparison of the different investigations must be done keeping the following limitations in mind:

(i) the building types, floor areas, and operation patterns are very different;

(ii) dwellings number 5 and 6 were located in Germany, while all the other dwellings were located in the UK (Kew or Sheffield);

(iii) many important building and conservatory design parameters (such as the partition window area and type) were unknown; and

(iv) the basic assumptions for the use of SPV (e.g. ventilation rates) were not always known.

(v) the result for building 6 was measured, whilst all the other results were obtained by simulation.

It was assumed that it is better to compare the absolute energy saving estimates (in terms of kWh/year) than the relative energy saving estimates (in terms of % of the total heating energy demand), since absolute savings are approximately independent of the total heating energy demand of the parent building (see section 9.8.1). But it is important to emphasise that the absolute energy savings are still highly dependent on the conservatory size and its coupling with the parent building (covered partition wall and window area). In addition, the absolute energy savings for buildings which use SPV are higher than for those which do not.

The two buildings, investigated in this study, the two-storey dwelling (section 9.11.2; number 8) and the living-room (section 9.7.1; number 7), can be best compared with the dwellings number 2 and 6. None of these buildings had SPV and they all had double glazed conservatories. The following relationships are apparent:

- dwellings 7 and 8 had similar absolute energy savings (for an explanation of the small differences, see section 9.11.2);
- the absolute energy savings for dwellings 7 and 8 are similar to those for dwelling 2 (which were obtained by simulations using the program SERI-RES); and
- the absolute energy savings for dwellings 7 and 8 (and 2) are clearly lower than those for dwelling 6 which were obtained by field measurements. It should be noted however, that dwelling number 6 was located at the foothills of the Alps in Germany (Rosenheim, Bavaria). This area is famous for its unusually long sunny weather periods. This diminishes the significance of this comparison.

A comparison of the dwellings 7 and 8 with the dwellings 1, 3, 4 and 5 is more difficult, because these dwelling consider the energy savings due to SPV. It was concluded in section 9.10 that, if the ventilation heat loss is half of the total heat loss of the building, the energy benefits of using SPV can be up to 20% - 25% of the building's energy demand. Thus, the absolute energy savings of dwellings 7 (with the extra benefit of SPV) would probably be something between 580 kWh/year and 1650 kWh/year. Assuming that the ventilation heat loss of dwelling 8 is not more than a quarter of the total building's heat loss, the absolute energy savings for dwelling 8 would be between 450 kWh/year and 3200 kWh/year. These ranges of energy savings would encompass the absolute energy savings obtained for all the other dwellings (1, 3 and 4) except of dwelling 5 which shows (compared to dwelling 7)

higher absolute energy savings. These high absolute energy savings could be a consequence of its very large partition area (28 m^2) and of its location (Germany). An investigation (section 9.6) showed that German locations and climates produce approximately the same relative energy savings as UK locations and climates, but slightly higher absolute energy savings.

It would have been interesting to compare the information in each source about the usability of conservatories, their susceptibility to overheating, and their energy demands when heated. However, none of the previous studies commented on their energy demand when heated and the information about the usability of- and comfort in- conservatories (see section 9.3) was too weak to permit satisfying comparisons.

These comparisons are not meant as a validation of any of the investigations. Rather, these comparisons show that, although the energy savings obtained are quite different, the new simulation results do not essentially contradict the previous results. All the investigations agree that an unheated, attached conservatory offers some energy savings. It was felt however, that the new, rigorous, conservatory simulations gave more detailed, and more accurate information, about the consequences of conservatory design than previous studies.

9.13 OBSERVATIONS ABOUT CONSERVATORY DESIGN

The following design observations summarise the important results for the conservatory design study (sections 9.7-9.11). Although the results were obtained for certain building arrangements and certain building operation patterns, it is likely that the massages are valid for typical UK and German dwellings with conservatories.

9.13.1 Performance of an attached, unheated, south-facing conservatory

a) Annual heating energy demand

(i) For a south-orientated direct-gain space, the annual solar radiation energy gains through double glazing, are on average, nearly equal to the heat losses through the glazing. Therefore, the net annual energy balance of the glazing is virtual zero. All other passive solar measures (triple glazing, quadruple glazing, low-emittance glazing, or a conservatory) lead to net energy gains.

(ii) The addition of a double glazed and unshaded south-facing conservatory reduces the annual energy demand of a double glazed room by about 14% (580 kWh/year). The same reduction could be approximately achieved by replacing the double glazing with quadruple or low-emittance glazing. However, the energy benefits of a conservatory of the same size would be small, compared with the energy demands of a whole building, (possibly lower than 2%). If low-emittance (or quadruple) glazing was used for all the south-facing windows in a house, the benefits (compared with double glazing) would still be 10% to 15%. In practice, therefore, passive solar houses are likely to be basically direct-gain designs.

(iii) Conservatories are added for their amenity value. Unheated conservatories offer extra living-space without an increase of the energy demand.

(iv) The addition of an unheated south-facing conservatory to a double glazed room reduces the energy demand throughout the year. The savings occur in winter, spring and autumn and, for rooms which are heated in summer, in summer also.

b) Usability

(i) The usefulness of a conservatory as a habitable room is greatest during the transitional period (spring, autumn). During this time a double glazed conservatory is four times more usable than an open-air garden. During summer, the external temperatures are generally higher, which reduces the relative benefits of a conservatory. While there is no possibility of living in the open-air in winter, the conservatory offers a small time period (10% - 20% of the hours between 7am and 11pm, which is approximately 2 to 3 hours per day on average), for which the air temperature is higher than 15°C.

(ii) The annual time-of-usability for an unheated double glazed conservatory is about 60% of the hours between 7am and 11pm. During this time, the average temperature in the conservatory exceeds the external air temperature by between 4 K and 11 K.

c) Heating an attached, south-facing conservatory

(i) The energy demand for heating a conservatory increases exponentially with the heating setpoint. It increases significantly for nighttime heating. The annual heating to produce an internal air temperature of 21°C (from 7am to 11pm) was much greater than the energy demand of a modern, well-insulated room. In comparison, restricted heating of a conservatory to under 10°C, is not very energy intensive and may be useful to protect plants. However, restricted heating to a setpoint lower than the comfort temperature, does not improve the time-of-usability.

(ii) To extend the habitable living-space, designers should choose a traditional construction instead of a conservatory. A conservatory should be an unheated space occupied adventitiously when its temperature makes this possible.

9.13.2 Influence of attached conservatory and dwelling design on performance

a) Construction of adjacent room

(i) For traditional poorly-insulated living-rooms, improvement in the levels of insulations can offer annual energy savings of up to 50%. By comparison, passive solar systems reduce the heating energy demand of the room by less than 15%. For energy saving purpose, it is therefore much more favourable to increase the insulation level of a room, before installing passive solar systems such as highly-insulated glazings or conservatories.

(ii) The reduction of energy demand due to adding an unheated south-facing conservatory to a room is independent of the insulation level (average U-value) of the room. The dwelling's construction mode has nearly no influence on the internal temperatures in the conservatory.

b) Shading a conservatory (with opaque panels)

(i) Opaque side-walls only marginally influence: the heating energy demand of the space attached to the (unheated) conservatory; the time-of-usability; and the amount of overheating in the conservatory. They reduce the energy demand if the conservatory becomes heated (by about 11%). For terraced houses with conservatories opaque side-walls may also be useful to increase privacy.

(ii) Opaque highly-insulated roof elements, significantly reduce the peak temperatures in the conservatory. Problems of overheating nearly disappear and the usability of the

space in the evening is increased. However, if the opaque roof shades the adjacent room from direct radiation, it increases its energy demand. Conservatory roof shading also unfavourable reduces the lighting level in the adjacent room, which is likely to be unwelcomed since the levels have been already reduced by the conservatory construction. In addition, the reduced lighting levels in the conservatory could have a negative effect on the growth of plants.

(iii) For the energy saving potential of an unheated conservatory to be realised, the transfer of radiation across the conservatory into the adjoining living-space is crucial. Any shading of the direct radiation into the living-space (e.g. by an opaque conservatory ceiling) reduces the energy saving potential of the conservatory. The heating energy demand of a totally shaded adjacent room (with conservatory) is similar to that of a double glazed direct-gain room. Hence, in the worst case, the energy benefits of an attached conservatory disappear completely.

c) Conservatory and partition glazing type

(i) The glazing type (clear single or double glazing) of the conservatory and of the partition window has virtually no influence on the energy demand of a room behind an unheated conservatory.

(ii) If low-emittance glazing is to be used for either the conservatory or the partition window, it is better to place the low-emittance glazing on the outside. The partition glazing is less important but more transparent partition glazings (i.e. single glazing) lead to reduced energy demands and improvements in the lighting of the living-space.

(iii) The time-of-usability of the conservatory increases as the insulation level of the conservatory glazing increases. Low-emittance glazing for the conservatory leads to the highest time-of-usability (73% of the hours between 7am and 11pm). In addition it reduces the heating energy expenditure, if the conservatory is continuously or intermittently heated.

d) Area of partition glazing

(i) From the energy saving point of view, it seems preferable to have big partition windows between the conservatory and the adjacent space.

(ii) Big partition glazing areas improve the lighting of the adjacent space. However, to prevent the living-space overheating, it is valuable to have manually operated shading devices on the partition windows (curtains or blinds).

e) Conservatory size

(i) Small unheated conservatories are comfortable more often than large conservatories.

(ii) The size of an unheated conservatory does not affect the energy demand of the adjacent living-room, provided the partition area remains unchanged.

(iii) Big heated conservatories use less energy per unit floor area to maintain comfort, than do similar small conservatories.

f) Conservatory thermal storage mass

(i) The storage mass in an unheated conservatory only marginally influences the energy demand of the adjoining room. Similarly, the storage mass has little impact on the energy demand of a heated conservatory.

(ii) Whilst the time-of-usability was only marginally improved by adding storage mass, it did improve the protection offered to plants against cold and frosty weather. Storage mass in the conservatory also reduces the space temperature variations, reduces overheating and increases the temperature level in the evening and night.

(iii) A storage mass of about 9 cm of concrete in the floor appears to be optimal but extra mass is not detrimental.

g) Surface reflectances

(i) The reflectance of surfaces in the conservatory has only a marginal influence on the thermal conditions in the conservatory and the adjacent room. The choice of the surface colour is more likely to be dictated by other issues like aesthetics or the choice of materials.

h) Partition wall-type

(i) The insulation level (U-value) of the partition wall has little influence on the operation of the conservatory, it is not an important factor in conservatory design. It may be tempting therefore, to reduce the costs of a new building by reducing the U-value of the partition.

9.13.3 Attached north-facing conservatories

(i) When a building permits, it is better to direct glazings towards the south, while keeping north glazings as small as possible. However, the energy saving produced of an unheated, double glazed conservatory on a north-facing wall is about the same as on a south-facing wall.

(ii) Compared with highly insulated (quadruple, low-emittance) glazings, an unheated, double glazed north-facing conservatory produces bigger energy savings in the adjacent space.

(iii) The time-of-usability of a north-facing conservatory is clearly lower than that for a similar south-facing conservatory (e.g. 50% of the time between 7am and 11pm compared to 62% of the time)

(iv) North-orientated conservatories very rarely exhibit overheating problems - this may be advantageous for temperature sensitive plants. In addition, it makes its operation very simple and cheap (no costly shading or ventilation devices are necessary).

9.13.4 Two-storey building with conservatories

(i) Unheated, semi-enclosed and corner conservatories, have a similar impact on the energy demand of the adjoining dwellings.

(ii) By replacing a heated living-space in a dwelling by an unheated, double glazed two-storey semi-enclosed or corner conservatory, the energy demand of the whole dwelling is reduced by 12% to 17%. In comparison, attaching a conservatory onto the outside of the dwelling produces energy savings which may be lower than 2%.

(iii) Semi-enclosed conservatories and corner conservatories have higher usabilities (for double glazed conservatories up to 70% of the annual hours between 7am and 11pm) than attached conservatories (60%). However, while the attached conservatories increase the usable living-space (at least for a limited time), semi-enclosed and corner conservatories reduce the usable living-space. With regard to the annual energy demand per m^2 of usable living-space there is virtually no difference between integrated (semi-enclosed or corner) and attached conservatories.

(iv) The glazing used in the conservatory has a large impact on the energy demand of the adjoining building and the usability of the integrated conservatories. In contrast, the influence of the partition glazing type is generally marginal. The time-of-usability increases as the insulation level of the external glazing increases. The energy demand of the adjoining building decreases as the insulation level of the external glazing increases.

(v) Compared to attached conservatories, integrated conservatories are less critical concerning their heating. The energy demand of a heated integrated conservatory is comparable with that of a similar direct-gain space.

(vi) The frequency of overheating in integrated conservatories is low.

9.13.5 Solar pre-heating of ventilation air (SPV)

(i) By using pre-heated air from the conservatory to ventilate the adjoining living-space (SPV), the energy used to heat ventilation air can be reduced. For a modern one- or two-storey dwelling, a double glazed conservatory can reduce the ventilation energy

demand by 40% - 50%. If all the ventilation air is recovered by the conservatory (best case) and the ventilation heat loss is half of the total heat loss of the adjoining house (modern highly-insulated dwelling), SPV offers a maximum energy saving of about 20% to 25%. In comparison, a conservatory, which acts only as a solar heated buffer space, reduces the energy demand of the whole dwelling by less than 10% to 15%. This reduction could be as low as 2% for some conservatory and dwelling designs.

(ii) If SPV can only be used to recover the ventilation air for those rooms, which directly adjoin the conservatory, the saving of 20% to 25% refers only to the heating energy demand of the adjoining rooms.

(iii) Since the average annual air temperature in the conservatory is higher, integrated conservatories are better suitable for the use of SPV than attached conservatories. In addition integrated conservatories border more spaces and thus offer greater potential for ventilating these spaces with pre-heated conservatory air.

(iv) The energy savings by using SPV can be further improved by using low-emittance glazing instead of double glazing for the conservatory.

(v) South-orientation of the conservatory is clearly better for SPV than north-orientation.

CHAPTER 10

CONCLUSIONS AND SUGGESTIONS FOR FUTURE WORK

10.1 CONCLUSIONS

This Chapter summarises the conclusions which can be drawn from the pieces of work outlined in Chapters 4 to 9.

10.1.1 Diffuse radiation transfer

i When modelling glazing, the transmittance and absorptance of the diffuse radiation are normally taken as the values for the direct transmittance and absorptance at an incidence angle of 60°. This value appropriately represents the diffuse radiation conditions on vertical clear glazings. In the cases of non-vertical windows or special glazing, this value is inaccurate.

ii Existing, but more accurate models of diffuse radiation neglect either, the dependence of the diffuse transmission on the surface inclination, or, the specific incidence angle dependent transmission behaviour of the glazings. No model could be found which considered real sky and ground radiance distributions.

iii A new technique has been developed, which calculates the glazing transmittance and absorptance for diffuse sky radiation. The technique has been produced as a program (GLSIM-DIF). It generates values which can be fed directly into DSMs.

iv GLSIM-DIF considers: the radiance distribution of the sky (overcast or clear); the ground reflected radiation; the inclination and orientation of the glazings; the glazing type; the time of day; and the season. The sky models used are the standard, anisotropic, CIE-radiance distributions of DIN 5034.

v For windows in built-up areas (e.g. in city centres), or in other places where there is a high horizon (e.g. in a valley), the influence of obstructions on the diffuse radiation transfer can become considerable. Within GLSIM-DIF the problem was solved by assuming that the radiance of the obstructions corresponds to that of the ground.

vi On overcast days, the diffuse transmittance and absorptance values predicted by GLSIM-DIF depend on the surface inclination, the ground reflectance, and the glazing type. The dependence on the surface inclination is very pronounced. The

diffuse transmittance, and therefore the predicted diffuse radiation energy transmission, varies by up to 10% as the surface inclination is varied.

vii The accurate definition of the diffuse glazing properties is essential for inclined surfaces on overcast days. Inclined glazings are used for conservatories, atria and glazed halls. Programs to predict the environmental conditions in such spaces should take advantage of the improved diffuse radiation properties for glazings.

viii On clear days, the diffuse transmittance and absorptance depends on the time-of-day and the season. However diffuse radiation transfer is usually swamped by higher energy directly-transmitted radiation. Hence, any inaccuracies in the clear-day diffuse glazing properties, hardly effects the inside climate. Hourly values for the diffuse glazing properties appear to be unnecessary on such days. Instead, daily effective glazing properties could be used. A method of calculating these has been explained.

ix Annual simulations require the distinction between clear and overcast sky conditions. DSMs can use a cloud-cover statement to switch from clear to overcast diffuse glazing properties or to interpolate between them.

10.1.2 Radiation transfer through special glazing

i DSMs normally calculate the radiation transfer through glazings using the incidence angle dependent transmittance and absorptance values. In the case of clear glazing these values can be easily predicted from the Fresnel equations. For special glazing however (coated, low-emittance, or sun-reflective glazing, and absorbing tinted glazing) these values are usually unknown.

ii The derivation of more accurate properties for special glazing requires: a calculation technique which considers thick layers (glass panes) as well as thin layers (coatings); the detailed optical constants of the glass panes and coatings; and the information about the structure of the glazing systems. No calculation technique was found, which offered an appropriate solution and which considered all these points.

iii A program GLSIM-FILM has been produced which is capable of predicting the variation of solar transmittance and solar absorptance with wavelength, and the variation of transmittance and absorptance with the angle of solar incidence, for any type of glazing system.

iv The calculations were based on multiplying matrices rather than a recursive technique. They are applicable to any combination of coating and glass with no limitation on the number or sequence of the layers.

v A database of the most important (clear and tinted) glass panes, absorbing noble metal films (gold, silver, copper) and dielectric films (metal oxides, metal sulphides) has been created and incorporated within the program GLSIM-FILM.

vi Strategies have been developed for calculating the variation of the relative transmittance with the angle of incidence using standard published manufacturers' data. These strategies are applicable to glazing systems of clear, or tinted glass, or systems incorporating a single noble metal layer, multiple layers of noble metal and dielectric (metal oxide) films, or glazings with pure dielectric coatings.

vii The predictions of the program compared favourably with published measured data for glazing systems. However, the limited data which was available gave incomplete descriptions of the glazings and no estimates of the measurement uncertainty were given. Further data to evaluate this software would be useful.

viii GLSIM-FILM is valuable as a pre-processor for dynamic thermal simulation programs. It enables them to produce more accurate predictions for buildings with special glazing.

ix The clarity afforded by the matrix formulation enables different glazing systems to be quickly modelled. The equations can be quickly solved on a PC. GLSIM-FILM therefore offers a cost-effective route to generating a database of glazing properties which could be used by detailed thermal simulation programs.

x The improved calculation technique indicated that the conventional Fresnel-based approach (valid for clear glazing) is not sufficiently accurate for coated and tinted glazings. The incidence angle dependent transmittances of such special glazings are shown to be considerably different from those for clear glazing.

xi It has been shown that the conventional method could lead to significant under-, or over-estimating of the annual heating and cooling energy demands of buildings. Such errors occur in both extreme continental, and temperate, climatic regimes.

xii Simulations using HTB2 demonstrated that the wrong decision may be made concerning the best type of glazing to choose, if clear glass properties are adopted for special glazings (conventional method).

xiii The results of detailed thermal simulation programs which use simple Fresnel-based recursive calculations to generate glazing transmission properties (valid for multi-layered systems of clear glazing) should be interpreted with caution.

xiv The predicted maximum cooling power needed in a small office has been shown to be influenced by the glazing calculation method. In some circumstances, the conventional method could lead to an under-sizing of the cooling equipment.

10.1.3 Total solar energy transmittance

i In simplified thermal models of buildings, the total solar energy transmittance and the thermal transmittance (U-value) are the energy related properties which are used to describe the thermal impact of a glazing system.

ii The conventional total solar energy transmittance for normal radiation incidence, which is used in many international standards and quoted by glazing manufacturers, is higher than the value which is obtained in practise (for non-normal radiation incidence). The use of this value for the calculation of heating or cooling energy demands or heating and cooling powers can lead to an over-estimation of the solar energy contribution.

iii Monthly and/or annual effective total solar energy transmittance values were introduced. These values were calculated by a new computer module GLSIM-TOT, which integrates the total amount of radiation entering a space over the appropriate time-frame. It uses hourly solar radiation data and the known solar radiation transmittance and absorptance characteristics of the glazings.

iv The monthly effective total solar energy transmittance values were shown to be considerably lower than the values for normal incidence. In addition, they were strongly dependent on the season, window orientation and window inclination.

v For clear glazing systems exposed to typical German solar data, the effective annual reduction of the conventional value for normal incidence was found to be about 0.85. This reduction factor was accepted in the latest German heat protection law (WärmeschutzVO 1993) and in DIN 4108 (1993).

vi The conventional (producer quoted) total solar energy transmittance values were not accurate enough to show the thermal differences between two glazing systems. The newly introduced, climate and location dependent, annual effective total solar energy transmittance values, indicated the imposed heating and cooling trends correctly and permitted a more accurate calculation of cooling and heating demands.

vii The introduction of annual effective total solar energy transmittance values can further improve the characterisation of special glazings.

10.1.4 Radiation transfer through slat-type blinds

i There are well known modelling methods for frames, side fines, overhangs and obstructions, and these are implemented in many DSMs. There are, however, no calculation methods for slat-type blinds. So it is not possible to accurately simulate blind systems.

ii None of the current standardised or producer quoted time-fixed shading factors meet the requirement of DSMs, which usually need the net-reductions of the different radiation components (transmitted or absorbed, direct or diffuse). Moreover, none of the given values consider the time-dependent changing of the shading as the beam radiation incidence angle varies.

iii A pre-processing program GLSIM-BLIND has been produced which is capable of predicting the necessary input values for DSMs to accurately simulate blind systems.

iv The theory upon which the computer module GLSIM-BLIND is based, was developed for quick calculation. Therefore, analytical solutions were preferred before time-consuming numerical procedures or ray-tracing techniques. Although the algorithms were realised in a pre-processing program, they are also appropriate for implementation directly into thermal programs.

v The radiation transfer through a blind and glazing system is calculated by considering: the unshaded transmittance of the direct beam; the reflected direct beam at the slat surfaces (the reflectance may be pure diffuse, pure specular or any combination between these); the unshaded transmission of the diffuse radiation; and the reflected diffuse radiation at the slat surfaces.

vi The program works for any orientation, window inclination angle, slat width, slat distance, slat inclination angle, slat colour, and slat material (shining factor). The slats may be located at the outside (external blinds) or at the inside (internal blinds) of the glazing. At present, GLSIM-BLIND can only model horizontal slats.

vii The theory considers the inter-reflections between the slats and between the glass pane and the slat. The transmittance through glazing at the inner side of external blinds is treated by considering the incidence angle of the directly received radiation and the radiation reflected from the slats. It has been shown that the significance of the radiation incidence angle should not be under-estimated.

viii The effect of curved slats is approximately considered, however, an investigation showed that, for normal blind geometries, the influence of the slat curvature is negligibly small. For most practical cases it seems acceptable to assume that the slats are flat.

ix GLSIM-BLIND is able to model different manual, or automatic, slat control strategies.

x The predictions of the program compared favourable with the available measured and calculated data for blind systems. Further data to evaluate this software would be useful.

xi For a dynamic treatment of blinds, GLSIM-BLIND produces the incidence angle dependent transmittance and absorptance values of a blind/glazing system. These can be used directly as an input to DSMs. The values depend on the date and the geographical latitude of the site.

xii The program can calculate effective (annual or monthly) total solar energy transmittance values or shading factors for blinds. These values can replace the conventional standard values currently used for quasi-stationary calculations of heating and cooling demands (or loads) or by simpler DSMs such as SERI-RES.

xiii By using daily effective blind properties rather than incidence angle dependent properties (dynamic blind treatment) the amount of data needed can be reduced. For investigations of the thermal conditions in rooms with shaded south-facing glazing the use of daily effective blind properties is sufficient. However, for east- and west-facing rooms, a rigorous dynamic treatment of blinds yields more accurate results.

xiv Annual effective shading factors are not suitable for daily or seasonal investigations of the environmental conditions in rooms with shaded south-facing glazing. They may however be useful for comparing, or ranking, different blind systems, or for approximate thermal calculations. They appear to be more accurate than the conventional (fixed) standard shading factors.

xv For GLSIM-BLIND to be most effective, the treatment of the radiation energy absorbed by internal blinds is also important. DSMs which use a rigorous solar-to-air approach are preferred to those which adopt a simplified treatment in which the absorbed radiation is added to the radiation incidence on internal surfaces.

xvi The clarity afforded by the analytical formulations enables different blind systems to be analysed quickly on a PC. GLSIM-BLIND therefore offers a cost-effective route to generating a database of blind properties which could be used by DSMs.

xvii GLSIM-BLIND can be used to investigate, compare, and optimise blind arrangements during the design phase of a building.

10.1.5 Internal solar radiation distribution

i A significant weakness of the current solar distribution models within DSMs is that the programs require the user to input the relative amounts of direct solar radiation falling on the various interior surfaces. The direct radiation distribution is normally assumed to be fixed over the whole simulation period. In the case of highly glazed spaces, the internal solar radiation distribution depends strongly on the time-of-day, the season of the year, and the sky conditions.

ii The DSMs usually calculate: the internal distribution of the diffuse radiation; the distribution of the reflected radiation around the internal surfaces; the radiation re-transmission; the radiation backloss; and the interzonal radiation transfer. However, the models used are normally crude approximations. For example, none of the DSMs reviewed ESP, HTB2 and SERI-RES could model the immediate loss of direct radiation (re-transmission).

iii The consequences of using simplified internal solar distribution models on the predicted air temperatures in a conservatory, and on the energy demand of an adjoining living-room, were investigated. The different, simplified, solar distribution models produced marked variations in the absolute predictions and, more seriously, different trends as the design of the building changed. Credible design conclusions for the test building with a conservatory could not be derived from the DSM predictions.

iv Existing, more detailed solar distribution programs, were reviewed, ESP-INS, ATRIA and the TRNSYS sunspace model. These programs were either incapable of accurately simulating highly glazed spaces or they were unable to work in connection with more than one particular DSM. They could not therefore solve the solar *distribution problem in highly glazed spaces* for a wider number of DSMs.

v An investigation showed that daylight programs (such as SUPERLITE and RADIANCE) are unsuitable for produce the necessary solar distribution values required by DSMs. A linkage between daylight and thermal programs appeared to be difficult. Daylight programs calculate the detailed lighting levels on internal surfaces, while DSMs usually need one value for the absorbed radiation on each surface. In addition, daylight programs predict the internal distribution for certain fixed sky conditions, while DSMs need the dynamic distribution for each hour of the day.

vi A new geometric solar distribution model, called SUNSIM, which considers all the important aspects of dynamic internal radiation distribution (including radiation re-transmission, radiation backloss, and interzonal radiation transfer) was created. It produces the hourly absorbed radiation energy quantities for all internal surfaces for the whole simulation period. In this way, the solar processing is totally separated from the thermal processing.

vii The solar distribution program SUNSIM can model one room, which is enclosed by any number of opaque or transparent planes. The room can be attached to a building (like most conservatories) or it can be totally embedded (like many atria). To simplify the definition of certain room geometries, a pre-processing program GEOSIM was created which permits the automatic digitising of the room's geometry. At present six distinct room shapes are offered: rectangular room with flat roof; pent roof; gable roof; hipped roof; barrel roof; or round room with domed roof.

viii SUNSIM uses a matrix solution method which produces a mathematically complete simulation of all inter-reflections in the room without any limitation on the number of reflections. The solution method considers very accurate view factors between all the surfaces.

ix SUNSIM is independent of a particular DSM. For demonstration and testing purposes, a new interface was created which allows its connection with HTB2.

x Since SUNSIM does not use empirical relationships (except those for the standard sky models) the validation was restricted to a code debugging task. (The correct reproduction of the sky models was tested by inter-model comparisons with HTB2.)

xi The simplified solar distribution models (as typically used within DSMs) and the improved model, SUNSIM, were compared in a sensitivity study. The predicted differences, in the conservatory peak air temperatures and the energy demands of the adjoining room, confirmed the need for a rigorous treatment of solar distribution. The simplified models predicted daily heating energy demands, which were between 30% and 200% too high. The error in the predicted conservatory peak air temperatures was sometimes more than 5 K (in the temperature range between 20°C and 30°C). This is clearly to high for reliable comfort assessments.

xii Using SUNSIM, the specific effects of interzonal radiation transfer could be investigated. The treatment of interzonal radiation transfer had a significant impact on the predicted peak air temperatures in conservatories and the energy demands of adjacent rooms. The neglect of interzonal radiation transfer (as is often done by DSMs) led to an incorrect assessment of the effect of the internal glazing (between the conservatory and the adjacent room).

xiii Using SUNSIM, the specific effect of not modelling radiation re-transmission and backloss could be studied. It was shown that radiation loss is an important aspect, which can have a marked impact on the predicted internal air temperatures in conservatories. It also affected estimates of the energy demands of adjacent spaces. Reliable comfort predictions for highly glazed spaces are only possible when radiation losses are accurately considered.

xiv SUNSIM can not replace the internal solar radiation distribution routine of a DSM. However, it is a very useful tool for simulating one particular highly glazed space, such as a conservatory or atrium, within a complex, multi-zone, building.

xv Since SUNSIM uses numerical procedures, the calculation time is relatively long. However, it is possible to simulate different building designs which have the same highly glazed space rapidly because it is only necessary to calculate the solar distribution once.

10.1.6 Application of improved modelling methods to the study of conservatory designs

i Many previous design guidelines for conservatories were derived from DSM predictions. However, the sensitivity studies conducted within this work have indicated that the approximate methods used to model glazings, internal solar distribution, and solar shading, can severely compromise the accuracy of DSM predictions. It was concluded that design studies of conservatories based on current DSM predictions (which do not appropriately consider the above modelling aspects) must be treated with caution.

ii To determine what the most important design questions might be, different conservatory studies were reviewed. Most of the research has been concerned with the potential energy savings resulting from the use of conservatories as passive solar systems. The estimated energy savings, due to adding an unheated conservatory to a building, differed markedly between the sources studied (i.e. from "very low", to 25 - 28% of the dwelling's heating energy requirement).

iii In the conservatory design guidelines found in the literature, there was conflicting (or different) information about: conservatory size; conservatory glazing type; partition (i.e. wall between house and conservatory) glazing type; partition glazing area; conservatory orientation; opaque element insulation, and the benefits of embedded (integrated) conservatories.

iv The program HTB2 was used to investigate the influence of design variations on: the usability of conservatories; the energy demand of the adjacent dwelling; and the internal comfort conditions in the conservatory. In this study all the new simulation models (for glazing, blind modelling and internal solar distribution) were used. This produces more authentic predictions than was hitherto possible.

The results of this study are summarised in the conclusions v to xvi for conservatories acting only as buffer spaces. The effects of using the conservatory to pre-heat ventilation air are considered in conclusions xvii and xviii.

v The addition of a double glazed and unshaded south-facing conservatory to dwellings reduced the energy demand of a double glazed living-room in the UK (Sheffield) by about 14% (580 kWh/year). The same reduction could be approximately achieved by replacing the double glazing with quadruple or low-emittance glazing.

vi Conservatories are added for their amenity value. An unheated conservatory offers extra living-space without an increase in the overall energy demand. The annual time-of-usability for an unheated double glazed conservatory in the UK is about

60% of the hours between 7am and 11pm, which is nine to ten hours per day on average.

vii The attachment of a conservatory to a living-room with a south-facing window yields the same relative reduction in the overall energy demand (14%) in Sheffield (UK) and North-Württemberg (Germany). In addition, the time-of-usability and the temperatures in the conservatory are similar for Sheffield and North-Württemberg. Based on these results, it is assumed that, for moderate or continental middle European climates, the thermal behaviour of a conservatory is similar. Conclusions about conservatory design based on a UK climate, could be transferred to locations and climates in Germany.

viii When a double glazed south-facing conservatory is heated to 21°C between 7am and 11pm, the heating energy demand exceeds the energy demand of a room insulated to current UK standards (325 kWh/m²). To extend the heated living-space, designers should adopt a traditional construction (with insulated opaque walls) instead of a conservatory.

ix The energy demand of a room with an attached, unheated, south-facing conservatory is virtually unaffected by whether single or double glazing is used in the conservatory and partition window. However, if low-emittance glazing should be used for either the conservatory or the partition, the lower energy demands are obtained if the conservatory is made of low-emittance glass. Low-emittance glazing also leads to the highest time-of-usability in the conservatory (73% of the hours between 7am and 11pm!). In addition, it reduces the heating energy expenditure, if the conservatory is (partly) heated.

x From an energy saving point of view, it is preferable to have a large area of glazing in the partition wall. However, the insulation level of the adjoining room, the floor area of the conservatory (for the same partition area), the thermal storage mass in the conservatory and the reflectance of the conservatory surfaces hardly influence the energy demand of the living-room or the usability of the conservatory.

xi If the side-walls of the conservatory are well-insulated and a large area of glazing is used in the partition wall, the energy demands of a heated conservatory will be reduced.

xii The energy demand for heating a conservatory when expressed as a fraction of its floor area, decreases as the conservatory floor area increases (provided the conservatory height remains the same).

xiii High ventilation rates in summer do not completely solve the overheating problem in a south-facing conservatory. Thus, additional shading devices are important. Highly-

insulated, opaque elements in the conservatory roof significantly reduce the overheating in the conservatory. However, the opaque roof elements can have an unfavourable influence on the heating energy demand of the adjacent space.

xiv In passive solar house design, it is better to direct glazings to the south, while keeping north glazings as small as possible. However, when a large north-facing glazed area is covered by an unheated, double glazed, conservatory the absolute energy savings are about the same as for the same south-facing conservatory design. In contrast, the time-of-usability of a north-facing conservatory is much lower than for one with a southerly orientation.

xv An unheated, double glazed, integrated (semi-enclosed or corner) conservatory reduces the overall energy demand of the dwelling by 12% - 17% (relative to a dwelling with a heated living-space instead of the enclosed conservatory). In comparison, an attached conservatory leads to energy savings which are possibly lower than 2% of the energy demand of a whole dwelling. Thus, unless an attached conservatory is used to pre-heat ventilation air its overall energy benefits are unlikely to be worth pursuing.

xvi Semi-enclosed conservatories and corner conservatories have higher usabilities than attached conservatories (e.g. a double glazed, integrated, conservatory may be usable for up to 70% of the annual hours between 7am and 11pm whereas the similar attached conservatory may be usable for 60% of the time). However, while the attached conservatories increase the usable living-space (at least for a limited time), enclosed conservatories reduce the usable living-space. With regard to the heating energy demand per m^2 of usable living-space there is virtually no difference between integrated and attached conservatories.

xvii By using pre-heated air from the conservatory to ventilate the adjoining living-space (SPV), the ventilation energy expenditure of a building can be reduced. If all the ventilation air is recovered from the conservatory (the best case) and the ventilation heat loss is half of the total heat loss of the adjoining house (e.g. a modern highly-insulated dwelling), SPV offers an maximum energy saving of 20% - 25%. This must be regarded as upper limitation.

xviii Since the average annual air temperature in integrated conservatories is higher than in attached conservatories, they are better suited for SPV. In addition, integrated conservatories border more spaces and thus offer greater potential for ventilating these spaces with pre-heated conservatory air. The energy saving of using SPV can be further improved by using low-emittance glazing instead of double glazing for the conservatory. South orientation for the conservatory is clearly better than north orientation.

xix The predicted energy savings, due to the addition of a south-facing conservatory to a dwelling has been compared with results of previous investigations. This comparison showed that, although the energy savings obtained are quite different, the new simulation results do not essentially contradict the previous results. All the investigations agree that an unheated, attached conservatory offers some energy savings.

10.2 SUGGESTIONS FOR FUTURE WORK

10.2.1 Radiation transfer through special glazing

i The program GLSIM-FILM, and GLSIM-DIF, can be used to generate databases of glazing properties. As a first step, the incidence angle dependent relative direct and diffuse transmittance and absorptance values of important glazing systems have been determined (Appendix C). To use these values for a particular glazing, its coating and/or glass types must be known. In addition, this method requires the user to calculate the absolute transmittance and absorptance values from the relative values, which is ponderous and time-consuming. Therefore, the database of glazing properties could be improved by replacing the relative values with the absolute transmittance and absorptance values of currently available glazings.

ii The predictions of GLSIM-FILM compared favourable with published measured data for glazing systems. However, the limited data which was available, gave incomplete descriptions of the glazings and no estimates of the measurement uncertainty were given. More reliable measured values are needed for a thorough validation.

iii So far, the theory of thin films and the program GLSIM-FILM, has been used to produce the incidence angle dependent properties for solar radiation transmittance. However, they could also be adapted to calculate the incidence angle dependent light transmittance through special glazing. These light transmittance values could further improve the accuracy of daylight calculations (in programs such as SUPERLITE and RADIANCE).

iv Effective total solar energy transmittance values depend not only on the window orientation and inclination, but also on the geographical location (latitude) and on the particular climate conditions. More work is needed to investigate the significance of these dependencies. An investigation could show to what extent the values are constant over geographical areas (e.g. over the UK; middle Europe; or all Europe etc.). The consequences of this investigation could be considered in a database of effective solar energy transmittance values. This database could improve simplified calculations of heating and cooling demands (loads) and/or internal temperatures.

10.2.2 Radiation transfer through slat-type blinds

i The theory of blind calculations outlined in Chapter 7 permits a great number of different blind and glazing systems to be simulated. Nevertheless, there are some blind configurations which cannot be modelled by the latest version of GLSIM-BLIND. These are calculations of:

- blinds between glass panes;
- blinds with vertical slats;
- special blind geometries (prismatic; honeycombed etc.); and
- blinds in connection with transparent material other than glazing (e.g. transparent insulation material).

The development and implementation of appropriate algorithms to cover such configurations would improve the scope of the program GLSIM-BLIND.

ii The incidence angle dependent or effective transmittance and absorptance values of glazing and blind systems depend on the geographical location of the site, the location of the window (orientation; inclination) and on the particular system characteristics (glazing type; slat inclination angle; slat surface colour etc.). Thus, a database of glazing/blind properties would contain a huge number of different systems. The plausibility of such a database has not been tested.

iii To calculate the incidence angle dependent radiation transfer through glass panes at the inner side of external blinds, within GLSIM-BLIND, the direct and diffuse radiation distribution behind the blinds is considered. However, the affect of the blinds on the internal solar radiation distribution in the room is not considered. This is a necessary simplification as long as blinds are pre-calculated and expressed in terms of glazing/blind input properties. As soon as blinds are incorporated into the solar calculation routine of a DSM, the consideration of internal solar distribution becomes possible. It would, for example, be useful to implement the blind algorithms into the internal solar distribution program SUNSIM and consider the consequences of blinds on the direction of the direct and diffuse radiation. This would further extend the area of application of the program SUNSIM.

iv The present treatment of blinds does not consider any thermal effects, which blinds may have on the energy transport to, and from, the outside. Often, the air gap between the glass and internal blinds is ventilated with outside air. Likewise, blinds may be located in a ventilated space between glazings. Issues of ventilation and conduction are treated separately by DSMs in the simulation of temperatures and energy flows. It would be an interesting task to try and model the thermal effects of internal or internal-glazing blinds.

v Verification of the blind modelling system was mainly done using analytical investigations during the model development process. Inter-model comparisons were however possible, by using programs which use a different (ray-tracing) technique to calculate the radiation transfer through blind systems. The measured data of one blind system was also available, but this was the only empirical validation that was possible. Clearly, further data to evaluate the software would be useful. This could be from full-scale field measurements, or from models placed outside or in artificial sky conditions. Both the solar transmission characteristics of blinds and their thermal consequences could be measured.

10.2.3 Internal solar radiation distribution

i The solar distribution program SUNSIM can simulate any convex room shapes with any number of opaque and transparent planes. However, these room geometries must be generated by a graphical computer module. A pre-processing program (GEOSIM) has been created which can generate six different conservatory and atrium room geometries. The number of possible room shapes could be extended by replacing the graphical interface, GEOSIM, by a sophisticated CAD computer program, which generates these room shapes.

ii Since SUNSIM can simulate only one zone at a time, interzonal radiation transfer across more than one glazed room can not be modelled. In addition, the detailed solar distribution in the adjacent rooms can not be modelled. More precise calculations may be possible and could be objective of further improvements.

iii SUNSIM could be further improved by implementing routines for calculating the shading effect of obstructions, trees, sky lines etc.

iv SUNSIM uses an isotropic (ISO) sky model to calculate the diffuse radiation incidence onto inclined surfaces. The program could therefore be improved by using more accurate anisotropic sky models (e.g. the sky model used to calculate the diffuse radiation transfer through glazings (Chapter 4)).

v Since the distribution of radiation and light is similar, SUNSIM could also be used to predict time-varying lighting levels on room surfaces. This would, for example, be useful to investigate the time-changing or time-average lighting-levels in greenhouses. For the growth of plants, the time-averaged lighting-levels are much more important than very accurate calculations of the lighting-levels at one certain time (as predicted by daylight programs).

10.2.4 Application of improved modelling methods to the study of conservatory designs

i It would be useful to validate the program HTB2 (with all the new glazing and blind calculation possibilities) by comparing its predictions with high quality field data collected in a conservatory. It would be possible to validate the energy saving predictions due to adding an unheated conservatory to a room, the predicted time-of-usability of a conservatory, and the predicted energy demand for heating a conservatory.

ii In this work, the problems of air flow and temperature stratification in highly glazed spaces were not investigated in detail. However, it would be useful to combine the latest developments in the area of solar radiation modelling (as considered in this work) with those in the field of air flow modelling (treated elsewhere). This would, for example, permit design studies of commercial atria in which the effects of air flow, convection, temperature stratification etc. are particularly important. A more rigorous simulation of air flow would also be useful to investigate in detail the energy saving potential associated with solar pre-heated ventilation air (SPV).

iii The conservatory design study investigated the influence of design variations on the thermal performance of conservatories subjected to the weather data for Sheffield (UK). It would be interesting to repeat the design study for other geographical locations and climate conditions. This would permit more detailed design statements for particular locations. It could also show if there are favourable or unfavourable locations for conservatories.

iv In the conservatory design study, the adjacent living-space was continuously heated to 21°C with a night set-back to 16°C. Since the heat losses into the unheated conservatory depend highly on the heating regime in the adjacent living-space, it would be useful to study the effect of continuous heating, not heating at night, and different heating setpoints. It would also be useful to study the impact of insulating the partition window at night.

v The influence of fixed slat-type external blinds on the predicted thermal performance of conservatories and adjacent rooms has been investigated. The results clearly demonstrated that more work is necessary to derive suitable design guidance about the appropriate use and control of blinds.

vi The conservatory design study could be improved by considering day lighting, moisture transfer, and thermal comfort in more detail. It would also be useful to consider economy issues.

vii The heating and cooling loads- and the heating and cooling energy demands-, of rooms with attached, unheated, conservatories are often approximated by reducing the U-value of the partition walls (and glazings) by a fixed amount (e.g. by a factor of 0.6 for a double glazed conservatory). Typically, such reduction factors (e.g. WärmeschutzVO, 1993) do not consider the particular design of the conservatory. It would be useful to calculate more accurate reduction values which take the important design aspects into consideration.

REFERENCES

Alexander D.K. 1993: "HTB2 version 1.1", Welsh school of Architecture, UWIST, Cardiff (UK)

Allen J.P., Whittle J.K. 1988: Chapter 8 of BRE/SERC Final Report "An investigation into analytical and empirical validation techniques for dynamic thermal models of buildings", Volume II, Part 2, (pp-119)

Anderson B.R. et al. 1985: "BREDEM - BRE Domestic Energy Model", Building Research Establishment Report, Garston Watford (UK)

Andres H. 1965: "Dünne Schichten für die Optik", Wissenschaftliche Verlagsgesellschaft mbH, Stuttgart (D)
"Thin films in the optic", Sience Publication Company Stuttgart (Germany)

ASHRAE Handbook 1981: "1981 Fundamentals", American Society of Heating, Refrigerating and Air-Conditioning Engineers, Inc., (IV27.1 - 27.48), Atlanta (USA)

Aydinli S. 1981: "Über die Berechnung der zur Verfügung stehenden Solarenergie und des Tageslichtes", Fortschrittsberichte der VDI-Zeitschriften, Reihe 6, Nr. 79, VDI-Verlag GmbH, Düsseldorf (D), (172-pp)
"Calculating the available solar energy and daylight", Research Reports of VDI-Journals, Record 6, No. 79, VDI publication, Düsseldorf (Germany)

Baker N.V. 1985: "The use of passive solar gains for the pre-heating of ventilation air", Energy Technology Support Unit (ETSU) Report No. ETSU-S-1142, (242-pp)

Balcomb J. et al. 1983: "Passive Solar Design Handbook", Volume 3, American Solar Energy Society, New York (USA)

BDP 1991: "Using ESP in the PAS non-domestic design studies" Building Design Part., Energy and Environment, Report. under Warrant 6 - Development of Performance Assessment Issues, For the DEn., (62-pp)

Beckman W.A., Parsons B.K. 1980: "Performance prediction of attached sunspaces", Proceedings of AS/ISES at Phoenix, Arizona, American Section of the International Solar Energy Society, Inc., (pp 671-675)

Bergmann L. 1978: "Lehrbuch der Experimentalphysik", Bergmann-Schaefer, Berlin, New York, de Gruyter, 7. Auflage
"Manual of the Experimental Physics", Bergmann-Schaefer publication Berlin and New York, de Gruyter, 7. edition

Berning P.H. 1983: "Principles of design of architectural coatings", Applied Optics, Vol. 22, No. 24, (pp 4127-4141)

BINE Informationsdienst 1989: "Demonstrationsprojekt Landstuhl - Energieeinsparung und Solarenergienutzung in Eigenheimen", Gesellschaft für wissenschaftlich-technische Information mbH Eggenstein-Leopoldshafen, Nr. 9
BINE Information service 1989: "Demonstration project Landstuhl - Energy saving and use of solar energy in dwellings", Society of scientific- technical information Eggenstein-Leopoldshafen (Germany), No. 9

BINE Informationsdienst 1991a: "Grüne Solararchitektur bei Reihenhäusern - Energiebilanzen und biologische Aspekte", Gesellschaft für wissenschaftlich-technische Information mbH Eggenstein-Leopoldshafen, Nr. 7
BINE Information service 1991a: "Green Solar-architecture at terraced houses - energy balances and biological aspects", Society of scientific- technical information Eggenstein-Leopoldshafen (Germany), No. 7

BINE Informationsdienst 1991b: "Einfamilienhäuser und passive Energiesparmaßnahmen - eine experimentelle Untersuchung", Gesellschaft für wissenschaftlich-technische Information mbH Eggenstein-Leopoldshafen, Nr. 9
BINE Information service 1991b: "Dwellings and passive energy saving measures - an experimental investigation", Society of scientific- technical information Eggenstein-Leopoldshafen (Germany), No. 9

Bland B.H., Allen J.P., Higgs F.S. 1988: Appendix 1 of BRE/SERC Final Report "An investigation into analytical and empirical validation techniques for dynamic thermal models of buildings", Volume II, Part 2

Bland B.H. 1992: "Conduction in Dynamic Thermal Models: Analytic Tests for Validation", Building Services Eng. Res. and Tech., Vol. 13, No. 4, (pp 187-208)

Bloomfield D., Eppel H., Lomas K.J., Martin C. 1993: "Multi-national validation using high quality data sets", IEA Task 12 /Annex 21, CIBSE Conference Paper

Borresen B.A., Harsem T.T. 1990: "Displacement ventilation in glazed atria", Roomvent'90 conference, Session A1-8, (18-pp)

Bowman N.T. and Lomas K.J. 1985: "Empirical validation of dynamic thermal computer models of buildings", Building Services Eng. Res. and Tech., Vol. 6, No. 4, (pp 153-162)

Brandemuehl M.J., Beckmann W.A. 1979: "Transmission of diffuse radiation through CPC and flat plate collector glazing", Solar Energy, Vol. 24, (pp 511-513)

CEN TC 129, 1992: "Glass in buildings - determination of light transmittance, solar direct transmittance, total solar energy transmittance and ultraviolet transmittance, and related glazing characteristics", final draft prEN 410, (31-pp)

Chu W.L, Oreszczyn T. 1991: "The energy duality of conservatories: should conservatories be exempt from Building Regulations?", The Bartlett School of Architecture and Planning London, Building Technical File No. 32, (pp 9-13)

Chuard D. 1992: "ATRIA, solar distribution computing program", IEA Solar R&D, task 12, project A3, Lausanne (CH), (10-pp)

CIBSE Guide 1986: Volume A - Design Data, London

CIE Committee E - 3.2, 1955: "Natural Daylight", Offical Recommendations Compte Rendu, 13th session, Bd. 13, Paris (France)

CIE 1973: "Standardisation of luminance distribution on clear skies", Publication No. 22 (TC-4.2)

Clark J.P., McLean D. 1988: "ESP - A building and plant energy simulation system", version 6, release 8, Energy Simulation Research Unit, Univ. of Strathclyde and ABACUS Simulations Limited, Glasgow (UK)

Clark J.P., Maver T.W. 1991: "Advanced design tools for energy conscious building design: development and dissemination", Building and Environment, Vol. 26, No. 1, (pp 25-34)

***Diegmann* V. 1991:** "*Der hemisphärisch-hemisphärische* Transmissionsgrad von transparenter Wärmedämmung und Verschattungsvorrichtungen", Diplomarbeit an der Fakultät für Physik, Frauenhofer-Institut für solare Energiesystems, Universität Freiburg (D)
"The hemispherical-hemispherical transmittance of transparent insulation and shading devices", diploma work at the department of physics, Frauenhofer-Institude for solar Energy-Systems, University of Freiburg (Germany)

Dietrich U. 1994: "Tageslichtmodell TYP 70 für TRNSYS", TRNSYS - News 1/94, TRANSSOLAR Energietechnik GmbH Stuttgart (D)
"Daylightmodel TYP 70 for TRNSYS", TRNSYS - News 1/94, TRANSSOLAR Energy technique company, Stuttgart (Germany)

DIN 1349 Blatt 1, 1972: "Durchgang optischer Strahlen durch Medien", Deutsche Industrie Norm, Beuth Verlag Berlin und Köln
"Transmission of optical radiation through material", German standard, Beuth publication Berlin and Cologne

DIN 4108, 1981: "Wärmeschutz im Hochbau", Deutsche Industrie Norm, Beuth Verlag, Berlin und Köln
"Heat protection of buildings", German standard, Beuth publication Berlin and Cologne

DIN 4108, 1993: "Wärmeschutz im Hochbau", Entwurf zum Beiblatt, Deutsche Industrie Norm, Beuth Verlag, Berlin und Köln
"Heat protection of buildings", draft of new insert, German standard, Beuth publication Berlin and Cologne

DIN 4701, 1983: "Regeln für die Berechnung des Wärmebedarfs von Gebäuden", Deutsche Industrie Norm, Beuth Verlag, Berlin und Köln
"Rules for calculating the heat requirement of buildings, Basic rules for calculation", German standard, Beuth publication Berlin and Cologne

DIN 5034, 1983: "Tageslicht in Innenräumen", Deutsche Industrienorm, Beuth Verlag Berlin und Köln
"Daylight in interiors", German standard, Beuth publication Berlin and Cologne

DIN 67507, 1980: "Lichttransmissionsgrad, Strahlungstransmissionsgrad und Gesamtenergiedurchlaßgrade von Verglasungen", Deutsche Industrie Norm, Beuth Verlag, Berlin und Köln
"Light transmittance, radiant transmittance and total energy transmittance of glazings", German standard, Beuth publication Berlin and Cologne

Dislich H. 1984: "Herstellung von transparenten Oxidschichten beim Tauchen", Glastechnische Berichte 57, Deutsche Glastechnische Gesellschaft Frankfurt, Nr. 9, (pp 229-236)
"Preparation of transparent oxide coatings by dipping", Glass-technical Reports 57, German Glass-technical Society Frankfurt (Germany), No. 9

Erhorn H. 1983: "Möglichkeiten zur Verbesserung des Wärmeschutzes von Mehrfachverglasungen", Fenster und Fassade, Nr. 4, (pp 105-110)
"Possibilities to improve the heat protection of multi-layered glazing systems", Window and Façade, No. 4

Erhorn H. 1989: "Solarenergiehäuser in der Praxis - Welche Energiesparergebnisse erbringen sie wirklich", Bauphysik 11, Heft 1, (pp 70-73)
"Buildings using solar energy - How much energy do they really save in practical application", Building-Physics, Vol. 11, No. 1

Erhorn H., Szerman M. 1993: "Neue Planungsinstruments für energiegerechte Verwaltungsgebäude", Ernst & Sohn Verlag für Architektur und technische Wissenschaften, Berlin (D), (3-pp)
"New design tools for energy efficient commercial buildings", Ernst & Sohn publication for architects and technical science, Berlin (Germany)

Erhorn H., Szerman M. 1994: "ADELINE - an advanced computer tool to design and evaluate day- and electric lighting applications in buildings", proceedings of BEP'94 conference, Building Environmental Performance Facing the Future, University of York (UK), (pp S19-S25)

Everett R. et al. 1985: "Performance of passive solar houses at Great Linford, Milton Keynes" Final Report to the Energy Technology Support Unit, Contract No: E/SA/CON/1025/174/020, Milton Keynes: Open University (UK)

Flachglas AG 1975: "Infrastop® - Sonnenschutz-Isolierscheiben mit der Garantie der Flachglas AG", Prospekt 1.42 75/5, (19-pp)
"Infrastop® - Sun-protection insulation glazing with guaranty of the Flachglas Company", public prospectus 1.42 75/5

Frank T., Püntener T. 1987: "Report carried out under step 4 of IEA Annex XII, window and fenestration", EMPA, Dübendorf (Switzerland), (104-pp)

Gläser H.J. 1980: "Improved insulating glass with low emissivity coatings based on gold, silver, or copper films embedded in interference layers", Glass Technology, Vol. 21, No. 5, (pp 254-261)

Gläser H.J. 1990: "Solar control glass", Glastechnische Berichte 63, Deutsche Glastechnische Gesellschaft Frankfurt, Nr. 9, (pp 266-276)
"Solar control glass", Glass-technical Reports 63, German Glass-technical Society Frankfurt (Germany), No. 9

Groth R. 1977: "Vakuumbeschichtete Sonnenschutzgläser für die Bauindustrie", Glastechnische Berichte 50, Deutsche Glastechnische Gesellschaft Frankfurt, Nr. 10, (pp 239-247)
"Vacuum-coated solar control glazing for the building industry", Glass-technical Reports 50, German Glass-technical Society Frankfurt (Germany), No. 10

Hauser G. 1984: "Eneretische Auswirkungen und sommerliches Temperaturverhalten eines Wintergartens", Kunststoffe im Bau, Heft 4, (pp 170-173)
"Thermal effect and summer temperature behaviour of a conservatory", Synthetic Building Materials, No. 4

Hauser G. 1986: "Unter Einzelwerten muß der Nutzer wichten - bauphysikalische Aspekte bei Wintergärten", Glaswelt, Nr. 5, (pp 10-21)
"Building physical aspects of conservatories", Glazing World, No. 5

Hauser G. 1987: "Beeinflussung des Innenklimas durch Außenwände und durch Wintergärten", Bauphysik, No. 5 (pp 155-162)
"Influences on the internal climate by external walls and by conservatories", Building-Physics, No.5

Harbeke B. 1986: "Coherent and Incoherent Reflection and Transmission of Multi-Layer Structures", Applied Physics B 39, Springer-Verlag, (pp 165-170)

Heinz B. 1991: "Optische Konstanten von Halbleiter Mehrschichtsystemen", Dissertation RWTH Aachen (D), (140-pp)
"Optical constants of semiconductor multi-layer systems", dissertation RWTH Aachen (Germany)

Hensen J.L.M. 1991: "On the thermal interaction of building structure and heating and ventilation system", Thesis, Technische Universiteit Eindhoven (Netherlands)

Hensen J.L.M., Hand J., Clark J.A. 1991: "Building design assessment through coupled heat and air-flow simulation: two case studies", Eindhoven University of Technology, University of Strathclyde (UK), (10-pp)

Hogan W.D, Loxsom F.M. 1981: "Preliminary validation of models predicting insolation on tilted surfaces", Proceedings of the 1981 Annual Meeting, AS/ISES, Philadelphia, Pennsylvania (USA), (pp 1521-1525)

Hofmann A. 1981: "Energiebilanz eines Wohnhauses mit passiver Solarnutzung über ein Gewächshaus mit Hypokausten-Heizung", Diplomarbeit im Studiengang Bauphysik, FHT Stuttgart
"Energy balance of a passive solar heated dwelling with greenhouse and air heating system", diploma work, department of Building-Physics, FHT Stuttgart (Germany)

Hottle H.C., Woertz B.B. 1942: "The performance of flat-plate solar-heat collectors", Trans. ASME 64, 91

Hunter-Douglas 1979: "Sonnenschutz durch Jalousien", Produktinformation, 74.942 Ge
"Sun protection by slat-type blinds", public prospectus (Germany)

Hutchins M.G. 1988: "Solar Optical Materials", Proceedings of the Conference Applications & Performance of Coatings & Materials in Building & Solar Energy Systems, Oxford (UK), Pergamon Press, (180-pp)

Interpane 1990: "Gestalten mit Glas", Produktinformationen, Interpane, Lauenförde (D)
"Designing with glass" public prospectus, Interpane Lauenförde (Germany)

ISO 9164, 1992: "Thermal Insulation - Calculation of space heating requirement for residential buildings", CEN prEN 832

Judkoff R.D. 1988: "Validation of Building Energy Analysis Simulation Programs at the Solar Energy Research Institude", Energy and Buildings, No. 10, (pp 221-139)

Kataja S., Kalema T. 1992: "Energy Analysis Test for Commercial Buildings", IEA TASK 12 & 21 C, Tampere University of Technology, (12-pp)

Keeble E. 1990: "Availability of UK climatic data for use in simulation", Air Infiltration and Ventilation Centre, Coventry (UK), (32-pp)

Khalifa A.J.N, Marshall R.H. 1990: "Validation of heat transfer coefficients on interior building surfaces using a real sized indoor test cell", Int. J. Heat Mass Transfer, Pergamon Press, Vol. 33, No. 110, (pp 2219-2236)

Klein S.A. et al. 1988: "TRNSYS, A Transient System Simulation Program", Manual, Solar Energy Laboratory University of Wisconsin, Madison (USA)

Krochmann J., Wang X.Y., Masuch J. 1992: "Winkelabhängige Strahlungstransmission durch Sondergläser", Ki 7-8, (pp 247-251)
"Incidence angle dependent solar transmission by radiation through special glass types", Climate - Cooling - Heating, No. 7-8

Küster O. 1992: "Thermische Simulation von Folienaufbauten", Diplomarbeit im Studiengang Bauphysik, FHT Stuttgart
"Thermal Simulation of halls with plastic tent-roofs", diploma work, department of Building-Physics, FHT Stuttgart (Germany)

Landlt-Bornstein 1962: "Optische Konstanten", Zahlenwerte 2. Band, 8. Teil, Springer Verlag
"Optical constants", Landlt-Bornstein numerical values 2. book, chapter 8, Springer publication Germany

Lewis P.T., Alexander D.K. 1985: "HTB2 - A model for the thermal environment of buildings in operation", Users Manual Release 1 Rev. 0, (154-pp), Technical Reference Manual Release 1 Rev. 0, Vol. 1 (378-pp), Vol. 2 (434-pp)

Linden P.F., Lane-Serff G.F., Smeed D.A. 1990: "Emptying filling boxes: the fluid mechanics of natural ventilation", J. Fluid Mech., No. 212, (pp 309-335)

Löber H. 1974: "Zur Berechnung der Sonneneinstrahlung in Räumen bei Verwendung starrer Sonnenschutzeinrichtungen", Dissertation an der TU Dresden
"To calculate the solar radiation gains in rooms by using fixed sun protection devices", dissertation at the Technical University of Dresden (Germany)

Lomas K.J. 1988: "Modelling adjacent zones in a non-explicit manner", Applicability Study 1, Research Note 1, De Montfort University Leicester (UK), (16-pp)

Lomas K.J., Bowman N.T. 1988: "Applicability Study 1, Phase II - Programme Proposals", Environmental Design Unit Leicester Polytechnic (UK), Report for ETSU, (75-pp)

Lomas K.J., Bloomfield D.P., Parand F., Pinney A.A. 1989: "Applicability Study 1: A UK initiative to determine the error characteristics of detailed thermal simulation models", Proc. Science and Tech. at the Service of Arch., Paris (France), (pp 559-563)

Lomas K.J., Mardaljevic J. 1990: "The effect of convective internal heat transfer coefficients on the prediction of detailed simulation models", Applicability Study 1, Research Report 16, De Montfort University Leicester (UK), (32-pp)

Lomas K.J., Bloomfield D.P., Cole A., Parand F., Pinney A.A. 1991: "Dynamic thermal models: Reliability for domestic building design", Building Services Eng. Res. and Tech., Vol. 12, No. 4, (pp 115-128)

Lomas K.J. 1992: "Applicability Study 1, Executive Summary", De Montfort University Leicester (UK) for ETSU, Contract Number E/5A/CON/1213/1784, (73-pp)

Loxsom F. 1985-86: "Meteorological data for the passive solar programme", Polytechnic of Central London Research and Building Unit, Collection of reports for the Energy Technology Support Unit, Model Refinement Study

Martin C., Seale C.F., Eppel H. 1994: "Analytical testing of detailed thermal simulation programs", Proceedings of BEP'94 conference, Building Environmental Performance Facing the Future, University of York (UK), (pp s27 - s32)

McLean D. 1981: "WINDOW: A computer program for the analysis of architectral glazing configurations", ABACUS Occasional Paper No. 84, Department of Architecture, University of Strathclyde (ABACUS) Glasgow (UK), (68-pp)

McLean D. 1988: "Case studies in thermal modelling", ABACUS - modelling tomorrow, ABACUS Simulations Limited, Transcripts of Papers given at the Autumn Workshop SERIES, (8-pp)

Memarzadeh K., Woollam J.A., Belkind A. 1988: "Variable angle of incidence spectroscopic ellipsometric characterization of TiO2/Ag/TiO2 optical coatings", Applied Physics, Vol. 64, No. 7, (pp 3407-3410)

Moon P., Spencer D.E. 1942: "Illumination from non-uniform sky", Illum. Engng. 37, (pp 707-726)

Mørck O.C. 1986: "Simulation model validation using test cell data", IEA task VIII, passive and hybrid solar low energy buildings, Report no. 176, Thermal insulation laboratory, Technical University of Denmark, (158-pp)

Niels P.W.B. 1984: "Determining the distribution of absorbed sun inside direct gain buildings", Proceedings of the 9th National Passive Conference, Ohio, American Solar Energy Society, Inc., (pp 91-94)

Nikolic V. 1983: "Bau und Energie - Bauliche Maßnahmen zur verstärkten Sonnenenergienutzung im Wohnungsbau", Verlag TÜV Rheinland, (pp 108-123)
"Building and Energy - building measures to increase the solar energy use in domestic buildings", publication TÜV Rheinland (Germany)

Ohlwein K. 1992: "Möglichkeiten zur Energieeinsparung durch Wintergärten", elektrowärme international (eta) 50, (pp 15-19)
"Possibilities to save energy with conservatories", electric heat international (eta) 50

Oreszczyn T 1992: "Energy use in conservatories", Conservatory Questionnaire, University College London, Reference No: E/5A/1369/2796/05, (23-pp)

Otter M. 1961: "Optische Konstanten massiver Metalle", Zeitschrift der Physik, Nr. 161, (pp 163-178)
"Optical constants of bulk metals", Journal of the Physics, No. 161

Palik E.D. 1985: "Handbook of optical Constants of Solids", Academic Press, Inc., (pp 275-798)

Palmiter L., Wheeling T. 1983: "Solar Energy Research Institute residential energy simulator version 1.0", Solar Energy Research Institute, Golden, CO (USA), (356-pp)

Parand F., Lomas K.J. 1988: "Short-wave radiation: a comparison of the theoretical basis of the three detailed simulation models ESP, HTB2 and SERI-RES", De Montfort University Leicester (UK), AS1 Research Report 7, presented at PEER GROUP review, (12-pp)

Parand F., Lomas K.J. 1989a: "The theoretical basis of the dynamic thermal model ESP 1. shortwave radiation", Applicability Study 1, Research Report 10, De Montfort University Leicester (UK), (43-pp)

Parand F., Lomas K.J. 1989b: "Optical and thermal properties of a low emissivity double glazing system", Applicability Study 1, Research Note 8, De Montfort University Leicester (UK), (10-pp)

Penz F. 1983: "Passive Solar Heating in existing dwellings"; Martin Centre report to ETSU (UK Department of Energy)

Pfrommer P., Kupke Chr., Lomas K.J. 1993a: "Transmissionswerte für Scheiben", Glaswelt, Gentner Verlag Stuttgart, 46. Jahrgang, Heft 9, (pp 20-32)
"Transmission properties of panes", Glazing-world, Gentner publication Stuttgart (Germany), Vol. 46, No. 9

Pfrommer P., Kupke Chr., Lomas K.J., 1993b: "Der Einfluß von Himmelsrichtung, Neigungswinkel und Sonnenschutzvorrichtung auf den Strahlungstransmissionsgrad und effektiven Gesamtenergiedurchlaßgrad von Mehrfachverglasungen", wksb (Grünzweig + Hartmann AG), Nr. 32, (pp 9-13)
"The influence of orientation, inclination and shading on the solar radiation transmittance and total solar energy transmittance of multi-layered glazings", Heating-Cooling-Sun-Fire Protection (magazin of Grünzweig and Hartmann AG Germany), No. 32

Pfrommer P. 1994a: "Thermal simulation of a butterfly house", Poceedings of BEP'94 conference, Building Environment Performance Facing the Future, University of York (UK), (pp 157-163)

Pfrommer P., Lomas K.J., Kupke Chr. 1994b: "Influence of Transmission Models for Special Glazing on the Predicted Performance of Commercial Buildings", Energy and Buildings, Elsevier, Nr. 21, (pp 101-110)

Pfrommer P., Lomas K.J., Seale C., Kupke Chr. 1995a: "The radiation transfer through coated and tinted glazing", Solar Energy, Elsevier, Vol. 54, Nr. 5

Pfrommer P., Lomas K.J., Kupke Chr. 1995b: "Radiation transfer through slat-type blinds: a new model and its application in thermal building simulation", Solar Energy, Elsevier, in press

Pilkington 1988: "Glass and Transmission Properties of Windows", public prospectus, Pilkington Glass Limited, St Helens (UK), (12-pp)

Pilkington 1990: public product information on special glazing, Pilkington Glass Limited, St. Helens (UK)

Pilkington 1992: "Glass and solar control performance of blinds", public prospectus, Pilkington Glass Limited, St. Helens (UK), (10-pp)

Pinney A. 1990: "The theoretical basis of the dynamic thermal program SERI-RES 1. shortwave radiation", Systems Performance Prediction Section, Building Research Station Garston Watford (UK), (25-pp)

Pulker H.K. 1984: "Coatings on Glass", section 8.6 "Optical properties of thin films", The Film Science and Technology 6, Elsevier, (pp 359-381)

Reilly S., Selkowitz S., Winkelmann F. 1992: "Optical Properties Database for High Performance Glazings", IEA Task 12, Subtask A.1, working documents, Lawrence Berkeley Laboratory, California (USA)

Rodriguez E.A., Guerra J., Alvarez S. 1988: "Modelling the effect of remote and facade obstructions on the radiation at the outdoor surface of windows", Proc. of the 6th International PLEA Conference, Energy and Buildings for Temperate Climates, Porto (Portugal), (pp 285-290)

Rodriguez E.A., Alvarez S. 1991: "Solar shading analytical tests", technical description, Universidad de Sevilla (Spain), denoted as IEA21RN136/91

Rouvel L. 1972: "Berechnung des wärmetechnischen Verhaltens von Räumen bei dynamischen Wärmelasten", Brennstoff - Wärme - Kraft 24, Nr. 6, (pp 245 - 262)
"Calculation of the thermal behaviour of rooms with dynamic heat loads", Fuel - Heat - Force, Vol. 24, No. 6

Rubin 1982: "Solar optical properties of windows", Energy Research Vol. 6, (pp 123-133)

Rudolph I. 1978: "Beitrag zur Berechnung der Wirksamkeit von äußeren Verschattungseinrichtungen", Dissertation an der TU Dresden
"Contribution to the calculation of the impact of external shading devices", dissertation at the Technical University of Dresden (Germany)

Schott 1982: "Calorex - Planen und bauen mit dem absolut farbneutralen Sonnenreflexionsglas von Schott", Prospekt, Schott Glaswerke, 7065/3 VII/82, Mainz (D), (15-pp)
"Calorex - Planning and building with the absolute colour-neutral sun-reflective glass of Schott", public prospectus, Schott Glazing Factory Mainz (Germany)

Schulze R.W. 1970: "Strahlenklima der Erde", Steinkopf-Verlag, Darmstadt (D)
"Radiation climate of the earth", Steinkopf-publication, Darmstadt (Germany)

Semen A. 1994: "Parameterstudie zur Untersuchung der Einflußgrößen, die auf den Abminderungsfaktor z von Jalousien einwirken", Diplomarbeit im Studiengang Bauphysik, FHT Stuttgart
"Parametric study to investigate the influences which affect the shading factor z of slat-type blinds", diploma work, department of Building-Physics, FHT Stuttgart (Germany)

Snatschke C., Künzel H. 1974: "Verfahren zur Ermittlung des strahlungsbedingten Wärmetransports durch Fenster", Ki 5, (pp 3-12)
"Method for the Determination of Heat Transfer through Windows from radiant sources", Climate - Cooling - Heating, No. 5

Spitzner M. 1991: "Vergleich thermischer Simulationsprogramme", Diplomarbeit im Studiengang Bauphysik, FHT Stuttgart
"Comparison of thermal simulation programs",diploma work, department of Building-Physics, FHT Stuttgart (Germany)

Strachan P. 1990: "Addition of Blind/Shutter Control to Transparent Multi-Layer Constructions and Other Improvements to the Solar Routines of ESPsim", Information for ESP users, Energy Simulation Research Unit, Univ. of Strathclyde (UK), (11-pp)

Tschegg, Heindl, Sigmund 1984: "Grundzüge der Bauphysik", Wien, New York, Springer Verlag
"Rudiments of Building-Physics", Springer publication Vienna and New York

VDI 2078, 1977: "Berechnung der Kühllast klimatisierter Räume (VDI-Kühllastregeln)", Verein Deutscher Ingenieure
"Calculation of the cooling load of air-conditioned rooms (VDI cooling load charts)", publication Club of German Engineers

VDI Wärmeatlas 1988: 5. Auflage, Einstrahlzahlen Kb, VDI-Verlag Düsseldorf (D)
"Heat-atlas 1988", 5. edition, View factors Kb, publication Club of German Engineers Düsseldorf (Germany)

Vegla 1985: "Sonnenschutzglas", öffentliche Produktinformationen, Vereinigte Glaswerke GmbH, Aachen (D)
"Sun-protective glazing", public prospectus, United Glazing Factories Aachen (Germany)

Voss K. 1992: "Lamellensysteme zur Steuerung der Strahlungsdurchlässigkeit transparenter wärmegedämmter Bauteile," Frauenhofer-Institut für solare Energiesysteme, Freiburg (D), (10-pp)
"Slat-type systems to control the radiation transmittance of transparent, insulated building elements", Frauenhofer-Institut for Solar Energy Systems Freiburg (Germany)

Ward G.J. 1989: "RADIANCE: A software program for computing luminance and synthetic images", Lawrence Berkeley Laboratory (USA), IES Annual Conference

Ward G.J. 1992: "Measuring and Modelling Anisotropic Reflection", Lighting Systems Research Group, Lawrence Berkeley Laboratory (USA), (8-pp)

WärmeschutzVO 1993: "Verordnung über einen energiesparenden Wärmeschutz bei Gebäuden", Referentenentwurf 1993, gültig ab 1.1.1995
"German law for the heat protection of buildings", referee draft of 1993, comes into force on 1.1.1995

Wilde M. 1985: "SUPERLITE 1.0 Evaluation Manual", Windows and Daylighting Group, Lawrence Berkeley Laboratory (USA)

Wright J.L., Sullivan H.F. 1992: "VISION3: Glazing System Thermal Analysis Program", User Manual (29-pp), Reference Manual (32-pp), Advanced Glazing System Laboratory, Department of Mechanical Engineering, University of Waterloo, Waterloo, Ontario (Canada)

Yannis S. 1994 "Solar Energy and Housing Design", Pub. Architectural Association for UK Department of Trade & Industry; Vol.1 Principles, Objectives, Guidelines", (146-pp); Vol.2 Examples, (127-pp)

Zimmermann and Becker 1992: "ZB-SIMULAP Gebäudesimulation, user manual", Zimmermann + Becker Software und Systemhaus Heilbronn (D)
"ZB-SIMULAP building simulation, user manual", Zimmermann + Becker Software and System-house Heilbronn (Germany)

BIBLIOGRAPHY

During the course of this research a number of internal reports, and other documents, were produced. These are listed here and are available from either the author, Professor C. Kupke at FhT Stuttgart [Fachbereich Bauphysik, Willi-Bleicher Str. 29, 70174 Stuttgart, Germany] or Dr. K. Lomas at De Montfort University [ECADAP Research Group, The Gateway, Leicester LE1 9BH, UK]. They were written merely as an internal record charting the progress of the research and they are not fully polished public domain documents, prospective readers should recognize this.

IR1: The effect of window modelling methods on the prediction of detailed simulation programs

IR2: The modelling of conservatories with detailed simulation programs

IR3: The diffuse transmittance through windows

IR4: The radiation transfer through external blinds

IR5: The radiation transfer through coated glazing

IR6: The radiation transfer through glazing with internal or external blinds

IR7: The influence of glazing and blind calculation methods on the thermal simulation of highly glazed spaces - sensitivity study

IR8: Calculation of the incidence angle dependent transmittance of coated and tinted glazing

IR9: The influence of the incidence angle dependent transmittance on the thermal simulation of commercial buildings

IR10: Solar distribution module for HTB2

IR11: The influence of solar distribution methods on the thermal simulation of highly glazed spaces

IR12: Conservatory design questions - review and discussion

IR13: Conservatory design study

IR14: Conservatory design guidance

User manual of GLSIM 1.0, 1994 "Glazing Simulation Program"

User manual of SUNSIM 1.0, 1994 "Internal Solar Distribution Simulation"

A.1 DIRECT-GAIN LIVING-ROOM

A.1.1 Introduction

To predict the influence of glazing calculation models on the environmental conditions in a room (Chapters 2, 4 and 7), a one-zone module of a typical living-room in a UK domestic building was chosen The module was devised by studying the features of real dwellings and published 'standard' building descriptions (Lomas et al. 1989). The advantage of the module was that it bore a close resemblance to real structures and operating conditions, yet was sufficiently simple that: protracted computer run-time was avoided; compatible program inputs could be assured; results for other dwellings could be inferred; and the effects of individual thermal processes could be disaggregated.

A.1.2 The room module

The living-room was a corner room with two walls connected to the outside air and two walls and the ceiling treated as internal elements (Fig. A.1). The room had a rectangular shape with a floor area of 16 m^2 and a volume of 40 m^3.

The west and south walls were external and heavy-weight (cavity brick walls). The east and north walls were internal and heavy-weight (one layer of brick). The ceiling was internal and light-weight (two layers of board). The floor was heavy-weight and on the ground.

The base-case room was south orientated. When other orientations were studied, the whole room structure (shape; window; internal and external walls) was rotated.

The adjacent zones were treated as unheated buffer zones and were modelled in an non-explicit manner. This was done by adding a material layer to the partition/ceiling which represented approximately the thermal behaviour of the buffer zone. A method of selecting the properties of this material was devised by Lomas (1988).

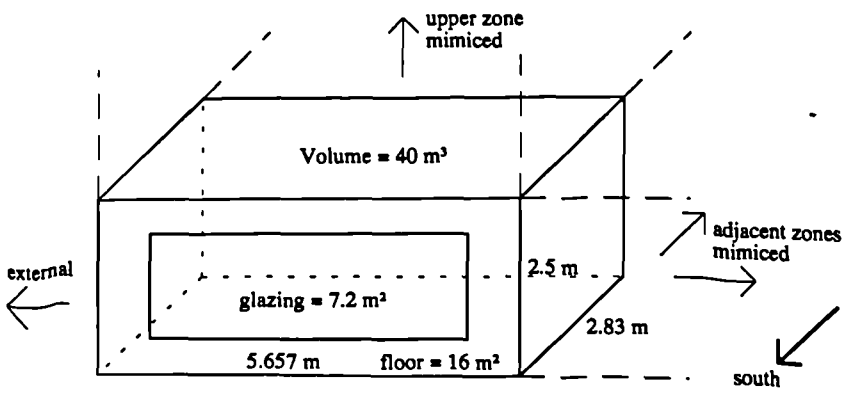

Figure A.1:
One-zone module of a typical living-room in a UK domestic building.

A.1.3 Construction

Three alternative insulation levels of the external walls (and floor) were investigated in different studies. These reflect traditional and modern constructional practise.

- Traditional low-insulated: average U-value = 1.4 W/m²K (pre-1985 UK-regulations); used walls W1, I1; ceiling C1; and floor F1.
- Modern-insulated: average U-value = 0.5 W/m²K (post 1985 UK-regulations); used walls W2, I1; ceiling C1; and floor F1.
- Advanced highly-insulated: average U-value = 0.3 W/m²K; used walls W3, I2; ceiling C1; and floor F2.

The structure of the walls given from the outside to the inside, and for the floor (and ceiling) given from the top to the bottom are given in the Tables A.1 to A.8. For air cavities the thermal resistance is given instead of the conductivity.

Material	thickness, mm	conductivity, W/mk	density, kg/m³	specific heat, J/kgK
Brick	105	0.84	1700	800
Cavity	65	0.18 m²K/W		
Brick	105	0.62	1700	800
Plaster	16	0.26	800	1000

Table A.1: Heavy-weight external wall (U-value = 1.4 W/m²K) as used for traditional insulation (W1).

Material	thickness, mm	conductivity, W/mk	density, kg/m³	specific heat, J/kgK
Brick	105	0.84	1700	800
Cavity	50	0.18 m²K/W		
Fibre glass	50	0.04	12	840
Brick	100	0.62	1700	800
Plaster	16	0.26	800	1000

Table A.2: Heavy-weight external wall (U-value = 0.5 W/m²K) as used for modern insulation (W2).

Material	thickness, mm	conductivity, W/mk	density, kg/m³	specific heat, J/kgK
Brick	105	0.84	1700	800
Fibre glass	100	0.04	12	840
Brick	100	0.62	1700	800
Plaster	18	0.26	800	1000

Table A.3: Heavy-weight external wall (U-value = 0.3 W/m²K) as used for advanced insulation (W3).

Material	thickness, mm	conductivity, W/mk	density, kg/m³	specific heat, J/kgK
Plaster	16	0.26	800	1000
Brick	105	0.62	1700	800
Plaster	16	0.26	800	1000

Table A.4: Internal wall (U-value = 1.9 W/m²K) used for traditional and modern insulation (I1).

Material	thickness, mm	conductivity, W/mk	density, kg/m³	specific heat, J/kgK
Plaster	16	0.26	800	1000
Block	100	0.51	1400	1000
Plaster	16	0.26	800	1000

Table A.5: Internal wall (U-value = 1.79 W/m²K) as used for advanced insulation (I2).

Material	thickness, mm	conductivity, W/mk	density, kg/m³	specific heat, J/kgK
Carpet	5	0.06	1000	1000
Chipboard	20	0.16	950	2093
Cavity	200	0.17 m²K/W		
Plasterboard	18	0.16	950	840

Table A.6: Ceiling (C1).

Material	thickness, mm	conductivity, W/mk	density, kg/m³	specific heat, J/kgK
Carpet	5	0.06	160	1000
Screed	50	0.41	1200	840
Concrete	150	1.4	2100	840
Hardcore	150	1.83	2200	712
Earth	1300	1.4	100	500

Table A.7: Floor (U-value = 0.6 W/m²K) as used for traditional and modern insulation (F1).

Material	thickness, mm	conductivity, W/mk	density, kg/m³	specific heat, J/kgK
Carpet	5	0.06	160	1000
Screed	50	0.41	1200	840
Concrete	150	1.4	2100	840
Polystyrene	90	0.03	25	1400
Hardcore	50	1.83	2200	712
Earth	1300	1.4	100	500

Table A.8: Floor (U-value = 0.3 W/m²K) as used for advanced insulation (F2).

All external surfaces were medium coloured with an absorptance of 0.8. The internal surfaces were light coloured (absorptance = 0.5) except for the carpet which was medium coloured (absorptance = 0.8). All surfaces have been assumed to have a high emittance of 0.9.

It should be noted, that these constructions and surface characteristics were also used for other buildings or room modules, which are described in Appendices A.2, A.4 and A.5. In these Appendices a certain construction is defined by the insulation level of the building. The wall, ceiling and floor constructions (and surface characteristics) for a certain insulation level correspond to those listed above.

A.1.4 Window

The window of the base-case room was south orientated and had a basic area of 7.2 m² which was 45% of the floor area and about half of the total south orientated wall area. The window was located in the centre of the wall. However, until the modelling of shading and

internal solar distribution becomes important, the location of a window is thermally unimportant. Window frames were ignored. In different studies the glazing area was varied:

- 3.2 m² (20% of the floor area);
- 5.3 m² (33% of the floor area);
- 7.2 m² (45% of the floor area) - base-case;
- 8.8 m² (55% of the floor area);
- 14.1 m² (88% of the floor area) - south surface completely glazed.

Within different studies the following window types were used:

- clear single glazing (U-value = 5.6 W/m²K);
- clear double glazing (U-value = 2.9 W/m²K);
- low-emittance glazing (U-value = 1.9 W/m²K).

The glazing properties of the low-emittance glazing were chosen to represent Pilkingtons Kappa-float® double glazing as used in previous studies at DMU (Lomas et al. 1989).

a) Thermal glazing properties

All glass was assumed to be 6 mm thick and, in double glazed units, a 12 mm cavity was used. The thermal resistance of the air cavity between clear glass panes was 0.17 m²K/W. However, the thermal resistance of the air cavity between one clear and one low-emittance coated glass pane of the Kappa-float glazing was assumed to be 0.345 m²K/W. The thermal properties of the glass panes are given in Table A.9.

Material	thickness, mm	conductivity, W/mk	density, kg/m³	specific heat, J/kgK
Floatglass	6	1.05	2500	750

Table A.9: Thermal properties of the used glass panes.

b) Solar glazing properties

The incidence angle dependent direct transmittance τ and direct absorptance α for clear single and clear double glazing (listed in Tables A.10 and A.11) were derived from the fundamental optical constants of the glass panes: refraction index = 1.526; extinction coefficient = 0.03 1/mm.

incidence angle:	0	10	20	30	40	50	60	70	80	90
τ:	.77	.77	.77	.76	.75	.73	.68	.57	.34	.0
α:	.16	.16	.16	.17	.17	.18	.19	.19	.18	.0

Table A.10: Incidence angle dependent transmittance τ and absorptance α of 6 mm clear single glazing.

incidence angle:	0	10	20	30	40	50	60	70	80	90
τ:	.59	.59	.58	.58	.57	.54	.49	.37	.16	.0
α:	.29	.29	.30	.30	.31	.32	.33	.33	.29	.0

Table A.11: Incidence angle dependent transmittance τ and absorptance α of 2×6 mm clear double glazing.

For the low-emittance glazing, the incidence angle dependent transmittance and absorptance values as used in previous studies at DMU (Lomas et al. 1989) were accepted. These values were obtained by Parand and Lomas (1989b) using an approximate calculation technique (Table A.12).

incidence angle:	0	10	20	30	40	50	60	70	80	90
τ:	.45	.44	.44	.43	.42	.39	.35	.26	.11	0
α:	.46	.46	.46	.47	.49	.49	.50	.49	.41	0

Table A.12: Incidence angle dependent transmittance τ and absorptance α of 2×6 mm low-emittance glazing.

For all glazings the diffuse transmittance and absorptance the values for direct radiation at an equivalent incidence angle of 60° were used.

In clear double glazing units, 59% of the radiation energy was absorbed in the outer pane (41% in the inner pane). For low-emittance glazing the radiation split was: 64% outer pane; 36% inner pane.

A.1.5 Heating (cooling) and ventilation

The room was continuously heated to set-points of 18°C or 21°C. The radiators had an output which was assumed to be 100% convective. The capacities were so great that the hourly loads never exceeded the capacities. The efficiency of the heat generation was 100%. Occupancy, lighting and small power heat gains were neglected.

In one study the effect of cooling the room was investigated. In this study the cooling set-point was 30°C.

The room was well sealed and had a low constant air change rate of 0.35 ach.

A.1.6 Location

The room was located at Kew near London (UK): latitude = 51.5° North; longitude = 0°.

The site was flat and unobstructed with respect to the wind and sun (no shading from other buildings was considered). The ground reflectance was 0.2.

A.2 LIVING-ROOM WITH ATTACHED CONSERVATORY

A.2.1 Introduction

To study the influence of thermal glazing and solar distribution models on the performance of buildings with attached conservatories (Chapters 2 and 8), a two-zone module of a typical UK domestic living-room and a typical single glazed conservatory was used (Fig. A.2). The conservatory design was chosen considering the results of extended investigations into the design of state of the art conservatories (Oreszszyn 1992).

A two-zone model was preferred before a multi-zone model of a realistic house with attached conservatory for the following reasons:

(i) a two-zone model involves a relatively quick and uncomplicated calculation while considering all the complex thermal interactions;

(ii) a conservatory has a considerable affect on the heating energy demand of the adjacent room, however, it has an energy impact which is small in comparison to the total energy demand of the whole house. So, if a whole dwelling is considered, the comparison and evaluation of very small differences in heating energy would be necessary.

(iii) The likely-hood of modelling mistakes is lower for simple building arrangements.

A.2.2 The two-zone module

The living-room corresponded to the room of Appendix A.1 with an heavy-weight, advanced highly-insulated construction (average U-value = 0.3 W/m²K). The south wall and south window bordered onto the conservatory. The common wall between living-room and conservatory had the same insulation level as the external walls (W3, see Table A.3). More details of the room are described in Appendix A.1.

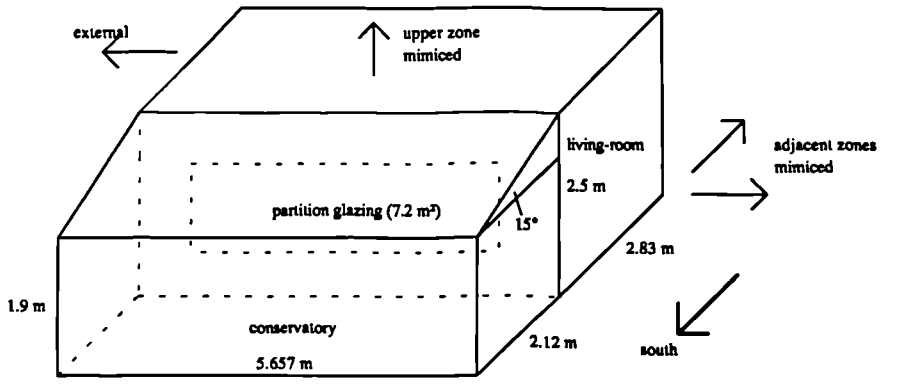

Figure A.2:

Two-zone module of a typical UK domestic living-room with attached conservatory.

The conservatory was rectangular and had a basic floor area of 12 m² and a volume of 26 m³. The construction of the conservatory floor corresponded to that of the living-room floor

(F2, see Table A.8). The conservatory ceiling was slightly inclined with an inclination angle of 15°. The surface reflectance of all opaque internal surfaces was 0.2 (dark colour).

A.2.3 Windows

In the base-case, there was a 7.07 m^2 glazing area between living-room and conservatory, which corresponded to the half of the total partition area. The window was located in the centre of the partition wall. In different studies the glazing areas were varied:

- 0 m^2 (no partition window);
- 7.07 m^2 (half of the partition area) - base-case;
- 14.14 m^2 (total partition area).

The base-case partition window was double glazed. The base-case conservatory was single glazed. Window frames were not considered. In addition, a conservatory shading device was not considered. In different studies the partition and conservatory glazing types were varied:

- single glazing (U-value = 5.6 W/m^2K);
- double glazing (U-value = 2.9 W/m^2K);
- low-emittance glazing (U-value = 1.9 W/m^2K).

The thermal and solar glazing properties are given in Table A.9 to A.12 (section A.1.4).

A.2.4 The floor area

As described above, the conservatory had a basic floor area of 12 m^2. However, in one study the floor area of the conservatory was varied: 0 m^2; 6 m^2; 12 m^2; 18 m^2. This was done by varying the depth from 1 m to 3.18 m while keeping the same partition area of 14.14 m^2. The case (0 m^2) represented the living-room without the conservatory, but with a double glazed external window.

A.2.5 Heating

The living-room was continuously heated to 21°C. The conservatory was unheated.

A.2.6 Ventilation

The living-room was well sealed and ventilated (with outside air) at a low basic air change rate of 0.35 ach.

The base-case conservatory was not ventilated. Interzonal air-flow between conservatory and living-room was not considered. However, in one study the effect of interzonal air flow was examined. In this case, the following air flow path was modelled: external -> conservatory -> living-room -> external. The following air change rates were considered: 14 m^3/h; 14 m^3/h (80 m^3/h between 12am and 4pm); 14 m^3/h (200 m^3/h between 12am and 4pm).

A.2.7 Location

The building was located at Kew near London (UK): latitude = 51.5° North; longitude = 0°.

The site was flat and unobstructed with respect to the wind and sun (no shading from other buildings was considered). The ground reflectance was 0.2.

A.3 COMMERCIAL BUILDING TEST MODULE

A.3.1 Introduction

To study the impact of glazing properties on the predicted performance of commercial buildings (Chapter 5), a three-zone test module was chosen. The module was similar to that being used by the IEA Annex 21 and Task 12 model evaluation groups (Kataja and Kalema 1992).

The use of the test module had the following advantages:

(i) It is appropriate for exploring specially coated and tinted glazings. These are increasingly popular in commercial buildings to reduce the solar load in highly glazed office rooms.

(ii) The simulation results of the base-case building could be compared with reference results from other DSMs (e.g. BLAST (Italy), ESP (UK), S3PAS (Spain) etc.) which took part in the IEA evaluation study. Thus, the likelihood of simulation mistakes (e.g. due to incorrect input parameters) could be reduced.

(iii) The three-zone commercial building module was part of a larger building, chosen to represent the thermal conditions in a typical office. It had the advantage of a quick and uncomplicated calculation.

In the sensitivity studies, the clear double glazing used in the IEA work was replaced by different types of special glazing. These glazings are detailed described in Chapter 5 (section 5.6.2)

A.3.2 The test module

The test module consisted of two rooms with a corridor between them (Fig. A.3). The corridor was separated from the office rooms by an internal wall and a door. The area of the window on each external wall was 2.52 m². The building was orientated so that the windows face North and South. Adjacent spaces were thermally identical to the space bounding it. The corridor was closed by the internal walls and doors.

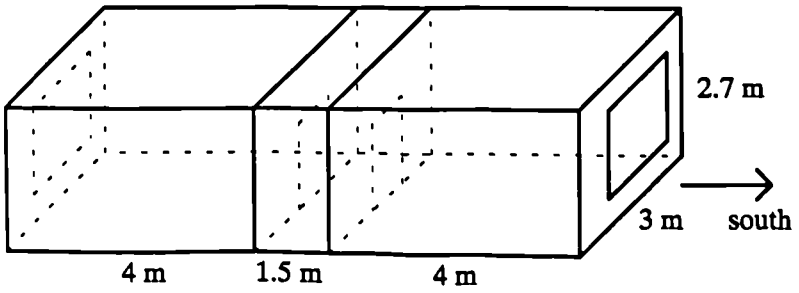

Figure A.3:
Three-zone test module of a commercial building.

The detailed description of the test module including all wall constructions are presented in an IEA Task 12 Annex 21 report (Kataja and Kalema 1992). The most important building details are presented in Table A.13.

WALLS:	The outside walls are well-insulated and heavy-weight (U = 0.53 W/m²K) The inside walls are light-weight The floor/ceiling is of heavy concrete		
VENTILATION RATE:	8°° - 17°°	2.47 ach	
	17°° - 8°°	0.41 ach	
INTERNAL HEAT LOADS:	9°° - 16°°	Room1: 500W Room2: 500W	
HEATING AND COOLING:	Heating set point:	8°° - 17°°	20°C
		17°° - 8°°	18°C
	Cooling set point:		25°C

Table A.13: Design and performance of the commercial building test module.

A.3.3 Modified building version

The basic IEA building had: an extremely high ventilation rate (2.47 ach in the daytime); high internal lighting heat gains (500 W in every room); and a relatively small window size (2.52 m²). All three aspects reduce the influence of solar radiation on the inside climate. In commercial buildings with less ventilation, lower casual heat gains, and bigger windows, the impact of the energy transmission through the glazing will be greater. Therefore, any inaccuracies in the glazing properties will have a greater impact.

To produce a building which was more sensitive to glazing properties, three changes were made to the basic IEA building description:

(i) the lighting system was switched off;
(ii) the day-time ventilation rate was reduced to a constant 0.41 1/h; and
(iii) the areas of the window were increased to 8.1 m² (i.e. the total external wall area).

A.3.4 Locations

The building was subjected to the climatic conditions in two different locations:

(i) Kew (UK), latitude 51.5° North, longitude 0°; and
(ii) Denver, Colorado (USA), latitude 39.8° North, longitude 104.9° West.

The building site was flat and unobstructed with respect to the wind and sun (no shading from other buildings was considered). The ground reflectance was 0.2.

A.4 DWELLING WITH ATTACHED CONSERVATORIES

A.4.1 Introduction

In contrast to the conservatory sensitivity study (Appendix A.2) the conservatory design study (Chapter 9) required a more realistic building design.

In selecting a useful building arrangement the following three effects were considered:

(i) the benefit of any passive solar feature depends strongly on the utilisation of the solar energy, which, in turn, depends on the solar energy available, the heat loss, and the thermal storage of the room;

(ii) the inside climate of the conservatory (and therefore its impact on the energy demand of the parent building) is strongly influenced by the thermal coupling with the parent building; and

(iii) the climatic conditions in the adjacent room influences the conservatory temperatures and therefore its time-of-usability.

Three different cases were investigated for the space attached to the conservatory:

(i) a virtual space with a defined heat loss and a defined storage mass, but without an explicitly modelled room envelope;

(ii) a typical domestic living-space, which considers neighbourhood zones in a non-explicit manner; and

(iii) a realistic multi-zone domestic building.

The investigation showed that virtual spaces can not reflect the thermal conditions in the room realistically enough. The temperature level in the room and the heat flow into the conservatory turned out to be strongly influenced by the thermal coupling of the walls, the window and the air. If a conservatory was modelled in connection with a comparable realistic room (same total heat loss; same storage mass), the conservatory climate and its impact on the energy demand of the room differed noticeably from those using a virtual space model. This was because a realistic room treats the longwave interaction between walls and window, and the convective energy transport between air and windows (and walls) separately. In contrast, the virtual space model assumed a combined convective and radiative connection between the air and the window surface. This led to different energy balances.

The investigation also showed that the use of a multi-zone dwelling to study the energy benefits of attached conservatories is unfavourable. A conservatory has a considerable affect on the heating energy demand of the adjacent room, however, it has an energy impact, which is small in comparison to the total energy demand of the whole house. So, if a whole

dwelling is considered, the comparison and evaluation of very small differences in heating energy would be necessary.

These considerations led to the conclusion, that the best arrangement would be to consider conservatories connected to a single adjacent room (Fig. A.4). This method also has the advantage of a quick and uncomplicated calculation while considering all the complex thermal interactions of realistic rooms.

The following sections describe the base-case arrangement of conservatory and adjacent room. Design variations (except of the glazing types) are not described here. These are discussed in detail in Chapter 9.

A.4.2 The two-zone module

For the adjacent room the typical UK living-room as described in Appendix A.1 was used. The base-case room had a heavy-weight, modern-insulated construction with an average U-value of 0.5 W/m²K (for wall constructions see Tables A.1 to A.8, section A.1.3). The south wall adjoined the conservatory. The common wall between living-room and conservatory had the same insulation level as the external west wall (W2, see Table A2). The north and east partition walls, and the ceiling, bordered adjacent zones, which were not modelled explicitly (see section A.1.2).

The conservatory was very similar to that used in the sensitivity studies (Appendix A.2). However, to consider a more realistic inclination for the conservatory roof (30°), the roof had to be connected to the external wall of the upper living-zone (which was not modelled explicitly). In practise, such a design permits the pre-heated conservatory air to ventilate the upper zone through openings in the wall. The construction of the conservatory floor corresponded to that of the living-room (F1, see Table A.7). The surface reflectance of all opaque internal surfaces was 0.2 (dark colour).

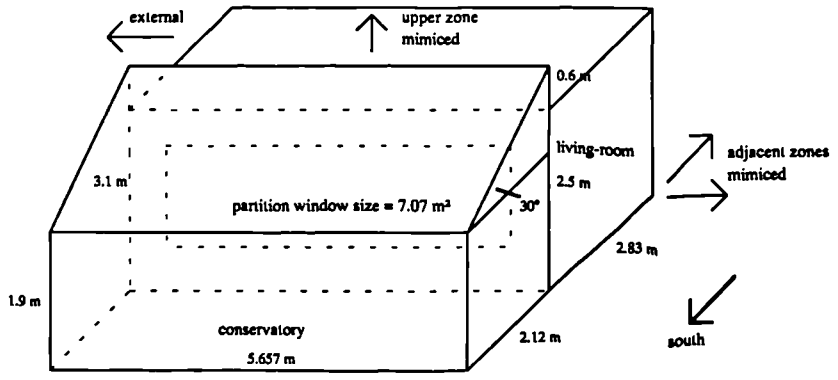

Figure A.4:

Two-zone module of a typical UK dwelling with attached conservatory.

A.4.3 Windows

There was a 7.07 m² glazing area between living-room and conservatory, which corresponded to half of the total partition area. The window was located in the centre of the partition wall. The partition window, as well as the conservatory, were double glazed. The conservatory window frames were assumed to cover 15% of the whole glazing area. The U-value of the frames was the same as the U-value of the glazings. Shading devices were not used in the base-case building.

In different studies the partition and conservatory glazing types were varied. The following glazing types were considered:

- single glazing (U-value = 5.6 W/m²K; total solar energy transmittance = 0.83);
- double glazing (U-value = 2.9 W/m²K; total solar energy transmittance = 0.72);
- triple glazing (U-value = 2.0 W/m²K; total solar energy transmittance = 0.59);
- quadruple glazing (U-value = 1.5 W/m²K; total solar energy transmittance = 0.55); and
- low-emittance glazing (U-value = 1.9 W/m²K; total solar energy trans. = 0.62) which corresponded to Pilkington's Kappa-float (neutral) 74/62® (Pilkington 1988).

All glass panes were assumed to be 6 mm thick. The thermal properties of the glass panes and cavities were the same as those described in section A.1.4 and Table A.9.

The solar properties of the glazings were calculated using the improved calculation possibilities of the program GLSIM. The incidence angle dependent direct transmittance τ and absorptance α, as well as the diffuse transmittance and absorptance (index f), are listed in the Tables A.14 to A.18.

Inc. angle:	0	10	20	30	40	50	60	70	80	90	f
τ:	.764	.763	.761	.755	.744	.722	.675	.571	.343	.0	0.673
α:	.166	.167	.170	.174	.180	.186	.192	.192	.174	.0	0.18

Table A.14: Incidence angle dependent transmittance τ and absorptance α and the diffuse transmittance and absorptance (f) of 6 mm clear single glazing.

Inc. angle:	0	10	20	30	40	50	60	70	80	90	f
τ:	.601	.600	.595	.588	.575	.550	.498	.383	.174	.0	0.502
α:	.288	.289	.294	.300	.308	.317	.322	.316	.273	.0	0.304

Table A.15: Incidence angle dependent transmittance τ and absorptance α and the diffuse transmittance and absorptance (f) of 2×6 mm clear double glazing.

Inc. angle:	0	10	20	30	40	50	60	70	80	90	f
τ:	.481	.479	.475	.467	.455	.433	.385	.274	.098	.0	0.390
α:	.381	.382	.387	.395	.404	.413	.415	.399	.327	.0	0.393

Table A.16: Incidence angle dependent transmittance τ and absorptance α and the diffuse transmittance and absorptance (f) of 3×6 mm clear triple glazing.

Inc. angle:	0	10	20	30	40	50	60	70	80	90	f
τ:	.390	.389	.385	.378	.368	.350	.308	.205	.060	.0	0.311
α:	.453	.455	.459	.467	.476	.483	.482	.455	.357	.0	0.458

Table A.17: Incidence angle dependent transmittance τ and absorptance α and the diffuse transmittance and absorptance (f) of 4×6 mm clear quadruple glazing.

Inc. angle:	0	10	20	30	40	50	60	70	80	90	f
τ:	.504	.503	.501	.495	.484	.462	.417	.318	.143	.0	0.421
α:	.310	.311	.315	.321	.329	.337	.341	.332	.283	.0	0.323

Table A.18: Incidence angle dependent transmittance τ and absorptance α and the diffuse transmittance and absorptance (f) of 2×6 mm double glazing consisting of a clear outer pane and a low-emittance coated inner pane (Pilkington Kappa-float (neutral) 74/62®)

The absorbed radiation was distributed between the different glass panes of the glazings as follows (absorbed radiation split):

clear double glazing - outer pane 59%, inner pane 41%;
clear triple glazing - outer pane 50%, middle pane 33%, inner pane 17%;
clear quadruple glazing -outer pane 33%, 2.pane 28%, 3.pane 22%, inner pane 17%; and
low-emittance glazing - outer pane 54.5%, inner pane 45.5%.

A.4.4 Heating

The living-room was heated to 21°C from 7am to 11pm. During the night there was a 'set-back' to 16°C.

The base-case conservatory was not heated. To study the energy demand of heating a conservatory additional investigations considered a conservatory heated to a setpoint of 21°C. It was assumed, that conservatories are very unlikely to be heated throughout the night, when they are not occupied. Thus, the heating period was restricted to the occupied period, which was 7am to 11pm.

A.4.5 Ventilation

The living-room was ventilated with a fixed infiltration rate of 1.0 ach (5 ach when the inside air temperature exceeded 27°C).

The conservatory was ventilated at a rate of 1.0 ach (15 ach when the air temperature exceeds 27°C). Inter-zonal air-flow (SPV) between conservatory and living-room was not considered.

A.4.6 Locations

The building was simulated for three different locations:

(i) Kew (UK), latitude 51.5° North, longitude 0°;
(ii) Denver, Colorado (USA), latitude 39.8° North, longitude 104.9° West; and
(iii) North-Württemberg (G), latitude 48.8° North, longitude -15° East.

Because errors were inferred in the climate data for Kew, data for Sheffield were used in this study. Nevertheless, the location for Kew was kept (see also Appendix B).

The building site was flat and unobstructed with respect to the wind and sun (no shading from other buildings considered). The ground reflectance was 0.2.

A.5 DWELLINGS WITH INTEGRATED CONSERVATORIES

A.5.1 Introduction

Compared to attached conservatories, integrated conservatories usually have more than one adjacent space. Because the coupling between the conditions in the building and the conservatory is more pronounced, the conservatory has a greater impact on the whole building. It was therefore decided, to study both semi-enclosed conservatories and corner conservatories connected to realistic multi-zone domestic dwellings.

A.5.2 The dwelling

The semi-enclosed and corner conservatories were integrated into a two-storey UK dwelling. The conservatories covered both storeys (Fig. A.5 and A.6). For comparison purposes, the same dwelling was investigated in connection with a two-storey attached conservatory (Fig. A.7).

The dwelling was treated as a three-zone arrangement of heated living-space, unheated roof-space and conservatory.

In the case of integrated (semi-enclosed and corner) conservatories, the living-space had a ground floor area (and partition floor area) of 60 m^2 and a volume of 312 m^3. The conservatory had a floor area of 12 m^2 and a volume of 72.8 m^3. The unheated roof-space had a volume of 51.9 m^3.

In the case of attached conservatories, the living-space ground floor area increased to 72 m^2, its volume increased to 374 m^3 and the roof-space volume increased to 62.3 m^3. The attached conservatory also had a floor area of 12 m^2, but its volume was 62.3 m^3.

The construction and insulation level of the dwelling was the same as for the two-zone living-room and conservatory (see section A.4.2) with the exception of the living-space ceiling (construction C1, see Table A.6). Since the roof-space was unheated an additional layer of insulation (100 mm fibre glass) was added. The roof itself had the same construction as the ceiling, but without additional insulation (construction C1). The roof was inclined with an inclination angle of 30°.

Although the different rooms of the living-space were not explicitly modelled, the internal storage mass was partly considered (100 mm thick internal concrete partition floor). The common walls between the living-space (and roof-space) and the conservatory had the same construction and insulation level as the external walls (W2, see Table A.2).

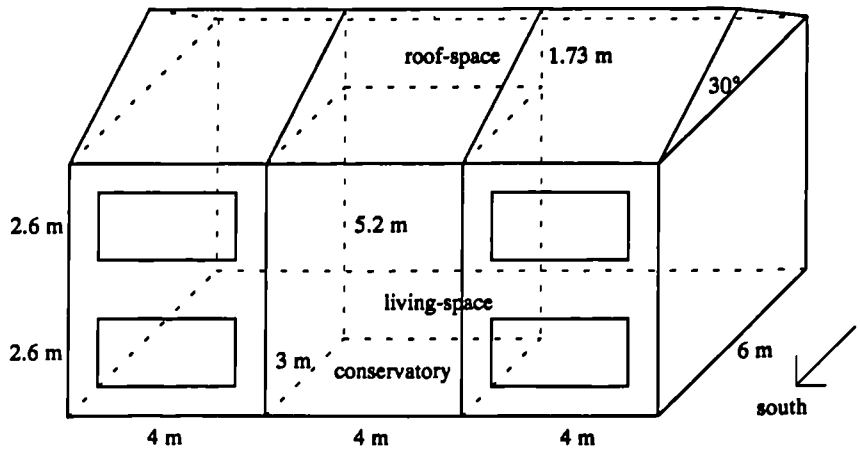

Figure A.5:

Three-zone dwelling with semi-enclosed conservatory.

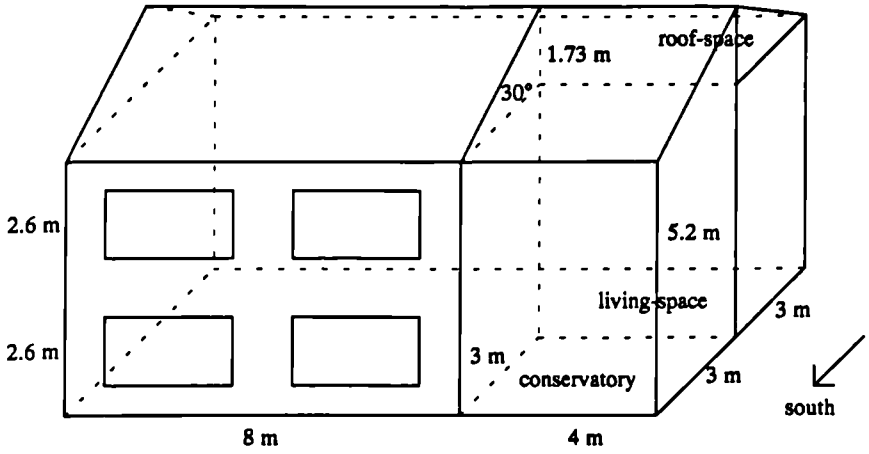

Figure A.6:

Three-zone dwelling with corner conservatory.

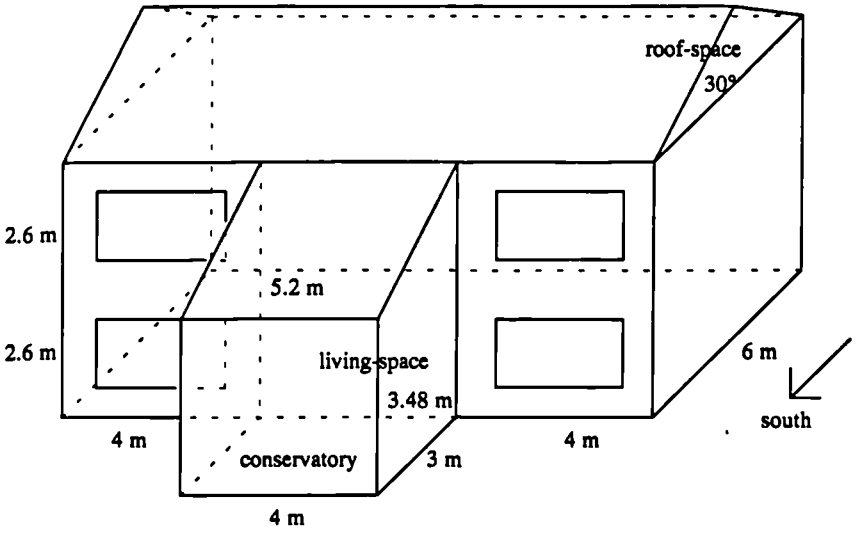

Figure A.7:

Three-zone dwelling with attached conservatory.

A.5.3 Windows

The dwelling had four exposed south-facing windows with a total area of 20.8 m². This represented about 50% of the exposed south wall area. In addition, the dwelling had north-facing windows with a total area of 6.24 m² which represented 10% of the north wall area. Since the simulation program HTBSOL (HTB2 connected with the solar distribution model SUNSIM) did not consider the geometry of conventional zones (living-room) explicitly, the exact location of the windows in the walls was not defined.

The conservatory was simulated as a special 'greenhouse zone', with the geometry of the zone, the walls and the windows considered in detail. The partition glazing, between the heated space and the conservatory, was 50% of the total partition area, i.e. 26 m^2 for the semi-enclosed conservatory, 18.2 m^2 for the corner conservatory and 10.4 m^2 for the attached conservatory. The glazing was located in the centre of each partition wall.

The external windows of the dwelling were, in all simulations, double glazed. However, the glazing type of the partition windows and conservatory windows were varied:

- single glazing (U-value = 5.6 W/m^2K; total solar energy transmittance = 0.83);
- double glazing (U-value = 2.9 W/m^2K; total solar energy transmittance = 0.72);
- low-emittance glazing (U-value = 1.9 W/m^2K; total solar energy trans. = 0.62) which corresponded to Pilkington's Kappa-float (neutral) 74/62® (Pilkington 1988).

The glazing types correspond to those described in the Tables A.14 to A.18 (section A.4.3). Frames were only considered for the conservatory. These were assumed to cover 15% of the whole glazing area. The U-value of the frames was the same as the U-value of the glazing. Conservatory shading devices were not modelled.

A.5.4 Heating and ventilation

The heating and ventilation was the same as that for the two-zone module (living-room plus conservatory) described in sections A.4.4 and A.4.5.

A.5.5 Location

The dwelling was located at Kew (UK), latitude 51.5° North, longitude 0°.

Sheffield climate data were used in this study because of errors in the climate data of Kew. Nevertheless, the location Kew was kept (see also Appendix B).

The building site was flat and unobstructed with respect to the wind and sun (no shading from other buildings considered). The ground reflectance was 0.2.

B.1 DAILY SIMULATIONS

For daily simulations UK design day data devised by Loxsom (1985) were used. These data files consist of one single day of hourly data. To facilitate use by DSMs, a number of these days have been strung together to produce 20 days of repeating values (thus a pre-simulation time of 19 days can be considered).

Single day simulations permit numerous inter-model comparisons to be made because simulation times are very short. It is also possible to isolate the specific meteorological conditions for which different program algorithms produce good agreement and the conditions for which they do not. The meteorological conditions considered are listed in Table B.1.

Day	Description	Date
1	cold, pure diffuse winter's day	1/1
2	cold, sunny winter's day	1/1
3	pure diffuse spring day	1/4
4	sunny spring day	1/4
5	pure diffuse summer's day	1/7
6	hot, sunny summer's day	1/7

Table B.1: Single design days after Loxsom (1985).

The winter design conditions were generated from a statistical analysis of the January conditions during a ten year period from 1958 to 1967 at Kew. The spring conditions were generated by analysing data for April and the summer conditions by examining the data for July.

Each day contains 24 values for each of the climate parameters. These are

- for the programs HTB2 and SERI-RES - direct normal irradiation (kJ/m²), total horizontal irradiation (kJ/m²), air temperature (°C), dew point temperature (°C), wind speed (m/s), and wind direction (deg from North); or
- for the program ESP - diffuse horizontal irradiation (W/m²), air temperature (°C), direct normal irradiation (W/m²), wind speed (m/s), wind direction (deg from North), relative humidity (%).

Table B.2 summarises the minimum temperature, the maximum temperature, the maximum total horizontal irradiation and the total daily horizontal radiation energy of the design days. The total horizontal irradiation includes direct and diffuse radiation.

Day	Minimum daily temperature, °C	Maximum daily temperature, °C	Maximum total horizontal irradiation, W/m²	Total daily horizontal radiation energy, kWh/m²
1	-2.4	-0.4	47	0.25
2	2.2	5.5	240	1.12
3	5.8	13.8	241	2.28
4	5.8	13.8	688	5.41
5	13.5	20.0	278	2.6
6	13.3	24.4	763	7.05

Table B.2: Characteristics of the design day data.

Because the design days represented Kew (London) climate conditions, the same geographical location was used for the buildings: latitude = 51.5° North, longitude = 0°.

Fixed ground temperatures were used for all the design days. The values of 7.28°C for January (day1 and day2); 7.33 °C for April (day3 and day4); and 13.5°C for July (day5 and day6), are quoted as being typical of the UK at 1.3 m depth (see Clark and McLean 1988).

B.2 ANNUAL SIMULATIONS

Annual simulations were conducted using CIBSE Example Weather Years (EWY) for Kew (UK) and Finningley near Sheffield (UK), an EC (European Community) Test Reference Year (TRY) for North-Württemberg (Germany) and a NCC (National Climatic Centre) Typical Meteorological Year (TMY) for Denver, Colorado (USA) (for definition of Reference Years see for example Keeble 1990). Each year contains 8760 values of the climate parameters. These are

- for the programs HTB2 and SERI-RES - direct normal irradiation (kJ/m²), total horizontal irradiation (kJ/m²), air temperature (°C), dew point temperature (°C), wind speed (m/s), and wind direction (deg from North); or
- for the program ESP - diffuse horizontal irradiation (W/m²), air temperature (°C), direct normal irradiation (W/m²), wind speed (m/s), wind direction (deg from North), relative humidity (%).

It should be noted that the original Reference Years include several more climate parameters which are, however, not used by the DSMs.

To characterise the different climate files, the annual average of the external air temperature, the annual degree-days to the base of 15.5°C and the annual total horizontal irradiation per m² were calculated (Table B.3).

Location (code)	Average annual external air temperature, °C	Degree-days to base 15.5°C, Kelvin×days	Total annual horizontal irradiation, kWh/m² year
Kew	10.0	3482	928
Finningley	9.0	3906	878
North-Württemberg	9.0	3895	1119
Denver	9.7	3829	1832

Table B.3: Characteristics of the annual climate data.

In addition, to demonstrate the annual external temperature distribution, the hourly average external air temperatures were attributed to 5 K temperature ranges (Figs. B.1 and B.2). The numbers quoted are the absolute annual numbers of hours, for which the average temperature lies in a certain range. The Kew and Denver climate conditions, as used in Chapter 5 to study the influence of glazing properties, are shown in Fig. B.1. The Sheffield and North-Württemberg climate conditions, which were important in the conservatory design study (Chapter 9), are compared in Fig. B.2.

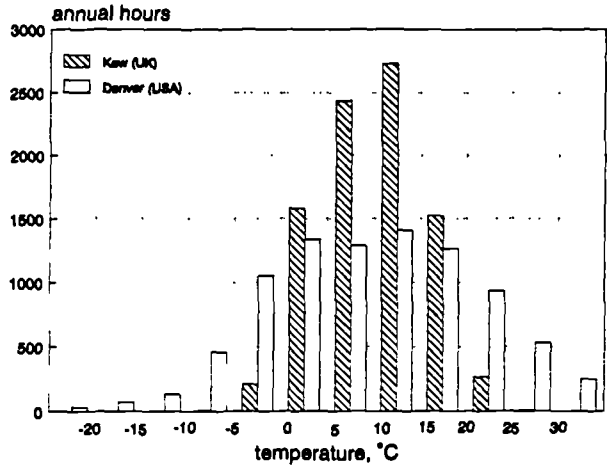

Figure B.1:

Absolute number of hours for which the external air temperature lies in a certain range.

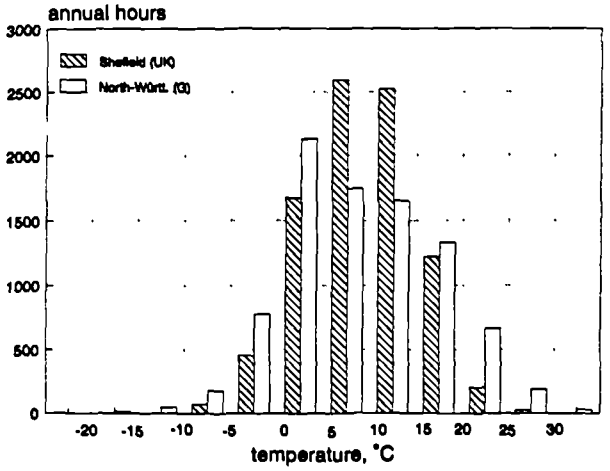

Figure B.2:

Absolute number of hours for which the external air temperature lies in a certain range.

Kew and Sheffield represent moderate maritime climates with reduced seasonal temperature variations and relatively frequent overcast conditions (low solar irradiation). North-Württemberg has a typical middle European continental climate with cold, clear winters and warm, sunny summers (high solar irradiation). Denver represents an extreme continental climate with very cold and clear winters and very sunny summers (solar irradiation is very high).

The different climate files represented the following geographical locations:

- Kew and Sheffield - latitude: 51.5°, longitude = 0°;
- North-Württemberg - latitude: 48.8°, longitude = 15° East;
- Denver - latitude: 39.8°, longitude = 104.9° West.

To minimise the differences between Kew and Sheffield climate conditions in the conservatory design study (Chapter 9), the latitude of Kew was used in conjunction with the Sheffield climate.

The climate files represented the local climate conditions and local sun time. Since the buildings were located at the weather data site, the longitude difference was zero.

For all annual simulations, a ground temperature of 10°C was used.

APPENDIX C GLAZING PROPERTIES

C.1 GLAZING PROPERTIES OF DIRECT RADIATION

Usually, the glazing properties for the direct radiation at normal (0°) incidence (e.g. τ^n, α^n) are published (in the literature or by the glass producers, see Table C.6). In practise, of course, the incidence angle of the solar radiation is not fixed; it varies with the sun position and is therefore highly dependent on the geographical location and the time of day. For vertical surfaces the incidence angle is usually greater than 40°; normal incidence rarely happens. DSMs normally use the incidence angle dependent glazing properties (transmittance τ; absorptance α; and reflectance ρ) to take account of the changing sun positions and incidence angles. For special (coated and tinted) glazings these values are generally unknown.

Within this research, the program GLSIM-FILM has been used to calculate the incidence angle dependent glazing properties for most of the current glazing systems. To describe the shape of the glazing properties versus incident angle curves (as produced by GLSIM-FILM), the relative transmittance representation of Krochmann et al. (1992) was adopted. The relative properties p^r (transmittance τ^r; absorptance α^r; reflectance ρ^r) are simply the ratio of the properties at any given angle of incidence p to the value of the corresponding property at normal incidence p^n. All relative properties therefore vary from 1 (at 0° incidence) to 0 (at 90° incidence). The absolute properties p are found by multiplying the relative values p^r by the known, usually published, properties at normal incidence p^n.

(C.1) $$p = p^n * p^r$$

The relative transmittance τ^r and absorptance α^r for the incidence angles 10° to 80° (in steps of 10°) for many common glazing systems (see section C.3) are listed in the Tables C.2 to C.5. The values for the incidence angles 0° (normal incidence) and 90° are not shown, since the corresponding relative glazing properties are always "1.0" or "0" respectively. The reflectance can be calculated from the absolute transmittance and absorptance values as follows:

(C.2) $$\rho = 1 - \tau - \alpha$$

C.2 GLAZING PROPERTIES OF DIFFUSE RADIATION

To describe the diffuse radiation transfer through glazings two different representations are commonly used: (i) the diffuse glazing properties p_f (transmittance τ_f, absorptance α_f, and reflectance ρ_f); and (ii) the equivalent beam incidence angle θ_f, such that, for the particular glazing system τ_f corresponds to the direct transmittance at an incidence angle of θ_f.

Many DSMs need either the diffuse glazing properties or the equivalent incidence angles to calculate the diffuse radiation transfer through glazings. The program GLSIM-DIF has been used to produce these values. To describe the diffuse glazing properties the relative representation has been adopted. The relative diffuse glazing transmittance τ_f^r, absorptance α_f^r and the equivalent incidence angle θ_f for the most common glazing systems are listed in the Tables C.2 to C.5. These values are valid for vertical windows on overcast (purely diffuse) days and for a ground reflectance of 0.2. The absolute diffuse radiation properties p_f can be found by multiplying the relative values p_f^r by the given glazing properties at normal (0°) radiation incidence p^n (see equation C.1).

To take account on non-vertical windows, within this research, a tilt correction c_η (Table C.1) has been introduced which approximately represents the variation of the equivalent incidence angle as the window inclination angle η varies. (The window inclination angle η is the angle between the surface normal and a vertical plane, i.e. 0° for horizontal). An investigation using GLSIM-DIF has shown that this correction is approximately valid for all glazing types listed in Tables C.2 to C.5 (see Fig. 4.4 in Chapter 4 for clear glazings). Thus, the equivalent incidence angle for inclined windows $\theta_f(\eta)$ can be calculated from the equivalent incidence angle for vertical windows θ_f as follows:

(C.3) $$\theta_f(\eta) = \theta_f - c_\eta$$

inclination angle η	0°	15°	30°	45°	60°	75°	90°
tilt correction c_η	6.5°	12.4°	15.6°	13.2°	7.5°	2.1°	0°

Table C.1: Tilt correction of the equivalent beam incidence angle for non-vertical windows.

C.3 GLAZING TYPES

It has been found (see Chapter 5) that most glazing systems can be divided into one of the following five groups:

(i) systems with one or more clear glass panes (Table C.2);

(ii) systems with single noble metal coatings (Table C.3);

(iii) glazings with multi-layered coating systems consisting of noble metal and dielectric coatings (usually metal oxides) (Table C.4);

(iv) glazings with tinted glass panes (Table C.5); and

(v) glazings with pure dielectric (oxide) coatings.

For each group, characteristic relationships exist between the angle of radiation incidence and the glazing properties. A method to calculate the glazing properties for glazings with

pure dielectric coatings (system v) is outlined in Chapter 5, section 5.5.2. For the systems (i) to (iv), the relative glazing properties are listed in the Tables C.2 to C.5. The following points are important.

- The glazing properties listed (in the Tables C.2 to C.5) are valid for glazing systems consisting of one or more 6 mm thick glass panes, with or without additional coating systems. However, since the thickness of the glass panes rarely influences the relative glazing properties, the values can also be used for glazing systems consisting of panes with other thicknesses.
- The location of the coating system (and the tinted glass pane) does not influence the relative transmittance and rarely influences the relative absorptance. It is therefore appropriate to use the given values for different locations of the coating system in a multi-layer glazing. For example, there is nearly no difference, when a coating system (in a double glazing unit) is located at the inside of the outer pane or at the outside of the inner pane.
- GLSIM-FILM calculates only one value of absorptance for each incidence angle. This value corresponds to the total absorptance in a glazing system. For multi-layer glazing systems, the knowledge of the absorptance-split between the different panes is necessary. The following formulation can be used to derive, for double glazing units, the ratio of the net-absorptance α^i in the inner glass pane to the total absorptance α^T of both panes:

(C.4) $$\frac{\alpha^i}{\alpha^T} = \frac{\tau^n_{tot} - \tau^n_d}{U * \alpha^T * (1/U - R_o - R_i)} - \frac{R_o}{1/U - R_o - R_i}$$

  where τ^n_{tot} is the total solar energy transmittance for normal incidence, τ^n_d the direct transmittance for normal incidence, and U the U-value of the glazing. These properties are usually quoted by the glazing producers. R_o and R_i are the outside and inside surface resistances respectively (see CIBSE-Guide 1986 or DIN 67507, 1980). It should be noted that this method approximately assumes that the relative absorptance split is independent of the radiation incidence angle.
- The glazing properties for glazing systems with single noble metal coatings (system ii) depend on the thickness of the noble metal layer. This can be derived by using the method outlined in Chapter 5, section 5.5.2 (Fig. 5.5).

Methods by which a particular glazing system can be recognised from the producers' data are outlined in Chapter 5, sections 5.2 and 5.5.2.

panes	θ:	10°	20°	30°	40°	50°	60°	70°	80°	diffuse	θ_f
single	τ^r:	.999	.995	.988	.973	.944	.883	.746	.449	.880	60°
	α^r:	1.006	1.022	1.049	1.083	1.12	1.152	1.153	1.048	1.083	
double	τ^r:	.998	.991	.979	.957	.915	.829	.637	.289	.836	59°
	α^r:	1.00	1.02	1.04	1.07	1.10	1.12	1.10	.949	1.06	
triple	τ^r:	.997	.988	.972	.946	.900	.801	.570	.205	.801	60°
	α^r:	1.004	1.017	1.037	1.061	1.083	1.090	1.047	.858	1.032	

Table C.2: Relative transmittance and absorptance of clear glazings with 6 mm glass panes.

thickness	θ:	10°	20°	30°	40°	50°	60°	70°	80°	diffuse	θ_f
5 nm	τ^r:	.999	.993	.982	.964	.930	.858	.683	.325	.854	60°
	α^r:	1.003	1.017	1.037	1.064	1.091	1.108	1.082	.927	1.047	
10 nm	τ^r:	.998	.993	.985	.971	.949	.896	.746	.382	.877	61°
	α^r:	1.004	1.017	1.036	1.063	1.09	1.105	1.081	.925	1.045	
15 nm	τ^r:	.998	.993	.987	.977	.964	.926	.801	.440	.898	62°
	α^r:	1.006	1.018	1.038	1.065	1.090	1.107	1.083	.926	1.047	
20 nm	τ^r:	.998	.992	.987	.980	.973	.949	.846	.490	.913	63°
	α^r:	1.004	1.019	1.039	1.065	1.091	1.107	1.081	.929	1.047	

Table C.3: Relative transmittance and absorptance of double glazing systems with 2 × 6 mm clear glass panes and one noble metal coating. The thickness of the noble metal coating is varied.

	θ:	10°	20°	30°	40°	50°	60°	70°	80°	diffuse	θ_f
	τ^r:	.998	.993	.981	.956	.905	.800	.595	.267	.822	58°
	α^r:	1.004	1.016	1.035	1.060	1.083	1.094	1.064	.904	1.038	

Table C.4: Relative transmittance and absorptance of double glazing systems with 2 × 6 mm clear glass panes and a multi-layered coating system.

tint	θ:	10°	20°	30°	40°	50°	60°	70°	80°	diffuse	θ_f
green	τ^r:	.996	.984	.962	.928	.874	.774	.587	.255	.806	57°
	α^r:	1.003	1.011	1.025	1.041	1.055	1.053	1.008	.821	1.008	
grey	τ^r:	.994	.978	.949	.905	.840	.734	.540	.222	.774	58°
	α^r:	1.004	1.015	1.033	1.054	1.074	1.081	1.045	.857	1.027	
bronze	τ^r:	.995	.980	.954	.914	.854	.750	.555	.230	.788	56°
	α^r:	1.004	1.015	1.034	1.056	1.076	1.086	1.053	.874	1.031	

Table C.5: Relative transmittance and absorptance of double glazing systems with 2 × 6 mm glass panes consisting of one one clear and one tinted glass pane with the given colour.

To illustrate the link between glazing types and the Tables C.2 to C.5, Table C.6 summarises the transmittance and absorptance values for normal incidence of some glazings used within this thesis (see Chapter 5 and Chapter 9). For every glazing, the Table number, where the appropriate relative glazing properties p^r are listed, is given.

glazing type	transmittance τ^n	absorptance α^n	Table for p^r
6mm clear single glazing	0.764	0.166	C.2
2×6mm clear double glazing	0.601	0.288	C.2
3×6mm clear triple glazing	0.481	0.381	C.2
4×6mm clear quadruple glazing	0.390	0.453	C.2
Pilkington Kappa-float 74/62®	0.504	0.310	C.4
Pilkington SunCool 20/34®	0.160	0.660	C.3
Pilkington Antisun grey 36/48®	0.350	0.590	C.5
Schott Calorex A0 50/48®	0.440	0.230	see section 5.5.2

Table C.6: Glazing properties for normal radiation incidence as used in the thesis and number of the Table where the relative incidence angle dependent properties are listed.

C.4 EXAMPLE

As an example suppose that the incidence angle dependent transmittance and absorptance of the direct radiation and the transmittance and absorptance of the diffuse radiation for the sun-reflective double glazing Interpane Ipasol-blau 53/38® has to be calculated. The following glazing-data are given by the producer (Interpane 1990):

direct normal transmittance $\tau^n = 0.33$;
direct normal absorptance $\alpha^n = 0.41$;
total solar energy transmittance at normal incidence $\tau^n_{tot} = 0.38$; and
U-value = 1.4 W/m²K.

The coating system of the glazing is most likely to be multi-layered (dielectric and noble metal films), because of the low-emittance quality of the glazing (this can be supposed because the U-value of a glazing is lower than 2.9 W/m²K) and the bluish colour (quoted by the producer) which is typical for dielectric coatings (see also Gläser 1990).

The incidence angle dependent glazing properties of the direct radiation and the diffuse radiation properties can be derived by multiplication of the relative properties listed in Table C.4 (for multi-layered coating systems) with the known properties for normal incidence (see above). The resultant absolute incidence angle dependent transmittance and absorptance values are listed in Table C.7.

incidence angle θ:	0	10	20	30	40	50	60	70	80	90
τ:	.330	.329	.328	.323	.315	.299	.264	.196	.088	0
α:	.410	.412	.417	.424	.435	.444	.449	.436	.371	0

Table C.7: Incidence angle dependent transmittance τ and absorptance α of Ipasol-blau 53/38®.

The absolute transmittance for diffuse radiation τ_f is 0.271 which is equal to the direct transmittance at 58° (θ_f). The absolute diffuse absorptance α_f is 0.426. These values are valid for vertical windows on overcast days.

The absorptance split between the two glass panes can be calculated using equation (C.4). By considering an internal surface resistance R_i of 0.14 m²K/W and an external resistance R_o of 0.04 m²K/W the net-absorptance of the inner pane becomes 9 % of the total absorptance. The net-absorptance of the outer pane is obtained by taking the difference from one (91 %).

D.1 BASIC PRINCIPLES

The radiation transmission through slat-type blinds is divided into four different radiation paths:

1. the unshaded transmission of the direct beam (direct transmittance);
2. the direct-reflected beam at the slat surfaces (direct-reflected transmittance)
   The reflectance may be pure diffuse, pure specular (metallic) or any combination between both;
3. the unshaded transmission of the diffuse radiation (diffuse transmittance);
4. the reflected diffuse radiation at the slat surfaces (diffuse-reflected transmittance).

The calculation considers the inter-reflections between the slats and between the glass panes and the slats. The incident angle dependent transmittance through a glazing behind a blind (external device) is treated by considering the true or effective incidence angle of both the directly received radiation and the radiation reflected from the slats. The effect of curved slats is approximately considered.

The following sections concentrate on the calculation principles of the different radiation portions. The basic symbols used to describe blind systems are demonstrated in Fig. D.1 Since the slats are assumed to be of infinite length, the spatial blind geometry is reduced to two dimensions. The slat geometry is fully described by the slat width (*sw*) the slat distance (*sd*) and the slat inclination angle (*si*). Usually the slat width corresponds approximately to the slat distance. This is called *regular* blind geometry.

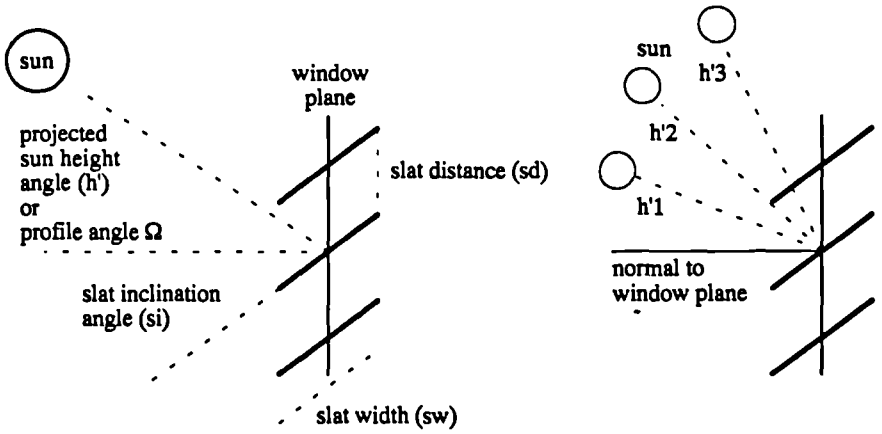

Figure D.1: Basic symbols and angles used to describe the blind systems. The right Figure demonstrates the projected sun height angles (h'1 - h'3) for different illumination situations.

The ability of horizontal panels or slats to intercept the direct component of solar radiation depends on their geometry and on the projected (effective) sun height angle *h'*. The pro-

jected sun height angle h' determines the effective incidence angle of the direct beam radiation onto the slat surfaces. It is defined as the angular difference between a plane normal to the window and a plane inclined about a horizontal axis in the plane of the window until it includes the sun. It can be calculated from the real sun height angle h_s as follows,

$$h' = \arctan\left(\frac{\sin(h_s)}{\cos(az_s - az_w)*\cos(h_s)}\right) - 90° + \eta \qquad \text{(D.1)}$$

where az_s is the azimuth angle of the sun, az_w the azimuth angle of the window and η the inclination angle of the window (0° for horizontal).

The corresponding angle, which determines the effective incidence angle of a diffuse radiation portion from a certain sky (or ground) point, is called the profile angle Ω. If the sky (or ground) vault is cut into slices, all sky (or ground) points on the same slice surface have fortunately the same height projection (profile angle). It is therefore possible to reduce the two-dimensional integration of diffuse radiation portions (along a height and a slice angle) to a one-dimensional integration along the profile angle Ω (Fig. D.2).

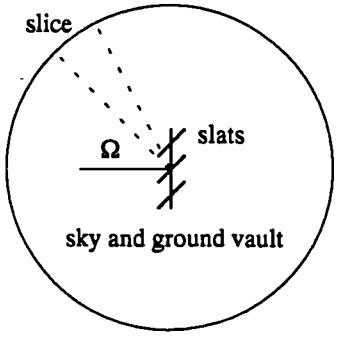

Figure D.2:

Cross-section through the sky and ground vault. The slice surface area corresponds to that area on the sky or ground vault which lies between two curves with constant projected height (or profile) angles.

D.2 DIRECT TRANSMITTANCE

One portion of the direct radiation is shaded by the slats, the other portion enters the room through the unshaded open space between the slats. The direct transmittance τ_d^b is simply the ratio between the unshaded space and the total space between the slats,

$$\tau_d^b = 1 - \frac{sh}{sd} = 1 - sw*\frac{\sin(h' - si)}{\sin(90° - h')*sd} = 1 - (sw*\sin(si) - sw*\cos(si)*\tan(h'))/sd \quad \geq 0 \qquad \text{(D.2)}$$

where sh is the shaded area, sd the slat distance, sw the slat width, and h' the projected sun height angle (Fig. D.3).

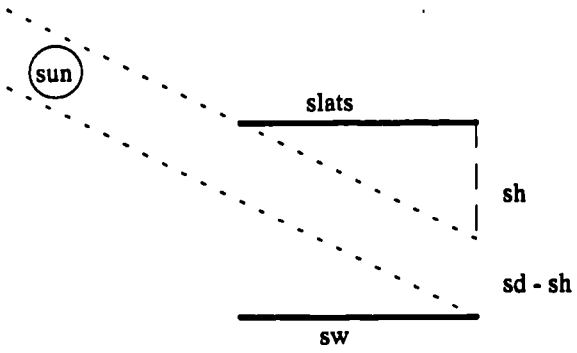

Figure D.3:

Relationship between sunposition and slat geometry to illustrate the shading of direct solar radiation.

D.3 DIRECT-REFLECTED TRANSMITTANCE

The direct-reflected radiation consists of two parts: a direct-to-diffuse reflected radiation portion τ^b_{df} and a specular-reflected radiation portion τ^b_{ds}. The relation between both components depends on the slat material and is defined by the shining factor σ of the material. The shining factor becomes 1 for pure diffuse reflection or 0 for ideal specular reflection.

The radiation split into specular and diffuse-reflected radiation components is considered only for the first reflection. All higher order reflections are either ideal diffuse or ideal specular. This simplification may lead to some inaccuracies, especially when both radiation components occur in similar portions (σ = 0.5). However, the inaccuracy of the shining factor itself is certainly much more important.

D.3.1 Direct-to-diffuse transmittance

The calculation of the direct-to-diffuse reflected radiation considers the multi-reflections between the slats up to the second reflection. This is an appropriate approximation, since the radiation portions after the second reflection becomes very low. The error in this radiation path was found to be lower than 5% for light slats (reflectance, ρ = 0.6) or lower than 1% for dark slats (ρ = 0.2). The direct-to-diffuse reflected radiation is given by

$$\tau^b_{df} = (\rho * f_1 + \rho^2 * f_2 * f_3) * (1 - \tau^b_d) \tag{D.3}$$

where ρ is the slat reflectance and f_1 is the view factor between the illuminated slat area and the inside, f_2 is between the illuminated slat area and the upper slat and f_3 is between the upper slat and the inside. The term (1 - τ^b_d) defines the absorbed or reflected direct radiation component. Substituting the reflectance of the slats by the absorptance (1 - ρ), the total direct absorptance α^b_{df} is given by,

$$\alpha^b_{df} = ((1-\rho) + \rho * f_2 * (1-\rho)) * (1 - \tau^b_d) \tag{D.4}$$

The view factor between the illuminated (lower) slat surface and the inside f_1 corresponds to the relationship between the projection (*pr*) of the slat distance (*sd*) onto the directly il-

luminated slat width (*isw*) and the illuminated slat width (calculation of view factors see also VDI Wärmeatlas 1988),

(D.5) $$f_1 = \frac{pr}{isw} = 0.5*(1-\cos(o1))$$

where *o1* is the opening angle within which the reflected radiation reaches the inside (Fig. D.4). The opening angle *o1* results from the sine-law by considering the opening line (*z1*), the slat distance (*sd*) and the enclosed angle (90°- *si*),

(D.6a) $$o1 = \arcsin\left(\frac{sd*\sin(90°-si)}{z1}\right)$$

(D.6b) $$z1^2 = (sw-0.5*isw)^2 + sd^2 - 2*sd(sw-0.5*isw)*\cos(90°-si)$$

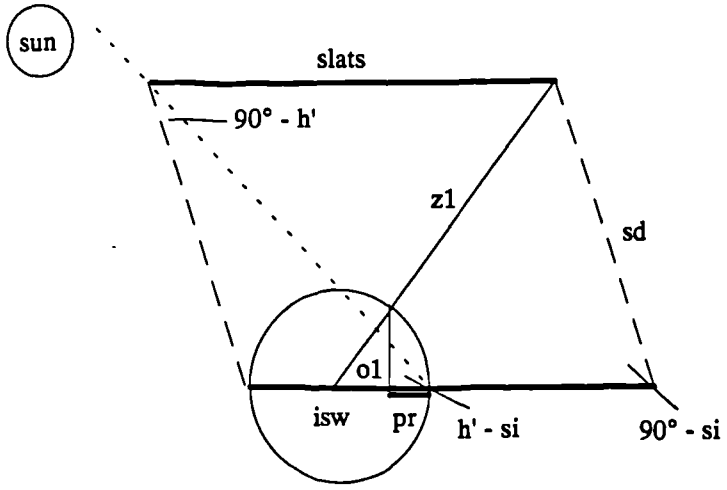

Figure D.4:

Relationship between illuminated slat width and inside to illustrate the view factor f_1.

The illuminated slat width (*isw*) depends on the projected sun height angle (*h'*), on the slat geometry and on the slat inclination (*si*):

(D.7) $$isw = sd*\frac{\sin(90°-h')}{\sin(h'-si)} \le sw$$

When the upper slat is illuminated ($h' < si$) equation (D.7) becomes:

(D.8) $$isw = sd*\frac{\sin(90°+h')}{\sin(h'+si)} \le sw$$

All other equations remain unchanged. The view factor between the illuminated (lower) slat and the upper slat f_2 (Fig. D.5) can be obtained by:

(D.9a) $$f_2 = 0.5*(\cos(o1)+\cos(180°-o1-o2))$$

(D.9b) $$o2 = \arcsin\left(\frac{sw*\sin(o1)}{z2}\right)$$

(D.9c) $$z2^2 = sw^2 + z1^2 - 2*sw*z1*\cos(o1)$$

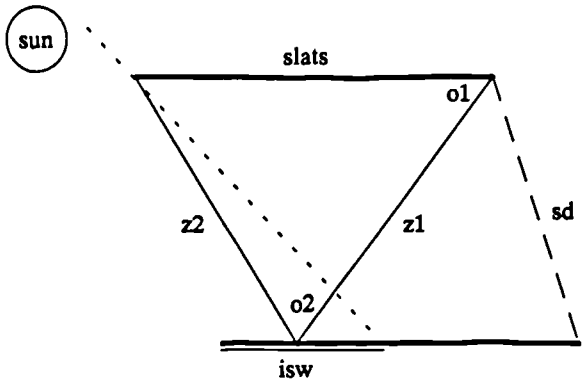

Figure D.5:

Relationship between illuminated slat width and upper slat to illustrate the view factor f_2.

Similarly the view factor between the upper slat and the inside (Fig D.6) is given by,

(D.10a) $$f_3 = 0.5*(1-\cos(o3))$$

(D.10b) $$o3 = \arcsin\left(\frac{sd*\sin(90°+si)}{z3}\right)$$

(D.10c) $$z3^2 = 0.25*sw^2 + sd^2 - sd*sw*\cos(90°+si)$$

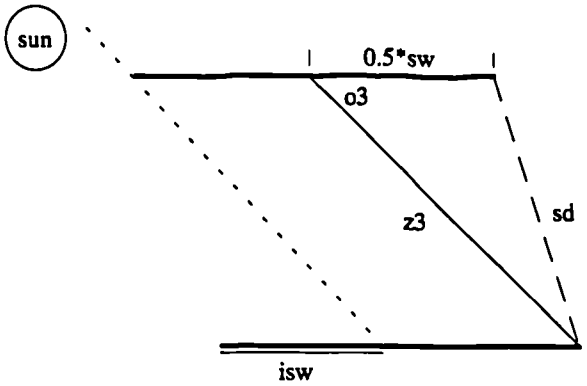

Figure D.6:

Relationship between illuminated upper slat and the inside to illustrate the view factor f_3.

The described view factor formulations are correct for infinitely small illuminated slat areas. In most cases, there is an error which increases as the illuminated slat width (*isw*) increases. The error was found to be at maximum about 4% (compared to the rigorous numerically predicted value), when the total slat width was illuminated. It is lower than 1%, when half of the slats or less are illuminated.

D.3.2 Specular-reflected transmittance

The calculation model for the specular-reflected radiation portion uses a rigorous analytical solution with no approximations. It considers all higher-order reflections. The total transmitted radiation τ_{ds}^{b} consists of, at most, three different radiation components, which represent a different number of inter-reflections *nr*,

(D.11) $$\tau_{ds}^{b} = \tau_{ds1}^{b} + \tau_{ds2}^{b} + \tau_{ds3}^{b}$$

When there is no reflectance back to the outside, the absorptance α_{ds}^{b} is simply the difference between τ_{ds}^{b} and one. When there is radiation backloss, α_{ds}^{b} can be obtained from the sum of all the single absorptance portions in the sequence of inter-reflections:

(D.12) $$\alpha_{ds_i}^{b} = (1-\rho) * \frac{\tau_{ds_i}^{b}}{\rho^{nr}} * \sum_{j=0}^{nr-1} \rho^{j}$$

The calculation of the different radiation components must also distinguish between the cases a) "no radiation backloss" or b) "radiation backloss", which are determined by the reflecting slat width (*rsw*). The reflecting slat width (*rsw*) is defined to be the slat area, which may reflect specularly to the inside (or to the outside).

(D.13a) $h' > si$: $$rsw = sd * \frac{\sin(90° - h' + 2 * si)}{\sin(h' - si)} \leq sw$$

(D.13b) $h' < si$: $$rsw = sd * \frac{\sin(90° + h' - 2 * si)}{\sin(si - h')} \leq sw$$

When the reflecting slat width (*rsw*) is positive, all radiation (after the first reflection) is multi-reflected to the inside. When *rsw* is negative, there is one radiation component, which is (after the first reflection) lost to the outside.

a) *rsw* > 0 (no radiation backloss)

When *rsw* is positive, three radiation components, which are inter-reflected with a different number of reflections (*nr*), are transmitted to the inside (Fig. D.7). In a sequence of inter-reflections these components are finally reflected by either the lower or the upper slat surface.

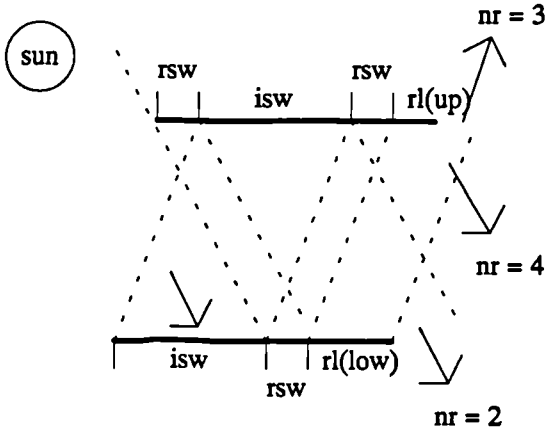

Figure D.7:

Specular inter-reflections of direct radiation between slat surfaces (without radiation backloss).

The reflectance length (*rl*) is defined to be the final (inner) slat area (in a sequence of inter-reflections), which actually gets reflected sunlight. It may be at the lower slat (rl_{low}) or at the upper slat (rl_{up}). It can be calculated by,

(D.14a) $$rl_{low} = sw - 0.5 * mnr * (isw + rsw)$$

(D.14b) $$rl_{up} = sw - 0.5 * mnr * (isw + rsw) - rsw$$

where *mnr* is the minimum number of reflections:

(D.15) $$mnr = 2 * \left| \frac{sw}{isw + rsw} \right|$$

The following relations must be regarded:
$$rl_{low} < 0 \Rightarrow rl_{low} = 0$$
$$rl_{up} < 0 \Rightarrow rl_{up} = 0$$
$$rl_{low} > isw \Rightarrow rl_{low} = 0$$
$$rl_{up} > isw \Rightarrow rl_{up} = 0$$

If rl_{low} is greater than rl_{up} the radiation component with the lowest number of reflections is (in the sequence of inter-reflections) finally reflected by the upper slat. In this case, the radiation components can be obtained from equations (D.16):

(D.16a) $$\tau^b_{ds_1} = \rho^{mnr} * \frac{isw - rl_{low}}{isw} \qquad mnr = 0 \Rightarrow \tau^b_{ds_1} = 0$$

(D.16b) $$\tau^b_{ds_2} = \rho^{(mnr+1)} * \frac{rl_{low} - rl_{up}}{isw}$$

(D.16c) $$\tau^b_{ds_3} = \rho^{(mnr+2)} * \frac{rl_{up}}{isw}$$

If rl_{low} is lower or equal than rl_{up} the radiation component with the lowest number of reflections is (in the sequence of inter-reflections) finally reflected by the lower slat. In this case, the radiation components can be obtained by equations (D.17):

(D.17a) $$\tau^b_{ds_1} = \rho^{(mnr+1)} * \frac{isw - rl_{up}}{isw}$$

(D.17b) $$\tau^b_{ds_2} = \rho^{(mnr+2)} * \frac{rl_{up} - rl_{low}}{isw}$$

(D.17c) $$\tau^b_{ds_3} = \rho^{(mnr+3)} * \frac{rl_{low}}{isw}$$

b) rsw < 0 (radiation backloss)

When *rsw* is negative, there are two radiation components, which are transmitted to the inside and one component, which is lost to the outside (Fig. D.8).

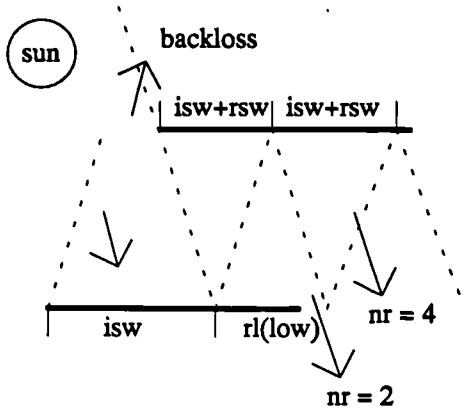

Figure D.8:

Specular inter-reflections of direct radiation between slat surfaces (with radiation backloss).

The two transmitted components can be obtained as follows,

(D.18a) $$\tau^{b}_{ds_1} = \rho^{mnr} * \frac{(isw + rsw) - rl_{low}}{isw}$$

(D.18b) $$\tau^{b}_{ds_2} = \rho^{(mnr+2)} * \frac{rl_{low}}{isw}$$

where

(D.19) $$mnr = 2 * \left| \frac{sw + rsw}{isw + rsw} \right|$$

and

(D.20) $$rl_{low} = (sw + rsw) - 0.5 * mnr * (isw + rsw)$$

D.4 DIFFUSE TRANSMITTANCE

The diffuse radiation on a surface consists of a portion from the sky and a portion from the ground (see Chapter 4). The sky radiance distribution was assumed to be isotropic (ISO).

The unreflected diffuse radiation enters the room through the open space between the slats, which is defined by the cutoff angles $\Omega 1$ and $\Omega 2$ (Fig.D.9).

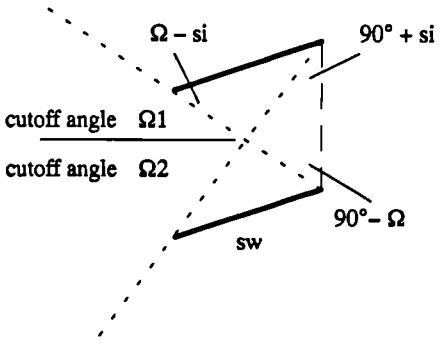

Figure D.9:

Geometrical presentation of the cutoff angles. Any radiation from above the cutoff angle Ω1 and below the cutoff angle Ω2 is totally shaded.

From Fig. D.9 it can be seen that

(D.21a) $$\Omega 1 = \arctan\left(\frac{sd + sw*\sin(si)}{sw*\cos(si)}\right)$$

(D.21b) $$\Omega 2 = -\arctan\left(\frac{sd - sw*\sin(si)}{sw*\cos(si)}\right)$$

The diffuse transmittance τ_f^b follows by integrating the radiation from each slice of the sky (or ground) across the vault between the cutoff angles. The net-transmittance $\tau(\Omega)$ of the diffuse radiation from each slice is calculated in a similar way to the direct transmittance $\tau_d^b(h')$ (see section D.2). Here, the projected sun height angle h' is substituted by the profile angle Ω of a certain sky (or ground) slice. When Ω is the integration angle, $\tau(\Omega)$ the diffuse transmittance of radiation from a slice and L the radiance of the sky (or ground), the formulation becomes,

(D.22a) $$\tau_f^b = \frac{I_{in}}{I_{on}} = \frac{\int_{\Omega 1}^{\Omega 2} L*\cos(\Omega)*\tau(\Omega)*d\Omega}{\int_{-90°}^{90°} L*\cos(\Omega)*d\Omega}$$

(D.22b) $$\tau(\Omega) = 1 - (sw*\sin(si) - sw*\cos(si)*\tan(\Omega)) / sd$$

I_{on} and I_{in} are the total incident and transmitted diffuse radiation intensities. For isotropic sky and ground radiance distributions the integrals can be solved analytically.

Since the calculation distinguishes between sky and ground radiation (dependent on the window inclination angle η; 0° for horizontal), it must be executed for both components separately. In addition, the particular sign of the integration must be considered (if the absolute value of Ω is greater than the absolute value of si, the integration of I_{in} in equation (D.22a) has a negative sign!), which leads to five different calculation cases for I_{in}. A simplified notation is used to illustrate the integration limits:

For $\Omega 2 > \eta - 90°$ (no ground radiation) and $si > 0$ $\quad I_{in} = \int_{\Omega 2}^{si} + \int_{si}^{\Omega 1}$

For $\Omega 2 > \eta - 90°$ (no ground radiation) and $si < 0$ $\quad I_{in} = \int_{\Omega 1}^{si} - \int_{si}^{\Omega 2}$

For $\Omega 2 < \eta - 90°$ and $si > 0$ $\quad I_{in} = \int_{\eta-90°}^{si} - \int_{si}^{\Omega 1} - \int_{\Omega 2}^{\eta-90°}$

For $\Omega 2 < \eta - 90°$ and $si < 0$ and $si > \eta - 90°$ $\quad I_{in} = \int_{\Omega 1}^{si} - \int_{si}^{\eta-90°} - \int_{\eta-90°}^{\Omega 2}$

For $\Omega 2 < \eta - 90°$ and $si < 0$ and $si < \eta - 90°$ $\quad I_{in} = \int_{\Omega 1}^{\eta-90°} - \int_{\eta-90°}^{si} - \int_{si}^{\Omega 2}$

The analytical solutions of the integrals are not shown here (but are given in IR6). Noting that the ground radiance for a (pure) overcast day corresponds to the sky radiance multiplied by the ground reflectance ρ_{gr}, the solution of the incident intensity I_{on} reduces to one simple formulation:

(D.23) $$I_{on} = 1 - \sin(\eta - 90°) + \rho_{gr}(\sin(\eta - 90°) + 1)$$

D.5 DIFFUSE-REFLECTED TRANSMITTANCE

The reflectance of the diffuse radiation on the slat surfaces is either diffuse, specular or any combination of these. The calculation of the specular reflectance needs numerical solution techniques. The solution simply assumes the diffuse radiation from slices of sky (or ground) is like direct radiation so the calculation principle for specular reflection outlined in section D.3.2 is used. The sum of the specular transmitted radiation contributions (for each slice of sky (or ground) vault) corresponds to the specular-reflected diffuse transmittance τ_{fs}^{b}. Numerical solutions were not considered within the basic version of GLSIM-BLIND (but added to a later version of the program).

For an analytical solution, the reflectance of the diffuse radiation on the slat surfaces was assumed to be purely diffuse. Thus, the calculation of the reflected radiation from each slice is similar to the calculation of the direct-to-diffuse reflection calculation (section D.3.1). Here, the projected sun height angle h' is substituted by the profile angle Ω of a certain sky (or ground) point. The diffuse-reflected transmittance τ_{ff}^{b} is obtained by considering the inter-reflections of each diffuse radiation portion and the corresponding view factors f up to the second reflection.

(D.24a) $$\tau_{ff}^{b} = \frac{I_{in}}{I_{on}} = \frac{\int_{-90}^{90} L * \cos(\Omega) * (1 - \tau(\Omega)) * (\rho * f_1(\Omega) + \rho^2 * f_2(\Omega) * f_3) * d\Omega}{\int_{-90}^{90} L * \cos(\Omega) * d\Omega}$$

(D.24b) $$1 - \tau(\Omega) = (sw * \sin(si) - sw * \cos(si) * \tan(\Omega)) / sd$$

When the reflectance at the slat surfaces is substituted by the absorptance (1 - ρ), the following equation for the total diffuse absorptance α_{f}^{b} is obtained.

$$\alpha_f^b = \frac{I_{in}}{I_{on}} = \frac{\int_{-90}^{90} L*\cos(\Omega)*(1-\tau(\Omega))*\left((1-\rho)+\rho*f_2(\Omega)*(1-\rho)\right)d\Omega}{\int_{-90}^{90} L*\cos(\Omega)*d\Omega} \qquad \text{(D.25)}$$

The view factors f are calculated according to equations (D.5) to (D.10) (section D.3.1). Here, the first illuminated slat can be either the upper slat or the lower slat. For lower slat illumination, the view factors f (index "low") can be obtained directly from equations (D.5) to (D.10). For upper slat illumination (index "up") the same equations can be used, but the slat inclination angle (*si*) must be substituted by (*-si*).

Again, the integration must be split into different parts, which consider either ground or sky radiation portions. In equations (D.24) and (D.25) the view factors f_1 and f_2 depend on the illuminated width of the slats, which again depends on the profile angle Ω of a certain radiation slice. To get an analytical solution, a simplified assumption was applied, which uses either half or total illumination of the slats (for *isw* in equations (D.5) to (D.10)). Half illumination (*isw* = 0.5**sw*; index "h") is assigned to all radiation slices in the sky (or ground) vault above or below the cutoff angles, which is approximately the energy-weighted average. Total illumination (*isw* = *sw*; index "t") actually occurs for all radiation slices with a profile angle between the cutoff angles. The error of the total transmittance due to this simplification was found to be lower than 1%.

There are again five different cases (see section D.4) which consider the sign of integration and the window inclination angle η (0° for horizontal). For every radiation slice, the corresponding view factors for upper (index "up") or lower (index "low"), as well as for half (index "h") or total (index "t") slat illumination must be used. This simplified notation is used to demonstrate the integration limits and the corresponding view factors.

For Ω2 > η - 90° (no ground radiation) and *si* > 0

$$I_{in} = \int_{\Omega 2}^{si}(f_{up}^t) - \int_{si}^{\Omega 1}(f_{low}^t) + \int_{\Omega 1}^{90°}(f_{low}^h) + \int_{-90°}^{\eta-90°}(f_{up}^h) + \int_{\eta-90°}^{\Omega 2}(f_{up}^h)$$

For Ω2 > η - 90° (no ground radiation) and *si* < 0

$$I_{in} = \int_{\Omega 1}^{si}(f_{low}^t) - \int_{si}^{\Omega 2}(f_{up}^t) + \int_{\Omega 1}^{90°}(f_{low}^h) + \int_{-90°}^{\eta-90°}(f_{up}^h) + \int_{\eta-90°}^{\Omega 2}(f_{up}^h)$$

For Ω2 < η - 90° and *si* > 0

$$I_{in} = \int_{\eta-90°}^{si}(f_{up}^t) - \int_{si}^{\Omega 1}(f_{low}^t) - \int_{\Omega 2}^{\eta-90°}(f_{up}^t) + \int_{\Omega 1}^{90°}(f_{low}^h) + \int_{-90°}^{\Omega 2}(f_{up}^h)$$

For $\Omega 2 < \eta - 90°$ and $si < 0$ and $si > \eta - 90°$

$$I_{in} = \int_{\Omega 1}^{si}(f_{low}^{t}) - \int_{si}^{\eta-90°}(f_{up}^{t}) - \int_{\eta-90°}^{\Omega 2}(f_{up}^{t}) + \int_{\Omega 1}^{90°}(f_{low}^{h}) + \int_{-90°}^{\Omega 2}(f_{up}^{h})$$

For $\Omega 2 < \eta - 90°$ and $si < 0$ and $si < \eta - 90°$

$$I_{in} = \int_{\Omega 1}^{\eta-90°}(f_{low}^{t}) - \int_{\eta-90°}^{si}(f_{low}^{t}) - \int_{si}^{\Omega 2}(f_{up}^{t}) + \int_{\Omega 1}^{90°}(f_{low}^{h}) + \int_{-90°}^{\Omega 2}(f_{up}^{h})$$

The analytical solutions of the integrals are not shown here (but can be found in IR6). But it should be noted, that in equations (D.24) and (D.25) $\tau(\Omega)$ is zero for all radiation components above or below the cutoff angles (index "h"). In these cases, the integration function reduces to one simple cosine-function. The incident intensity I_{on} is the same as for the diffuse transmittance (section D.4).

D.6 CURVED SLATS

In GLSIM-BLIND curved slats are treated as surface-slices of a cylinder. The curvature of the slat is described by the radius *sr* of the cylinder (Fig. D.10). The influence of curved slats on the transmittance of the different radiation components is considered as follows.

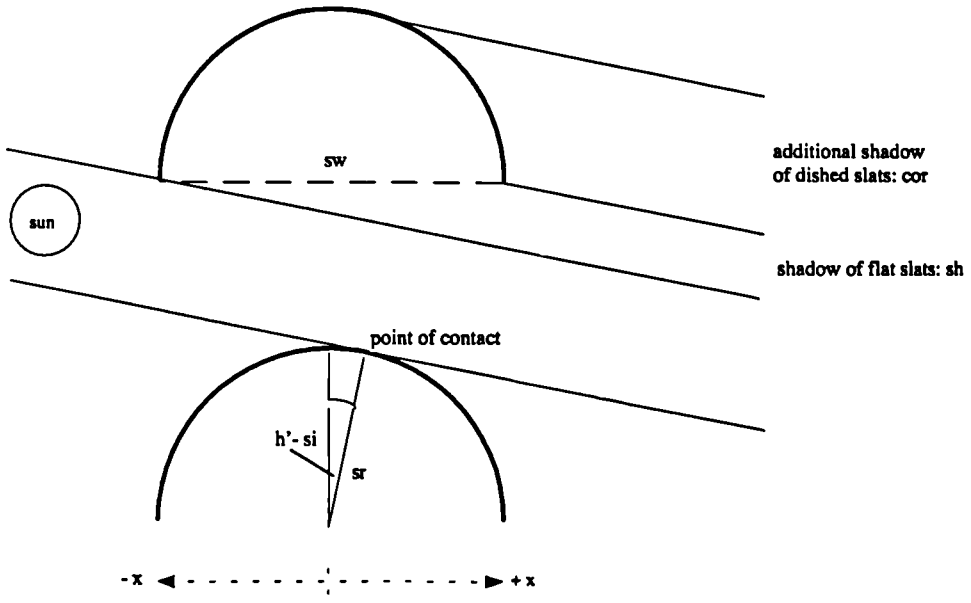

Figure D.10: Relationship between sun position and curved slat geometry to illustrate the shading of direct radiation.

D.6.1 Direct transmittance

The direct transmittance is reduced by an additional shadow due to the slat curvature. A correction (*cor*) was introduced which represents the additional shadow correctly (no approximation). It is calculated from first principles dependent on the angular position of the sun and the exact blind geometry. The calculation is based on a geometrical consideration of the point of contact, where the sun beam touches the slat (a detailed description of the derivation is given in IR6).

When *sr* is the slat radius of curvature (always greater than 0.5**sw*) and x_c the point of contact on an axis along the slat width, the correction (*cor*) can be obtained as follows,

(D.26a) $$x_c = sr\sin(h'-si) \qquad -0.5sw < x_c < 0.5sw$$

(D.26b) $$for\ x_c > 0 \qquad cor = \sqrt{(sr^2 - x_c^2)} - \sqrt{(sr^2 - 0.25sw^2)} - (0.5sw - x_c)\tan(h'-si)$$

(D.26c) $$for\ x_c < 0 \qquad cor = \sqrt{(sr^2 - x_c^2)} - \sqrt{(sr^2 - 0.25sw^2)} - (x_c - 0.5sw)\tan(h'-si)$$

As a result of the correction (*cor*) equation (D.2) for the direct transmittance modifies to:

(D.27) $$\tau_d^b = 1 - \frac{sh + cor}{sd} = 1 - sw * \frac{\sin(h'-si)}{\sin(90°-h')*sd} - \frac{cor}{sd} = 1 - \frac{(sw*\sin(si) - sw*\cos(si)*\tan(h'))}{sd} - \frac{cor}{sd}$$

D.6.2 Direct-to-diffuse transmittance

The influence of the slat curvature on the direct-to-diffuse transmittance is approximately considered by three single corrections to the view factors f_1 and f_2.

a) When a sun beam touches the slat curvature, the slat is illuminated between the outer end of the slat and the point of contact. The corrected illuminated slat width (*isw**) results from,

(D.28) $$isw^* = 0.5*sw + sr*\sin(h'-si)$$

b) The opening angle *o1* used to calculate the view factor f_1 is reduced due to the reflectance characteristic of the curved surface:

(D.29) $$o1^* = o1 - \arctan\frac{\sqrt{(sr^2 - x_c^2)} - \sqrt{(sr^2 - 0.25sw^2)}}{isw}$$

c) The slat distance (*sd*) is reduced due to the height of the central point of the curved slat:

(D.30) $$sd^* = sd + \sqrt{\left(sr^2 - 0.25\,sw^2\right)} - sr$$

In equations (D.3) to(D.9) *isw**, *ol**, and *sd** replace *isw*, *ol* and *sd* to yield the amended view factors. These view factors are approximate values. For flat slats the error due to these simplifications was found to be lower than 4% (in comparison with the rigorous analytical value). Since the rigorous analytical view factor for curved slats is difficult to obtain, the error was not investigated. However, it is probable that the uncertainty is similar to that of smooth slats.

D.6.3 Specular-reflected transmittance

To avoid numerical calculations, the effect of the slat curvature on the specular-reflected transmittance was neglected.

D.6.4 Diffuse transmittance

To avoid numerical calculations, the effect of the slat curvature on the diffuse transmittance was neglected.

D.6.5 Diffuse-reflected transmittance

The influence of the slat curvature on the diffuse-reflected transmittance can be treated in the same way as the direct-to-diffuse reflected radiation (section D.6.2) considering three corrections of the view factors given within section D.5.

D.7 INTERACTION BETWEEN BLIND AND GLAZING

Interaction between the blind and the glazing occurs in two ways:

- by the effect of blinds on the beam direction, which determines the incidence angle (and hence the transmittance and absorptance) in the glass panes; and
- by multiple-reflections between the glass panes and the slats.

D.7.1 Effect of blinds on the beam direction

For internal blinds, the incidence angle of the direct or diffuse radiation is not influenced by the slats. Thus the radiation transfer through the glass pane can be calculated by considering the usual direct and diffuse transmittance and absorptance values of glazings without blinds (as explained in Chapters 4 and 5).

For external blinds, however, the direction of the radiation is normally changed by reflection at the slat surfaces (one exception is for the direct transmitted radiation (section D.2) which is not influenced by the slats). Thus, the transmittance and absorptance values of the glass

panes (at the inner side of external blinds) must be calculated by considering the altered incidence angles of the radiation. This is done for the primary radiation ray (first order transmittance). The following transmittance values must be considered:

a) the glazing transmittance for the specular-reflected radiation τ^g_{ds};
b) the effective glazing transmittance for the direct-to-diffuse reflected radiation τ^g_{df};
c) the effective glazing transmittance for the diffuse-reflected radiation τ^g_{ff}; and
d) the effective glazing transmittance for the unreflected diffuse radiation τ^g_f.

The glazing absorptance values for the different radiation paths can be calculated using the same procedures as for the transmittance values. The direct radiation glazing transmittance in equations (D.32) to (D.34) τ^g_d must simply be replaced by the direct radiation absorptance α^g_d. Thus, in the following sections, only the prediction of the transmittance values - which are usually more important - is demonstrated.

a) The glazing transmittance for the specular-reflected radiation

The glazing transmittance for the specular-reflected radiation τ^g_{ds} corresponds to the direct radiation transmittance at the incidence angle θ. For specularly reflected direct beam radiation (section D.3.2) the incidence angle θ can be calculated by considering the reflection angles at the slat surfaces. As described in section D.3.2, the specular transmitted radiation consists of, at most, three different radiation portions which represent a different number of inter-reflections (*nr*). When the number of inter-reflections (*nr*) is even (2; 4; 6 etc.) the incidence angle θ of the direct radiation onto the glass pane corresponds to that incidence angle, which would occur without the blind (thus, in this case, the slats do not influence the incidence angle of direct radiation onto the glass pane).

When the number of inter-reflections is uneven (1; 3; 5 etc.) the direction of the direct beam radiation is changed by reflection at the slat surfaces. The new incidence angle of the radiation onto the glass pane corresponds to the sum of the incidence angle (say θ_1) of the direct radiation onto the slat surfaces and the inclination angle (*si'*) of the slats (projected into the beam direction) (Fig. D.11).

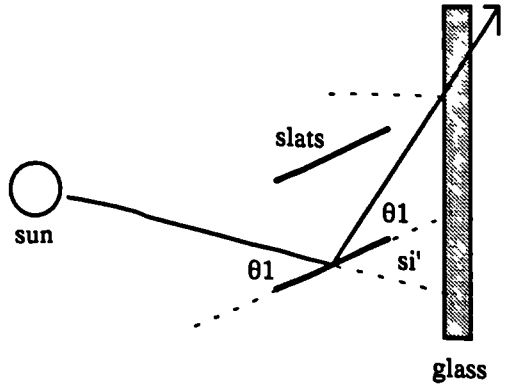

Figure D.11:

Direct radiation incidence onto a glass pane at the inner side of external blinds, which is reflected specularly at the slat surfaces (with an uneven number of inter-reflections).

The incidence angle of the direct radiation onto the slat surfaces (θ_1) can be calculated with the same (well-known) algorithms, which are used to calculate the incidence angle of direct radiation onto any inclined surfaces (walls; roofs; ground etc.). These are not described here.

Knowing the azimuth angle of the window (az_w) and the sun (az_s), the projection of the slat inclination angle (si) into the beam direction is given by,

$$si' = \arctan\left(\tan(si) * \cos(az_s - az_w)\right) \tag{D.31}$$

It should be noted that for slats which are inclined downwards (the normal case for vertical blinds), the radiation is more likely to be inter-reflected on an even number of times. Thus, in GLSIM-BLIND it was assumed that the incidence angle of the direct radiation onto the glass pane always corresponds to that, which would occur without the blind. The consequences of this assumption was not investigated.

b) The effective glazing transmittance for the direct-to-diffuse reflected radiation

The glazing transmittance for direct-to-diffuse reflected radiation τ_{df}^{g} corresponds to the average of the (incidence angle dependent) transmittance values for all the reflected radiation portions onto the glass pane (Fig. D.12).

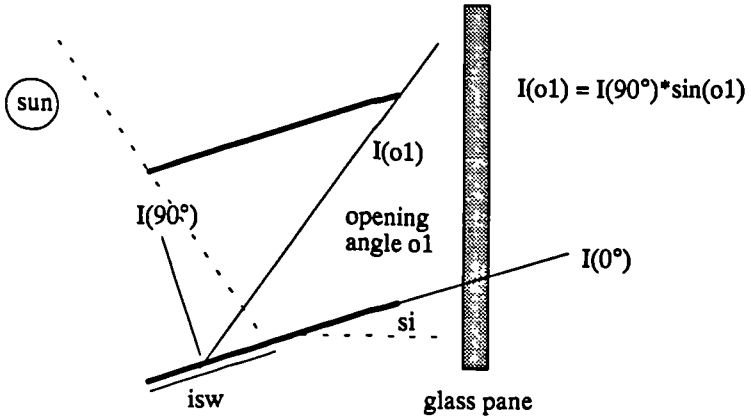

Figure D.12: Incidence of direct-to-diffuse reflected radiation onto a glass plane at the inner side of an external blind.

The Law-of-Lambert states that the radiation intensities above an ideal diffusing (reflecting) surface decrease with the sine of the emittance angle. Thus, the effective direct-to-diffuse transmittance τ_{df}^{g} for a glass pane behind a diffusing slat surface is given by,

$$\tau_{df}^{g} = \frac{\int_{0}^{o1} \sin(\Omega) * \tau_{d}^{g}(\Omega - si) * d\Omega}{\int_{0}^{o1} \sin(\Omega) * d\Omega} \tag{D.32}$$

where τ_d^g is the direct radiation glazing transmittance for incidence angle (Ω - si) and *o1* is the opening angle, within which the reflected radiation reaches the glass pane. The opening angle (*o1*) is calculated by considering equation (D.6) and the actual illuminated slat width (*isw*).

c) The effective glazing transmittance for the diffuse-reflected radiation

The calculation of the effective glazing transmittance for the diffuse-reflected radiation τ_{ff}^g is similar to that of τ_{df}^g, however the illuminated slat width always corresponds to the total slat width (*isw* = *sw*). In addition, in the case of diffuse-reflected radiation, both sides of the slats are illuminated simultaneously. It is therefore necessary to consider two different opening angles, one from the lower slat ($o1_{low}$) and one from the upper slat ($o1_{up}$).

$$\tau_{ff}^g = \frac{\int_0^{o1_{low}} \sin(\Omega) * \tau_d^g(\Omega - si) * d\Omega + \int_0^{o1_{up}} \sin(\Omega) * \tau_d^g(\Omega + si) * d\Omega}{\int_0^{o1_{low}} \sin(\Omega) * d\Omega + \int_0^{o1_{up}} \sin(\Omega) * d\Omega} \tag{D.33}$$

For lower slat illumination, the opening angle *o1* (subscript "*low*") can be obtained directly from equations (D.5) to (D.6). For upper slat illumination (subscript "*up*") the same equations can be used, but the slat inclination angle (*si*) must be replaced with (-*si*).

d) The effective glazing transmittance for the unreflected diffuse radiation

The calculation of the effective glazing transmittance for the unreflected diffuse radiation τ_f^g is more complicate. The diffuse radiation from the sky (or ground) vault which lies between the cutoff angles is not reflected by the slat surfaces (Fig. D.13). Thus, the direction of the radiation is not changed. The distribution of the unreflected diffuse radiation at the inner side of external blinds must consider its usual three-dimensional character.

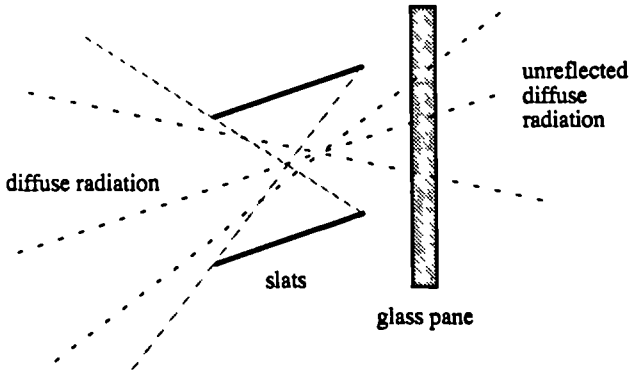

Figure D.13:

Incidence of unreflected diffuse radiation onto a glass plane at the inner side of external blinds.

The effective diffuse glazing transmittance τ_f^g is found by integrating the radiation from each point of the sky (or ground) vault which lies between the cutoff angles. Each radiation

portion is transmitted through the blind dependent on the *net* blind-transmittance $\tau(\Omega)$ (see section D.4). The *net* glazing-transmittance τ_d^g of each radiation portion considers the exact incidence angle θ of the radiation portions onto the glass pane.

For the integration, the sky (and ground) vault is cut into slices. The integration follows along a slice angle ξ and along the profile angle Ω. (Note: the profile angle corresponds to the height angle ζ used in this type of integration previously, see Chapter 4, section 4.2). By considering that $\tau_d^g(\theta)$ is the direct glazing transmittance at an incidence angle of θ, the integration becomes,

$$\tau_f^g = \frac{\int_{-90°}^{90°}\int_{-90°}^{90°} L*\cos(\theta)*\tau(\Omega)*\tau_d^g(\theta)*\sin(\xi)*d\Omega*d\xi}{\int_{-90°}^{90°}\int_{-90°}^{90°} L*\cos(\theta)*\tau(\Omega)*\sin(\xi)*d\Omega*d\xi} \tag{D.34a}$$

where

$$\tau(\Omega) = 1-(sw*\sin(si)-sw*\cos(si)*\tan(\Omega))/sd \tag{D.34b}$$

The incidence angle θ of the diffuse radiation portions can be calculated as follows,

$$\theta = \arccos\left[\cos\left(\arcsin(\sin\xi*\sin\Omega)\right)*\cos\left(\arctan\left(\frac{\sin\xi*\cos\Omega}{\cos\xi}\right)\right)\right] \tag{D.35}$$

Since the calculation distinguishes between sky and ground radiation (depending on the window inclination angle), it must be executed twice, once for each component.

Since glazing transmittances are usually given as discrete values at certain incidence angles (e.g. in 10° steps from 0° to 90° in HTB2) the integrals of equations (D.32) to (D.34) can not be solved analytically, instead numerical summations become necessary. These are the only numerical procedures in the basic version of GLSIM-BLIND. However, they are sufficiently simple that they can be solved quickly. Because the glazing properties for diffuse radiation stay the same over the whole simulation period, they only need to be solved once at the beginning of the program run.

D.7.2 Multi-reflections between blind and glazing

The multi-reflections between the blind and the glazing are considered using a recursive sequence of calculation steps up to the second reflection. An investigation showed that the error in the total transmittance values, due to neglecting of the third or higher order reflections, is in most cases lower than 1% (IR6).

The sequence of reflections is described by: the blind (superscript "*b*") transmittance τ^b; the blind reflectance ρ^b; the glazing (superscript "*g*") transmittance τ^g; and the glazing reflectance ρ^g. Each of these parameters must be considered for radiation which is: direct (subscript "*d*"); diffuse (subscript "*f*"); direct-to-diffuse reflected (subscript "*df*"); specularly reflected (subscript "*ds*"); or diffuse-reflected (subscript "*ff*"). Since the reflectance values are not calculated from first principles, they must be obtained from the transmittance and absorptance values. The sequence of reflections is different for internal or external blind device.

a) External blinds

For external blinds the reflectance values of the blind and glazing, for the different radiation components (*d, f, df, ff, ds*), can be calculated as follows:

(D.36a) Reflectance of diffuse radiation from the blind:

$$\rho_f^b = 1 - \tau_f^b - \tau_{ff}^b - \alpha_f^b$$

(D.36b) Reflectance of direct radiation from glazing:

$$\rho_d^g = 1 - \tau_d^g - \alpha_d^g$$

(D.36c) Reflectance of direct-to-diffuse reflected radiation from glazing:

$$\rho_{df}^g = 1 - \tau_{df}^g - \alpha_{df}^g$$

(D.36d) Reflectance of diffuse radiation from glazing:

$$\rho_f^g = 1 - \tau_f^g - \alpha_f^g$$

(D.36e) Reflectance of diffuse-reflected radiation from glazing:

$$\rho_{ff}^g = 1 - \tau_{ff}^g - \alpha_{ff}^g$$

(D.36f) Reflectance of specularly reflected radiation from glazing:

$$\rho_{ds}^g = 1 - \tau_{ds}^g - \alpha_{ds}^g$$

The total (superscript "T") transmittance and absorptance for the different radiation portions due to multiple reflections up to the second reflection (Fig. D.14) are given by the following equations.

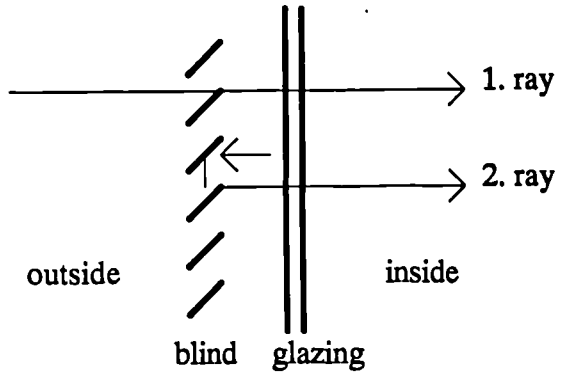

Figure D.14:

Sequence of multiple reflections between glazing and external blinds.

The total direct transmittance:

(D.37a) $$\tau_d^T = \tau_d^g * \left(\tau_d^b + \tau_{ds}^b\right)$$

The total direct-to-diffuse transmittance:

(D.37b) $$\tau_{df}^T = \left(\tau_d^b + \tau_{ds}^b\right) * \rho_d^g * \rho_f^b * \tau_{ff}^g + \tau_{df}^b * \tau_{df}^g + \tau_{df}^b * \rho_{df}^g * \rho_f^b * \tau_{ff}^g$$

The total diffuse transmittance:

(D.37c) $$\tau_f^T = \tau_f^b * \tau_f^g + \tau_f^b * \rho_f^g * \rho_f^b * \tau_{ff}^g + \tau_{ff}^b * \tau_{ff}^g + \tau_{ff}^b * \rho_{ff}^g * \rho_f^b * \tau_{ff}^g$$

The total direct absorptance of the glazing:

(D.37d) $$\alpha_d^{T,g} = \tau_d^b * \alpha_d^g + \tau_d^b * \rho_d^g * \rho_f^b * \alpha_{ff}^g + \tau_{ds}^b \alpha_{ds}^g + \tau_{ds}^b * \rho_{ds}^g * \rho_f^b * \alpha_{ff}^g + \tau_{df}^b * \alpha_{df}^g + \tau_{df}^b * \rho_{df}^g * \rho_f^b * \alpha_{ff}^g$$

The total diffuse absorptance of the glazing:

(D.37e) $$\alpha_f^{T,g} = \tau_f^b * \alpha_f^g + \tau_f^b * \rho_f^g * \rho_f^b * \alpha_{ff}^g + \tau_{ff}^b * \alpha_{ff}^g + \tau_{ff}^b * \rho_{ff}^g * \rho_f^b * \alpha_{ff}^g$$

Since the absorbed radiation energy in external blinds is lost to the ambient air, the total absorptance of external blinds is (thermally) unimportant.

b) Internal blinds

For internal blinds the important reflectance values of the blind and glazing can be calculated as follows:

(D.38a) Reflectance of direct radiation from the blind: $$\rho_d^b = 1 - \tau_d^b - \tau_{df}^b - \alpha_d^b$$

(D.38b) Reflectance of diffuse radiation from the blind: $$\rho_f^b = 1 - \tau_f^b - \tau_{ff}^b - \alpha_f^b$$

(D.38c) Reflectance for diffuse radiation from the glazing: $$\rho_f^g = 1 - \tau_f^g - \alpha_f^g$$

The total (superscript "T") transmittance and absorptance values for the different radiation portions are calculated by considering the multiple reflections between the blind and the glazing up to the second reflection (Fig. D.15).

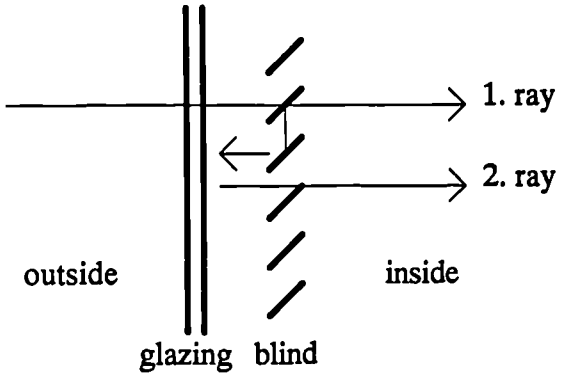

Figure D.15:

Sequence of multiple reflections between an internal blind and the glazing.

The total direct transmittance:

(D.39a) $$\tau_d^T = \tau_d^g * \left(\tau_d^b + \tau_{ds}^b\right)$$

The total direct-to-diffuse transmittance:

(D.39b) $$\tau_{df}^T = \tau_d^g * \tau_{df}^b + \tau_d^g * \rho_d^b * \rho_f^g * \left(\tau_f^b + \tau_{ff}^b\right)$$

The total diffuse transmittance:

(D.39c) $$\tau_f^T = \tau_f^g * \left(\tau_f^b + \tau_{ff}^b\right) + \tau_f^g * \rho_f^b * \rho_f^g * \left(\tau_f^b + \tau_{ff}^b\right)$$

The total direct absorptance of the glazing:

(D39d) $$\alpha_d^{T,g} = \alpha_d^g + \tau_d^g * \rho_d^b * \alpha_f^g$$

The total diffuse absorptance of the glazing:

(D39e) $$\alpha_f^{T,g} = \alpha_f^g + \tau_f^g * \rho_f^b * \alpha_f^g$$

The total direct absorptance of the blind:

(D39f) $$\alpha_d^{T,b} = \tau_d^g * \alpha_d^b + \tau_d^g * \rho_d^b * \rho_f^g * \alpha_f^b$$

The total diffuse absorptance of the blind:

(D39e) $$\alpha_f^{T,b} = \tau_f^g * \alpha_f^b + \tau_f^g * \rho_f^b * \rho_f^g * \alpha_f^b$$

LIST OF SYMBOLS

The following symbols are used in Appendix D. The list contains some additional symbols which are not considered in the common symbols list of the Chapters 1 to 10.

English Letter Symbols

az: azimuth angle, *deg* or *rad*
cor: correction, same unit as used for slat distance (*sd*)
f: view factor, -
h': projected sun height angle, *deg*
h: height angle, *deg*
isw: illuminated slat width, same unit as used for slat distance (*sd*)
*isw**: illuminated slat width for curved slats, same unit as used for slat distance (*sd*)
I: intensity, W/m^2K
L: radiance, $W/sr\ m^2$
mnr: minimum number of reflections (in a sequence of inter-reflections), -
nr: number of reflections (in a sequence of inter-reflections), -
o: opening angle, *deg*
*o**: opening angle for curved slats, *deg*
pr: projection of the slat distance onto the illuminated slat width, same unit as used for slat distance (*sd*)
rl: reflectance length, same unit as used for slat distance (*sd*)
rsw: reflecting slat width, same unit as used for slat distance (*sd*)
sd: slat distance, any unit
*sd**: slat distance for curved slats, same unit as used for slat distance (*sd*)
sh: shaded area, same unit as used for slat distance (*sd*)
si: slat inclination angle (positive upwards; negative downwards), *deg*
si': projection of the slat inclination angle into the direction of the direct radiation, *deg*
sr: slat curvature radius, same unit as used for slat distance (*sd*)
sw: slat width, same unit as used for slat distance (*sd*)
x_c: point of contact on an axis along the slat width, same unit as used for slat distance
z: opening line, same unit as used for slat distance (*sd*)

Greek Letter Symbols

α: absorptance, -
ζ: height integration angle, *deg*
η: inclination angle between window normal and a vertical plane (e.g. 0° for horizontal surface), *deg*
θ: angle between radiation incidence and surface normal, *deg*
ξ: slice integration angle, *deg*
ρ: reflectance, -
σ: shining factor, -
τ: transmittance, -
Ω: profile angle (projected height angle of diffuse radiation portions), *deg*
$\Omega 1$: cutoff angle1, *deg*
$\Omega 2$: cutoff angle2, *deg*

Subscripts

d: relating to direct radiation
df: relating to direct-to-diffuse reflected radiation
ds: relating to specular-reflected direct radiation
f: relating to diffuse radiation
ff: relating to diffuse-reflected diffuse radiation
fs: relating to specular-reflected diffuse radiation
gr: relating to ground
in: into the room
low: at the lower slat
on: onto the outer glazing surface
s: relating to sun
up: at the upper slat
w: relating to window surface

Superscripts

b: relating to blind
g: relating to glazing
h: half
t: total
T: total transmittance (absorptance; reflectance) of a multi-layered glazing and blind structure